8-2023

A larval zebrafish (Danio rerio) model of adherent-invasive Escherichia coli infections

Erika Flores

Erika Flores

A larval zebrafish (*Danio rerio*) model of adherent-invasive

Escherichia coli infections

by

Erika Flores, B.S

APPROVED:

_____
Anne-Marie Krachler, Ph.D.
Advisory Professor

_____
Heidi Kaplan, Ph.D.

_____
William Margolin, Ph.D.

_____
Charles Darkoh, Ph.D.

_____
Rosa Uribe, Ph.D.

APPROVED:

_____
Dean, The University of Texas
MD Anderson Cancer Center UTHealth Graduate School of Biomedical Sciences

A larval zebrafish (*Danio rerio*) model of adherent-invasive *Escherichia coli* infections

A
Dissertation

Presented to the Faculty of

The University of Texas

MD Anderson Cancer Center UTHealth

Graduate School of Biomedical Sciences

in Partial Fulfillment

of the Requirements

for the Degree of

Doctor of Philosophy

by

Erika Flores, *B.S.*

Houston, Texas

August, 2023

Acknowledgements

I would like to express my gratitude to Dr. Anne Marie Krachler for her invaluable support and guidance throughout my dissertation journey. Anne-Marie, thank you for welcoming me into your lab and fostering a supportive environment. I am grateful for your mentorship, encouragement to step out of my comfort zone, and for teaching me the importance of perseverance.

Next, I thank Dr. Heidi Kaplan for her support, mentorship, and for providing me with the opportunity to participate in the summer research program. Your patience and dedication to mentoring me have been greatly appreciated. I am grateful for the time you have invested in my development. I thank you and Anne-Marie for helping me meet my graduation timeline and pushing through the tight schedule.

I extend my gratitude to my current and former advisory committee members, Drs. Rosa Uribe, Charles Darkoh, William Margolin, and Anthony Maresso. Thank you for your patience and understanding with scheduling and for your valuable input during my committee meetings and defense.

I am thankful for every member of the Krachler lab, past and present. Your contributions have made this journey more enjoyable. I want to express my special thanks to Natalie, who played a significant role in mentoring me during my early years in graduate school and continues to provide support from a distance. Your guidance and friendship have been invaluable. To Max, thank you for taking your time to help me with statistics and to practice my oral presentations. I want to express my deep gratitude to Soumita for teaching me essential laboratory techniques, such as RNA isolation and RT-PCR, as well as for generating the deletion strains. Your lessons and

friendship are cherished. Kim, thank you for being a great friend and for your fun and generous personality that brought joy to the lab. I appreciate your role in organizing our hangouts and game nights. I would also like to thank Rachel for her assistance in homogenizing fish samples and for her friendship.

A special thank you goes to my undergraduate mentor, Dr. Poonam Gulati, for providing me with an opportunity to explore microbiology research. It was through this experience that I discovered my passion for this field.

I want to express my heartfelt appreciation to my family and close friends. To my mom, who played a crucial role in shaping my upbringing and instilling in me the courage to pursue my dreams, thank you for your hard work and sacrifices. To my fiancé, Andy, thank you for being a supportive listener and for believing in me. To my sister Monica, thank you for your constant support. To Mary, Jackie, Keyla, Leslie, and Steffany, thank you for being a friend and always lending an ear to my frustrations and for the good times. Your friendship has been a source of comfort and support during difficult moments. Lastly, I am thankful to my dogs Missy, Layla, and Emma for their unconditional love and company.

I am sincerely grateful to everyone who has contributed to my academic and personal growth throughout this dissertation process. Your support has been invaluable, and I am honored to have met such wonderful individuals throughout this journey.

Abstract

A larval zebrafish (*Danio rerio*) model of adherent-invasive

Escherichia coli infections

Erika Flores, B.S.
Advisory Professor: Anne-Marie Krachler, Ph.D.

Inflammatory bowel disease (IBD), including Crohn's disease and ulcerative colitis, is a broad term for chronic intestinal disorders that severely impact patient morbidity and quality of life. The global prevalence of IBD is rising, with over one million patients affected in the US alone. Adherent-invasive *E. coli* (AIEC) is a pathobiont frequently found in IBD biopsies. AIEC adhere to and invade epithelial cells, and can survive inside macrophages *in vitro*. However, how AIEC contributes to IBD *in vivo* remains unclear. Here a larval zebrafish (*Danio rerio*) model of AIEC was established, which facilitates the study of the role of pre-existing inflammation, and host- and pathogen-genetic factors during IBD pathogenesis. *Paramecium caudatum*, a natural prey of zebrafish larvae, was used as a vehicle for AIEC delivery to the gastrointestinal tract, and dextran sulfate sodium (DSS) pharmacologically induced colitis. AIEC colonized the zebrafish gut in higher numbers and persisted for longer compared to non-pathogenic *E. coli* in the absence of chronic inflammation. Further, bacterial burden and persistence in the host were higher in fish with pre-existing DSS colitis. The proinflammatory response was further exacerbated by AIEC, resulting in higher neutrophil recruitment to the gut and increased relative expression of the genes that encode proinflammatory cytokines. In addition, we showed that two AIEC virulence

factors, FimH and IbeA, play a role in AIEC colonization and contribute to intestinal inflammation in larval zebrafish, similarly to what has been observed in mice. In conclusion, we established a high-throughput, genetically tractable model to study AIEC–host interactions in the context of chronic inflammation.

Table of Contents

List of Abbreviations

AIEC: adherent-invasive *Escherichia coli*

ALR: AIM2-like receptor

AMPs: antimicrobial proteins

APEC: avian pathogenic *E. coli*

APOA1: antioxidant apolipoproteinA-I

ATG16L1: autophagy-related 16-like 1

c-di-GMP: cyclic dimeric GMP

CBD: chitin-binding domains

CD: Crohn's disease

CEACAM: Carcinoembryonic antigen-related cell adhesion molecules

CHI3L1: chitinase 3-like-1

ChiA: chitinase A

CHST5: carbohydrate sulfotransferase 5

CLRs:C-type: lectin receptors

COX: cyclooxygenases

CXCL9: chemokine 9

CYLD: cylindromatosis

DHODH: dihydroorotate dehydrogenase

DOC: sodium deoxycholate

Dpf: days post fertilization

Dpi: days post infection

DSS: dextran sulfate sodium

DUOX2: dual oxidase 2

ECM: extracellular matrix

EHEC: enterohemorrhagic *Escherichia coli*

ENU: N-ethyl-N-nitrosourea

FAE: Follicle-associated epithelium

GAL3ST2: galactose-3-O-sulfotransferase 2

GF: germ-free

GlcNAc6ST-2: N-acetylglucosamine 6-O-sulfotransferase-2

GWAS: genome-wide association studies

HPI: high-pathogenicity island

HtrA: high-temperature requirement A

IBCs: intracellular bacterial communities

IBD: inflammatory bowel disease

IbeA: invasion of the brain endothelium protein A

IECs: intestinal epithelial cells

Igs: immunoglobulins

IKK: IκB kinase

iKO: inducible knockout

IL: interleukin

IRGM: immunity-related GTPase M

ITLN1: human intelectin-1

KI: knock-in

KO: knockout

LPF: long polar fimbriae

LPS: lipopolysaccharide

M cells: microfold cells

MAM: multivalent adhesion molecule

MD-2: myeloid differentiation factor 2

MDP: muramyl dipeptide

meso-DAP: meso-diaminopimelic acid

MMPs: matrix metalloproteinases

mpi: minutes post infection

MUC2: mucin 2

MyD88: myeloid differentiation factor 88

NADPH: nicotinamide adenine dinucleotide phosphate hydrogen

NAG: N-acetylglucosamine

NANA: N-acetylneuraminic acid

NBS/LRR: nucleotide-binding site/leucine-rich repeat

NLRs: nucleotide-binding oligomerization domain-like receptors

NMEC: neonatal meningitis *Escherichia coli*

NOD1: nucleotide-binding oligomerization domain-containing protein 1

NOD2: nucleotide-binding oligomerization domain-containing protein 2

NOX1: nicotinamide adenine dinucleotide phosphate hydrogen oxidase 1

NOXO1: NADPH oxidase organizer 1

NSAID: nonsteroidal anti-inflammatory drug

OMP: outer membrane protein

OMV: outer membrane vesicles

PAPS: 3′-phosphoadenosine-5′-phosphosulfate

PGE2: prostaglandin E2

PI3K: phosphoinositide 3-kinase

PRRs: pattern recognition receptors

RIP2/RICK: kinase receptor interacting protein 2

RLRs: retinoic acid-inducible gene-I-like receptors

ROS: reactive oxygen species

SBA: secondary bile acids

SCFA: short chain fatty acid

SEPEC: sepsis-associated *Escherichia coli*

SULTs: sulfotransferases

SUMO: small ubiquitin-like modifier

Tg: transgenic

TLRs: Toll-like receptors

TRAM: TRIF-related adaptor molecule

UC: Ulcerative colitis

UDP-GlcNAc: uridine diphosphate N-acetylglucosamine

uhrf1: ubiquitin-like protein containing PHD and RING finger domains 1

ULK1: unc-51-like kinase 1

UMP: uridine monophosphate

UPEC: uropathogenic *Escherichia coli*

UT: untreated

UTP: uridine triphosphate

UVRAG: UV irradiation resistance-associated gene

WT: wild-type

ZO: zonula occludens

List of Figures

List of Tables

Chapter 1: Introduction

Overview of IBD

Inflammatory bowel disease (IBD) is a broad term for chronic intestinal disorders, with the two main types being Crohn's disease (CD) and ulcerative colitis (UC). The difference between CD and UC is based on the region of the gastrointestinal tract (GI) that is impacted. Inflammation experienced anywhere throughout the GI tract is referred to as Crohn's disease, whereas inflammation that occurs predominantly in the colon is termed ulcerative colitis (Fig. 1-1) [1]. IBD is a major problem in the United States and in other industrialized nations [2]. It is estimated that over 1.5 million residents in the USA and 2.5 million in Europe have IBD, and the number of cases in low-incidence areas is expected to keep rising [3]. IBD is most frequently observed in genetically susceptible adults under the age of 30, however the disease can also develop in pediatric and geriatric populations [4].

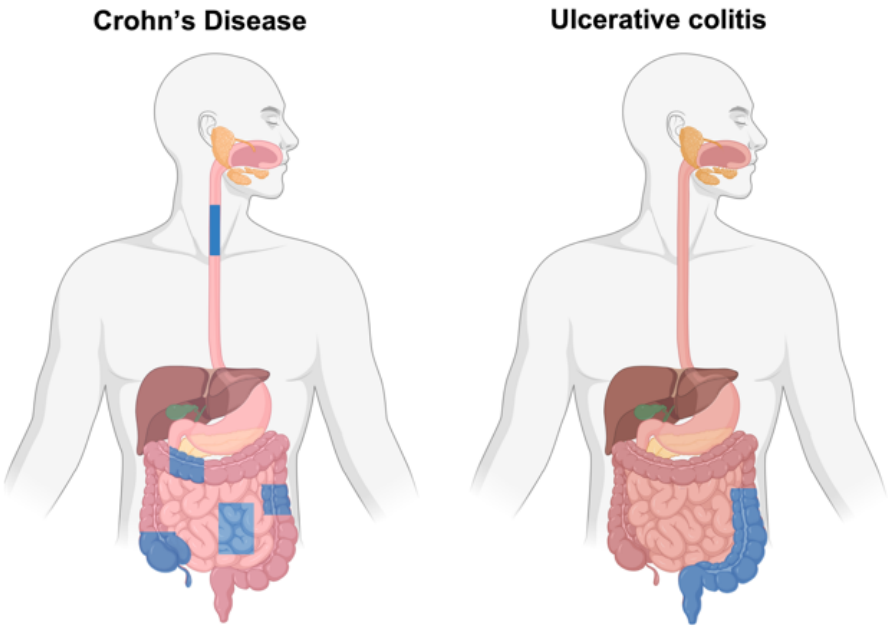

Figure 1-1. Crohn's disease and ulcerative colitis affect different regions of the intestine.

Inflammation (blue) may occur anywhere along the gastrointestinal tract in patients with Crohn's disease. However, patients with ulcerative colitis predominantly experience inflammation (blue) in the colon. Image was created with BioRender.

The common symptoms of CD and UC are diarrhea, mucus in the stool, abdominal pains, bowel obstruction, intestinal bleeding, and in some cases weight lossv[5]. Some patients may experience mild symptoms of the disease, but others experience recurrent episodes that can require surgical treatment [6]. Furthermore, inflammation associated with IBD can increase the risk of colorectal cancer [7]. There is currently no cure for IBD and treatment is based on symptom control with anti-inflammatory drugs, immune suppressors, and antibiotics [8]. Unfortunately, not all patients are responsive to treatment and prolonged exposure to immunosuppressants can increase the risk of cancer [9]. Studies suggest that 70% and 25% of patients diagnosed with CD or UC, respectively, will undergo partial or complete intestinal removal [10, 11]. Patients with UC that are unresponsive to medications will often undergo J-pouch surgery to remove the affected colon and rectum [12].

The exact cause of IBD is unknown, but the disease is modulated by various elements including host genetics, intestinal microbiota, and environmental factors [13]. To date studies suggest that IBD results from a hyperinflammatory immune response to intestinal microbes that is triggered by abnormal antimicrobial responses in genetically susceptible hosts. Hallmarks of IBD include a damaged intestinal epithelial barrier, defects in microbial recognition and elimination by immune cells, intestinal dysbiosis, and chronic intestinal inflammation [14].

Components of intestinal barrier and the innate immune system

A functional intestine relies on an intact intestinal epithelial barrier to regulate nutrient absorption and to mediate communication between the host and the environment. The intestinal epithelium maintains intestinal homeostasis by forming a

boundary between luminal microbes and the underlying host immune cells (Fig. 1-2) [15]. The intestinal barrier is made of an outer mucus layer, antimicrobial proteins (AMPs), immunoglobulins (Igs), a single layer of intestinal epithelium, and the lamina propria where the immune cells reside [16]. Changes to structural components within the intestinal barrier may compromise its protective role.

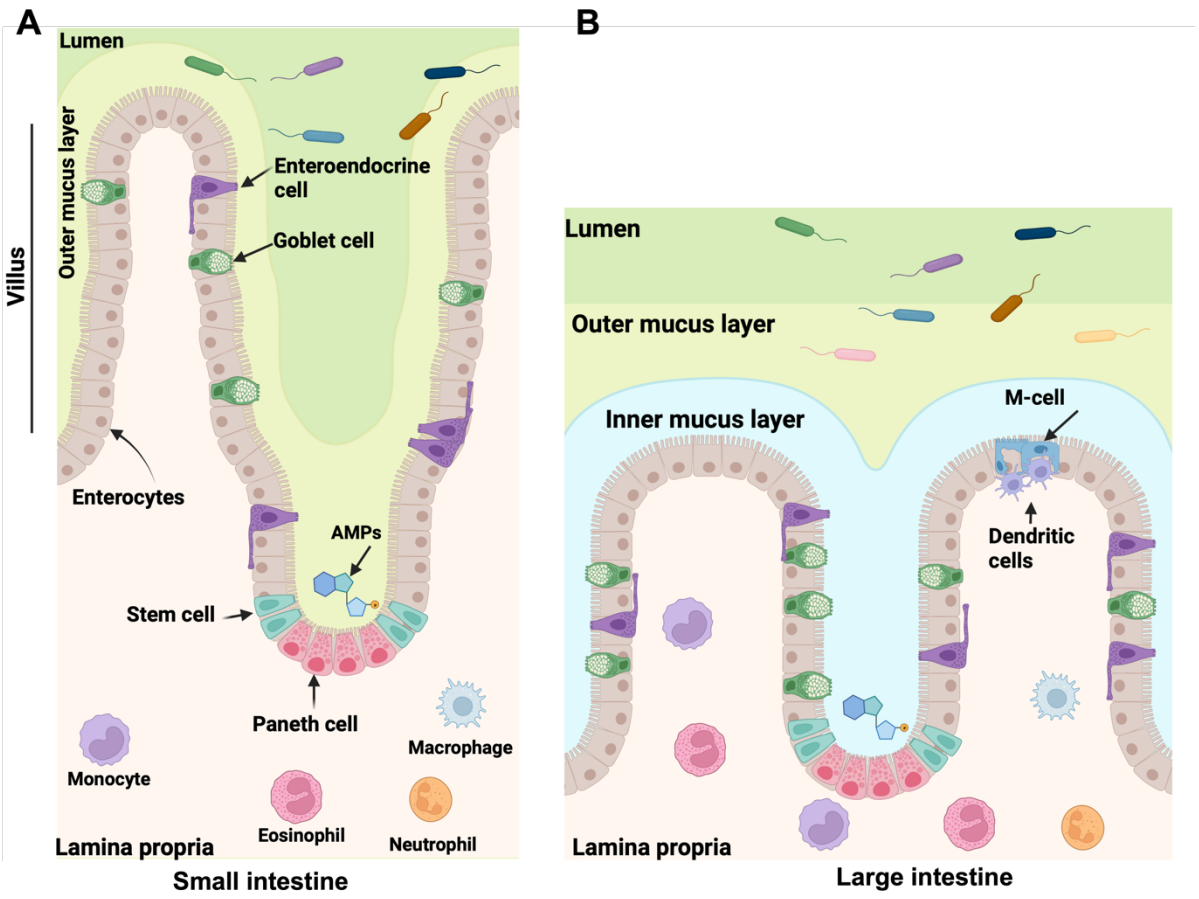

Figure 1-2.The large intestine is composed of two mucus layers.

The intestinal barrier consists of an outer mucus layer (light green), antimicrobial proteins (AMPs), the intestinal epithelial cell layer, and the lamina propria (bottom pink area) where the immune cells reside. The immune cells include monocytes (purple), eosinophils (pink), neutrophils (orange), and macrophages (blue). The intestinal epithelium is composed of enteroendocrine cells (purple), enterocytes (brown), stem cells (cyan), Paneth cells (dark pink), M-cells (blue), and goblet cells (green). The small intestine **(A)** has a single mucus layer, while the large intestine **(B)** has an inner (blue) and outer mucus layer. Intestinal microbes (colorful rods) primarily colonize the lumen (green) and outer mucus layer (light green). Image was created with BioRender.

The intestinal mucus layer

The intestinal mucus layer is composed the mucins, MUC5B, MUC6 and MUC2, that are secreted by goblet cells, however MUC2 is the predominant mucin expressed throughout the gut [17]. This mucus layer acts as the first line of defense against external molecules and the microbiota by limiting the direct contact of luminal contents from the underlying epithelium [18]. Intestinal mucus is hypothesized to consist of approximately 95% water, 0.5-5% glycoproteins, and 1% free proteins, such as AMPs and Igs [19]. The high water and glycoprotein contents create the viscous mucus texture that lubricates the epithelium and facilitates the clearance of the resident bacteria [20, 21].

The epithelium of the small intestine is protected by a single outer loose mucus layer, whereas the epithelial cells of the stomach and colon are covered by two mucus layers (Fig. 1-2) [22]. The first inner mucus layer of the colon is a thin sterile layer that is tightly adhered to the epithelium and the second layer is a thicker outer layer that has loosely distributed mucus [22]. Although the inner and outer layers have a similar protein composition, the outer layer is thought to expand in volume after bacterial proteolytic cleavage within the cysteine-rich regions of MUC2 [23]. Unlike the inner layer, the outer layer is in direct contact with the microbiota and serves as a nutrient and colonization source for the resident bacteria [23]. Further, it is hypothesized that the mucus layer of the small intestine is thinner to facilitate nutrient absorption and thicker in the colon because bacteria reside in there for longer time periods [22, 24].

The mucin backbone is composed of four von Willebrand D domains within the N- and C- terminals and a central PTS domain that has multiple repeats of proline,

threonine, and serine residues (Fig. 1-3) [22]. Mucin polymers are stabilized by disulfide bonds formed within the von Willebrand D domains and are protected against bacterial degradation because the PTS domains are highly O-glycosylated [19]. O-glycosylation occurs in the Golgi apparatus and promotes the binding of water to form a viscous protein [19] . Other post-translational modifications that fortify the MUC2 backbone against microbial degradation include the addition of galactose, fucose, sialic acid, sulfate, and N-acetylgalactosamine [25]. These residues dictate the overall size and charge of MUC2 [25].

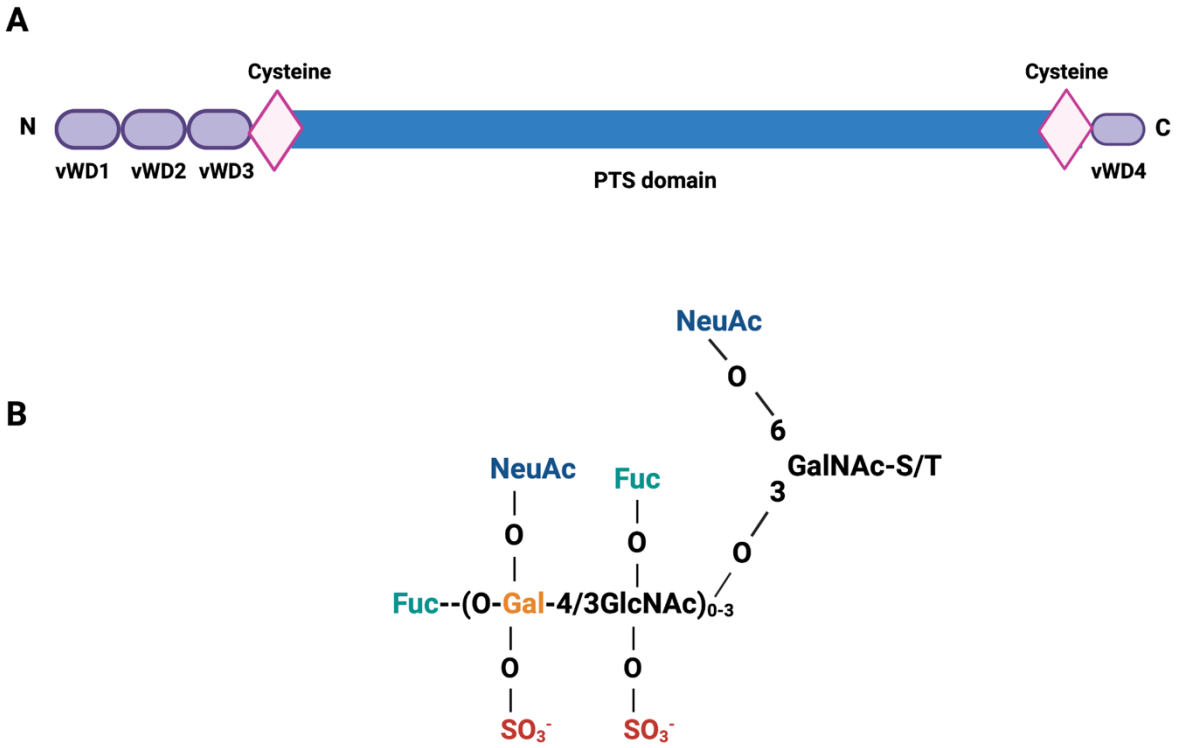

Figure 1-3. The MUC2 backbone is composed of a PTS domain and oligosaccharides.

(**A**) The N- and C- terminus of MUC2 have 3 and 1 von Willebrand D domains (purple), respectively. The MUC2 backbone is composed cysteines (pink) and a central PTS domain (blue) that has multiple repeats of proline, threonine, and serine residues. (**B**)The addition of galactose (Gal, orange), fucose (Fuc, green), sulfate (SO_3-,red), and N-acetylgalactosamine (GalNAc) fortifies the MUC2 backbone. Image was created with BioRender.

The epithelium

Underneath the mucus layer is the single layered intestinal epithelium that contains specialized cells. In the small and large intestine, the columnar epithelial cells are arranged in folds to increase the surface area (Fig. 2) [26]. The small intestine contains a higher number of folds that form finger-like projections, termed villi, to aid in nutrient absorption [26]. Within the villi are invaginations, knowns as crypts, that house the pluripotent stem cells that give rise to absorptive enterocytes, enteroendocrine cells, goblet cells, Paneth cells, and microfold cells (M cells) [27]. The absorptive enterocytes and colonocytes make up most of the intestinal epithelium in the small intestine and the colon, respectively [28]. The enteroendocrine cells are found throughout the whole intestine and secrete hormones that regulate appetite, digestion and mucosal immunity [29]. Paneth cells contain granules filled with AMPS, including lysozymes and α-defensins, and reside in the small intestine within the crypts of Lieberkühn [30]. Within the crypts reside the intestinal stem cells, that are regulated and protected by growth factors and AMPs, respectively [31]. Lastly, the M-cells are also found in the small and large intestine, specifically in a region termed the follicle-associated epithelium (FAE) [32]. The FAE covers the luminal surface of the gut-associated lymphoid tissue which includes, Peyer's patches, cecal patches, and colonic patches [32]. In the FAE, the M-cells regulate mucosal immune responses by transporting luminal antigens to the underlying gut-associated lymphoid tissues [32].

Passage of ions and large molecules through the intestinal epithelium is regulated by tight junctions, adherens junctions, and desmosomes (Fig.1-4) [33]. Tight junctions are found in the apical portion of the epithelium and maintain the cells'

polarity [34]. Tight junctions include zonula occludens 1 (ZO-1, ZO-2), claudins, and occludins [35]. The adherens junctions stabilize the cell-to-cell adhesions through cadherins and catenins [36]. Desmosomes are found near the basal layer of cells and link intermediate filaments to the cells' surface [37]. The desmosomal proteins include desmogleins and desmocollins [38]. In general, tight junction proteins are involved in the formation of the barrier and/or selective channels or pores, whereas desmosomes and adherens junctions mainly serve as communicators between neighboring cells [39, 40].

The lamina propria

The lamina propria is composed of loose connective tissue and separates the intestinal epithelial cells from the underlying smooth muscle cells [41]. The architecture of the lamina propria in the small intestine and the colon is similar and it is composed of elastin, collagen, lymphatic vessels and myofibroblasts [41]. Further, the lamina propria is well known to contain many types of immune cells both from the innate and adaptive immune systems. The most abundant immune cells found on the basal side are lymphocytes, monocytes, eosinophils, and plasma cells [42][43]. Macrophages, neutrophils, and dendritic cells are less abundant under homeostatic conditions and are primarily distributed along the superior part of the lamina propria, close to the tips of the villi [44, 45].

Cells of the innate immune system

The innate immune system consists of macrophages, neutrophils, dendritic cells, mast cells, eosinophils, basophils, and natural killer cells [46]. Neutrophils,

macrophages, and dendritic cells are classified as phagocytes because they engulf and remove microbes, foreign materials, and dead cells [47]. In addition to their phagocytic activity, neutrophils also have granules that contain enzymes that kill bacteria and fungi after ingestion [48]. All of these phagocytes have pattern recognition receptors (PRRs) that recognize and bind pathogen-associated molecular patterns (PAMPs) on microbes [47]. And like neutrophils, intestinal epithelial cells also have PRRs [49]. The PRRs families include the nucleotide-binding oligomerization domain-like receptors (NLRs), Toll-like receptors (TLRs), the retinoic acid-inducible gene-I-like receptors (RLRs), the C-type lectin receptors (CLRs), and the AIM2-like receptor (ALR) [50]. Proper expression of these PRRs is imperative for maintaining intestinal homeostasis.

Damage in the intestinal barrier during IBD

Forty to fifty percent of IBD patients with active disease are estimated to experience intestinal permeability (Fig. 1-4) [51]. To date it is unclear whether intestinal permeability occurs prior to inflammation/disease or if preexisting inflammation leads to intestinal permeability. There are case studies of individuals with increased intestinal permeability who have not been diagnosed with IBD and these cases suggest that a dysfunction in gut permeability occurs prior to disease [52, 53]. However, other studies suggest that treatment of cultured cells and patients with drugs that inhibit the proinflammatory cytokine, tumor necrosis factor alpha (TNF-α), alleviates intestinal permeability, suggesting that inflammation triggers intestinal permeability [54, 55].

Damage to the mucus layer

The thickness of the mucus layer of CD patients is similar and/or thicker than that of healthy controls [56, 57]. However, the amount of MUC2 protein (but not mRNA) is increased and the quality of the mucus is diminished [58]. These changes can be attributed to a decrease in post-translational sulfation and glycosylation [58, 59]. Patients with UC have been observed to have decreased thickness in colonic mucus layer and a decrease in goblet cell numbers [57, 60]. The difference in the thickness of the mucus layer maybe explained by the observation that *hath1* and *Krüppel-like factor 4*, two goblet cell differentiation factors, are actively induced in CD, but not UC [57, 61]. Although it is unclear whether mucin sulfation is reduced in CD, multiple studies have shown that the mucins of biopsy samples from UC patients have less sulfation than healthy controls [62, 63].

The sulfation of MUC2 protects against rapid microbial degradation of the outer mucus layer and has a protective function in mice with experimentally induced colitis [64, 65]. It is hypothesized that the sulfation of mucin confers negative charges that prevent excessive glycan degradation, increases the retention of positively charged AMPs, and increases its viscosity [62, 66, 67]. Mucin sulfation is catalyzed by sulfotransferases (SULTs) that transfer a sulfonate group from the universal sulfate donor 3′-phosphoadenosine-5′-phosphosulfate (PAPS) to an oligosaccharide in the mucin backbone, such as N-acetylglucosamine or galactose [68]. Moreover, SULTs also catalyze the sulfation of glycolipids, such as sulfatide and glycosaminoglycans, including heparin sulfate and chondroitin sulfate [69, 70].

Several studies have associated loss of SULTs with intestinal inflammation [71, 72]. For example, the expression of galactosylceramide 3'-sulfotransferase is reduced

in biopsy samples of individuals with gastritis and mice that do not express the colonic N-acetylglucosamine 6-O-sulfotransferase-2 (GlcNAc6ST-2) have less MUC2 sulfation and are more susceptible colitis [65, 69]. In addition, the levels of sulphotransferase 2A1 are also decreased in patients with active CD [73]. Although the exact mechanism by which the expression of SULTs is regulated are unknown, it appears that microbial and host factors may be responsible for SULT activity and mucin sulfation. Croix, et al. showed that addition of flagellin, interleukin 13 (IL-13), and TNF-α to the human colonic goblet cell line LS174T induced the expression of carbohydrate sulfotransferase 5 (CHST5) and galactose-3-O-sulfotransferase 2 (GAL3ST2) [74]. The expression of GlcNAc6ST-2 and mucin sulfation has also been shown to be induced after administration of butyrate to mice colonic epithelial cells and mice [65]. Further, sulfatases (enzymes that remove sulfate groups) of *Bacteroides thetaiotaomicron* are known to degrade colonic mucus and decrease the binding of *Escherichia coli* to the mucus layer [75, 76]. These reports suggest that although CD patients have a normal or thick mucus layer, it might not be as protective if post-translational modifications are lacking.

Damage to Paneth cells

Although Paneth cells are mainly found in the small intestine, individuals with IBD have been observed to have Paneth-like cells in the colon that secrete the AMP, human defensin 5 [77]. Chronic inflammation is thought to induce metaplastic Paneth cells in the large intestine to help defend against excessive bacterial invasion [78]. In contrast, the ileum of CD patients with active disease is known to have decreased human defensin 5 and human defensin 6 levels compared to healthy controls [79].

Abnormalities in Paneth cells have been attributed to genes that regulate multiple pathways. For example, the secretion of AMPS by granules within Paneth cells is reduced in mice with a hypomorphic *autophagy-related 16-like 1* (*ATG16L1*) gene and in CD patients carrying a mutation in the gene encoding the nucleotide-binding oligomerization domain-containing protein 2 (NOD2) protein [80, 81]. In addition to α-defensins, Paneth cells also secrete a lectin encoded by the *human intelectin-1 (ITLN1)* gene that binds acyclic vicinal (1,2)-diol residues on microbial cells [82]. Mutations in *ITLN1* have been identified by genome-wide association studies (GWAS) as markers of CD susceptibility and mice with null mutations in this gene are susceptible to chemically induced colitis [83]. Although the mechanism by which *ITLN1* confers protection against colitis is unknown, it is hypothesized that this lectin is important for the activation of the innate immune response upon microbial binding [83, 84].

Aside from genetic predisposition to malfunctional Paneth cells, environmental factors such as smoking, early-life antibiotic exposure, and vitamin D deficiency have also been found to negatively affect these cells in individuals with CD [85]. Berkowitz, el al. showed that intragastric administration of cigarette smoke condensate damages the ileum of mice [86]. The mechanism behind ileal damage was attributed to decreased secretion of AMPs by Paneth cells and dysbiosis of the fecal bacterial population [86]. Retrospective studies have shown that recurrent antibiotic exposure in children and adolescents under 18 years old is a risk factor of CD in susceptible hosts [87, 88]. Observations in mice have led to the speculation that early-life antibiotics alter the intestinal microbiota that are essential for the production of AMPS,

and for the maturation of the innate immune system [89, 90]. Other mice studies have shown that vitamin D deficiency in combination with high fat diets suppresses the production of α-defensin 5 and MUC2, and that vitamin D supplementation alleviates gut permeability [91].

Damage to tight junctions

As mentioned above, tight junctions control the integrity of the epithelial barrier. There are at least 27 different claudins in humans that are involved in the movement of ions, initiation of tight junction formation, and/or strengthening or weakening the epithelial barrier (Fig. 1-4) [92-94]. Different claudin family members affect the tension between one another to modulate the intestinal permeability [95]. Thus, a leaky or tight barrier is determined by the ratio of claudins that seal the paracellular intestinal barrier versus claudins that induce channel formation [96]. Claudins that maintain a tight barrier are claudin-1, -3, -4, -5, -6, -8, -12, -18, and -19, whereas the claudins that promote a leaky gut are claudins 2 and 15 [97-100] . In IBD, the expression of claudin -1, -2, and -18 is generally increased while the expression of the genes encoding claudin -3, -4, -5, -7, -8, and -12 is decreased [100, 101]. The tight junction protein, ZO-1, is also reduced in biopsy samples from IBD patients and has been shown to be critical for mucosal healing, but indispensable for barrier function [102, 103]. Specifically, ZO-1 regulates the mitotic spindle during cell division and failure to do so results in increased apoptosis in ZO-1 knockout mice [103].

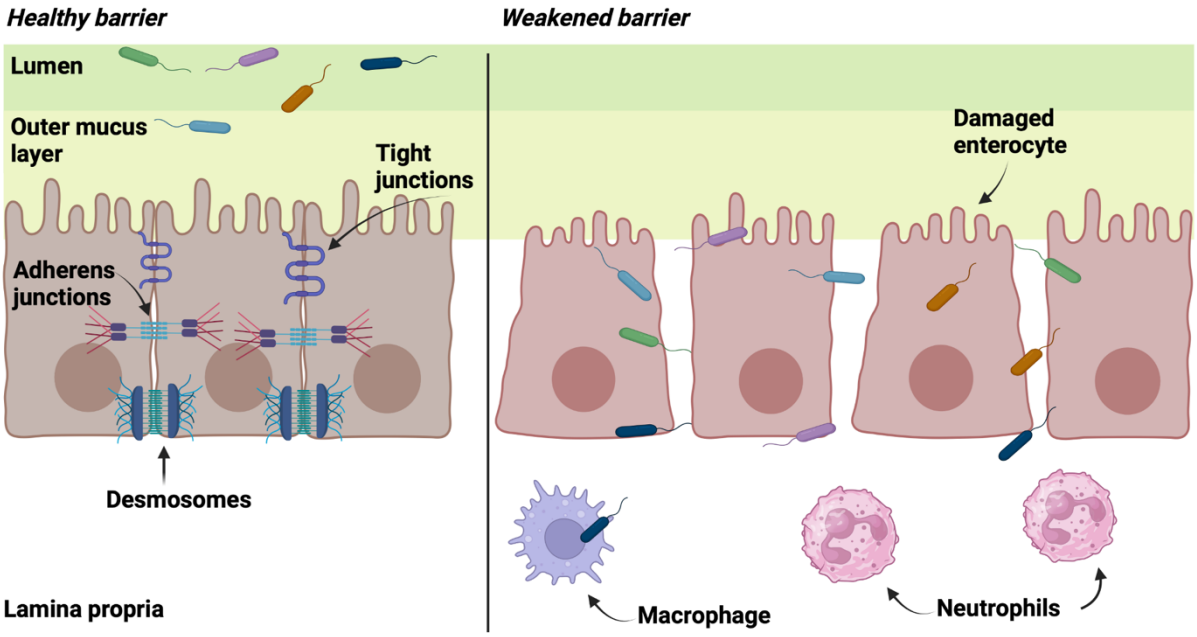

Figure 1-4. Loss of the intestinal epithelial barrier integrity facilitates intestinal inflammation.

The epithelial barrier is maintained by tight junctions, adherens junctions, and desmosomes. Decreases in the production of tight and adherens junction proteins may lead to intestinal permeability by weakening the barrier. A weak barrier (red enterocytes) fails to keep luminal bacteria (colorful rods) away from the lamina propria (bottom, white area) and away from immune cells. The interaction of the bacteria with macrophages and neutrophils contributes to intestinal inflammation in a susceptible host. Image was created with BioRender.

As previously mentioned, it is not clear whether changes in the production of proteins involved in tight junctions lead to chronic intestinal inflammation or if intestinal inflammation modulates the function of tight junctions. However, the expression of genes encoding claudin 2 has been shown to be increased by the proinflammatory interleukins (ILs) IL-13 and IL-6, and decreased by butyrate [104-106]. Thus, it is possible that continuous inflammation may change the function of tight junctions and induce epithelial damage through increased apoptosis and ulcerations.

Damage of the innate immune responses involved in microbial recognition

Failure of the first line of defense to keep the microbiota from invading the lamina propria results in increased immune cell activation and inflammation. In a non-diseased host, the innate immune system is capable of clearing bacteria that breach the epithelium and regulating the inflammatory response. However, individuals with IBD often have abnormal innate immune responses due to mutations in susceptible genes (Fig. 1-5) [107]. As a result, some essential immune cells fail to eliminate invasive or pathogenic bacteria, while other cells remain hypersensitive to the microbiota and fail to shut off proinflammatory pathways [107].

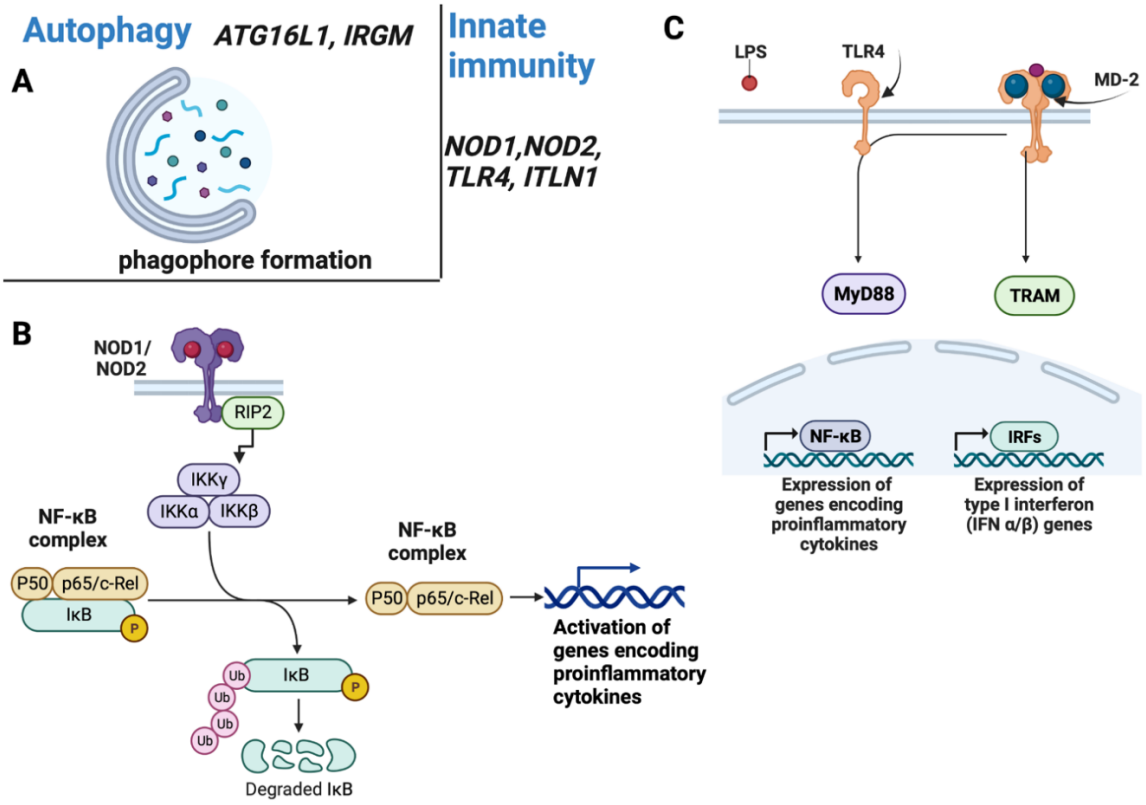

Figure 1-5. List of commonly affected genes in patients with IBD that lead to defective microbe sensing and elimination.

(A) Mutations in the *ATG16L1* and *IRGM* genes interfere with phagophore formation and autophagy. Mutations in the genes involved in innate immunity, (**A)** *NOD1*, *NOD2* and **(B)** *TLR4* and *ITLN1*, interfere with the activation of the NF-KB complex, and subsequent activation of proinflammatory and/or type 1 interferon genes. **(A)** Upon recognition of their respective target, the NOD1/NOD2 receptors oligomerize and recruit RIP2. Active RIP2 recruits the IKK complex that phosphorylates and ubiquitinates the NF-κB inhibitor-α, IKB, and released NFκB translocates into the nucleus to induce the transcription of genes encoding proinflammatory cytokines. **(B)** Binding of LPS to the TLR4/MD-2 complex triggers the homotypic interaction of 2 TLR4 receptors, followed by activation of MyD88 or TRAM pathway. Signaling in the

MyD88 or TRAM pathway, leads the activation of NFκB activation or the synthesis of type I interferons, respectively. Image was created with BioRender.

Autophagy

There are three pathways that mediate bacterial clearance and in which mutations have been identified that lead to IBD susceptibility. One of these pathways is macroautophagy, hereafter referred to as autophagy. Autophagy is a highly conserved process in eukaryotes by which damaged organelles, non-functional proteins, apoptotic bodies, and microbes are degraded and recycled [108]. The processes of autophagy are as follows: initiation, phagophore formation, phagophore elongation, autophagosome maturation/closure, and degradation (Fig. 1-6) [109]. Briefly, the inactivation of the regulator of cellular metabolism, mTOR, initiates autophagy through the formation of the autophagosome, which is mediated by a large complex of 18 ATG proteins and LC3-I lipidation [110]. When lipidated LC3-I becomes LC3-II, LC3-II recruits ubiquitinated p62 to tag cells for degradation [110]. During the final stages, the autophagosome fuses with lysosomes and the degraded products are released into the cytoplasm [111].

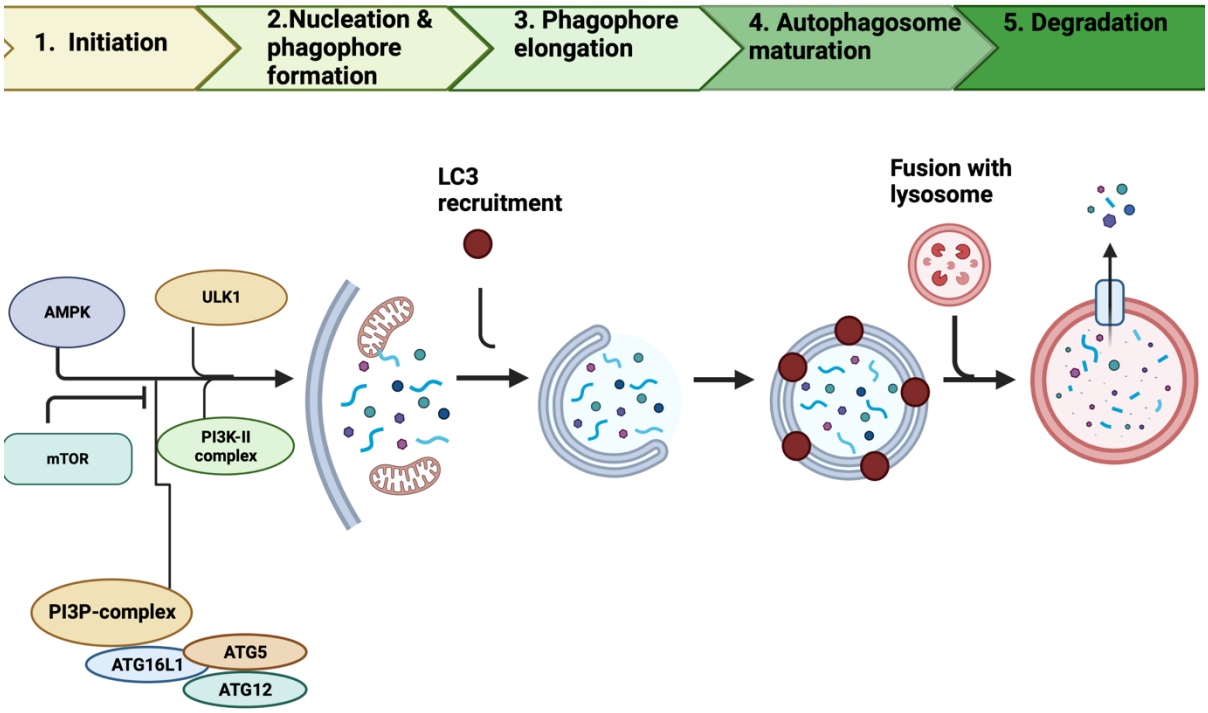

Figure 1-6. Schematic diagram of autophagy induction and completion.

Inactivation of the regulator of cellular metabolism (mTOR) and activation of AMP-activated kinase (AMPK) initiates the process of autophagy. During autophagy, cytoplasmic contents are engulfed by double membranes that are formed through 5 steps: (1) initiation, (2) phagophore formation, (3) phagophore elongation, (4) autophagosome maturation/closure, and (5) degradation. During the initiation step, ATG proteins assemble in the PI3KIII nucleation complex, Unc-51-like kinase 1 (ULK1) initiation complex, and the PI3P-binding complex. These complexes aid phagophore formation by facilitating the recruitment of the ATG conjugation system. In the ATG conjugation system, ATG12 binds ATG5 and ATG12-ATG5 bind ATG16L1. The ATG12-ATG5-ATG16L1 complex mediates LC3-I lipidation mediating the conjugation of phosphatidylethanolamine to LC3-1 form LC3-II. LC3-II is then incorporated into the autophagosome membrane during the elongation process and

recruits ubiquitinated p62 to tag cells for degradation. Following phagosome maturation, the autophagosome fuses with lysosomes and the degrades the internalized contents. Image created with BioRender.

The first autophagy gene that was linked to CD and shown to have single nucleotide polymorphisms by GWAS was *autophagy-related 16-like 1* (*atg16l1*) [112]. ATG16L1 is part of the large 18 protein complex required for autophagosome formation and lipidation of LC3-I to target membranes [113]. Crohn's disease-associated *atg16l1* mutations can occur in the coiled-coil domain, the WD domain, and/or the 3' untranslated region [114]. The most well studied variant is ATG16L1^{T300A}, which contains a point mutation in the WD domain [115]. Human epithelial cells expressing ATG16L1^{T300A} fail to clear intracellular bacteria and display increased secretion of proinflammatory cytokines [116]. Specifically, the point mutations in the WD domain increase caspase 3-mediated degradation of ATGl16L1 and prevent the association of the WD domain with transmembrane protein 59 that is required for labelling and targeting the compartment for autophagic degradation [115, 117]. In addition, ATG16L1 is also essential for the formation of the ATG12-ATG5-ATG16L1 complex, which generates LC3-II to tag the cells for degradation [113].

Autophagy and other immune response pathways converge to suppress the production of excess proinflammatory proteins. For example, Atg16l1-deficient macrophages secrete high levels of proinflammatory cytokines in response to LPS binding to Toll-like receptor 4 (TLR4) [118]. Furthermore, germ-free mice hypomorphic for *atg16l1* have increased type I interferon (an antiviral factor and member of a different pathway) signaling compared to the wild-type groups [119];[120].

Mutations in the *immunity-related GTPase M* (*irgm*) gene are also linked to CD susceptibility and to altered autophagy [121, 122]. IRGM regulates the

phosphorylation of autophagy regulators to initiate phagophore formation and mediates the interaction of ATG16L1 with NOD2 to initiate autophagy [123]. Further, IRGM is also hypothesized to be essential for the maturation of the phagosome, as it has been observed to form complexes with the regulator of autophagic maturation, UV irradiation resistance-associated gene (*uvrag*), and to displace proteins that inhibit maturation [123]. The CD-associated variants of *IRGM* have single nucleotide polymorphisms within the upstream region of the gene, which suggest that mutations in the regulatory region may affect transcription of this gene [124].

NOD2 signaling pathway

The second pathway is comprised of a family of membrane-bound receptors known as nucleotide-binding site/leucine-rich repeat (NBS/LRR) proteins [125, 126]. The n*ucleotide-binding oligomerization domain-containing protein 1* and *2* (*NOD1, NOD2*) genes encode proteins expressed by macrophages, dendritic cells, and epithelial cells [127]. Moreover, NOD2 is also expressed in Paneth cells [128]. NOD1 and NOD2 recognize *meso*-diaminopimelic acid (*meso*-DAP) and muramyl dipeptide (MDP), respectively in the peptidoglycan of Gram-positive and Gram-negative bacteria [129]. It is hypothesized that upon recognition of MDP, NOD1/NOD2 oligomerize and recruit the kinase receptor interacting protein 2 (RIP2/RICK)[129]. Active RIP2 recruits the IκB kinase (IKK) complex that phosphorylates and ubiquitinates the NF-κB inhibitor-α, IKBα, and released NFκB translocates into the nucleus to induce the transcription of genes encoding proinflammatory cytokines such as IL-8, TNF-α, and IL-1β (Fig. 1-5 B) [130]. NOD2 also plays an important role in autophagy through recruitment of ATG16L1 to the plasma membrane of target cells

[131]. Specifically, infected cells expressing the NOD2 variants linked to CD do not recruit ATG16L1 to the plasma membrane and fail to induce autophagy [131].

NOD2 is the first IBD-risk gene identified by transmission disequilibrium tests and mutations in this gene have been observed in 30-50% of CD patients [132]. There are three common *NOD2* gene variants (R702W, G908R, and L1007fs) and other minor variants with mutations in the LRR binding domain [133]. It is not clear how mutations in *NOD2* lead to CD pathogenesis, but there are 3 current hypotheses. The first and most common hypothesis is that mutations in the LRR binding domain code for a hypomorphic protein that does not activate the NFκB pathway upon MDP exposure [134]. Thus, it is possible that failure to remove bacteria leads to a hyperinflammatory response through NOD2-independent pathways [135]. The second hypothesis is that NOD2 variants cannot recruit ATG16L1 to the plasma membrane of infected epithelial cells, and as a result bacterial clearance is limited due to impaired autophagy [136, 137]. The last hypothesis is supported by minor evidence that NOD2 limits the activation of NFκB after the TLR2 pathway has been initiated and proposes that NOD2 mutations fail to limit the inflammation response through NFκB inhibition [138, 139]. Further, it is also hypothesized that having more than one NOD2 variant increases the chances of an individual developing CD. However, there are some people who are homozygous for NOD2 mutations and are not diseased [140]. Thus, this implies that other environmental factors may contribute to the pathology.

TLR4 signaling pathway

Mutations in the members of the Toll-like receptor 4 (TLR4) signaling pathway are also linked to CD and UC [141]. There are 13 types of TLRs in mammals and each recognize different bacterial components [142]. TLR4 associates with the extracellular molecule, myeloid differentiation factor 2 (MD-2), to recognize lipopolysaccharide (LPS) of Gram-negative bacteria [143]. TLR4 is expressed on the cell surface of macrophages and in the Golgi apparatus in intestinal epithelial cells [143]. Like NOD2, TLR4 is also a transmembrane receptor with leucine-rich repeats in the extracellular region [144]. The binding of LPS to the TLR4/MD-2 complex triggers the homotypic interaction of 2 TLR4 receptors [145]. This leads to the initiation of either the myeloid differentiation factor 88 (MyD88) or the TRIF-related adaptor molecule (TRAM) pathway [146]. Signaling in the MyD88 pathway results in the activation of NFκB and proinflammatory cytokine production, while the activation of TRAM pathway results in production of type I interferon (Fig.1-5 C) [146]. The expression of gene encoding TLR4 has been observed to be increased in CD and UC patients [147]. The increased synthesis of TLR4 in these individuals leads to an increased secretion of proinflammatory regulating proteins such as TNF-α, chemokine CCL2, cyclooxygenase 2 (COX-2), and prostaglandin E2 (PGE2) by macrophages [148]. This is a major problem because the affected epithelium fails to regenerate during constant inflammation [149].

Changes in the intestinal microbiome during IBD

The healthy human intestine contains more than 100,000 trillion microorganisms, with over 1,000 bacterial species that belong to the phyla Actinobacteria, Bacteroidetes, Firmicutes, Proteobacteria, and Verrucomicrobia

[150]. Firmicutes and Bacteroidetes make up 90% of the total bacterial population and indirectly affect gut homeostasis [150, 151].Primarily, these two bacterial phyla aid in the digestion of complex carbohydrates and the production of short chain fatty acids (SCFA) [152]. The three most abundant SCFAs include acetate, butyrate, and propionate[153]. These SCFA are all primarily produced by bacterial fermentation of carbohydrates in the distal colon [153]. Studies suggest that butyrate is the most important SCFA because it is the main energy source of colonocytes, stimulates MUC2 production, facilitates the assembly of tight junction proteins ZO-1, claudin-1 and -4, and inhibits activation of NF-κB in the colon [154-156].

16S rRNA gene sequencing of biopsy samples from patients show that in IBD the diversity of the gut microbiota is reduced, and the microbiome is primarily composed of microbes associated with proinflammatory properties [157-159]. Specifically, patients with CD and UC are reported to have a reduction of 50% and 30% in microbial diversity respectively, compared to healthy controls [160]. Interestingly a lower bacterial diversity is often observed during all stages of UC [161]. This is in contrast to what is observed in CD and J-pouch patients, who display a decrease in bacterial diversity only during the active stages of disease [161]. In IBD the most abundant bacterial phyla are Proteobacteria and Fusobacteria, and the least abundant is Firmicutes [162]. Further, butyrate concentrations and butyrate-producing bacteria including the *Faecalibacterium*, *Roseburia*, and *Ruminococcus* genera (all of which are members of the firmicutes phyla) are decreased in IBD patients [163-165]. In addition, patients with J-pouch surgeries have also been found to have less lithocholic acid and deoxycholic acid, two secondary bile acids (SBA) important for

colon homeostasis, and a decreased amount of SBA-producing *Ruminococcaceae* [166].

Colitis studies in mice show that enteric bacteria influence IBD pathogenesis. For example, mice with null mutations in the gene that codes for the anti-inflammatory cytokine, IL-10, develop colitis only in the presence known pathogenic bacteria [167]. Further, transgenic rats with the human major histocompatibility complex class I allele, *human leukocyte antigen B27* (*HLA-B27*), also develop intestinal inflammation only in the presence of the gut microbiota [168]. In both examples the germ-free transgenic rodents do not develop disease even though they are susceptible to intestinal inflammation.

Intestinal dysbiosis can be defined as loss of beneficial microbes and expansion of microbes that can contribute to a disease state [169]. The assessment of dysbiosis includes the identification of alpha and beta diversities and indexes that characterize the state of a disease and/or predict treatment outcomes [170]. Clinical studies show that there is a positive correlation in the pattern of gut dysbiosis and the severity of IBD. Dr. Kugathasan's group showed that a higher degree of gut microbial dysbiosis is positively associated with increased calprotectin levels, a protein biomarker of intestinal inflammation [4]. This study also showed that IBD patients that failed to respond to their treatments (non-responders) had a higher abundance of *Akkermansia* species and *Fusobacterium* species compared to responders [4]. *Fusobacterium* species, such as *Fusobacterium nucleatum,* are common in dental plaque, present in colorectal adenomas, and contributors of UC pathogenesis [171]. Whether *Akkermansia species* are beneficial bacteria in IBD is still a controversy.

Wang, et al. showed that a membrane protein of *A. muciniphila* reduces immune cell recruitment and alleviates intestinal inflammation in mice with chemically induced colitis [172]. However, Ganesh, et al. showed that *A. muciniphila* indirectly exacerbates intestinal inflammation by promoting the survival of *Salmonella typhimurium* in gnotobiotic mice [173].

Among the most abundant families frequently observed in CD and UC are *Enterobacteriaceae*, *Fusobacteriaceae,* and *Pasteurellaceae*, while the least abundant include *Bacteroidales*, and *Clostridiales* [174, 175]. Proteobacteria include the *Enterobacteriaceae*, family which are among the top microbes often identified in CD and UC [176]. Dr. Denson's group proposed a mechanism that associated the depletion of Firmicutes and Bacteroidetes with in an increase in Proteobacteria and showed that this shift in bacterial communities is closely linked to severe mucosal injury [175]. Briefly, they proposed that as the disease progresses the expression of the genes encoding the anti-inflammatory antioxidant apolipoproteinA-I (APOA1) is downregulated, and the expression of the gene encoding the dual oxidase 2 (DUOX2), an enzyme that generates reactive oxygen species (ROS) is increased. As DUOX2 increases, mature enterocytes begin to malfunction and the expression of the gene encoding the immune cell recruitment regulator, chemokine 9 (CXCL9), is upregulated. This generates an environment with high oxidative stress, expansion of Proteobacteria, and depletion of members within the Firmicutes and Bacteroidetes taxa. Altogether these processes result in severe mucosal injuries and epithelial ulceration [175].

Although many microbial species have been identified to be associated with IBD, there is not a single microbe that is known to be the cause of the disease. One pathobiont of the *Enterobacteriaceae* family that is abundantly present in the diseased mucosa of CD and UC is *E. coli.* In fact, *E. coli* has been reported to exceed more than 50% of the total number of bacteria in the mucosa of CD patients [177].

Adherent-invasive Escherichia coli in IBD

The presence of a*dherent-invasive Escherichia coli (AIEC)* has been more commonly reported in inflamed ileal biopsies of CD (55%) and to a lesser extent in the colonic samples associated with UC (35.7%) [178],[179-181]. AIEC is present in approximately 21-63% of CD patients, 0-35.7% in individuals with UC, and in 0-19% of healthy controls [180, 182, 183]. Furthermore, AIEC is hypothesized to be involved in the initial stages of CD and to cause disease relapses, because they are often isolated from lesions in patients with chronic CD as opposed to those in remission[180, 184].

Another reason that AIEC is hypothesized to be involved in the early stage of CD is because they induce infections with similar histopathological patterns to those observed in CD patients. Histological markers of CD include intestinal epithelioid granulomas that are characterized by aggregations of immune cells in small nodules at the site of inflammation [185]. Similarly, AIEC also induce granulomas in blood-derived mononuclear cells and in the colon of Boxer dogs [186-188]. In humans AIEC is reported to cause granulomas along the mucosal surface closer to lumen, whereas in dogs AIEC strains are generally observed to induce granulomas within the mucosa [187-189]. In addition, *E. coli* DNA has been detected in approximately 80% of

granulomas isolated from CD patients and detected in only 10% of non-CD individuals [190].

By definition AIEC adhere to and invade intestinal epithelial cells (IECs), survive inside of macrophages without inducing host cell death, and lack known virulence factors [191]. AIEC LF82 is the first identified strain and is currently used as a reference strain in AIEC- and IBD- associated studies [182]. Another well characterized AIEC prototype strain is NRG857c. Both strains were isolated from the ileum of CD patients and have a fully sequenced genome [192, 193]. Comparative genomics of AIEC LF82 and NRG857c show that both strains contain 35 genomic islands that encode fimbriae proteins, proteins required for capsular polysaccharide biosynthesis, and multidrug resistance efflux pumps that promote their survival in the host [193]. Thus far, it has been a challenge to identify AIEC-specific genetic factors due to their genotypic variability. AIEC LF82 and NRG857c belong to the B2 phylogroup, but other identified AIEC strains are members of the phylogroups A, B1, and D [193]. In general, *E. coli* strains from the B2, and to a lesser extent D phylogroups, are considered pathogenic since they carry more virulence genes than those in groups A and B [194, 195]. AIEC that belong to group A and B1 are generally considered transient strains, because they don't encode most adhesion and invasion genes [195]. Due to a lack in widely conserved genetic markers of AIEC, isolated *E. coli* strains are classified as AIEC by phenotypic analyses based on their ability to adhere to and invade intestine-407 cells, and survive inside of murine and human macrophages [196].

AIEC are most closely related to extraintestinal pathogenic *E. coli* (ExPEC) because both harbor similar virulence genes and both consist of strains that belong to the same phylogroups, A, B1, B2, and D[193, 197, 198]. In general, ExPEC strains do not adhere to epithelial cells of CD patients and most are classified as non-invasive, but there are a few isolates that invade IECs and macrophages [198-200]. Members within the ExPEC group include avian pathogenic *E. coli* (APEC), neonatal meningitis *E. coli* (NMEC), uropathogenic *E. coli* (UPEC), and sepsis-associated *E. coli* (SEPEC) [201]. Some AIEC strains have been found to carry unique virulence genes that set them apart from ExPEC. A study that looked at 36 AIEC isolates from biopsies of CD patients, including AIEC LF82, showed that these clinical strains express genes that regulate capsule synthesis (*k1, k5, kps mt II),* siderophore production (*fyuA)*, host cell invasion (*ibeA*) and serum resistance (*traT*) that set AIEC apart from ExPEC [179]. Furthermore, AIEC contain numerous virulence genes that may mediate their survival inside of a host with IBD (Fig. 1-7).

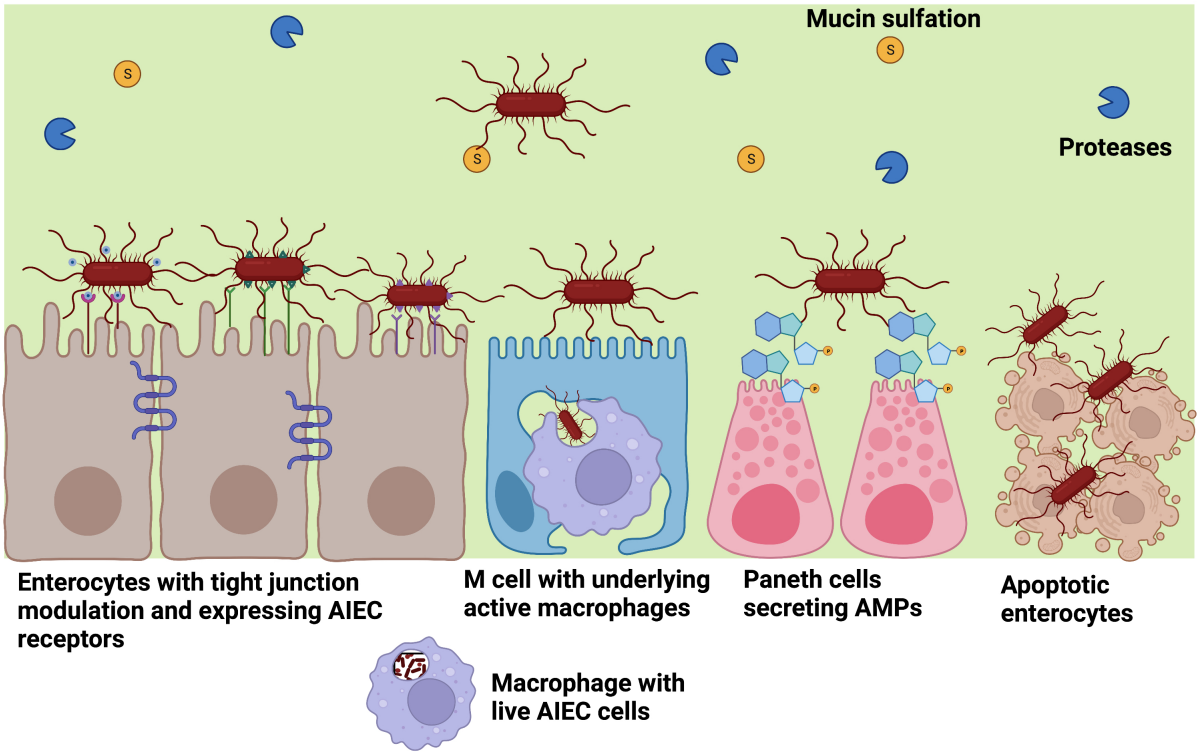

Figure 1-7. Summary of host and microbials factors that promote AIEC colonization and survival in patients with IBD.

Mucin sulfation and proteases secreted by AIEC (red) promote the invasion of AIEC through the mucus layer. AIEC express type 1 pili (short projections) that bind abnormally expressed CEACAM6 receptors (pink) in the ileum of patients. During inflammation, the CHI3L1 receptor (green) is abnormally expressed and binds to the chitin binding domains of the AIEC chitinase ChiA (green triangles). AIEC increase intestinal permeability by modulating the synthesis of tight junction proteins (purple). The binding of AIEC OmpA (purple triangles) to the host endoplasmic reticulum-localized stress response chaperone, Gp96 receptor (purple), induces bacterial internalization. AIEC are internalized through interactions of AIEC long polar fimbriae with M cells. AIEC survive inside of phagolysosomes and replicate inside of

macrophages. Defective AIEC clearance is further modulated by mutations in *atg16L1*, *irgm,* and *nod2,* and abnormal AMP production/secretion. In addition, AIEC also bind to oligomannosidic glycans displayed on the membranes of apoptotic cells through pili. All together these mechanisms may lead to AIEC colonization.

Virulence factors of AIEC used for adhesion to and invasion of epithelial cells

Type 1 pili

Type 1 pili are long hair-like structures on the surface of AIEC cells that bind mannosylated host proteins [203]. The assembly of type 1 pili is mediated by the periplasmic chaperone, FimC, which facilitates the assembly of the secreted pilus subunits and delivers them to the outer membrane assembly platform, FimD [204]. FimC and FimD facilitate the assembly of the other pilin subunits to form a pilus structure that is made of a pilus rod and tip fibrillum [204]. The large pilus rod consists of 500-3,000 subunits of FimA, and the smaller tip fibrillum is made up of two minor subunits FimF, FimG, and the terminal subunit/tip adhesin, FimH [205].

Type 1 pili were among the first identified virulence factors and are known to induce host cell membrane elongations to mediate the invasion of AIEC LF82 into intestinal epithelial cells (IECs) [203]. Upon invasion, infected colonic cells increase the production of nicotinamide adenine dinucleotide phosphate hydrogen (NADPH) oxidase 1 (NOX1) and NADPH oxidase organizer 1 (NOXO1) to generate ROS in response to AIEC infection [206]. Furthermore, this host response is known to be dependent on type1 pili, as ROS production does not occur when cells are infected with LF82Δ*fimA*. These observations suggest that AIEC may induce early inflammation in the ileum of CD patients.

Aside from inducing ROS production upon invasion, AIEC also induce intestinal permeability. A recently published study by Dr. McKay's group showed that IECs infected with wild-type LF82, but not LF82Δ*fimH,* displayed a decrease in barrier function due to AIEC-induced mitochondrial swelling and mitochondrial fragmentation

[207]. In accordance with these findings, two other studies also showed that the infection of cultured intestinal cells with LF82 decreases the integrity of the epithelial cell monolayers through the downregulation and disruption of ZO-1 [208, 209].

Flagella

Type 1 pili alone is not enough to trigger epithelial cell invasion by AIEC. This is corroborated by the observation that expression of type 1 pili in *E. coli* K-12 does not confer invasive properties [203]. AIEC and other pathogens rely on pili and flagellar motility to successfully colonize a host. AIEC LF82 defective in flagella have decreased motility, impaired adhesion and invasion to IECs, induce less host cell inflammation, and fail to induce colitis in mice compared to infections conducted with wild-type strains [210-213].

In *E. coli,* the genes that encode flagellar proteins are assembled in three categories (class I-III) and transcribed in a hierarchical manner to ensure that flagellar proteins are synthesized only when a functional flagellum will be produced [214]. Flagellar synthesis occurs when the class I master regulator, $FlhD_2C_2$, activates the alternate sigma factor, FliA[214]. FliA regulates the expression of the class II and class III genes [214]. Class II genes encode proteins that comprise the flagellar hook and basal body and class III genes encode proteins that comprise the flagellar filament, motor, and chemotactic signaling system [214]. The timing of transcription of the class III genes is tightly regulated by the cytoplasmic anti-sigma factor FlgM, which inhibits the FliA from associating with RNA polymerase until the assembly of the hook and basal body completed [214]. Once the assembly of the class II proteins is completed,

FlgM is secreted out of the cell and allows FliA to initiate the transcription of Class III genes [214, 215].

In AIEC, the expression of flagella and pili are interdependent. Studies show that the synthesis of type 1 pili and flagella are linked by the cyclic dimeric GMP (c-di-GMP) pathway and FliA [210]. In addition to regulating flagellar synthesis, FliA also regulates the transcription of *yhjH,* which encodes a phosphodiesterase that degrades c-di-GMP [216, 217]. The study showed AIEC cannot form type 1 pili when the master regulator of flagellar synthesis, $FlhD_2C_2$, and FliA are deleted. Their proposed model is that activation of $FlhD_2C_2$ results in accumulation of FliA, and FliA promotes the transcription of *yhjH*, which ultimately leads to lower concentrations of c-di-GMP and type 1 pili synthesis [210]. Through this proposed mechanism, AIEC may be able to differentiate when it needs to be motile versus when it is ready to colonize.

The RNA-binding protein Hfq of LF82 is a global regulator of posttranscriptional gene expression and required for the expression of type1 pili and flagella [211]. The deletion of *hfq* in LF82 decreases the invasion of LF82Δ*hfq* into HeLa cells and generates mutants defective in motility, compared wild-type strains [211]. However, it is unclear how Hfq mediates the production of these surface structures. In other *E. coli* strains, Hfq binds small regulatory RNA molecules and regulates stress response pathways, however in AIEC the role of Hfq in mediating virulence is independent of those pathways [211].

Long polar fimbriae and invasion of the brain endothelium protein A

Aphthous ulcers are early inflammatory lesions in CD patients and are predominantly observed in the FAE region within the ileum in the Peyer's patches or

along colonic Patches [218, 219]. As mentioned above, the FAE contains specialized M-cells that uptake and transport luminal antigens to the Peyer's patches and other gut-associated lymphoid tissues [32]. Studies suggest that AIEC may cause aphthous ulcers using long polar fimbriae (LPF). Infection of human monolayer cells and transgenic mice susceptible to IBD with AIEC LF82 results in the transcytosis of wild-type AIEC, but not LPF-negative mutants, across the M cells into the Peyer's patches and in increased intestinal permeability [220, 221]. Interestingly, AIEC isolated from CD patients, but not healthy controls express LFP [220]. The invasion of the brain endothelium protein A (IbeA) invasin also mediates the adhesion and transcytosis of AIEC NRG857c through M-like cells [222]. Wild-type NRG857c, and to a lesser extent NRG857cΔ*ibeA*, cause ulcerations in the caecum and ileum of infected mice [222].

Bile salts and ethanolamine, which are found in the ileum, may serve as AIEC signaling molecules that mediate recognition of the intestinal environment and induction of virulence genes. AIEC cells increase the production of LPF in the presence of bile acids and metabolize ethanolamine to obtain a fitness advantage in the intestine [221, 223-225]. Ethanolamine is abundant in inflamed mucosa and infected macrophages, and can only be metabolized by some pathogenic bacteria, including enterohemorrhagic *E. coli* (EHEC) and AIEC [225]. Bioinformatic analyses indicate that the LPF of LF82 is slightly similar (86%) to LFP of EHEC strain EDL-933 [224]. Since EHEC increases synthesis of LPF in the presence of ethanolamine, it is possible that AIEC also utilizes it as a signaling molecule to increase the production of LPF [226].

The components of long polar fimbriae are encoded in the *lpf* operon. This operon encodes the fimbrial subunits, LpfA, LpfD, and LpfE, the periplasmic chaperone LpfB, and the outer membrane usher LpfC [227]. The LPF tip adhesin is composed of LpfD subunits that bind the extracellular matrix (ECM) components; fibronectin, laminin, and collagen type V in intestinal epithelial cells [227]. During intestinal inflammation, ECM degradation occurs due to an increase in matrix metalloproteinases (MMPs) and ECM remodeling [228]. Thus, it is possible that exposed ECM proteins act as AIEC attachment sites in the disease epithelium of patients with active disease.

Outer membrane proteins

In addition to long surface appendages, AIEC also use outer membrane proteins (OMPs) to adhere to and invade IECs. Transposon mutagenesis experiments have shown that the *yfgL* gene of AIEC encodes for the YfgL lipoprotein, which regulates the release of OmpA and OmpC through outer membrane vesicles (OMVs) [229]. The OmpA of AIEC binds the endoplasmic reticulum-localized stress response chaperone, GP96, to fuse with the ileal mucosa of CD patients [230]. The expression of GP96 may be one of the reasons that AIEC colonize IBD patients, since GP96 is known to be significantly over synthesized in the apical plasma membrane of the ileal mucosa in patients with active and quiescent CD [230].

OmpC has been reported to be present in the mucosa of 37%-55% CD patients and to positively correlate with severe disease outcome [231, 232]. OmpC is a major porin in the outer membrane of *E. coli* and known to be predominantly present during high osmolarity [233]. The expression of OmpC is controlled by the EnvZ/OmpR two

component regulatory system [233]. EnvZ is a cytoplasmic sensor-transmitter and kinase that changes confirmation upon fluctuations in osmolarity and serves as the source of phosphate for the response regulator OmpR to induce transcription of *ompC* and *ompF* [233]. OmpC is essential for successful colonization of AIEC in the intestine because it protects against high osmolarity, a condition that might be encountered during the transition from the stomach to small intestine [234]. In addition, OmpC is also essential for the expression of pili and flagella in AIEC and is hypothesized to indirectly regulate the expression of these surface appendages through the σ^E pathway [234]. However, the exact mechanism by which OmpC and σ^E converge is unknown. Moreover, the response regulator, OmpR, also promotes the growth of AIEC in the presence of sodium deoxycholate (DOC), a major component of bile salts [235]. Survival of AIEC with *ompC* and *ompF* deletions suggest that OmpR mediates DOC tolerance through an unknown mechanism [235].

Another outer membrane protein that regulates the adhesion of LF82 to Intestine-407 cells is the lipoprotein NlpI [236]. AIEC LF82*ΔnlpI* mutants exhibit a 35-fold decrease in adherence and 45-fold decrease in invasion to IECs, compared to wild-type LF82 cells [236]. It is hypothesized that Nlp regulates an important pathway involved in pili and flagellar synthesis because LF82*ΔnlpI* mutants do not express flagella and produce small amounts of pili. However, this mechanism has not been elucidated.

AIEC survive inside of host cells without inducing host cell death

Survival in intestinal epithelial cells

The internalization of AIEC by cultured intestinal cells occurs through elongations of microvillar extensions in an actin-and-microtubule-dependent mechanism [237]. AIEC survive inside of intestinal epithelial cells for at least 24 hours post infection (hpi) without altering the architecture of the mucosa and without inducing cell death [237, 238]. Using an explant culture of colonic mucosa from a healthy individual, Dr. Laboisse's team showed that AIEC are unable to activate caspase-1 to induce cell death, but do activate the proinflammatory transcriptional regulator, NFκB [238]. Specifically, AIEC-infected IECs decrease the concentrations of the NF-κB regulator cylindromatosis (CYLD), to promote the degradation of the NF-κB inhibitor, IκB-α, and NF-κB activation [239]. Activation of NFκB results in the secretion of the proinflammatory cytokines, TNF-α, IFN-γ, and IL-8 by AIEC-infected cells [238, 240, 241].

Survival in macrophages

In vitro studies show that AIEC LF82 can survive inside of infected human and murine macrophages up to 24 hpi without inducing macrophage death [242]. In contrast, phagocytosis of non-pathogenic *E. coli* K12 results in macrophage death through apoptosis [243]. Intramacrophagic AIEC survival is shown to be dependent on the secretion of TNF-α, as neutralization of TNF-α decreases the number of intracellular AIEC [242]. Although TNF-α secretion is known to promote necroptosis during infections with Gram-negative bacteria, AIEC prevents cells death through TLR4 signaling [244, 245]. Infection of murine and human macrophages with LF82 leads to the activation of TLR4 signaling through the TRIF-related adaptor molecule (TRAM) and subsequently to caspase 8-dependent cleavage of CYLD [244].

Cleavage and removal of CYLD prevents the activation of the second pathway required for TNF-α-mediated necroptosis [244].

AIEC replicate inside of macrophages and resist degradation in the phagolysosome

In addition to being able to prevent infected macrophage death, AIEC also have unique genes that allow them to survive and replicate in the acidic environment of the mature phagolysosome [246]. A phagolysosome is defined as the product of fusion of a lysosome and other hydrolytic proteins with a phagosome (a membrane-bound vacuole) after phagocytosis. Of important note, studies suggest that AIEC does not modify the macrophage response, but rather employs mechanisms that permit bacterial survival [247]. Moreover, studies using compounds that interfere with phagolysosome formation reveal that acidification is a requirement for the replication of AIEC inside of macrophages [246].

In the mature phagolysosome, hydrogen peroxide and reactive oxygen species target the invading bacteria. Intracellular replication and survival of AIEC LF82 in J774-A1 macrophages relies on the stress protein, high-temperature requirement A (HtrA), and the periplasmic oxireductase, DsbA, respectively [248, 249]. HtrA is protein chaperone that degrades misfolded proteins and promotes proper protein folding [250]. AIEC has been shown to upregulate the expression of *htrA*, inside of the phagolysosome and use HtrA to protect against oxidative stress [248]. DsbA is a periplasmic protein that stabilizes membrane and exported proteins through the formation of intramolecular disulfide bonds between cysteine residues [251]. Deletion of *dsbA* in LF82 renders the intramacrophagic bacteria unable to survive to the acidic

pH and nutrient-poor environment [249]. It is hypothesized that HtrA and DsbA work together to ensure that other virulence factors required for intramacrophagic survival are properly folded in the periplasm and exported to the outer membrane.

The dihydroorotate dehydrogenase (DHODH), encoded by the *pyrD* gene, is an enzyme involved *in de novo* pyrimidine/nucleotide biosynthesis and is essential for the replication of LF82 inside of macrophage environment-mimicking medium [252]. Transposon mutagenesis experiments showed that a mutation in the *pyrD* gene prevents the growth of LF82 in low pH and nutrient poor medium, and inhibits the expression of curli fibers and type 1 pili [252]. The stunted growth of *LF82pyrD::Tn5* inside of macrophages may be exacerbated by the limited levels of purines and pyrimidines inside of macrophages [247]. This mechanism may also be conserved in other AIEC strains. Other studies showed that AIEC HM604 utilizes glycolysis to replicate inside of phagolysosomes and that this strain also utilizes the *de novo* pyrimidine biosynthesis pathway for replication [247].

During pyrimidine synthesis DHODH generates uridine monophosphate (UMP), which is then phosphorylated to yield uridine triphosphate (UTP) [253]. The uridine diphosphate N-acetylglucosamine (UDP-GlcNAc) pyrophosphorylase then synthesizes UDP-GlcNAc from UTP [253]. Increased O-GlcNAcylation post translational modifications occur in patients with CD and are known to interfere with appropriate NOD2 signaling responses [254]. In addition to increased host O-GlcNAcylation, AIEC infected cultured and murine IECs also upregulate UDP-GlcNAc and have increased O-GlcNAcylation in response to infection [255]. Moreover, high levels of O-GlcNAc in infected tissues promote O-GlcNAcylation of *IKKβ* and NF-kB

and result in the release of NF-kB from its inhibitor, IKKβ, which ultimately leads to nuclear translocation of NF-kB to activate the transcription of proinflammatory genes [255]. Thus, it may be possible that a similar mechanism occurs inside of infected phagolysosomes that produce high levels of TNF-α.

The SOS and stringent response pathways also play a role in intramacrophagic survival and replication of AIEC [256]. The bacterial stringent response controls the expression of genes required during nutrient limitation and the SOS response is induced by with DNA damage and repair [257] . Inside of macrophages, AIEC activate a phenotypic switch that controls the replicative and stationary phases [256] . Based on reported data, it is hypothesized that nutrient depletion inside of the phagosome activates the stringent response and subsequently a non-replicating state that lasts approximately 7 hpi [256]. After this lag phase, the SOS response is activated and induces replication in a subpopulation of the non-replicating cells [256]. Bacterial cells that persist without growing inside of macrophages are shown to be resistant to antibiotics and proposed to be the cause of relapsing chronic diseases. Further, studies show the multidrug resistance efflux pump, MdtEF, is highly expressed in AIEC inside of macrophages and is essential for the survival of LF82 in this environment [258].

AIEC subvert autophagy by inhibiting the elongation of phagophores

AIEC utilizes the intracellular communication of host cells to suppress autophagy. Early studies suggested that human intestinal cells and macrophages infected with AIEC LF82 release exosomes that stimulate NF-kB activation and proinflammatory cytokine secretion in recipient cells [259]. Later it was demonstrated

that the activation of NF-kB by AIEC-infected IECs increased the expression of 2 microRNAS, miR30C and miR130A, which decreased ATG5 and ATG16L1 levels [260]. Decreased expression of these ATG proteins prevent the completion of autophagy and lead to an increase in intracellular AIEC (Fig. 1-6) [260]. Recent findings have linked these two studies and shown that miR30C and miR130A are found inside of exosomes released by AIEC-infected T84 cells [261]. Of note, exosomes from uninfected epithelial cells and epithelial cells infected with *E. coli* K12 do not contain these miRNAs and do not inhibit autophagy [261]. Since then, other microRNA variants that inhibit ATG16L1 and autophagy upon AIEC infection have been identified [262]. Thus, AIEC cause infected cultured cells to release exosomes containing microRNAs that suppress autophagy to promote their survival.

AIEC also inhibit autophagy by decreasing host protein SUMOylation, a post-translational process that involves the attachment of a small ubiquitin-like modifier (SUMO) protein to a target acceptor protein to regulate signal transduction [263]. The adhesion of AIEC is necessary for host cell modulation, since wild-type AIEC, but not AIEC LF82Δ*fimH,* decreases global protein SUMOylation in T84 cells and mice [263]. The adhesion of AIEC is hypothesized to increase host cell expression of miR-18, a negative regulator of SUMO E3 ligase PIAS3 required for SUMOylation [263]. Since the inhibition of miR-18 was shown to induce autophagy in AIEC-infected cells, it is also hypothesized that SUMOylation of host cell proteins is required for autophagy.

Functional autophagy is essential for AIEC removal

Studies show that human macrophages initiate autophagy within 30 minutes post internalization of AIEC [264-266]. The AIEC yersiniabactin siderophore mediates

autophagy through activation of the transcriptional activator (HIF-1α) [267]. AIEC-mediated autophagy is carried out by the eukaryotic translation initiation factor 2 and 4 and the activating transcription factor 4 (EIF2AK4-EIF2α-ATF4) pathway, which also occurs in mammals in response to nutrient deprivation [265]. During macrophage and IEC infection there is a subpopulation of intracellular AIEC that is rapidly degraded by autophagy and another subpopulation survives inside of phagolysosomes,and subverts autophagy possibly through the aforementioned mechanisms [264, 266]. The induction of autophagy by rapamycin in IECs and macrophages shows that autophagy reduces the number of intracellular AIEC (almost by 100%), but only when rapamycin is administered at the same time of infection [264, 266]. One striking difference between autophagy in cultured macrophages and IECs, is that autophagy occurs within 30 minutes post infection (mpi) in macrophages, whereas in IEC it occurs after 1 to 6 hpi. Thus, AIEC might have higher chances of avoiding autophagy in IECs.

Host defects in autophagy increase intracellular AIEC

As mentioned above, variants of *ATG16L1*, *IRGM,* and *NOD2* are present in some CD patients. Separate studies showed that knockdown of *ATG16L1* and *IRGM* in macrophages and HeLa cells resulted in impaired autophagy, increased intracellular AIEC, and increased secretion of TNF- α and IL-6 [264, 266]. This group and others also showed that LC3-II (a marker for autophagy) failed to be induced in AIEC-infected macrophages and in dendritic cells isolated from *nod2* null mice [264, 268]. However, upon autophagy induction all host cells were able to effectively eliminate intracellular AIEC. Moreover, the overexpression of NOD2 in human colon cells also effectively cleared AIEC through autophagy, indicating that NOD2-mediated

autophagy is essential to control intracellular AIEC[269]. All of these studies suggest that host's defects in autophagy may be advantageous for the survival of AIEC and that AIEC may also affect autophagy even in patients who do not carry autophagy-related variants, as suggested by T84 studies.

AIEC form biofilms in host cells

Inside of the phagolysosome AIEC forms intracellular bacterial communities (IBCs) that have an extracellular matrix composed of exopolysaccharides and curli fibers [270]. During the lag phase of bacterial growth, non-replicating AIEC cells induce the expression of biofilm-forming genes and produce exopolysaccharides and curli fibers. Afterwards, when bacterial replication is resumed, AIEC cells grow in IBCs inside of macrophages and survive for up to 24 hpi [270]. The formation of IBCs is also mediated by the yersiniabactin iron capture system, which is tightly linked to the biofilm pathway [268]. Yersiniabactin is a siderophore encoded in the high-pathogenicity island (HPI) of AIEC and mediates the adhesion and invasion to T84 cells, colonization in mice, and induces inflammation-associated fibrosis in mice susceptible to colitis [267, 270, 271].

In AIEC, biofilm genes are encoded in the *waaWVL* operon and their expression is regulated by σ^E regulon [272]. This operon also mediates the adhesion of AIEC to cultured IECs, possibly through the indirect induction of type I pili and LPS synthesis [272]. Interestingly, the *waaWVL* operon of APEC, UPEC, and commensal *E. coli* strains do not encode biofilm forming genes [272].

The mechanisms behind how AIEC sense their environment inside of the phagosome and induce virulence genes are not well elucidated. However, it has been

shown that sugars and sugar-derivatives in the intestine can influence biofilm formation in AIEC. N-acetylneuraminic acid (NANA), N-acetylglucosamine (NAG), and fucose, components of the intestinal mucus, act as signaling molecules for biofilm inhibition in AIEC [273]. During NAG catabolism the NagC protein, a repressor of the *nag* operon, is inactivated and NAG is metabolized. However, how this mechanism converges with biofilm induction is unclear. In contrast, maltodextrin and propionic acid, two widely used food preservatives stimulate AIEC biofilm formation and increase the burden of AIEC in IECs and mice, respectively [274, 275].

Host factors that influence colonization of AIEC

The carcinoembryonic antigen-related cell adhesion molecule 6 (CEACAM6) is a cell surface glycoprotein that regulates many biological processes, such as cell adhesion and migration, immune responses, and inflammation [276]. CEACAM -1, -5, -6, - 7, and -20 are expressed in the intestine however, only CEACAM 5 and CEACAM 6 are abnormally upregulated in the apical surface of the ileum in 35% of CD patients [277, 278]. CEACAM6 is a highly mannosylated molecule and a well-known receptor of type 1 pili of AIEC [278]. Currently, there are two mouse models that express CEACAM6 in the intestine, CEABAC10 and Vill-hCC6 mice [278-280]. To date more data have been generated using CEABAC10 mice. CEABAC10 mice have increased AIEC LF82 burden and severe colitis compared to infected wild-type mice [280]. Severe colitis is characterized by high proinflammatory cytokine expression, rectal bleeding, reduced survival, weight loss, and erosive lesions.

The type 1 pili terminal subunit, FimH, is essential for the induction of colitis as CEABAC10 mice infected with LF82Δ*fimH* do not develop colitis[280]. LF82 FimH

consists of pilin domains and a mannose-binding lectin domain that binds mannose moieties of host cells and surfaces with high affinity [281]. Phylogenetic analyses show that LF82 and other AIEC strains isolated from CD patients have polymorphisms in the FimH adhesin that increase their adherence and dissemination in CEBAC10 mice [282]. AIEC strains harboring FimH polymorphisms were found to have mutations in the D-mannose binding pocket and in the intermediate domain located between pili and lectin domains [282]. It is hypothesized that these mutations increase the mannose binding affinity.

In addition to CEACAM6, AIEC LF82 also bind to oligomannosidic glycans displayed on the membranes of apoptotic cells through FimH [283]. The binding of LF82 to CEACAM6 cells through FimH has been demonstrated to induce apoptosis and AIEC is hypothesized to exploit this mechanism to colonize the intracellular spaces by binding to mannose residues on blebbing cells [283]. Further, it is proposed that apoptotic cells serve as entry points for AIEC to enter neighboring cells.

Another receptor that is abnormally upregulated in the intestine of IBD patients is chitinase 3-like-1 (CHI3L1) [284]. The expression of CHI3L1 is usually very low under homeostatic conditions, but during inflammation it is increased more than 10-fold in colonic epithelial cells [284, 285]. AIEC is known to bind N-glycosylated residues of CHI3L1 through the chitin-binding domains (CBD) of the chitinase, ChiA [286-288]. Binding of ChiA to CHI3L1 facilitates the invasion of AIEC into murine IECs, induces the secretion of proinflammatory cytokines, IL-22 and IL-6, and exacerbates colitis in mice chemically predisposed to intestinal inflammation [286-288].

Paneth cells and mucin minimize the contact of bacteria with the intestinal epithelium. However, when a patient is suffering from IBD cellular and structural changes occur to these host factors that render them nonfunctional. Analysis using *ex vivo* follicle-associated epithelium (FAE) from patients with CD show that the secretion of α human defensin 5 (HD5) is decreased by 2-fold in the FAE of CD patients stimulated by LF82 compared to the FAE of non-IBD control patients [289]. Decreased HD5 secretion by diseased FAE is thought to be the reason for increased AIEC transcytosis across diseased FAE compared to non-IBD FAE [289]. However, other studies show that the genome of AIEC NRG857, but not LF82, consists of a plasmid-encoded genomic island (PI-6) that encodes two genes, *arlA* and *arlC*, important for the resistance against HD5 and human β-defensin 2 (HBD2) [290]. PI-6 was shown to be essential for the survival of AIEC when exposed to cultured Paneth cells and in mice. Thus, it may be possible that even if the host has functional Paneth cells, it may not be sufficient to inhibit colonization of some AIEC strains.

Studies suggest that the intestinal mucus layer of IBD patients may not be enough to protect the intestinal epithelium against AIEC colonization. AIEC LF82 and other AIEC strains belonging to the B2 phylogroup harbor the VAT-AIEC mucinase that degrades intestinal MUC2 and facilitates colonization of AIEC in the colon of CEABAC10 mice [291]. *In vitro* experiments showed that AIEC uses VAT-AIEC to cleave and penetrate mucus to access the intestinal epithelial cells [291]. Furthermore, the transcription of *vat-AIEC* is induced in the presence of bile, mucins, and a pH below 7.5, which indicates that AIEC cells express virulence factors required to establish a niche in the intestine. In addition, comparative sequence analyses in

previously described genes have identified the presence of other potential metabolic genes that may degrade mucin in AIEC belonging to the B2 and D phylogroups [195]. Previous work in our lab has shown that the gut commensal *E. coli* strain HS possess a multivalent adhesion molecule (MAM) that is 99% identical to the AIEC MAM adhesin and binds sulfate moieties within MUC2 [76]. These data also suggest that sulfation of mucin improves retention of *E. coli* by the mucosal layer and removal of these sulfation groups by sulfatase-producing commensal microbes allows *E. coli* to translocate into the epithelium *in vitro* [76]. Thus, it is plausible that AIEC MAMs bind to intestinal MUC2 in a sulfation-dependent manner like the *E. coli* strain HS MAM.

Gaps in knowledge and significance of this work

It is clear that AIEC harbor unique virulence factors that facilitate pathogenesis in the intestine of a diseased host. To date it is still unknown whether the colonization of AIEC in a susceptible host triggers the onset of intestinal inflammation or if inflammation presents a favorable environment for the AIEC pathotype. However, given the high prevalence of AIEC in CD patients with active disease and in those predicted to have severe endoscopic postoperative recurrences post-surgery, studies using cultured cells are being conducted to identify therapeutics that target AIEC or protect the host from AIEC colonization [292, 293]. Current IBD treatment is based on symptom control with anti-inflammatory drugs, immune suppressors, and antibiotics. However, AIEC may influence the refractive nature of IBD because they are resistant to commonly used antibiotics in IBD treatment [294, 295].

Due to animal model limitations, the mechanisms of intramacrophagic AIEC are not well understood and have only been studied *in vitro*. Whether AIEC survive,

replicate inside of macrophages, and induce high secretion of proinflammatory cytokines *in vivo* is unknown. In addition, we do not fully understand how AIEC interacts with an intact innate system. Some questions that remain unanswered are: 1) do neutrophils eliminate infected macrophages, 2) does a healthy mucus layer with AMPS limit AIEC invasion, 3) does AIEC clearance alleviate host intestinal inflammation, 4) does targeting inflammation also clear AIEC, 5) does the activation of autophagy *in vivo* clear AIEC 6) what are the molecular signatures of AIEC, and 7) does AIEC express other essential virulence factors. Thus, it would be beneficial to have an *in vivo* high throughput animal model to address these gaps in knowledge. Furthermore, this *in vivo* model permits the visualization of bacterial adherence in real time in an animal amenable to genetic and pharmacological manipulation. Having a powerful *in vivo* model of AIEC may facilitate the investigation of how AIEC respond to anti-inflammatory therapeutics and antibiotics used during IBD treatment.

Current animal models of AIEC include CEABAC10 mice, conventional mice treated with broad-spectrum antibiotics, mice treated with colitis inducing agents (dextran sulfate sodium (DSS) and 2,4,6-trinitro-benzene sulfonic acid (TNBS)), and mice that are genetically susceptible to spontaneous colitis [296]. Moreover, a recent study has reported that CEACAB10 mice primarily express CEACAM6 in the colon rather than in the ileum, the region where AIEC is often observed [279]. Although mice are powerful tools, they have some limitations that include: expensive care, long development periods, small statistical power, and laborious genetic manipulation. Furthermore, pathophysiological changes in infected mice cannot be observed in a live animal, until after euthanasia. To address the gaps of knowledge in the AIEC, we

need an animal model that provides high throughput analyses and allows to us study AIEC infections in real-time.

The larval zebrafish (*Danio rerio*) model system presents numerous experimental benefits including: a fully sequenced genome, high fecundity and rapid experimental turnover, genetic tractability, rapid development, and optical transparency throughout development into early adulthood [297]. Zebrafish also harbor at least 70 percent of human genes, including some IBD susceptibility genes [298, 299]. Additionally, the gastrointestinal tract of larval zebrafish is physiologically and functionally similar to the human intestine (Fig.8) [297, 300, 301].

There are various epithelial subtypes in the zebrafish gut that permit the identification of functionally defined intestinal segments that are classified as the anterior, mid, and posterior axes [302, 303]. The anterior gut is analogous to the mammalian stomach and contains digestive enzymes. The midgut functions like the small intestine because it mediates nutrient absorption. The posterior gut carries out water absorption and resembles the colon [302]. Like mammals, the zebrafish intestine is made of absorptive enterocytes, mucin secreting goblet cells, enteroendocrine cells, and M-like cells arranged in single layer of epithelial folds that are positioned above a lamina propria (Fig. 8) [302, 303]. However, enteroendocrine cells and M-like cells are limited to the anterior and mid segments, respectively.

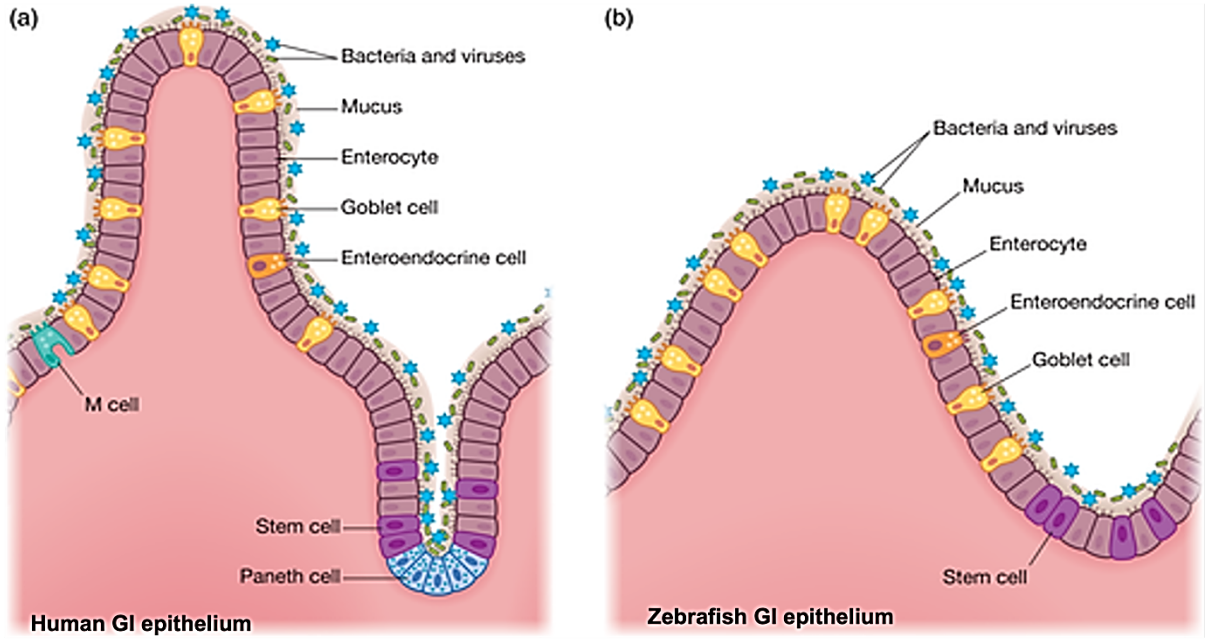

Figure 1-8. The human and larval zebrafish gastrointestinal epithelium share common features.

In humans (a) the intestinal epithelium is composed of intestinal folds with pronounced crypts and vili, and contains Paneth cells and M cells, which are not observed in zebrafish (b). The zebrafish epithelium has less pronounced intestinal folds. However, the zebrafish and human intestinal epithelium both contain goblet cells, enteroendocrine cells, enterocytes, and intestinal mucus.

Flores EM, Nguyen AT, Odem MA, Eisenhoffer GT, Krachler AM. The zebrafish as a model for gastrointestinal tract-microbe interactions. Cell Microbiol. 2020;22(3):e13152, Figure 1, by permission of John Wiley & Sons, Inc.

In contrast to mammals, zebrafish lack a stomach, Paneth cells, and the crypts of Lieberkuhn [302]. Despite the fact that zebrafish do not have a stomach, they do express several digestive enzymes that are functionally equivalent to those found in mammalian stomach, such as rennin, capthepsins, and lipases, and contain lysosome rich enterocytes in the mid gut that aid in protein adsorption [302, 304, 305]. In mammals, epithelial cell division occurs within the crypts of Lieberkühn house, however in zebrafish division occurs at the base of the epithelial folds [28];[297, 302, 306]. Moreover, even though zebrafish lack Paneth cells, they still express antimicrobial peptides and proteolytic enzymes, including the LPS degrading phosphatase alpi.2 and AMP ly97.2 [307, 308].

Zebrafish larvae have an innate immune system that is active by 28 to 30 hours post fertilization (hpf) and do not have a functional adaptive immune system until 4-6 weeks post fertilization [309]. Like mammals, the zebrafish innate immune system consists of signal transducers (NOD1, NOD2, TLRs, and the myeloid differentiation primary response 88 (MyD88), neutrophils, macrophages, mucin, cytokines, and the AMPS [308, 310]. Macrophages appear at 15 hpf and have phagocytic activity at 26 hpf [311]. Neutrophils develop at 18 hpf and secrete myeloperoxidase by 24 to 48 hpf[312]. One of many benefits of using larval zebrafish as a model organism is that transgenic lines that express fluorescently labeled proteins are available. These benefits have propelled the use of zebrafish as effective high-throughput models and have contributed to our understanding of numerous biological processes [313].

Recent studies show that human intestinal pathogens, including *E. coli,* can be studied in larval zebrafish [297]. Previous work from the Krachler lab suggests that

EHEC upregulates the expression of the locus of enterocyte effacement (LEE) pathogenicity island in response to the shear forces experienced in the gut and that zebrafish may be a suitable model to investigate how bacteria sense their environment [314]. In this work I attempt to characterize larval zebrafish as a model of adherent-invasive *E. coli* infections. In Chapter 3, a zebrafish model of intestinal inflammation, induced by DSS, is validated. This model is then used to characterize AIEC infections, as described in Chapter 4. Chapter 4 also discusses whether known virulence factors that are important for AIEC colonization in mice also play a role in the colonization of AIEC in the zebrafish intestine.

Chapter 2: Methods

Zebrafish maintenance and breeding

The zebrafish used in this study were wild-type (AB) and transgenic Tg*(mpo*::*egfp*)[315] and Tg (*mpeg1*:*egfp*)[316], which produce enhanced green fluorescent protein (GFP) in neutrophils and macrophages, respectively. Adult fish were kept in a recirculating tank system at the aquatics facility of The University of Texas Health Science Center CLAMC (Center for Laboratory Animal Medicine and Care) on a 14:10 h light:dark cycle at pH 7.4 and 28 °C. Eggs were obtained from the natural spawning of adult fish. Fertilized embryos were bleached for 30 sec. in 0.05% sodium hypochlorite solution (stock solution 4.00-4.99%, Sigma-Aldrich) and kept at 30 °C on a 14:10 h light:dark cycle at pH 7.4. Embryos were raised in petri dishes containing E3 buffer (10 mM HEPES, 5 mM NaCl, 0.17 mM KCl, 0.4 mM $CaCl_2$, 0.67 mM $MgSO_4$) buffered to pH 7.4. The amount of HEPES added to the E3 buffer was increased compared to the original recipe to neutralize the acidic (pH 3) solution that arose after dissolving DSS in standard E3 buffer. The additional HEPES maintained the E3 media containing DSS at pH 7.4. Larvae that were maintained past 6 days post fertilization (dpf) were fed GEMMA Micro 75 (Skretting) daily after 7 dpf until euthanized.

Bacterial strains and growth conditions

The bacterial strains used in this study were the non-pathogenic *E. coli* strain MG1655, and the adherent-invasive *E. coli* (AIEC) strain LF82 (parent strain obtained from the Torres Lab, University of Texas Medical Branch), and its derivatives LF82Δ*fimH*, LF82Δ*ibeA*, LF82Δ*fimH:fimH*, and LF82Δ*ibeA:ibeA*. The LF82 deletion strains were generated using gene doctoring [317]. Briefly, constructs were generated

by amplifying a kanamycin cassette from the plasmid pDOC-K using oligonucleotide pairs that contain at least 45 bp of homology to the DNA immediately upstream and downstream of the target genes (Table 1). The amplified fragment was inserted into the plasmid pDOC-C, and the construct sequence was verified by sequencing (Azenta Life Sciences). The constructed pDOC-C deletion plasmid and the recombineering plasmid pACBSCE were co-transformed into LF82 via electroporation and plated on LB agar containing chloramphenicol (35 µg/ml), ampicillin (200 µg/ml), and kanamycin (50 µg/ml). Selected colonies were grown in 1 ml of LB broth containing 0.5% glucose for 2 h and then induced with 0.5% arabinose for 4 h. The cells were then collected by centrifugation, resuspended in 50 ul of residual medium and spotted on LB plates without NaCl, but containing 5% sucrose and kanamycin. Sucrose insensitive and kanamycin resistant recombinant colonies were transferred to LB chloramphenicol plates to confirm loss of the pACBSCE plasmid. Loss of the pDOC-C plasmid was confirmed by using pDOC-specific oligonucleotides [317], instead of patching on LB-ampicillin plates, since the LF82 strain is resistant to ampicillin. Lastly, the gene deletion was confirmed by PCR analysis of the relevant chromosomal regions using oligonucleotide pairs (Table 2) and sequencing of the resulting PCR products. All strains were transformed with plasmid pME6032::mCherry by electroporation and plated on LB containing tetracycline (15 µg/ml). The resulting strains were grown in LB broth supplemented with 15 µg/mL tetracycline, at 37 ^{o}C in a shaker. Complementation strains were generated by introducing a copy of the gene of interest including its endogenous promoter into the attTn7 site on the LF82 chromosome using Tn7 transposition[318]. Briefly, 500 bp upstream and downstream of the *fimH* and

ibeA genes were taken (to include the promoters) and amplified by PCR from AIEC LF82 genomic DNA. The amplified DNA was purified, digested with SpeI/ApaI (*fimH*) or SpeI/KpnI (*ibeA*), ligated into the vector pGp-Tn7-Gm, and then introduced in DH5α-λpir competent cells by electroporation to construct pGp-Tn7-*fimH* and pGp-Tn7-*ibeA* vectors. Positive clones (gentamycin resistant) were checked by colony PCR and confirmed by Sanger sequencing. The Tn7 transposase encoding, temperature-sensitive plasmid pSTNSK-Cm was electroporated into the LF82Δ*fimH* and LF82Δ*ibeA* strains. Then the pGp-Tn7-*fimH* and pGp-Tn7-*ibeA* vectors were also introduced into LF82Δ*fimH* and LF82Δ*ibeA* by electroporation. The electroporated cells were spread on LB plates containing gentamycin (15 μg/ml) and chloramphenicol (20 μg/ml), and incubated at 30°C for 20 hours. Following a 20-hour incubation, 20-30 colonies were selected, streaked on LB agar plates without antibiotics, and incubated at 42 °C for 20 hours to promote the loss of plasmid pSTNSK-Cm. The colonies were passaged 4-5 times on LB agar plates, incubated at 37 °C and screened for resistance to gentamycin and sensitivity to chloramphenicol. The integration of the Tn7 transposon at the attTn7 site located downstream of the *glmS* gene of LF82 was checked by PCR (Table 3).

***Paramecium caudatum* maintenance and infection**

Paramecia stocks were maintained in T25 flasks at room temperature in 10 mL of E3 medium. Paramecia were propagated by adding 1 mL of the initial paramecia stock culture to 8 mL of fresh E3 medium and fed 10^8 CFU/mL of *E. coli* MG1655 resuspended in 1 mL of E3 medium. Paramecia were propagated one day prior to infection experiments, and every two weeks to maintain live cultures. Loading of

paramecia with AIEC LF82 and MG1655 was conducted as described previously[319]. Briefly, bacterial cultures were grown for 12 hours in LB broth (containing 15 μg/mL tetracycline when required), washed with E3 medium, and resuspended in 20 mL of paramecia cultures prepared the day before.

E. coli burden in Paramecium caudatum

After adding *E. coli* to 20 mL of the paramecia culture, the amount of AIEC or MG1655 in paramecia at the initial time point (T0) was assessed. The sample was washed to remove *E. coli* that was not initially taken up by spinning the sample at 300 RCF at 15 °C for 5 minutes. The sample was placed in 1% Triton X-100 and vortexed to lyse the paramecia. Serial dilutions (1:10) were performed, and 5 μL of each dilution was plated on CHROMagar™ O157 plates (Drg International Inc). The plates were incubated at 30 °C for 24 h, and then at room temperature for an additional 24 h to permit full growth of colonies. The number of colonies was assessed 48 h after plating.

Larval zebrafish infections

Following the 2 h incubation of paramecia and *E. coli*, the co-culture was placed in a 50 mL conical tube and centrifuged at 300 RCF at 15 °C for 10 minutes. Ten milliliters of the supernatant was removed, and the pellet was resuspended with an additional 10 mL of E3 medium and centrifuged again for 5 minutes at the same settings. This process was repeated two additional times to remove *E. coli* cells that were not engulfed by the paramecia. After the final wash, 500 μL of the co-culture was placed into a 2 mL microfuge tube and centrifuged again at 300 RCF for 5 minutes. Four hundred microliters of the supernatant were removed, and the pellet was gently

resuspended with the remaining solution and 20 μL of 37% formaldehyde. The number of live paramecia were counted using an automated cell counter (Life Technologies Countess II) and used to calculate the volume of the co-culture required to feed larvae at a final concentration of $2*10^5$ paramecia/mL in E3 medium. After setting up the paramecia containing medium, groups of 8 larvae were anesthetized with tricaine and transferred into 3 mL of the *E. coli*-containing-paramecia mixture in sterile 6-well tissue culture plates. The larvae were then incubated with the paramecia for 2 h at 30 °C. After feeding, the larvae were anesthetized and washed six times in 3 mL of fresh E3 medium containing 0.16 mg/mL tricaine in the 6-well plate. The larvae were gently transferred using a glass pipette to minimize excess volume transfer.

E. coli burden and persistence in larvae

Infected zebrafish larvae were euthanized with 1.6 mg/mL of tricaine, and then incubated with 100 μL of a 1 mg/mL filter-sterilized pronase solution, vortexed, and incubated at 37 °C for 6 minutes. The larvae were then homogenized by repeated passage through a 31-gauge needle attached to a 1 mL syringe. The solution was diluted 1:10 and 5 μL was spotted on CHROMagar™ O157 plates. The plates were incubated at 30 °C for 24 h and then at room temperature for an additional 24 h to permit full colony growth. The number of dark steel-blue (AIEC) and mauve (MG1655) colonies were assessed afterwards. Data was analyzed using Prism 9 software.

DSS administration and survival analysis of DSS-treated larvae

Colitis grade dextran sulfate sodium (DSS) (36,000-50,000 MW, MP Biomedical) was used to induce enterocolitis as previously described by Dr. Oehlers'

group[320]. DSS at a concentration of 0.5% (w/v) was made fresh every day in E3 medium at room temperature. At 3 dpf, 120 larvae were anesthetized with 0.16 mg/mL of tricaine and transferred to a 150 mm diameter petri dish containing 90 mL of 0.5% DSS (w/v). Survival or death was assessed daily, by the presence or absence of a heartbeat on anaesthetized larvae using an Olympus SZX10 stereomicroscope. Dead larvae were removed every day following assessment, and the surviving larvae were transferred to a new petri dish containing fresh DSS in E3 medium.

Measurement of intestinal and body length, and swim bladder assessment

All fish were imaged on an Olympus SZX10 stereomicroscope at 1.6 X magnification. Fish were anesthetized in 0.16 mg/mL tricaine and embedded in 1% low melt agarose (LMA). ImageJ was used for image analysis to assess whole body and intestinal length. To calibrate the measurements, 0.3 cm on a ruler was imaged at 1.6 X magnification, and the corresponding number of pixels was determined. Then, the ImageJ pixel value was converted to millimeters. The length of the intestine was measured from the beginning of the bulb to the end of the cloaca, and the total body length was determined from the mouth to the tip of the tail. The presence of a swim bladder was visualized under the stereomicroscope on anesthetized larvae embedded in 1% LMA, from 3-10 dpf. The data was analyzed using Prism 9 software.

Histological analysis

Zebrafish larvae were fixed in 4% formaldehyde diluted in PBS, overnight at 4 ^{o}C. Larvae were processed by the UTHealth Histopathology Lab. Briefly, larvae were embedded in paraffin, sectioned along the sagittal plane at 2 μm, and stained with hematoxylin and eosin (H&E). Imaging was performed on an AmScope microscope

with a MU1003 camera and the AmScope software version x64, 3.7.11443.20180326 (Courtesy of Dr. Rady, UTHealth Houston).

Neutrophil and macrophage recruitment

Zebrafish were anesthetized with tricaine, embedded in 1% LMA in a 6-well glass bottom plate, and imaged on an Olympus Fluoview FV3000 confocal microscope for 3-21 hours post infection (hpi). A Z-stack of 190 images of 2 uM slices was analyzed with Fluoview FV3S-SW. The images were then imported into the Imaris software, version 9 7.2, which was used to quantify the number of fluorescent cells. In Imaris, the “surfaces” feature was used to outline the larval intestine and the number of GFP-expressing neutrophils or macrophages within the intestine was counted using the “cell count” feature. Imaris tracked the number of individual neutrophils recruited to the intestine over the course of 3 to 21 hpi.

Immunofluorescence staining and microscopy

Larvae were euthanized with 1.6 mg/mL tricaine, placed in a 4% formaldehyde (diluted in PBS) solution and stored at 4 ^{o}C overnight. The following day, larvae were washed twice with phosphate buffered saline (PBS) solution, permeabilized in acetone for 15 minutes at -20 ^{o}C and incubated in blocking solution composed of PBS, 1% BSA, 1% DMSO, and 0.5% Triton-X100 (PBDT). Anti-laminin antibody (Sigma-Aldrich, L9393) was diluted 1:25 in PBDT and added to a 500 μL microfuge tube containing 4-8 larvae. The samples were incubated at 4 ^{o}C overnight with gently rocking. The following day, the samples were washed and incubated with solution containing goat anti-rabbit IgG secondary antibody conjugated with Alexa Flour 488 (2:500) (Thermo Fisher Scientific, A27034) and 1 μM/mL 4′,6-diamidino-2-

phenylindole (DAPI) overnight. The samples were kept at 4 ^{o}C overnight and imaged on a confocal microscope (Olympus Fluoview FV3000 confocal microscope at 60 X magnification) and then transferred to cellSENS version 2.3 for deconvolution with five iterations.

Quantification of bacteria inside of epithelium

The quantification of bacteria inside of the intestinal epithelium was performed on deconvoluted images taken after immunofluorescence imaging. ImageJ was used to quantify the fluorescent signal of the mCherry channel (representing bacteria). The data was plotted using Prism 9 software and assessed using an unpaired t-test.

RNA isolation and quantitative reverse transcription PCR

For each condition, 15 zebrafish larvae were infected with *E. coli*, euthanized, and used for RNA extraction. RNA isolation from groups of 15 larvae was performed as previously described[321]. Briefly, larvae were placed in a 2 mL microfuge tube and homogenized in 1 mL of TRIzol reagent (Thermo Fisher, 15596026) using a disposable pellet pestle (Fisher Scientific, 12-141-364). The concentration of the isolated RNA was quantified using a NanoDrop ND-1000 spectrophotometer. The RNA was treated with RNAase-free DNase (Qiagen RNase-Free DNase Set) and cleaned and concentrated using a Zymo Research RNA clean & Concentrator Kit. Removal of DNA contamination was verified by PCR using purified RNA as template. Reverse transcription was carried out using oligo(dT) primers and the SuperScript™ IV First-Strand cDNA Synthesis Reaction system. Synthesized cDNA was purified using a QIAquick PCR Purification Kit (QIAGEN Inc, Valencia, CA, United States) and the final cDNA concentration was determined using a NanoDrop spectrophotometer.

Each qRT-PCR reaction used 45 ng of cDNA. cDNAs and primers (listed in Table 4) were mixed with Luna Universal qPCR Master mix (New England Biolabs) and amplification was carried out in a BioRad CFX96 Real Time system. The reactions were performed in duplicate in a CFX96 Real-Time System C1000 Touch Thermal Cycler (Bio-Rad, Hercules, CA, United States). The *elfα* and *rpl13* genes were used as internal controls, and the relative fold-change for each gene of interest was expressed in 2-ΔΔCT, where ΔΔCT = [(CT gene of interest-CT internal control) one condition - (CT gene of interest- CT internal control) another condition[322]. For DSS experiments, the DSS data was normalized to the untreated group, whereas in the infection experiments the data was normalized to controls fed paramecia without added bacteria. PCR cycling conditions were 95 ºC for 1 min, 60 ºC for 30 s, 95 ºC for 15 s and 39 cycles, and 60 ºC for 31 s.

Table 2-1. List of primers used to amplify the pDOC-K plasmid with 45 base pair homology to the DNA upstream and downstream of *ibeA* and *fimH*.

The restriction site is in red and the region homologous to the kanamycin cassette is in green.

Gene	Forward primer sequence (5-3)	Reverse primer sequence (5-3)
ibeA	CGGAATTC**GCGCGGGGGATTGTTTTACTCAATTATTGAATACGGAGATAAAGTATGGAA**GACCGGTCAATTGGCTGGAG	CGGCTAGC**GCGCGACATAAAAACTGGGTTTTTCTCTCATAACTTTATTCCCTGTTAAAA**AATATCCTCCTTAGTTCCTATTCCGAAGTTC
fimH	CGGAATTC**TTAGCATCACCTATACCTACAGCTGAACCCGAAGAGATGATTGTAATGAAA**GACCGGTCAATTGGCTGGAG	CGGCTAGC**TCAGGTAATATTGCGTACCTGCATTAGCAATGCCCTGTGATTTCTTTATTG**AATATCCTCCTTAGTTCC

Table 2-2. List of primers used to verify deletion mutants.

Strain	Forward primer sequence (5-3)	Reverse primer sequence (5-3)
LF82*ΔfimH*	CAACCAAAACAGTTCAGGTGG	GCTGATTATTAGCATGGTAGCG
LF82*ΔibeA*	GGCAAAGAGAGATGATCTCCTT	CCCATAACACCGATGCCAATA

Table 2-3. List of primers used to analyze the integration of the Tn7 transposon system at the attTn7 site located downstream of the *glmS* gene.

Strain	**Forward primer sequence (5-3)**	**Reverse primer sequence (5-3)**
LF82 complementation strain	TGGCTTACCACGTTGCGCG	CATACACCGGCGCAGGGAAG

Table 2-4. List of primers used to analyze the transcription of proinflammatory genes and housekeeping genes.

Gene	**Forward Primer Sequence (5-3)**	**Reverse Primer Sequence (5-3)**
rpl13	TCTGGAGGACTGTAAGAGGTATGC	AGACGCACAATCTTGAGAGCAG
ilb	ATCAAACCCCAATCCACAGAGT	GGCACTGAAGACACCACGTT
cxcl8	TGTTTTCCTGGCATTTCTGACC	TTTACAGTGTGGGCTTGGAGGG
mmp9	CATTAAAGATGCCCTGATGTATCCC	AGTGGTGGTCCGTGGTTGAG
tnfα	GTTTATCAGACAACCGTGGCCA	GATGTTCTCTGTTGGGTTTCTGAC

Chapter 3: Characterizing a Larval Zebrafish Model of Colitis

Introduction

To date animal models of inflammatory bowel disease (IBD) have included rabbits, primates, rats, mice, and zebrafish. Although mice are the most widely used IBD models, larval and adult zebrafish have emerged as powerful tools to complement mouse IBD studies. In fact, there are zebrafish models for almost every IBD mouse model. There are numerous mouse and zebrafish colitis models and they have been generated by several methods [323, 324]. In these animals, colitis can be induced through administration of chemicals, targeted and spontaneous genetic modifications, adoptive T cell transfer, spontaneous mutations, and transplantation of pathogenic bacteria [325]. Although the methods used to induce colitis in these models differ, there are three common features shared by all: (1) immune system-mediated inflammation, (2) bacteria as a disease initiator, and (3) genetic background as a disease modifier.

Chemical induction of colitis

Chemical agents used to create IBD-like colitis in rodents include dextran sulfate sodium (DSS), 2,4,6-trinitrobenzene sulfonic acid (TNBS), oxazolone, acetic acid, carrageenan, peptidoglycan-polysaccharide and nonsteroidal anti-inflammatory drugs (NSAIDs) [326]. To date, only DSS, TNBS, oxazolone, and NSAIDs have been used in zebrafish. In general, chemicals are administered to zebrafish through immersion. Water-soluble chemicals are absorbed by zebrafish through their gills and skin, and can also be consumed orally by larvae starting a 72 hours post fertilization, (hpf) (corresponding to the protruding-mouth stage) [327].

DSS is a large negatively-charged and sulfated polysaccharide that is toxic to the colonic epithelial cells [328]. The consumption of DSS by animals through their

drinking water damages the intestinal mucosal barrier, thereby facilitating the entry of luminal contents into the underlying tissue, and ultimately results in large secretion of proinflammatory cytokines [329, 330]. The immersion of larval zebrafish in DSS results in all of the above and in neutrophil recruitment to the intestine, altered goblet cells in the intestine, and mucin accumulation in the intestinal bulb [320, 331, 332]. DSS is the most widely used method to induce colitis in mice and zebrafish and is ideal for studying aspects of the innate immune system and factors that modulate epithelial integrity [329].

TNBS is a small molecule that causes colitis through a delayed hypersensitivity response when it binds to host proteins [333]. TNBS is administered to mice and adult zebrafish intrarectally and to zebrafish larvae through immersion. In adult zebrafish and mice, binding of TNBS to colonic proteins initiates the T-helper 1 (Th1) response, in which CD4 positive T lymphocytes are activated [333]. These T cells secrete large quantities of interferon gamma (IFN-γ) and promote the recruitment of neutrophils and macrophages, which all together result in transmural colitis [325]. In contrast, TNBS is hypothesized to induce colitis in larval zebrafish by directly disrupting intestinal epithelial cell function or altering the secretion of mucin, since larvae do not have a developed adaptive immune system [332].

Fleming and colleagues were the first group to report that immersion of larval zebrafish in TNBS resulted in enterocolitis [334]. They showed that TNBS causes smoothening of the intestinal epithelium, expansion of the lumen, and an increased number of goblet cells at 6 days post TNBS exposure. Oehlers and colleagues further investigated the effects of varying TNBS concentrations on larval zebrafish, but did

not observe changes in goblet cell numbers or changes to the intestinal epithelium morphology [320, 332]. However, they showed that TNBS exposure primarily elicited an infiltration of neutrophils to the intestine and subsequently caused elevated secretion of proinflammatory cytokines IL-1β, Tnf-α, matrix metallopeptidase 9 (MMP9), chemokine ligand 20 (CCL20), and IL-8 and increased nitric oxide production [320, 332]. TNBS-induced colitis models are generally used studying immunotherapies and the adaptive immune system response. For instance, it has been shown that TNBS-induced colonic inflammation is IL-12-driven and can be decreased with monoclonal antibodies against IL-12 [335, 336].

Like TNBS, oxazolone is also a haptenizing agent that induces a hypersensitivity response after intrarectal injection [325]. However, oxazolone induces an IL-4-driven Th2 response that is characterized by a hypersecretion of IL-13 by natural killer T cells [337]. The Th2 response causes inflammation in the distal half of the colon that resembles the pathology observed in UC patients [337]. Although this method has not been used in larval zebrafish, it is commonly administered to adult zebrafish and mice. In adult zebrafish oxazolone causes thickening of the epithelium, loss of the intestinal folds, decreased goblet cells, and a significant infiltration of neutrophils and eosinophils [338]. In general, this model is used to identify therapeutics that target Th2 immune responses.

Other methods used in larval zebrafish for the disruption of the mucosal barrier are soybean meals and the nonsteroidal anti-inflammatory drug (NSAID) glafenine. Soybean meals have long been considered a primary source of protein for commercially important fish, however multiple studies show that the glucoside, IL-1β

saponin, found in soybeans causes intestinal inflammation [339-341]. Saponin consumption results in reduced production of tight junction proteins, increased transcription of the genes encoding proinflammatory cytokines, IL-1β and IL-8, and neutrophil infiltration [36;337;338]. Interestingly, this method is unique because intestinal inflammation is independent of the intestinal microbiota, as inflammation occurs in germ-free fish fed saponin [341]. NSAIDs, including ibuprofen and glafenine, reduce inflammation by inhibiting cyclooxygenases (COX) that form proinflammatory molecules, including prostaglandin and thromboxane [342]. Moreover, blockage of the COX enzyme by glafenine induces intestinal damage in humans, mice, and adult zebrafish [343]. Larval zebrafish immersed in glafenine exhibit epithelial cell shedding and apoptosis, but do not have increased intestinal permeability [343].

Genetic modifications

During the last 30 years, more than 74 transgenic mouse models of IBD, including 20 that carry human susceptibility genes, have been developed [344]. Genetically engineered mouse models fall into different categories including transgenic (Tg) animals that overexpress a gene, gene knockouts (KO), inducible knockouts (iKO), and knock-in models (KI) that carry a mutation in the gene of interest[344]. The most commonly used model is the IL-10$^{-/-}$ KO mouse that develops spontaneous colitis due to lack of T-cell mediated expression of the anti-inflammatory cytokine, IL-10, which is also a CD- and UC- susceptibility gene in children and adults [345];[346]. These mice develop inflammation in the colon due to infiltration of neutrophils, macrophages, and lymphocytes [347]. Recent zebrafish studies show that in addition to regulating leukocytes, IL-10 also regulates goblet cell differentiation through the Notch signaling

pathway [348]. Moreover, this mechanism is also conserved in mice and may provide a plausible mechanism by which mutations in the genes regulating IL-10 production lead to IBD.

Another study using the zebrafish line TgBAC(*tnf*α:*gfp*) showed that mutations in the *ubiquitin-like protein containing PHD and RING finger domains 1* (*uhrf1*) gene result in decreased methylation of the *tnfα* promoter and increased TNF-α production in the intestinal epithelium [349]. Increased TNF-α causes epithelial shedding and apoptosis and ultimately induces inflammation [349]. Further studies have confirmed that mutations in *uhrf1* also cause colitis in mice due to increased TNF-α secretion by macrophages upon exposure to LPS [350]. Together, these studies suggest that polymorphisms in *uhrf1* may be an indication of susceptibility to IBD in humans.

Adoptive T cell transfer

The adoptive T-cell transfer mouse model is created by the transfer of naïve $CD4^+$ T-cells from a healthy donor mouse to a recipient mouse with severe combined immunodeficiency (SCID) or a Rag1 mouse that lacks mature B and T lymphocytes [351]. These mice experience colonic inflammation driven by the Th1 response and are generally used to study the role of T cells in mucosal inflammation [325]. Adoptive T-cell transfers are also carried out in zebrafish to study the role of T cells in adaptive immunity. However, these studies are conducted in older zebrafish, as the adaptive immune system of zebrafish is not fully developed until three to six weeks post fertilization [352].

Spontaneous mutations

Senescence-accelerated P1 mice (SAMP1/YitFc) develop spontaneous mutations that recapitulate the pathology of CD due to inflammation in the ileum [353, 354]. These mice suffer from acute and chronic inflammation of the ileum and are used to identify therapeutics that interfere with the full development of disease [325]. However, one drawback of this model is that it takes approximately 30 weeks to develop disease. Spontaneous mutations of zebrafish have been conducted using the mutagenesis agent, N-ethyl-N-nitrosourea (ENU), for forward mutagenesis screens in a colorectal cancer model, however this method has yet to be used for IBD studies [355].

Transplantation of enteric pathogens

Germ-free (GF) IL-$10^{-/-}$ and SAMP mice have also been used to investigate the correlation of microbes with IBD. Recent studies show that engraftment of microbiota isolated from IBD patients in remission to SAMP mice induce severe ileitis, which suggests that proinflammatory bacteria continue to be present in the absence of disease [356]. Furthermore, inoculation of GF IL-10 ($^{-/-}$) with *Helicobacter hepaticus*, but not wild-type mice, results in acute inflammation mediated by IFN-γ and IL-12, suggesting that *H. hepaticus* only causes disease in susceptible hosts [357]. Human enteric pathogens also cause intestinal inflammation in zebrafish. Infections of zebrafish with *Salmonella enterica* result in significant recruitment of neutrophils to the site of infection and overexpression of the genes encoding heat shock proteins Hsp70*,* HSPA4b*, and* HSPA4a [358].

Together these studies highlight the use of zebrafish as a model organism for uncovering novel IBD pathways and for investigating how microbial pathogens

contribute to IBD. As highlighted here and in other studies, zebrafish complement mouse models well and offer faster turnover rates. For example, the induction of colitis in larval zebrafish takes approximately 3 to 5 days, whereas in mice it can take anywhere from 3 to 5 weeks. My overall goal for the project detailed in this chapter was to validate a larval zebrafish model of acute inflammation to use in further studies with AIEC. In this chapter I treat larvae with different DSS concentrations and characterize the resulting intestinal inflammation.

Results

To recapitulate the immunopathology of IBD in larval zebrafish I chose to use the DSS colitis model due to its practical approach and reproducibility. Previous groups have established a base line of DSS concentrations that induce colitis at different days post fertilization and these studies helped identify a starting point [320, 331, 332, 359, 360]. Prior studies suggested that the immersion of larvae in DSS for one day would not be sufficient to induce acute colitis, because larvae recover quickly upon DSS removal. As a result, larvae were immersed in DSS for 3 days at 3 dpf during the mouth protruding stage (Fig. 3-1A). A range of different DSS concentrations (0.25%, 0.5%, and 0.75%) were tested and the percent survival was recorded (Fig 3-1 B). The immersion of larvae in 0.75% DSS caused significant mortality at 2 days post DSS exposure and 99% of the fish did not survive 3 days post DSS treatment. In contrast, treatment of larvae with 0.25% DSS did not cause significant mortality and the fish did not display any signs of inflammation. However, the percent survival of larvae treated with 0.5% DSS was lower than fish administered 0.25% DSS and higher than larvae treated with 0.75% DSS. Furthermore, the surviving larvae of the 0.5% DSS group displayed slower bursts of swimming compared to untreated larvae, which is a sign of stress in zebrafish [361]. Thus, a DSS concentration of 0.5% was chosen and phenotypic changes in DSS-treated larvae were further characterized.

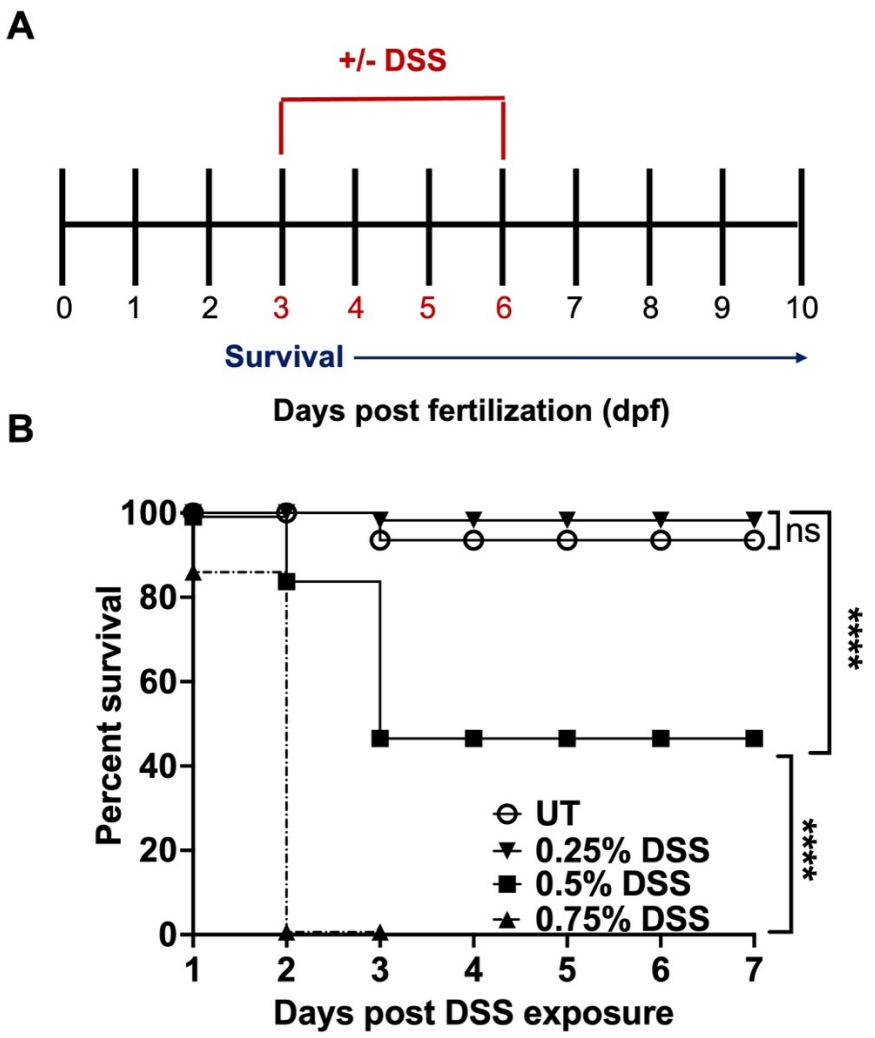

Figure 3-1. DSS immersion of larvae at 3 dpf induces mortality in a time- and dose-dependent manner.

(A) Schematic of DSS administration (red) from 3 to 6 dpf and survival experiment from 1-7 days post exposure **(B)** Survival of larvae administered 0.25%, 0.5%, or 0.75% DSS in E3 medium from 1 to 7 days post DSS exposure relative to untreated controls. Percent survival was analyzed using a Kaplan-Meier plot and Mantel-Cox test. The survival of fish treated with 0.5% DSS was significantly different than that of larvae exposed to 0.25% DSS and 0.75% DSS,****, $p < 0.0001$. n=20.

At two days post DSS exposure, some larvae were found lying on their side and unable to swim. Closer inspection revealed the absence of a fully developed swim bladder (Fig. 3-2 A) in a large percentage of treated fish, predominantly at 3 days post DSS exposure (Fig. 3-2 B). The swim bladder is a gas-filled organ essential for buoyancy and gas exchange [362]. Development of the swim bladder starts during embryogenesis and is completed by 5 dpf, once it becomes inflated [363]. It is possible that the swim bladder is not fully developed because the larvae are immersed in DSS for half of their development period. Other phenotypic changes that occurred were shortening of the intestine (Fig. 3-2 C) and stunted growth (Fig. 3-2 D). Shortening of the colon is a common phenotype in mice administered DSS due to excessive inflammation and edemas [329, 364]. Although the intestines of DSS-treated larvae were shorter, they were growing, although at a slower rate compared to untreated fish (Fig. 3-2 C and E). We did not anticipate DSS would cause shortening of the whole-body length. To assess whether shortening of the gut was caused by DSS and was not a result of overall stunted growth, linear regression analyses were conducted (Fig. 3-2 E). The negative slope of the linear regression graph suggested that during maturation the body length increases faster than length of the gut, indicating that shortening of the intestine was a result of DSS exposure.

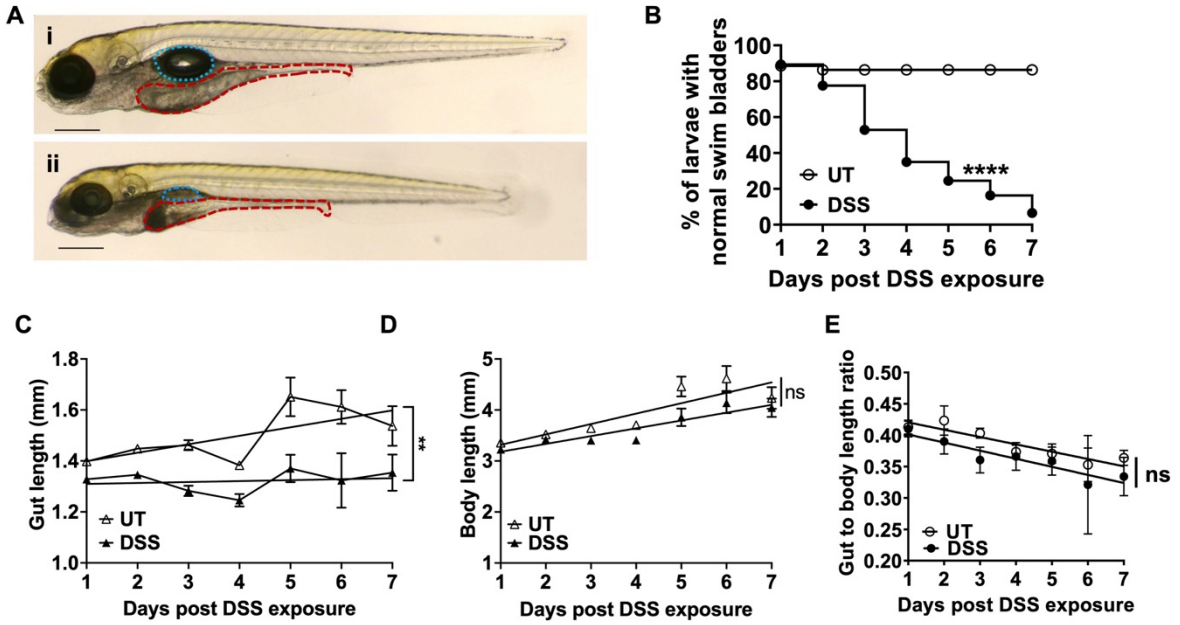

Figure 3-2. DSS inhibits full development of larval swim bladders and decreases the length of the gut and total body length.

(A) Representative images of untreated (UT) and DSS-treated larvae at 6 dpf (3 days post 0.5% DSS exposure), with the swim bladder (teal outline) and the intestine (red outline) highlighted. Scale bar = 0.3 mm. **(B)** Quantification of UT (black) or DSS-treated (red) larvae with fully developed swim bladders from 1 to 7 days post DSS exposure. Group differences were analyzed using Mantel-Cox test, ****, $p \leq 0.0001$. Quantification of the lengths of the intestine **(C)** and whole body **(D)** of UT and DSS exposed larvae from 1 to 7 days post DSS exposure in millimeters, n≥13. Group differences were analyzed with linear regression, *, $P \leq 0.05$; **, $P \leq 0.01$; ***, $P \leq 0.001$; ****$P \leq 0.0001$. **(E)** The gut to body length ratio was analyzed by linear regression. Larvae treated with DSS displayed a decreased growth rate of the gut and total body length compared to the untreated controls. The slopes of DSS and UT

groups were both negative and the elevation of the slopes were significantly different, ****P ≤ 0.0001.

The next goal was to investigate whether the histopathology of larvae exposed to 0.5% DSS recapitulated that of previously reported larval zebrafish and murine studies. At 6 dpf (3 days post DSS) larvae were collected for hematoxylin and eosin (H&E) staining, after paraffin embedding, and sectioning. The epithelium of untreated larvae displayed folds in the anterior, mid, and posterior intestine (Fig. 3-3 A). In contrast, H&E-stained sections of DSS-treated larvae showed epithelial corrosion with flat surfaces, loss of intestinal folds, and detachment of the epithelial layer from the basement membrane in all intestinal segments (Fig. 3-3 B). The midgut of untreated zebrafish was rich in mucus secreting goblet cells, whereas DSS-treated larvae showed a severe loss of goblet cells (Fig. 3-3 A vs 3B, which are the cells containing clear/light blue mucus droplets [365].

The recruitment of neutrophils is another method used to assess intestinal inflammation in zebrafish infections [331, 332]. Phagocyte recruitment is increased during DSS exposure due to disruption of the mucosal barrier, which promotes bacterial invasion and colonization of the intestinal epithelium. Neutrophils are the first responders to bacterial infections, whereas macrophages appear at later time points to mediate tissue repair and clearance of spent neutrophils [332, 366-368]; [369]; [320]. Transgenic larvae containing green fluorescent neutrophils (Tg(*mpo*::*egfp*)) or macrophages ((Tg(*mpeg1*:*egfp*)) were used to study phagocyte recruitment during DSS treatment. Neutrophil recruitment to the gut was significantly increased in DSS-treated larvae compared to the untreated controls at both 6 and 7 dpf (3 and 4 days

of DSS treatment, respectively, (Fig. 3-3 C, D)). There were also more neutrophils recruited to the intestine of DSS-treated fish at 7 dpf compared untreated groups. In contrast, macrophage recruitment was not significantly changed in untreated and DSS-treated groups (Fig. 3-4 A-B).

To evaluate the extent of inflammation, we also quantified the expression of proinflammatory marker genes at 6 and 7 dpf (3 and 4 days of DSS treatment, respectively). At 6 dpf, the expression of *cxcl8*, *il-1b*, and *mmp9,* corresponding to interleukin 8, interleukin-1β, and matrix metallopeptidase 9, respectively, were significantly increased in DSS-treated larvae compared to untreated groups, whereas *tnf*α expression was not significantly increased (Fig.3-3 E). Between 6 and 7 dpf, the expression of inflammatory markers decreased in DSS-treated fish, and expression of *cxcl8*, *il1b* and *tnfa* was similar in DSS-treated and untreated fish, whereas *mmp9* expression was still elevated (Fig. 3-3 F). Taken together, these data recapitulate key morphological and proinflammatory features described by previous groups and support our methodology of immersing larvae in DSS from 3 to 6 dpf to induce inflammation prior to introducing the bacteria.

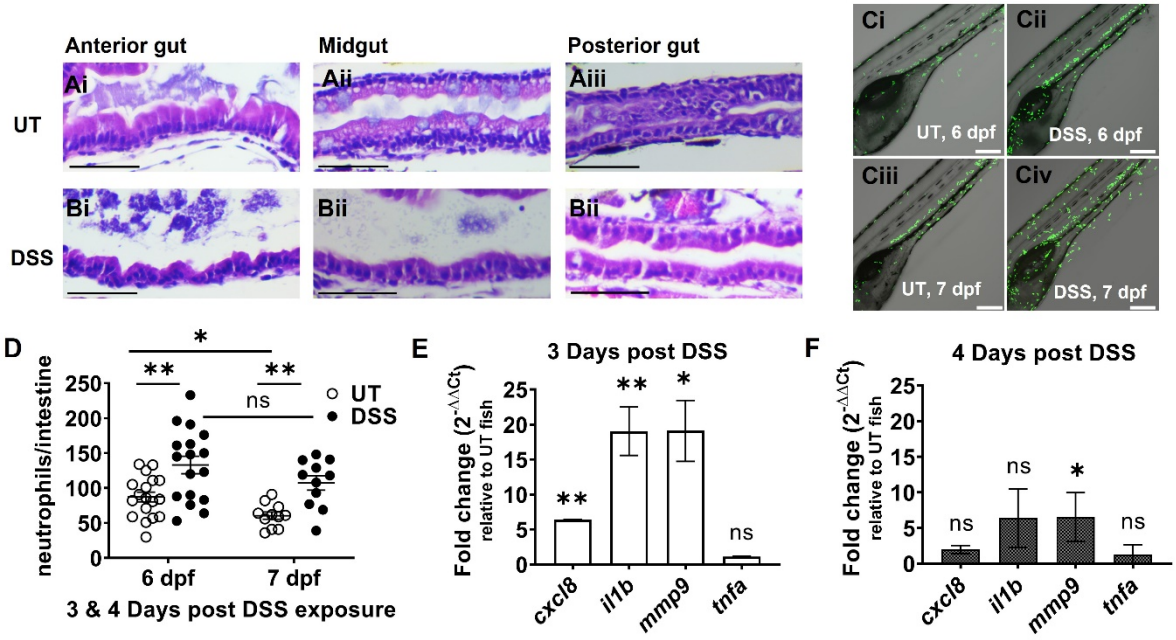

Figure 3- 3. DSS causes intestinal epithelial damage and inflammation.

(A) Longitudinal sections of the anterior, mid, and posterior intestine from control **(Ai-iii)** and DSS-treated **(Bi-iii)** larvae at 6 dpf; n=4. Scale bar = 50 μm. **(C)** Representative images of Tg(*mpo*::*efgp*) larval zebrafish. Recruitment of GFP-producing neutrophils to the whole gut (outlined by the red box) was analyzed using live-cell confocal analysis from 6-7 dpf **(Ci-iv)**. Larvae were imaged for 18 h (3-20 hpi), a complete Z-stack of 190 images is shown. Scale bar = 200 μm. **(D)** Quantification of neutrophils in the intestine at 6 and 7 dpf (3- and 4-days post DSS treatment); unpaired two-tailed t-test, n≥11, **(E)** qRT-PCR analysis of *cxcl8, il1b, mmp9,* and *tnfα* in DSS-treated larvae relative to untreated controls at 6 dpf and 7 dpf; n=3. **(F)**. Unpaired two-tailed t-test. Mean with SEM, *, P ≤ 0.05; **, P ≤ 0.01.

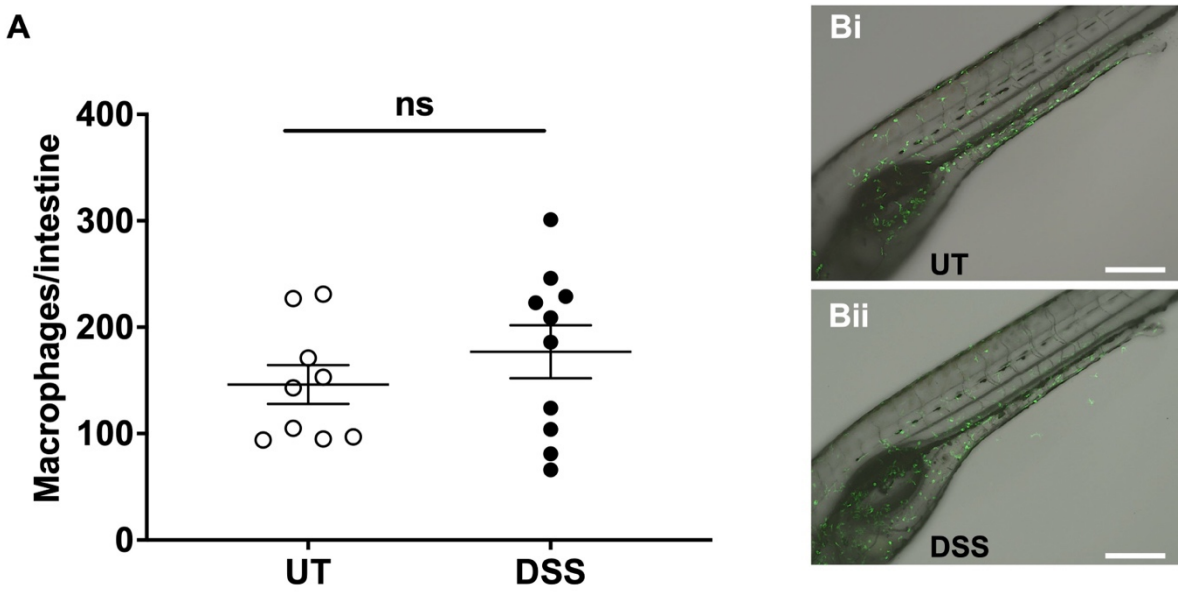

Figure 3-4. Macrophage recruitment to the intestine does not change after DSS treatment.

(A) Enumeration of macrophages recruited to the intestine of Tg(*mpeg1*::*egfp*) larvae treated with DSS for 3 days and control (UT) larvae. **(B)** Live imaging of whole-mount untreated **(Bi)** and DSS-treated **(Bii)** larvae with green, fluorescent macrophages; n≥9, unpaired two-tailed t-test. Mean with SEM. Scale bar = 200 μm.

To investigate why the expression of *tnfα* was not significantly expressed, PCR was performed on larvae that displayed significant inflammation after 3 days of exposure to DSS. These fish had a heartbeat, but were unable to swim and had intestinal edemas (Fig. 3-5A). The expression of *cxcl8*, *il1b*, mmp9 and *tnfα* were assessed relative to untreated (Fig. 3-5 B) and healthy DSS-treated larvae (Fig. 3-5 C). The expression of *il1b* and *mmp9* were significantly increased compared to healthy control fish (Fig. 3-5 B) and *mmp9* and *tnfa* transcripts were also slightly significantly increased in fish with severe inflammation compared to those that appeared normal after DSS exposure (Fig. 3-5 C). This data suggested that non-swimming and severely inflamed fish were suffering from severe inflammation and that an increase in the relative expression of the gene encoding TNFa does occur after DSS exposure. However, the relative fold change of *tnfa* may be less than that of other proinflammatory cytokines.

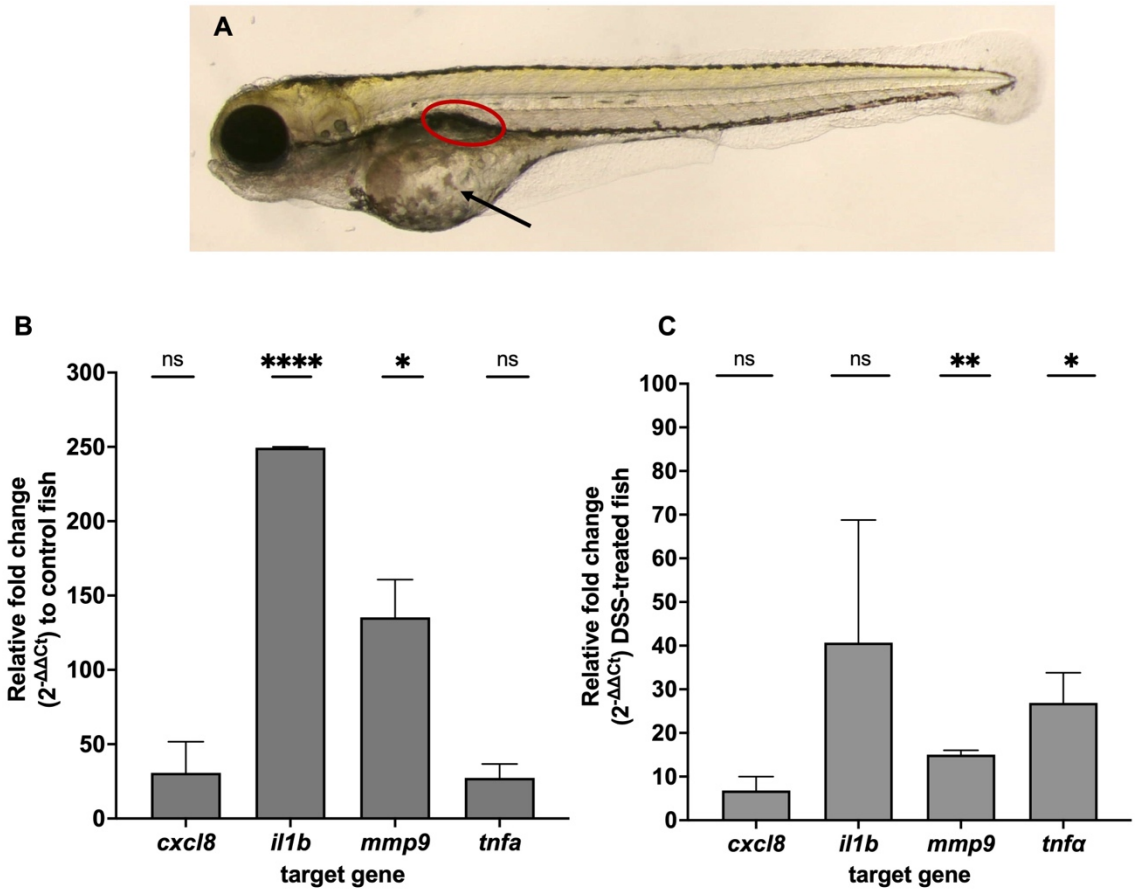

Figure 3-5. DSS creates severe inflammation in some larvae after 3 days of exposure.

(A) A representative image of severely inflamed fish without a swim bladder (outlined in red) and with intestinal edema (black arrow). **(B)** qRT-PCR analysis of *cxcl8, il1b, mmp9,* and *tnfa* in severely inflamed DSS-treated larvae relative to untreated controls; n=2, and **(C)** relative normal DSS-treated fish at 6 dpf (3 days post DSS); Unpaired two-tailed t-test, n=2. Mean with SEM, *, P ≤ 0.05; **, P ≤ 0.01; ****P ≤ 0.0001.

Discussion

The overall goal for this chapter was to generate a larval zebrafish model of acute inflammation. The data suggest that this is accomplished by repetitive administration of 0.5% DSS. Although inflammation is observed after immersion of larvae in DSS for 3 days, the state of inflammation is resolved by 1 day post DSS removal as suggested by histological analyses of the intestine and quantitative real-time PCR (qPCR) of the proinflammatory genes. It is hypothesized that the association of DSS with intestinal fatty acids facilitates its paracellular transport through the claudins and through this mechanism it disrupts the integrity of the membrane and induces a proinflammatory response [370]. Zebrafish larvae are known to have striking regenerative abilities. Others have shown that the intestinal injuries caused by DSS in larvae are promptly resolved 1 day after DSS removal and that burn wounds on the caudal fins of zebrafish heal 4 days post injury [359];[371].

Due to the mode of administration, DSS unintentionally has off-target effects including on the swim bladder and overall body length. Nonetheless, intestinal inflammation is still observed as indicated by the increased recruitment of neutrophils to the intestine, transcription of genes encoding proinflammatory cytokines, and smoothening of the intestine. The evaluation of intestinal inflammation varies between organisms. In mice readouts of intestinal inflammation caused by DSS include intestinal permeability, increased transcription of genes encoding proinflammatory cytokines, severe bleeding, diarrhea, decrease in mucin secretion and goblet cells, infiltration of neutrophils into the submucosa and occasionally in the crypts, and death [329]. The presence of diarrhea and rectal bleeding are difficult to visualize in larvae due to their size, however the other readouts can be observed in zebrafish. In contrast,

diagnosis of Crohn's disease and ulcerative colitis in humans is conducted by the analysis of blood and stool samples that identifies inflammation biomarkers in blood (c-reactive protein and erythrocyte sedimentation rate) and in stool samples (calprotectin and lactoferrin) and by endoscopy to visualize inflammatory bowel lesions [372]. Recent studies also show that adult zebrafish produce S100A-10b, a protein homologous to calprotectin, in response to intestinal inflammation [373]. Here, I have not assessed whether calprotectin produced by larvae is secreted in response to DSS, however it is something that could be performed in future studies.

One of the major differences between the DSS mouse and the zebrafish model is that DSS predominantly causes colitis in rodents and to a lesser extent inflammation in the ileum, whereas in fish DSS causes inflammation throughout the whole intestine (enterocolitis) [374]. The reason for this difference could be explained by the DSS delivery approach. Mice intake DSS ad libitum through drinking water, whereas zebrafish continuously up take DSS. Thus, it is possible that in mice most of the DSS is absorbed in the colon, whereas in zebrafish larvae DSS is continuously absorbed by various cell types due to the constant exposure. Of note, an aggregation of neutrophils was often observed in the cloaca of DSS-treated zebrafish (3-3 C i-iv), however histological sectioning showed that the whole intestine was damaged.

Upon intestinal barrier damage, commensal bacteria invade the epithelium, which results in intestinal inflammation. Neutrophil recruitment to the intestine was significantly upregulated in DSS-treated fish relative to untreated controls, possibly as an effort to control bacterial invasion to the epithelium. However, the average number of macrophages was not significantly changed between DSS and untreated fish (Fig.

3-4 A). Larval zebrafish studies show that although neutrophils efficiently phagocytose bacteria on the surface of tissue, macrophages specialize in engulfing bacteria located in fluid-filled cavities and or blood [375]. Macrophage recruitment to the intestine may not be significantly changed in untreated and DSS-treated fish since the role of macrophages is to clear microbes from fluid environments.

Neutrophils are key players in the initial stages of inflammation. After migrating to the site of infection, neutrophils phagocytose microbes, release antimicrobials peptides, and produce cytokines that activate macrophages and initiate tissue repair [376]. Here the relative expression of the genes encoding the proinflammatory cytokines interleukin 8 (*il8 or cxcl8*), interleukin-1-β (*il1b*), and matrix metallopeptidase 9 (*mmp9*) was observed to be increased relative to the untreated controls. IL-1β, IL-8, and TNF-α are primarily produced by macrophages. However, IL-8 is mainly associated with the activation and mobilization of neutrophils, whereas IL-1β and TNF-α are involved in signaling pathways that regulate apoptosis and cell survival [377]. During inflammation MMP9 degrades the extracellular matrix and through this process it activates cytokines to that mediate tissue/wound healing [378]. A decrease in the expression of proinflammatory cytokines at 7dpf (24 h post DSS) may suggest that inflammation is resolved in DSS-treated larvae, a process that is necessary to prevent chronic inflammation.

TNF-a appeared to be the only proinflammatory cytokine that was not significantly upregulated. Figure 3-5 suggests that the relative expression of *tnfa* is less than that of *il1b* and *mmp9* in healthy DSS-treated fish (fish able to swim) and surprisingly also in fish that appear have elevated inflammation as characterized by edemas in the gut

and failure to swim. Moreover, the relative expression of the gene encoding TNF-α in fish with severe inflammation is increased 30-fold relative to DSS-treated fish with less diseased phenotypes (Fig. 3-5 C). Thus, this might explain why *tnfa* is not significantly upregulated in the larvae that were previously assessed (Fig. 3-3 F). To conduct bacterial infection experiments (detailed in the next chapter) it is important that DSS-treated larvae can swim properly and for this reason only healthy DSS-treated larvae will be used in future experiments.

Chapter 4: Larval Zebrafish as a Model Organism for AIEC Infections

Introduction

Several approaches have been used to introduce foreign bacteria into zebrafish. The simplest route of bacterial inoculation is the bath immersion model. This method involves the immersion of larval or adult zebrafish in an environment containing high concentrations of bacterial pathogens (10^{10} CFU/ml), such that the fish take up the pathogen *ad libitum*. This model is advantageous for investigating how the immune system responds to local infections after the zebrafish have been externally injured [379]. However, one drawback of this model is that the amount taken up by the zebrafish varies between fish and it is difficult to retain a high bacterial burden for subsequent colonization by mammalian pathogens. Another drawback is that this method cannot be used to inoculate zebrafish with obligate anaerobic bacteria, which include many intestinal pathogens.

In contrast to immersion, a precise bacterial load at a specific anatomical site may be introduced to zebrafish using microinjection. The site of administration may be chosen based on the desired response (Fig. 4-1). Systemic bacterial infections are accomplished through microinjection into the duct of Cuvier (cardinal vein that empties blood into the first chamber of the heart), the caudal vein (largest vein in tails of vertebrates) and with intraperitoneal injections [380, 381]. Local infections can be established through intramuscular injections or injections in the notochord [379]. The zebrafish notochord is a tissue that is similar to cartilage and analogous to the human bone, and is inaccessible to neutrophils and macrophages [382, 383]. Other microinjection sites that result in localized infections include the hindbrain ventricle, otic vesicles, yolk sac, and the tail fin [313]. Interestingly, hindbrain infections show

that *Bdellovibrio bacteriovorus* synergizes with the innate immune system to clear infections of antibiotic resistant *Shigella flexneri[384]*.

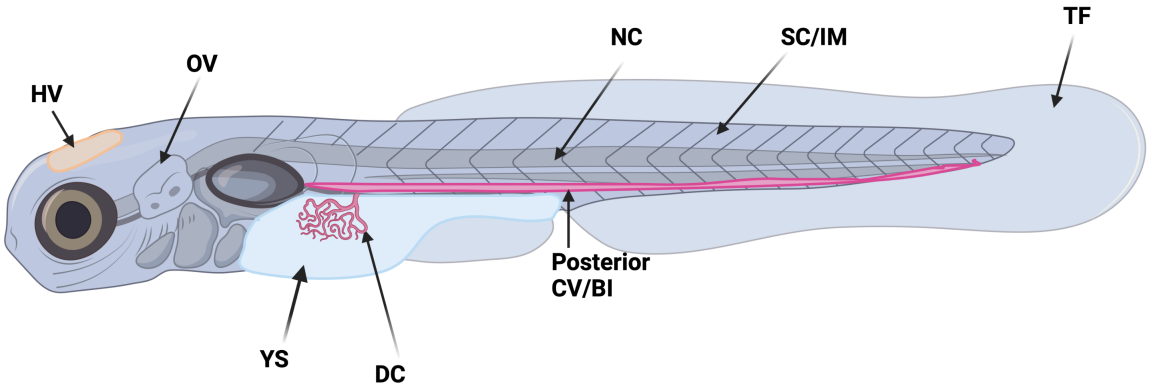

Figure 4- 1. Localized and systemic infections in larval zebrafish are achieved by inoculation at different anatomical regions.

Intravenous injections of microbes at the caudal vein (CV), blood island (BI), or the duct of Cuvier (DC) results in microbial dissemination throughout the bloodstream. Immune cell recruitment studies can be performed by intramuscular (IM) or subcutaneous (SC) injections or by injections within the hindbrain ventricle (HV), otic vesicle (OV), tail fin (TF). Localized infections may occur within the yolk sac (YS), HV, TF, and OV. Injections at the notochord (NC) permit the study of bone and cartilage inflammation. Image was created with BioRender.

Alternatively, a bacterial suspension may be administered to adult and larval zebrafish through oral gavage [385, 386]. However, this approach requires specialized equipment for the insertion of a needle into the mouth of the fish through the esophagus and into the anterior intestinal bulb, a procedure that can be challenging to learn and apply reproducibly. More recently, our lab has established a model of food-borne infections using the protozoan *Paramecium caudatum* as a way to deliver the pathogen into the gastrointestinal tract [297, 314]. Paramecia prey on bacteria and are a natural food source of larval zebrafish. Ingestion of bacteria by paramecia is followed by bacterial internalization in an acidifying storage vacuole, which is hypothesized to prime gastrointestinal pathogens, similarly to the mammalian stomach, prior to consumption of the bacteria-loaded paramecia by larvae [297]. This approach has been shown to efficiently deliver EHEC into the zebrafish intestine [314]. Colonization of EHEC in the larvae intestine prompts the expression of virulence genes and decreases the survival of infected larvae [314].

Other gastrointestinal pathogens previously modeled in larval zebrafish include major aquaculture and opportunistic human pathogens. *Edwardsiell*a and *Aeromonas* species are acquired by consumption of contaminated food and cause gastroenteritis in immunocompromised humans and zebrafish [387, 388]. Infection studies of zebrafish with *Edwardsiella tarda* suggest that the type III secretion system is essential for bacterial replication in phagocytic cells and have contributed to the identification of novel invasins and flagellar components involved in adhesion and biofilm formation [389-391]. Similarly, the immersion of zebrafish with *Aeromonas sp*. results in

intestinal inflammation, alters the intestinal microbiota of the host, and induces the secretion of extracellular enzymes that degrade host cells [379, 392, 393].

Some members of the *Vibrio* genus are natural fish pathogens and are transmitted to humans through contaminated food [394]. Once colonized, the host may develop vibriosis, an illness involving diarrhea, nausea, and fever, and may be susceptible to bacteremia depending on the colonizing strain [395]. *V. cholerae* is the causative agent of cholera and a good colonizer of the zebrafish intestine [396]. Using zebrafish as a model organism, studies show that although the cholera toxin is dispensable for colonization and pathogenesis in zebrafish, the accessory toxins RTX and hemolysin A (HlyA) are essential during intestinal colonization and are regulated by the metabolic regulator cAMP receptor protein (CRP) during host infection [397].

Other enteric bacteria that are not natural fish colonizers, but have been successfully modeled in zebrafish larvae are *Salmonella enterica* serovar Typhimurium and *E. coli*. Infection of larvae with *Salmonella* causes inflammation in the intestine and cloaca and causes neutrophil recruitment to the site of infection, a process that is dependent on IL-8 and leukotriene B4 [398]. Further, human commensal *E. coli* strain Nissle and *E. coli* 40, also colonize larval zebrafish, and reduce the colonization of *V. cholerae* by decreasing the intestinal pH due to glucose metabolism [399].

Altogether these studies support the establishment and characterization of larval zebrafish as a model organism for adherent-invasive *E. coli* infections (AIEC). Here, paramecia were used as delivery vehicles for AIEC to the zebrafish intestine. This model was chosen because it facilitates the introduction of AIEC into the lumen

following the ingestion of AIEC-loaded paramecia and allowed us to investigate whether AIEC invades the host or is successfully cleared.

Results

Clinical AIEC strains isolated from the ileum and colon exhibit antibiotic resistance

In the previous chapter a larval zebrafish model of colitis was characterized to investigate whether larvae with preexisting inflammation are a suitable model organism of AIEC infection. Current AIEC studies in mice suggest that AIEC are true pathobionts, as they only cause disease in animals suffering from intestinal inflammation attributed to genetic or environmental factors [202]. Since numerous clinical studies suggest that AIEC are important disease modifiers, the search for AIEC targeting-strategies is on-going. Early studies are generally conducted in tissue culture cells prior to advancing to a mammalian system. However, the results obtained *in vitro* may not always be translatable *in vivo*. Thus, it would be advantageous to have a high-throughput animal model with similar hallmarks of infection to the mammalian model, for the identification of therapeutics and the discovery of novel mechanisms of AIEC pathogenesis. For this reason, I set out to investigate whether the larval zebrafish model is suitable for the modeling of AIEC infections.

The first aim of this project was to investigate the antibiotic susceptibility of AIEC strains isolated from IBD patients to establish the model. These AIEC strains were acquired from the Diehl lab (in Baylor College of Medicine) and were used in prior studies to identify genes associated with the AIEC phenotype and pathways involved in virulence [178]. The susceptibility to ampicillin, kanamycin, tetracycline, and chloramphenicol in AIEC strains 50, 341, 342, 343, 344, 345, 346, 347, 356, 365, 366, and LF82 was assessed using the Kirby-Bauer disc diffusion susceptibility test to identify an appropriate marker of fluorescent protein-expressing plasmids.

Susceptibility or resistance to the antibiotics was determined based on previously published cutoff values of the diameter of the zone of inhibition [400]. Quantification of the zone of inhibition (Table 4-1) suggested that 50% of the strains (AIEC 342, 345, 346, 347, 356, and LF82) are resistant to ampicillin (as no growth inhibition was observed) and that all strains are susceptible to either tetracycline or chloramphenicol, except for AIEC 366.

To complement these results, AIEC strains were grown in liquid cultures with the same antibiotics, but at different concentrations (Fig. 4-2). The reference strain, AIEC LF82 (Fig. 4-2 A) did not grow well in low concentrations of tetracycline (10 μg/mL) and chloramphenicol (25 μg/mL), but grew in the liquid culture containing kanamycin (50 μg/mL), which was in accordance with the data quantified in Table 4-1. Likewise, the growth of the AIEC strains 50, 341, and 343 was inhibited by tetracycline and chloramphenicol (Fig. 4-2 B,C,D), which was also observed in the disk diffusion assays (Table 4-1). Surprisingly, increasing the concentration of ampicillin by 10-fold remained ineffective at inhibiting the growth of the AIEC stains (Table 4-1 and Fig. 4-2). Consequently, we decided to use a tetracycline resistance marker for future experiments. These AIEC strains were transformed with a plasmid encoding mCherry and the tetracycline repressor (for tetracycline resistance) and kept for future experiments.

Table 4- 1. Most of the AIEC strains that were isolated from patients are susceptible to tetracycline and/or chloramphenicol.

After streaking bacteria on LB plates, antibiotic discs were added, and the plates were incubated at 37 ^{o}C for 24 hr. Following the incubation, the diameter of the zone of inhibition was measured in centimeters (cm). Based on previously established values, ampicillin (10 µg), kanamycin (30 µg), tetracycline (30 µg) and chloramphenicol (30 µg) discs were considered effective antimicrobial agents if the measured zone of inhibition was greater than 1.6, 1.7, 1.8, and 1.7 cm, respectively [400]. The dimeter measurements that were above the cutoff values and a sign of antibiotic susceptibility are shown in bold.

AIEC Strain	Amp (10)	Kan (30)	Tet (30)	Chl (30)
50	**1.7**	1.5	**2**	**2.3**
341	**1.7**	1.6	**1.9**	**2**
342	No inhibition	No inhibition	1.7	**2.8**
343	1.6	**2**	1.7	**2.1**
344	1.5	1.7	1.8	**1.9**
345	No inhibition	**1.9**	1.9	2.3
346	No inhibition	1.6	1.8	**2.1**
347	No inhibition	1.5	1.7	**1.8**
356	No inhibition	1.5	**1.9**	1.6
365	**1.9**	**1.8**	No inhibition	**2.3**
366	**1.7**	**1.9**	No inhibition	No inhibition
LF82	No inhibition	1.7	**2**	**2**

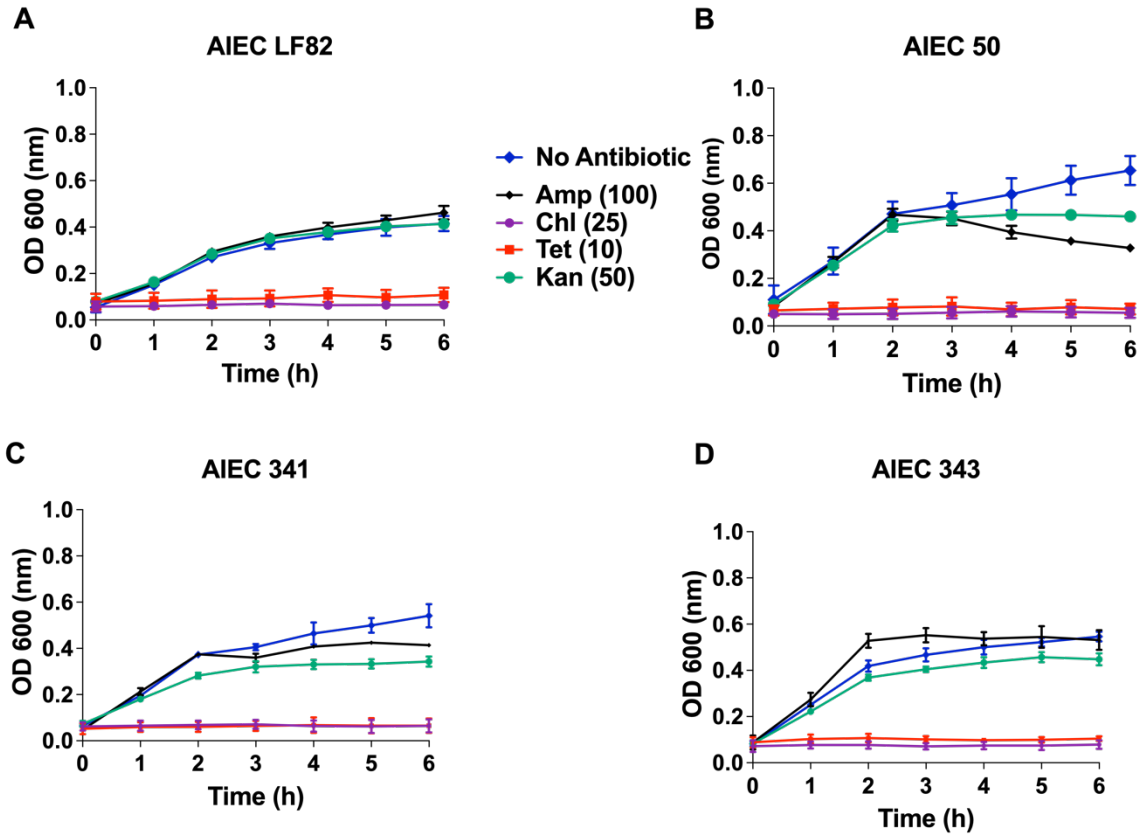

Figure 4- 2. The growth of AIEC reference strains LF82, 50, 341, and 343 is suppressed by tetracycline and kanamycin.

AIEC strains **(A)** LF82, **(B)** 50, **(C)** 341, and **(D)** 343 were adjusted to an initial OD of 0.1 and the growth in a 96-well plate was assessed every hour for 6 hours in the presence or absence of antibiotics. n=3. Mean and SEM. Blue= no antibiotic, black = ampicillin (100 µg/mL), purple = chloramphenicol (25 µg/mL), red = tetracycline (10 µg/mL), green = kanamycin (50 µg/mL).

Paramecia engulf and deliver AIEC to the zebrafish intestine

As mentioned in the introduction, paramecia were used as vehicles to deliver of AIEC into the zebrafish intestine. In the model AIEC are fed to paramecia and the AIEC-loaded paramecia are incubated with zebrafish larvae (Fig. 4-3 A). To approximate the bacterial dosage consumed by the zebrafish following a 2-hour incubation of larvae with AIEC-loaded paramecia, I first determined the AIEC LF82 half-life (the time at which the initial AIEC quantity inside of the paramecia is halved) following uptake by paramecia. This was an important step since bacteria consumed by paramecia are internalized in a storage vacuole that acidifies and degrades its contents over time [401]. The reference AIEC strain LF82 was transformed with the mCherry plasmid pME6032, containing tetracycline resistance, to visualize LF82 inside of paramecia and zebrafish.

The uptake of AIEC by paramecia occurred almost instantly, as the presence of 790 colony-forming units (CFUs) per paramecia was observed minutes after the introduction of LF82 (Fig.4-3 B, Time 0). This is in accordance with other studies that show that paramecia engulf their targets within seconds to minutes after their identification [314, 402]. Based on the number of CFUs per paramecia over the course of 6 hours, the LF82 half-life (τ) was shown to be 2.3 hours (Fig. Fig.4-3 B). The LF82 decay rate (k) inside of paramecia was then determined based on the LF82 half-life (2.3 h) and found to be 0.30 h^{-1} (Fig. 4-3 C). The rate at which larvae feed on paramecia (prey rate) was also determined based on video analysis (Fig. 4-3 E,F). Based on the half-life, decay rate, number of CFUs at time 0, and prey rate, the

theoretical LF82 dosage consumed by fish following a 2-hour incubation of larvae with LF82-containing paramecia was approximated to be 6.7 x 10^5 CFUs (Fig. 4-3 D).

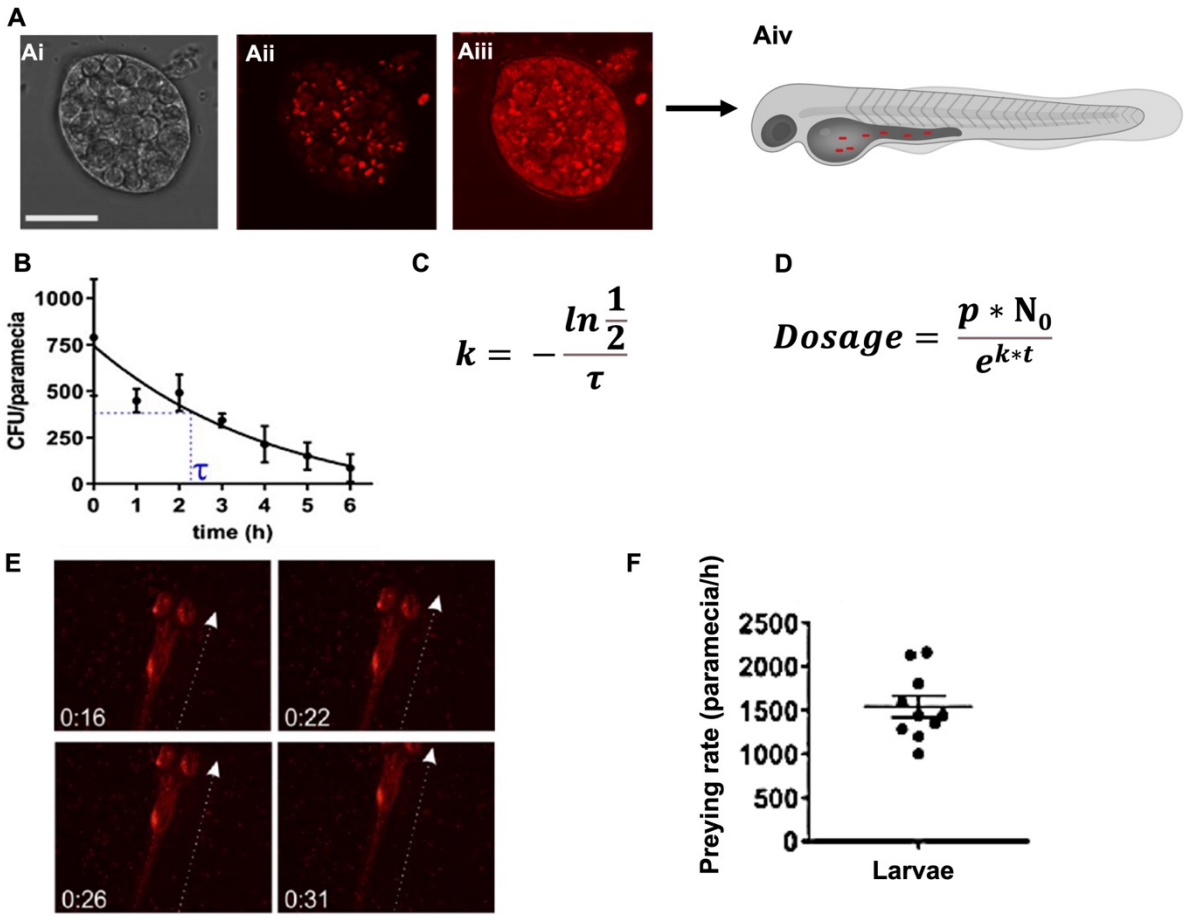

Figure 4- 3. The bacterial dosage is dependent on the half-life of AIEC LF82 inside of paramecia and the prey rate of larval zebrafish on AIEC-containing paramecia.

(A) Paramecia (Ai) were co-cultured with 10^8 mCherry-expressing AIEC LF82 (Aii,Aiii, red). Following a 2-hour co-incubation of paramecia and AIEC LF82, paramecia-containing AIEC were fed to larval zebrafish (Aiv), scale bar = 20 μm. **(B)** AIEC-loaded paramecia were sampled from 0-6 hours post incubation to count CFUs of AIEC per paramecia and to determine the paramecia concentration, and CFUs/ paramecia was calculated. The number of AIEC CFUs per paramecia was 790 at time 0. The half-life (τ) of AIEC LF82 in paramecia is 2.3 hours. Error bar, mean +/- SEM **(C)** The decay

constant (k) is determined based on the half-life (τ) of AIEC LF82 and is 0.30 h^{-1}. (Non-linear fit, first order decay); Half-life: 2.3 hrs, n=3. **(D)** The equation used to calculate the bacterial dosage consumed by larval zebrafish after a 2-hour incubation (t) of larvae with AIEC-containing paramecia. This equation takes into account the rate at which larvae prey on paramecia (p), the initial bacterial quantity at time 0 (N_0), and the decay rate of AIEC (k). **(E)** Still images from a video used to determine the prey rate of larvae on paramecia. The prey rate was 1539/h based on video analysis, n= 10 **(F)**. Plugging in these values into **(D)** results in a bacterial dosage of 6.7 x 10^5 CFUs following a 2-hour incubation of AIEC-containing paramecia with larval zebrafish.

Flores, E., Thompson, L., Sirisaengtaksin, N., Nguyen, A. T., Ballard, A., Krachler, A. M. Using the protozoan *Paramecium caudatum* as a vehicle for food-borne infections in zebrafish larvae. J. Vis. Exp. (143), e58949, doi:10.3791/58949 (2019), by permission of JoVE Journal.

Adherent-invasive *E. coli* LF82 and non-pathogenic *E. coli* MG1655 colonize the gut with a similar burden, but AIEC persists longer

After establishing the bacterial dosage consumed by fish, the next task was to investigate how AIEC would interact with the GI tract of healthy zebrafish larvae (hereafter referred to as untreated (UT) fish). The survival of larvae infected with LF82 or the nonpathogenic *E. coli* strain MG1655 was also assessed. Surprisingly, fish infected with either LF82 or MG1655 had 100% survival from 2 to 48 hpi (Fig. 4-4 A). To determine whether LF82 exhibits different colonization patterns compared to MG1655, infected larvae were homogenized and plated on selective CHROMagar™. Here, AIEC LF82 formed dark, steel-blue colonies that were distinguishable from MG1655 (mauve), and the larva's endogenous microbiota (white, Fig.4-4 B). PCR analysis further confirmed that the steel-blue and mauve colonies were indeed LF82 and MG1655, respectively (data not shown).

Following food-borne delivery, AIEC and MG1655 were taken up by the larvae at similar concentrations (Fig. 4-4 C, 2 hpi), however at later time points, AIEC formed a significantly higher burden within fish than *E. coli* strain MG1655 (6-24 hpi). The number of detected MG1655 CFUs in homogenized zebrafish samples decreased after 6 hpi and by 24 hpi no MG1655 CFUs were detected (Fig. 4-4 C). Interestingly, the number of LF82-infected fish with a burden below the detection limit also began to increase from 6 to 24 hpi, and by 30 hpi the burden of LF82 was significantly decreased compared to prior timepoints. To get a better representation of the difference in colonization between these two *E. coli* strains, the bacterial persistence was analyzed and quantified as the percent of fish that contained AIEC and MG1655

burdens above the detection limit (10 CFUs). As shown in Fig. 4-4 D, AIEC LF82 was significantly more persistent than non-pathogenic *E. coli* MG1655 from 2 to 24 hpi. Altogether these data suggests that AIEC LF82 forms a slightly higher burden and persists longer inside larval zebrafish compared to nonpathogenic *E. coli*.

The next task was to investigate the localization of AIEC inside of the larval zebrafish intestine. Following administration of AIEC LF82::mCherry and MG165::mCherry to UT larvae, AIEC was observed in the foregut, lumen, and attached to the midgut epithelium (Fig. 4-5 A). Closer observation of LF82 and MG1655 in the midgut revealed that both strains were internalized by the intestinal epithelium and located within the cytoplasm, which was outlined by phalloidin (shown in cyan) (Fig. 4-5 B). At 2 hpi individual red LF82 and MG1655 cells were predominantly observed (Fig. 4-5 Bi, Biv). However, LF82 clusters became more prominent at 24 and 30 hpi (Fig. 4-5 Bv-vi). In contrast, individual MG1655 cells observed at 2 hpi gradually disappeared from 24 to 30 hpi (Fig. 4-5 Bii-iii). These observations were in agreement with the burden data shown in Fig 4-4, C-D.

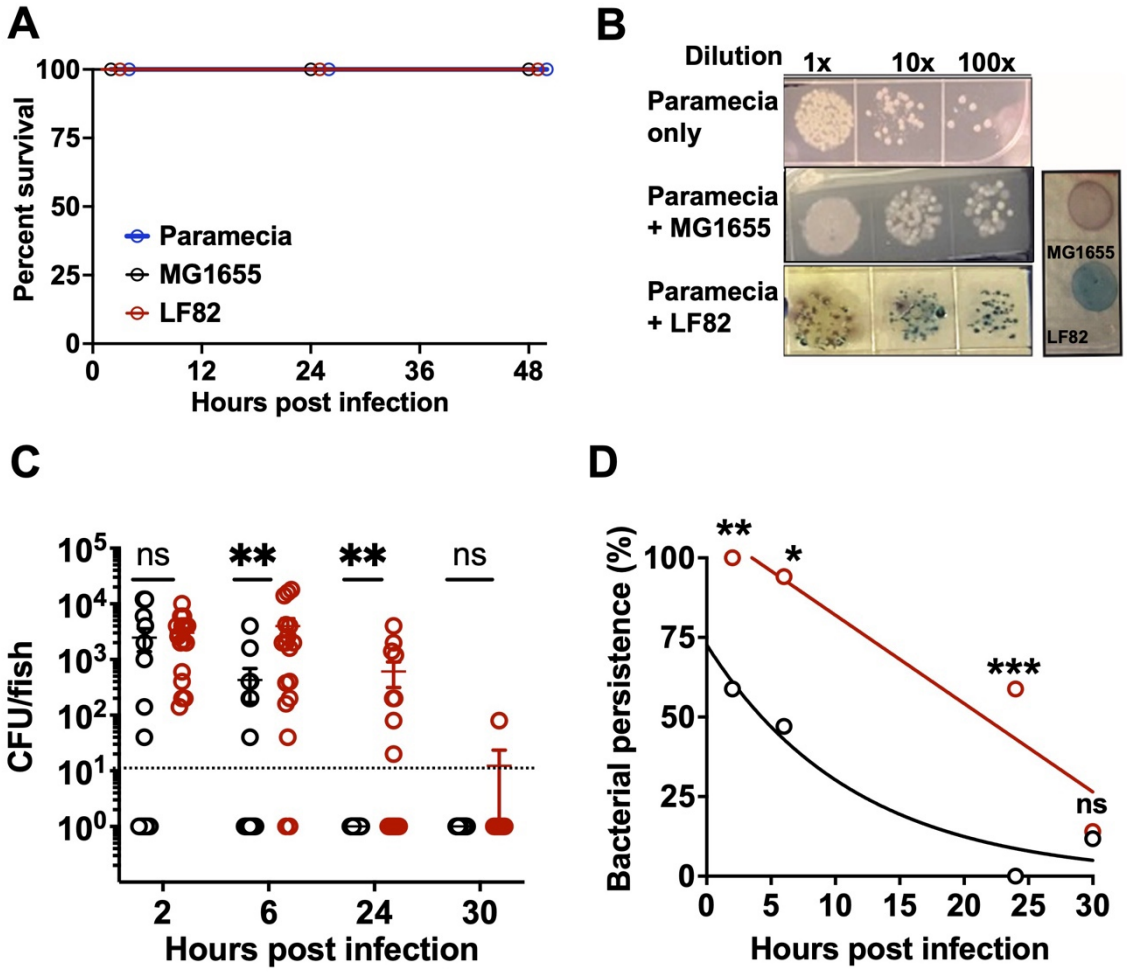

Figure 4- 4. AIEC LF82 persists longer than nonpathogenic *E. coli* MG1655 in healthy larval zebrafish but does not cause mortalities in infected fish.

(A) Survival of larvae fed paramecia and paramecia with or without *E. coli*. **(B)** Bacterial colonies grown on a CHROMagar™ plate. The zebrafish microbiota forms white colonies and is distinguished from AIEC LF82, which forms dark steel-blue colonies, and *E. coli* MG1655, which forms mauve colonies. **(C)** Quantification of LF82 (red) and MG1655 (black) CFUs per fish. The detection limit was 10^1 (dashed line), this was the lowest CFU number that was detected in all dilutions. Fish that did not have any detectable *E. coli* were annotated as "1". n <15 fish/condition, p values; **,P=

0.0099, *P = 0.0312. Non-linear regression first order decay, ROUT outlier test with Q=0.2%, Paired t-test and Wilcoxon test. **(D)** Bacterial persistence was quantified as percentage of fish that contained a burden of AIEC and MG1655 above the detection limit from 0 to 30 hpi. Significance in persistence **(D)** at 2, 6, 24, and 30 hpi were: **,P= 0.0019, *,P= 0.0104, ***, P=0.006, and ns, P > 0.05, respectively. Persistence was analyzed using a Fisher's exact test.

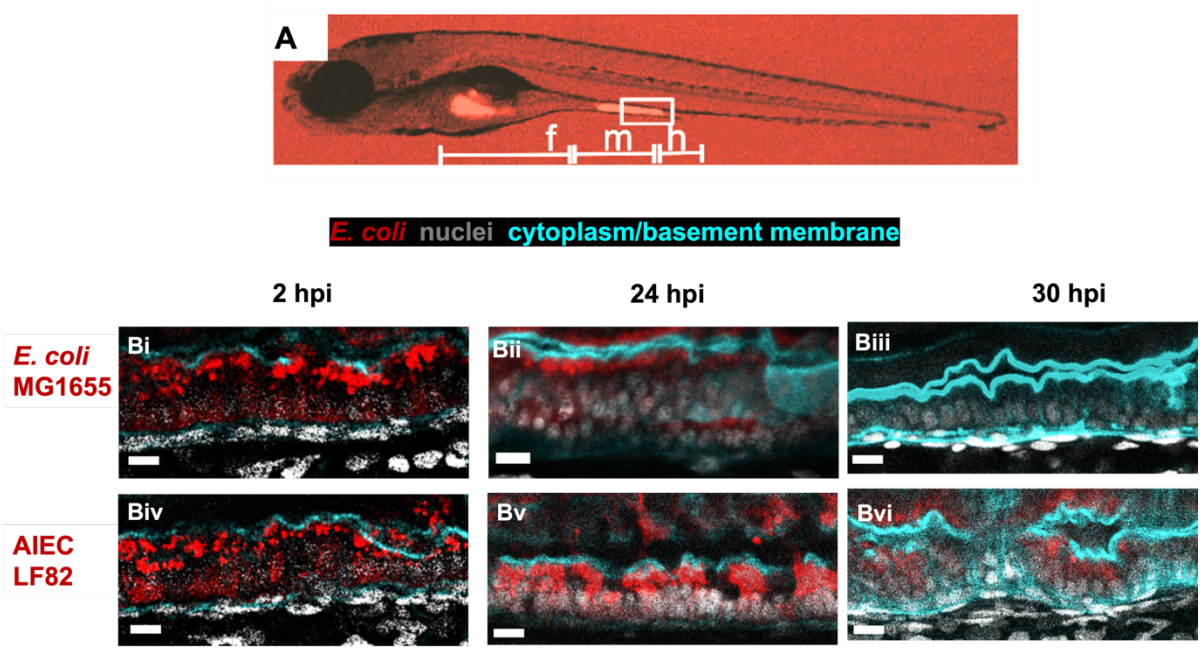

Figure 4- 5. LF82 and MG1655 colonize the cytoplasm of intestinal epithelial cells after 2 hpi.

(A) Larvae infected with LF82 and imaged at 10X. The intestinal segments are separated into the foregut (f), midgut (m), and hindgut (h). Figure B are magnified (60X) images of the area identified by the box in A. **(Bi-vi)** Sagittal views of the midgut of larvae infected with MG1655 **(Bi, Bii, Biii)** and LF82 **(Biv, Bv, Bvi)** at 2, 24, and 30 hpi. Scare bar = 100 um. *E. coli* (red) inside of the cytoplasm (cyan, stained with anti-laminin) of the columnar intestinal epithelium (white) at 2, 24, and 30 hpi. The basement membrane is slightly outlined by anti-laminin (parallel horizontal teal lines at the bottom edge of the intestine) and contains flat endothelial cells that comprise the vasculature.

Preexisting colitis and AIEC infection synergize to increase proinflammatory responses

Although AIEC colonizes the gastrointestinal tract of healthy hosts, it is more prevalent in hosts experiencing chronic inflammation, such as with patients suffering from IBD [186, 240, 241]. Consequently, the larval model was expanded to address whether preexisting inflammation affects AIEC colonization. Following the protocol established in the previous chapter, DSS was administered to larval zebrafish from 3 to 6 dpf, at which point DSS treatment stopped, and *E. coli* was introduced (Fig. 4-6 A). AIEC LF82 were administered to larvae at 6 dpf because at this stage the intestine is fully functional [306]. Larvae that were moribund or had defective swim bladders were excluded from bacterial infection experiments to prevent the paramecia from preying on the sick fish.

The burden of LF82 in DSS-treated zebrafish at 2 hpi was bimodal with half of the larvae containing more LF82 than the rest and slightly more than untreated fish, (Fig. 4-6 B), but not significantly different than the average burden of AIEC in untreated fish. Although the burden of LF82 fluctuated, the average burden remained within the range of 100-10,000 CFUs per fish from 2 to 48 hpi and was significantly higher than that of untreated controls at 6 and 12 to 48 hpi (Fig. 4-6 B). Further, the persistence of LF82 in DSS-treated larvae was significantly higher compared to untreated fish (Fig. 4-6 C). These results suggested that preexisting inflammation enhances the persistence of LF82 in the intestine of larval zebrafish. Further, these results are in accordance with those of published murine studies that show that AIEC persists longer in mice with IBD compared to healthy controls [234, 403, 404].

To investigate whether the colonization of AIEC was enhanced due to pre-existing inflammation or due to AIEC's pathogenicity, the colonization patterns of MG1655 in DSS-treated larvae were also assessed. The burden of LF82 was significantly higher than MG1655 at 2, 6, 24 and 48 hpi (Fig. 4-6 D). Surprisingly the burden of MG1655 was higher in some larvae sampled at 30 hpi compared to those sampled at 24 hpi. However, by 48 hpi, the number of fish that contained MG1655 significantly decreased and the persistence of MG1655 was lower than that of LF82 (Fig. 4-6 E). Moreover, CFUs of MG1655 and LF82 were not detected at 72 hpi (data not shown). These results reveal that although the treatment of larvae with DSS enhanced the burden of both LF82 and MG1655, AIEC LF82 still colonized and persisted better compared to nonpathogenic *E. coli* in fish with colitis (Fig. 4-6 D-E). Overall, these data suggest that the colonization of LF82 in fish with preexisting inflammation might be due to its unique virulence genes.

Data presented in Chapter 3 showed that larvae have reduced survival after DSS treatment. Thus, next I investigated whether the persistence of LF82 in DSS-treated larvae affected their survival. The percent survival of DSS-treated larvae infected with LF82 was decreased relative to that of DSS-treated uninfected fish and DSS-treated fish fed the paramecia vehicle only (Fig. 4-7 A). Moreover, the introduction of LF82 also lowered the survival of DSS-treated larvae relative to those infected with MG1655 (Fig. 4-7 B).

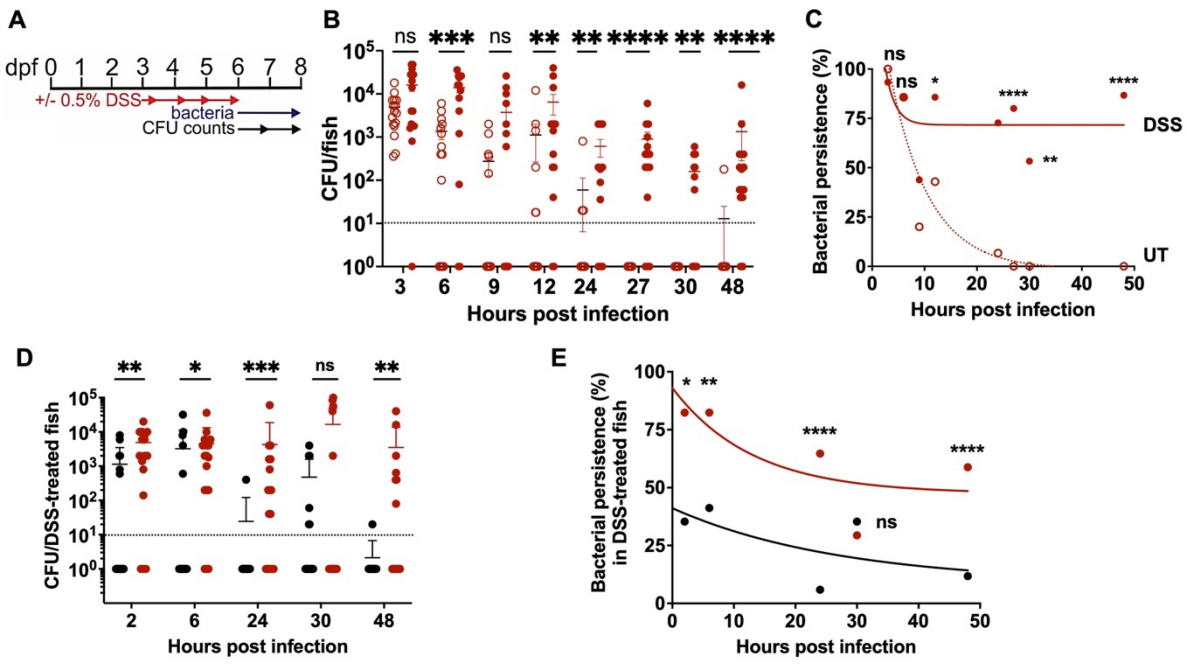

Figure 4-6. Preexisting inflammation enhances the colonization and persistence of AIEC LF82, but not of nonpathogenic *E. coli* MG1655.

(A) Timeline of DSS administration, infection of larvae with AIEC LF82 or MG1655, and CFU monitored. **(B)** Quantification of LF82 CFUs per larva with (solid black circles) and without (open circle) prior DSS treatment, n<15. The detection limit was 10^1 (dashed line)**. (C)** Bacterial persistence (% fish with a burden of AIEC above the detection limit) from 2-48 hpi. The half-life of LF82 in larvae either DSS-treated (solid black) or untreated (open circles) is 30 and 10 hours, respectively. Non-linear regression first order decay, ROUT outlier test with Q=0.2%, Paired t-test and Wilcoxon test. **(D)** Quantification of MG1655 (red) and LF82 (black) CFUs per fish treated with DSS. Fish that did not have any detectable *E. coli* were annotated as "1", n = 17 fish/condition. (E) Bacterial persistence (% fish with a burden of AIEC and MG1655 above the detection limit) from 0-48 hpi. Persistence was analyzed using a

Fisher's exact test. The half-life of LF82 is 18 hours and 6 hours for MG1655. *, P ≤ 0.05; **, P ≤ 0.01; ***, P ≤ 0.001; ****, P ≤ 0.000.

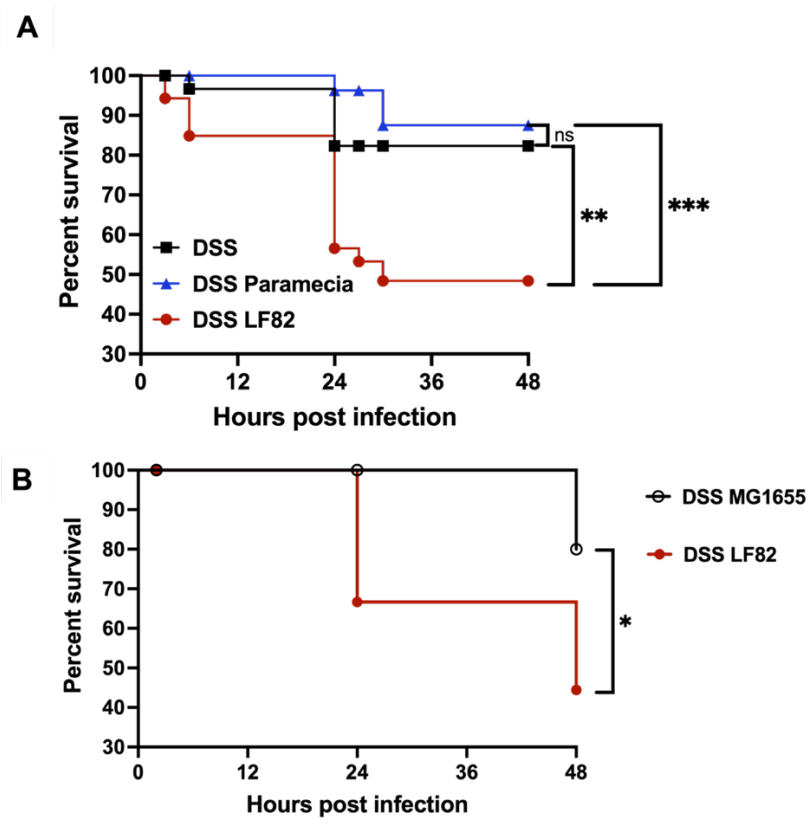

Figure 4- 7. DSS-treated larvae infected with LF82 have decreased survival compared to the control groups.

(A) Percent survival of DSS-treated larvae that were uninfected (black), fed the vehicle control (blue), or vehicle and AIEC (red). Mantel-Cox test, followed by a Bonferroni correction test n = 17. **, P ≤ 0.01; ***, P ≤ 0.001. **(B)** Percent survival of DSS-treated fish infected with MG1655 (black) and AIEC LF82 (red). Gehan-Breslow-Wilcoxon test, n=6. *, P ≤ 0.05.

One of the major benefits of using larval zebrafish to model infections is that bacterial colonization in the intestine may be visualized without disturbing the tissue. To capitalize on this, I attempted to generate an algorithm that quantified bacterial translocation from the lumen into the epithelium to assess whether AIEC invades the epithelium deeper than MG1655. Two hours post infection, larvae were euthanized and stained with phalloidin to visualize *E. coli* relative to the cytoplasm (Fig. 4-8 A). The images were compressed to 10 by 20-pixel images (Fig. 4-8 B), with pixel (bin) 0 corresponding to the lumen and bin 20 corresponding to the basement membrane (Fig. 4-8 A and B). The fluorescence intensity of the mCherry channel (*E. coli*) was quantified for each "bin" in untreated fish infected with LF82 and MG1655, respectively. However, no significant changes in fluorescence intensities were identified (Fig. 4-8 C). Approximately 50 fish were analyzed at 2, 24, and 30 hpi and the same results were observed. We reasoned that this approach was not reliable due to differences in the widths of zebrafish intestines (see for example Fig. 4-5 B). This method would probably be suitable for samples with equal measurements, however after looking at several images it was clear that there was too much variability and thus this approach was abandoned.

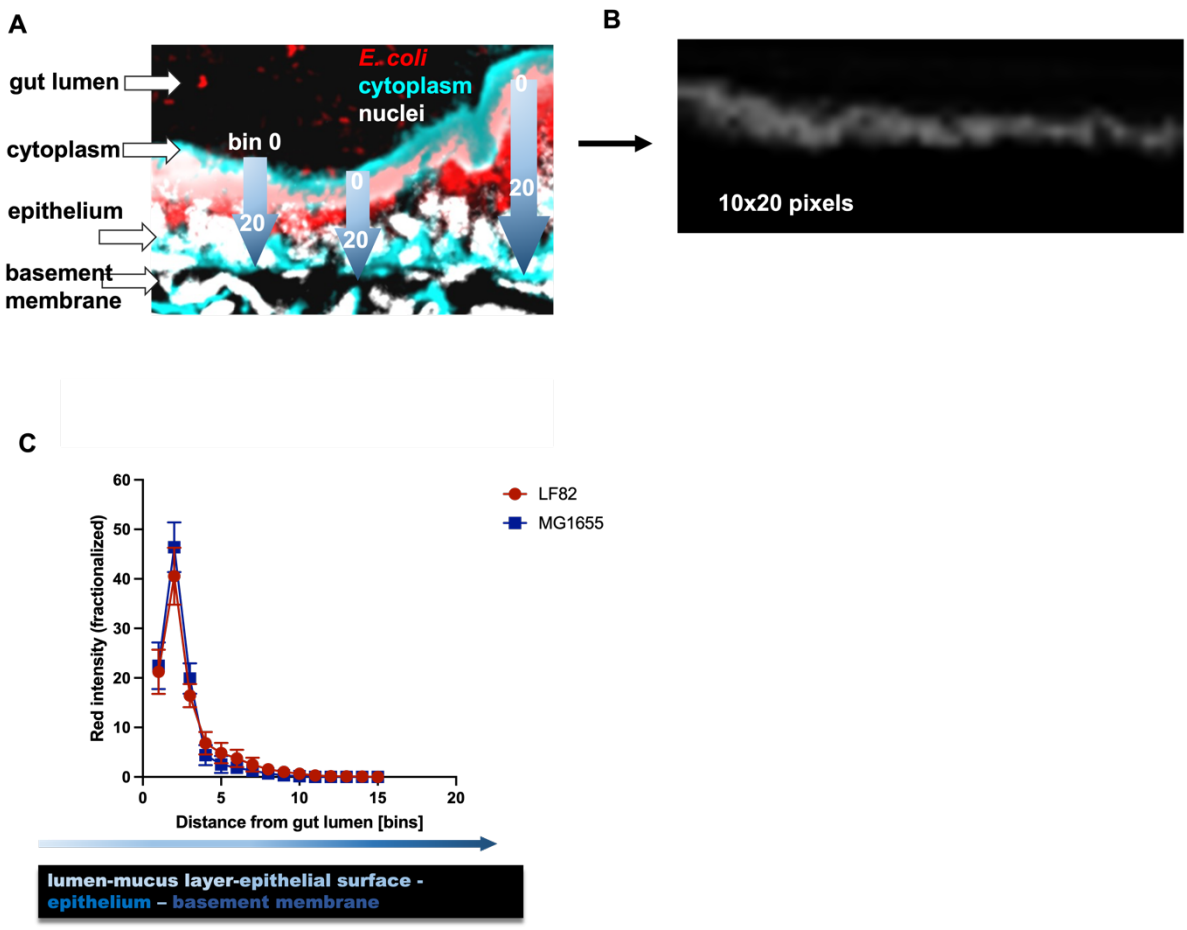

Figure 4- 8. An approach to quantify *E. coli* invasion into the epithelium.

(A) Representative image of a larval zebrafish intestine containing *E. coli* (red). All images were converted to grey scale and compressed into a 10 X 20 (length x width) pixel image **(B**). The compressed images consisted of 20 bins that represented vertical slices from the cytoplasm to the basement membrane and 10 horizontal bins that represented the length of the intestine. The fluorescence intensity of the red channel was then quantified in each bin. An example of the readouts is illustrated in **(C)** in which the fluorescence intensity of the red channel (y) is quantified in 20 bins (x) that extend from the lumen to the basement membrane. n=15, data showed no significant differences.

Based on immunofluorescence analysis, it was clear that there was a difference in the colonization patterns of LF82 in larvae exposed to DSS compared to the control group. Since the approach described above did not work, the fluorescent intensity of the mCherry channel inside of the intestinal epithelium was quantified as a measure of invading AIEC cells. DSS-treated and UT larvae were infected with LF82, euthanized at 2, 24, and 48 hpi, and labeled with anti-laminin to assess the localization of LF82::mCherry inside of the epithelium (delineated by the white lines) in between the lumen (asterisk) and basement membrane (right above the blood vessel "V") (Fig.4-9 A-B). In UT fish, individual LF82 cells were observed at 2 hpi, and by 24 hpi aggregates appeared (Fig. 4-9 Ai-ii) however by 48 hpi individual cells were not observed rather the mCherry protein appeared to have been internalized by specialized epithelial cells (Fig. 4-9 Aiii)[305]. Based on burden analysis, the signal appeared to be solely due to the mCherry protein since no LF82 CFUs in UT fish was observed during CFU counts at 48 hpi (previous figure, Fig. 4-6 B). Further studies are required to investigate why the mCherry protein was internalized in UT fish.

Similarly, individual AIEC cells were found inside of the epithelium at 2 hpi in DSS-treated larvae and aggregates were observed at 24 and 28 hpi (Fig. 4-9 Bi-iii). Throughout 2 to 48 hpi, the number of internalized AIEC was significantly greater in larvae with preexisting inflammation compared to healthy UT fish (Fig. 4-9 C). Moreover, AIEC were found localized closer to the basement membrane (thick blue line above the blood vessel "V") in the DSS group, whereas in UT fish AIEC mainly remained on the apical surface of the cells (Fig. 4-9 A vs B). Thus, it was hypothesized that the localization of AIEC closer to the basement membrane may modulate

intestinal inflammation since adhesion to the basement membrane may induce a proinflammatory response.

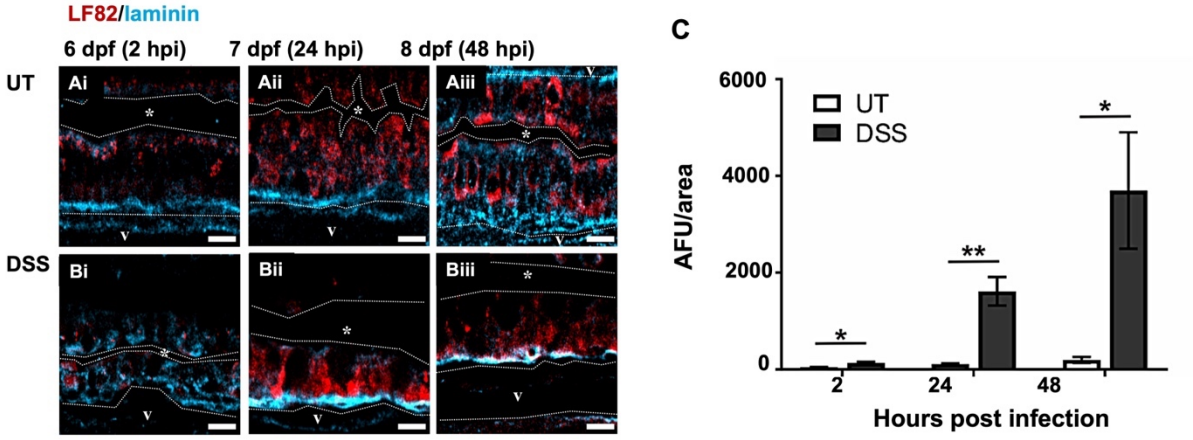

Figure 4- 9. DSS enhances the invasion of AIEC LF82 in the larval zebrafish intestine.

LF82 (red) in the mid-intestine of control **(Ai-ii)** and DSS-treated **(Bi-iii)** larvae relative to the basement membrane (blue) from 2 to 48 hpi or 6-8 dpf. Internalized mCherry protein was observed in specialized intestinal cells **(Aiii)** [305]. The dotted white line outlines the intestinal epithelium and separates it from the lumen, indicated by *, and the blood vessel below the basement membrane (V). Scale bars represent 10 μm. **(C)** Quantification of the fluorescent mCherry signal (arbitrary fluorescence units (AFU)) which represents AIEC inside of the intestinal epithelial cells at 2, 24, and 48 hpi, x= 6, *, $P \leq 0.05$; **, $P \leq 0.01$.

Murine studies show that colonization of AIEC LF82 exacerbates intestinal inflammation in DSS-treated animals and causes an immunopathology similar to the one observed in IBD patients [404-406]. Thus, next I investigated whether AIEC could exacerbate inflammation in UT- or DSS-treated larvae, respectively. The midgut of untreated fish infected with LF82 presented mucus secreting goblet cells at 2, 24, and 48 hpi that were not observed in UT fish fed the paramecia control (Fig. 4-10, Ai-iii vs Bi-iii, cells containing clear/light blue mucus droplets)[365]. As mentioned in Chapter 3, DSS disrupts the intestinal folds at 6 dpf (3 days post-DSS treatment) however these folds are restored at 7 and 8 dpf (4-5 days post-DSS treatment) (Fig. 4-10 Cii-iii). These observations suggest that the intestine may partially recover upon DSS removal. In contrast, DSS-treated larvae infected with LF82 were unable to fully recover from colitis by 48 hpi; they did not recover the original intestinal fold architecture and exhibited a thinner epithelial cell layer compared to DSS-treated larvae that were not infected (Fig. 10 Di-iii vs Ci-iii). Altogether these data suggested that AIEC LF82 alters the architecture of the intestine of larvae, in UT fish LF82 increases goblet cell number, and in DSS-exposed fish it prevents epithelial healing. The increased presence of mucin-producing goblet cells may indicate a host-defense response to fight off bacterial infections whereas flattening of the intestinal villi may be due to inflammation [67].

To further examine the effect of LF82 on inflammation, neutrophil recruitment was assessed, and induction of inflammatory markers was quantified using qRT-PCR. For these experiments, UT- and DSS-treated larvae fed the paramecia vehicle only (without *E. coli*) were used as controls. Neutrophil recruitment to the intestine was not

changed in UT fish infected with LF82 compared to UT paramecia-fed fish (Fig. 4-10 Ei and Eiii, F). However, infection of DSS-treated larvae with LF82 significantly increased neutrophil recruitment to the intestine compared to DSS-fish fed paramecia only (Fig. 4-10 Eii and Eiv, F). The infection of DSS-treated larvae with LF82 increased the relative expression of proinflammatory CXCL8, IL-1β, and MMP9 encoding genes compared to UT fish infected with LF82 (Fig. 4-10 G). To further investigate whether LF82 could enhance the proinflammatory response in DSS-treated larvae, the relative expression of CXCL8, IL-1β, MMP9, and TNF-α encoding genes was assessed in DSS-treated fish with LF82 and paramecia only. Here we saw that the expression of CXCL8 and MMP9 encoding genes were increased in DSS-treated fish infected with LF82 compared to DSS-fish fed paramecia only and relative to the UT paramecia control group (Fig. 4-10 Eii, H). All together these data suggested that AIEC do not induce intestinal inflammation in untreated larvae, but do exacerbate inflammation in hosts with existing colitis. Interestingly, although the number of macrophages recruited to the intestine was unchanged across samples (Fig. 4-11), in some DSS-treated fish LF82 was observed to replicate inside macrophages over time (Fig. 4-12).

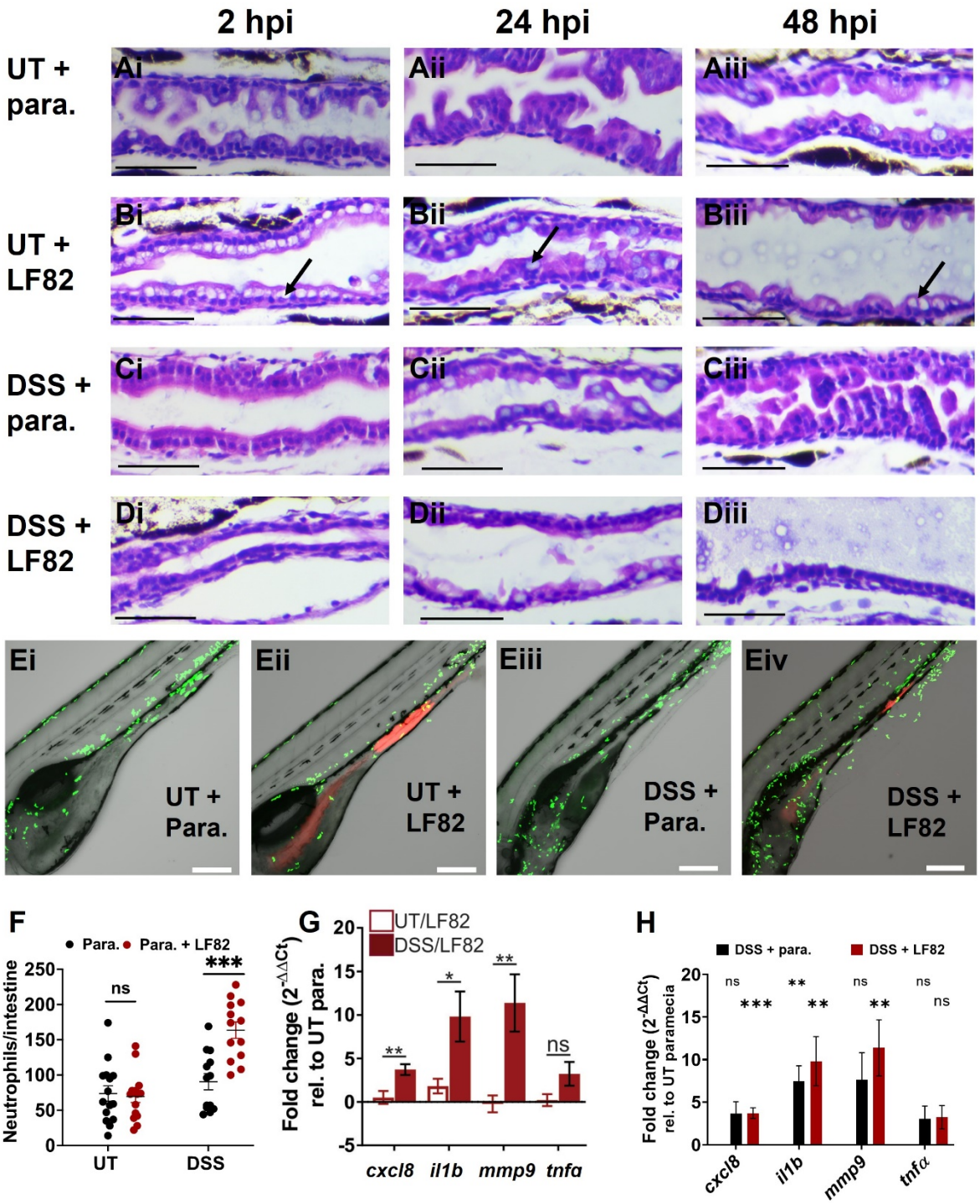

Figure 4- 10. Figure 4-10. AIEC LF82 exacerbates intestinal inflammation in DSS-treated larvae.

(A-D) H&E-stained longitudinal sections of the mid-intestine of larvae fed paramecia with **(C)** and without DSS **(A),** and those infected with paramecia plus LF82 **(B and D)** at 6, 7, and 8 dpf (2, 24, and 48 hpi). n=3. Black arrows point to goblet cells. Scale bars represent 50 μm. **(E)** Representative confocal images (10X) of Tg(*mpo*::*egfp*) larvae fed paramecia only or LF82 at 6 dpf. Larvae were imaged for 18 h (3-20 hpi), maximum intensity projection of 190 images; neutrophils (green) and bacteria (red). Neutrophils were also seen on the ventral fin underneath the intestine. Scale bars represent 200 μm. **(F)** Quantification of neutrophils per intestine in UT- and DSS-treated fish fed with paramecia only (black) or infected with LF82 (red); n ≥10. **(G)** qRT-PCR analysis of *cxcl8, il1b, mmp9,* and tnfα in UT (white) and DSS-treated (red) larvae infected with LF82 relative to UT paramecia only controls at 6 dpf, n=6. **(H)** qRT-PCR analysis of *cxcl8, il1b, mmp9,* and tnfα in DSS-treated (red) larvae infected with LF82 and DSS-treated larvae fed paramecia (black) relative to UT paramecia controls at 6 dpf, n=7 Unpaired two-tailed t-test. Mean with SEM, *, $P \leq 0.05$; **, $P \leq 0.01$; ***, $P \leq 0.001$.

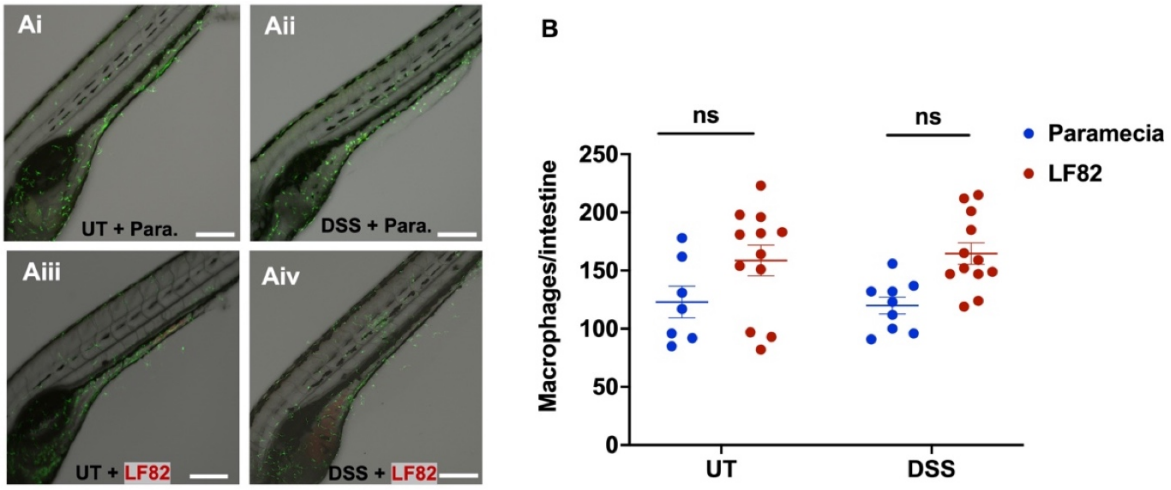

Figure 4- 11. Macrophage recruitment to the intestine does not change in fish infected with AIEC LF82.

(A) Representative confocal images of untreated **(Ai)** and DSS-treated **(Aii)** Tg(*mpeg1*::*egfp*) larvae with LF82 (red) with green macrophages during live imaging from 2 to 24 hpi. Scale bars represent 200 μm. **(B)** Enumeration of macrophages recruited to the intestine of larvae treated with DSS and control untreated larvae infected with LF82. n ≥10, unpaired two-tailed t-test. Mean with SEM. ns= not significant.

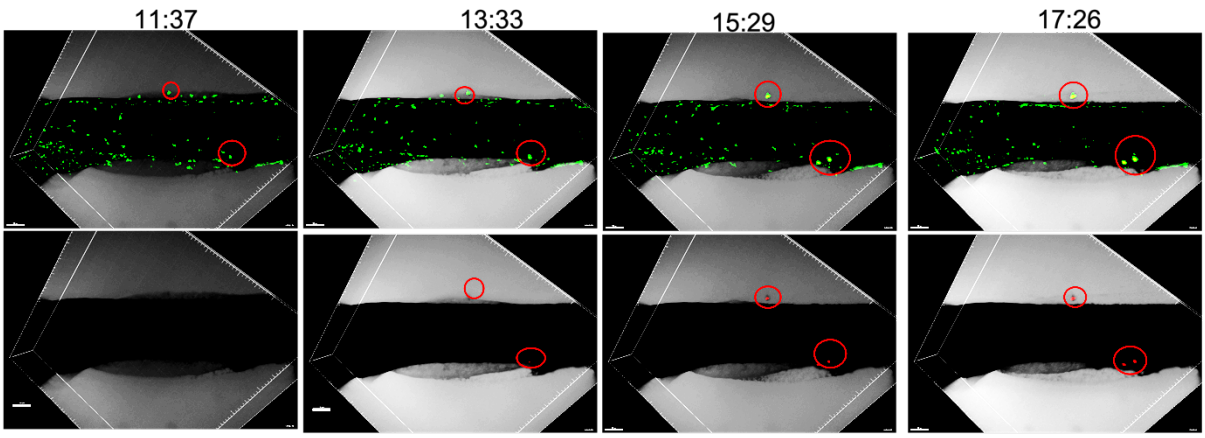

Figure 4- 12. AIEC LF82 may replicate inside of zebrafish macrophages over time.

Images collected during overnight imaging using Tg(*mpeg1*::*egfp*) infected with mCherry expressing LF82 (red). The GFP channel (top images) and the mCherry channel (bottom images). At roughly 13 hpi (11 hours of imaging) two macrophages (green) stop circulating and remain in a fixed location (circled in red). Over the course of the next 6 hours, the macrophages expand in size, and individual LF82 colonies form within. n=3. Scale bar: 100 μm.

The fimH adhesin and ibA invasin mediate the pathogenicity of AIEC LF82 in the larval zebrafish intestine

Next, I investigated whether previously characterized AIEC virulence factors played a role in bacterial pathogenesis in larvae with preexisting inflammation. Among the identified AIEC virulence factors that mediate adhesion and invasion of intestinal epithelial cells are the fimbrial adhesin FimH and the invasion of the brain endothelium protein A (IbeA), respectively [222, 282]. FimH is the terminal subunit of type I pili and binds collagen type I and type IV, laminin, fibronectin, and mannosylated glycoproteins [407] . Moreover, FimH of AIEC LF82 adheres to the human carcinoembryonic antigen-related cell adhesion molecule 6 (CEACAM6) that is abnormally expressed in ileal samples of CD patients and in transgenic CEABAC10 mice [280, 282]. It is hypothesized that the presence of CEACAM6 receptors in a host promotes the colonization of AIEC and indirectly contributes to intestinal inflammation, since binding of AIEC to CEACAM6 through FimH triggers intestinal inflammation in CEACAM6-expressing, CEABAC10 mice [408]. Further, *in vitro* studies suggest that the secretion of IFN-γ and TNF-α induces the synthesis of CEACAM6 receptors, which could indicate a positive feedback loop that leads to AIEC colonization [278].

IbeA is an invasin and outer membrane protein conserved in the *E. coli* B2 phylogenetic group that includes avian pathogenic *E. coli*, newborn meningitis-causing *E. coli*, and AIEC strains NRG857C and LF82 [222] . BLAST analyses show that the IbeA protein in these pathogenic *E. coli* strains are 100% identical. IbeA binds to vimentin proteins found in macrophages, fibroblasts, and endothelial cells and mediates the invasion of AIEC NRG857c to Caco-2 and M-like cells [222]. Moreover,

since the deletion of *ibeA* decreases intramacrophagic AIEC NRG857c survival and sensitizes APEC to H_2O_2, this suggests that IbeA contributes the replication of AIEC in macrophages and to resistance to the ROS response [222, 409]. However, *in vivo* data suggests that IbeA does not play a role in colonization of AIEC NRG857c to the mouse intestine and that colonization of NRG857cΔ*ibeA* leads to moderate intestinal epithelial damage compared to colonization of wild-type AIEC NRG857c [222].

To further investigate whether FimH and IbeA play a role in the colonization and invasion of AIEC LF82 in zebrafish larvae, these genes were deleted from the parent strain and complemented by inserting *fimH* or *ibeA* with their endogenous promoters into the chromosome. Deletion and complementation of both genes did not affect the overall growth of AIEC LF82 in LB media over the course of 20 hours (Fig. 4-13 A). The survival of larvae infected with the parent strain LF82 and complemented strain LF82Δ*fimH:fimH* was significantly lower than that of fish infected with the *fimH* deletion strain (LF82Δ*fimH*) (Fig. 4-13 B). On the contrary, the survival of larvae infected with LF82Δ*ibeA* was not significantly different when compared to larvae infected with the parent strain and LF82Δ*ibeA:ibeA* (Fig. 4-13 C).

Interestingly, the burden of LF82Δ*fimH* and LF82Δ*ibeA* was higher than that of the parent strain at 2 hpi, while the burden of LF82Δ*fimH:fimH* and LF82Δ*ibeA:ibeA* was not statistically different than that of LF82 (Fig.14 A and C, 2 hpi). At 24 hpi, the burden of LF82Δ*fimH* remained similar to of the parent strain (Fig. 14 A, 24 hpi) and, although not statistically significant, there was a 2-log difference in the average number of CFUs of LF82Δ*ibeA* compared to the parent strain (Fig. 14 C, 24 hpi). Further, for unknown reasons, the burden of the LF82Δ*fimH:fimH* and LF82Δ*ibe:ibeA*

strains was lower than that of WT at 24 hpi (Fig. 14 A and C). By 48 hpi, the burden of LF82Δ*fimH* and LF82Δ*ibeA* was significantly lower than that of the parent strains and complemented strains (Fig. 4-14 A and C, 48 hpi). Due to similarities in the number of fish with undetected *E. coli*, the bacterial persistence of LF82Δ*fimH* was not significantly different than that of LF82 and LF82Δ*fimH:fimH* (Fig. 4-14 B). However, the persistence of LF82Δ*ibeA* was lower than that of LF82 (Fig.4-14 D). Based on CFU analyses, it is possible that FimH is important for the retention of AIEC in the zebrafish intestine throughout the infection. Although, previous studies suggest that IbeA does not play a role in colonization, this data suggest that IbeA may also be essential for the retention of AIEC inside of larvae across 48 hpi.

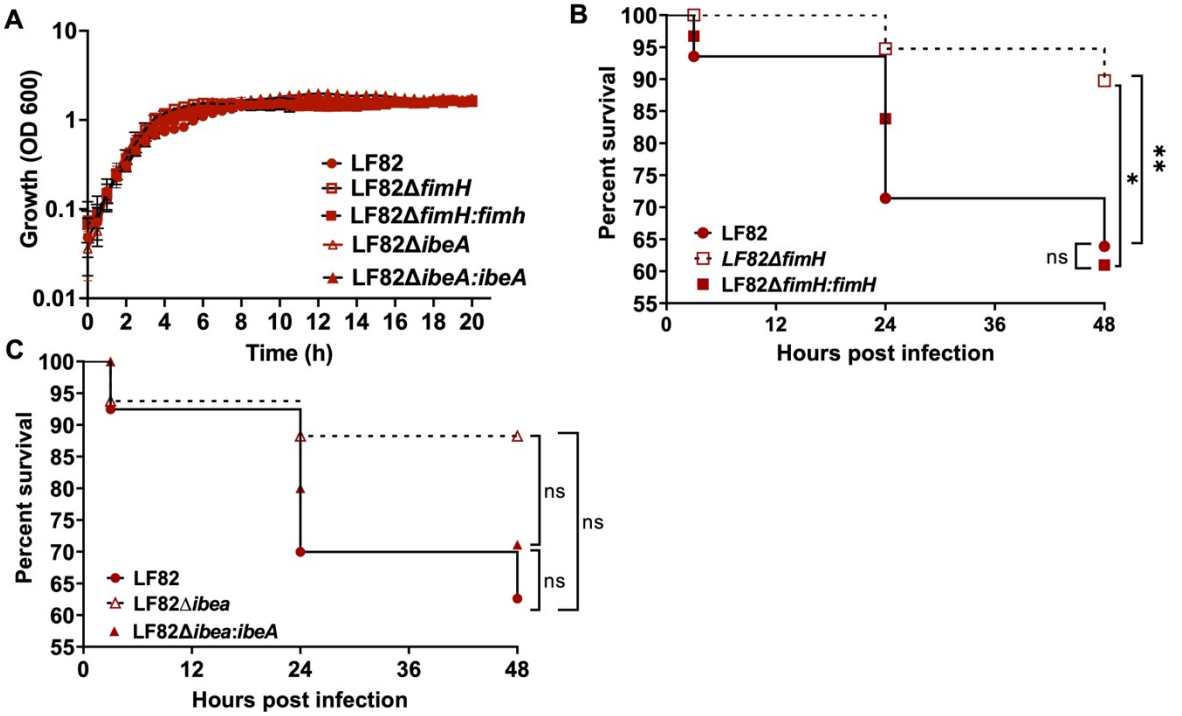

Figure 4- 13. Deletion and complementation of fimH and ibeA in AIEC LF82 does not affect LF82 growth and results in changes in the survival of infected larvae.

(A) Growth of LF82, LF82Δ*fimH*, LF82Δ*fimH:fimH*, LF82Δ*ibeA*, LF82Δ*ibeA:ibeA* in LB over 20 hours n=3. Survival of larvae infected with **(B)** LF82, LF82Δ*fimH*, LF82Δ*fimH:fimH* or **(C)** LF82, LF82Δ*ibeA*, LF82Δ*ibeA:ibeA* at 2, 24, and 48 hpi. Kaplan-Meier and Mantel-Cox test, followed by a Bonferroni correction test, n=20.

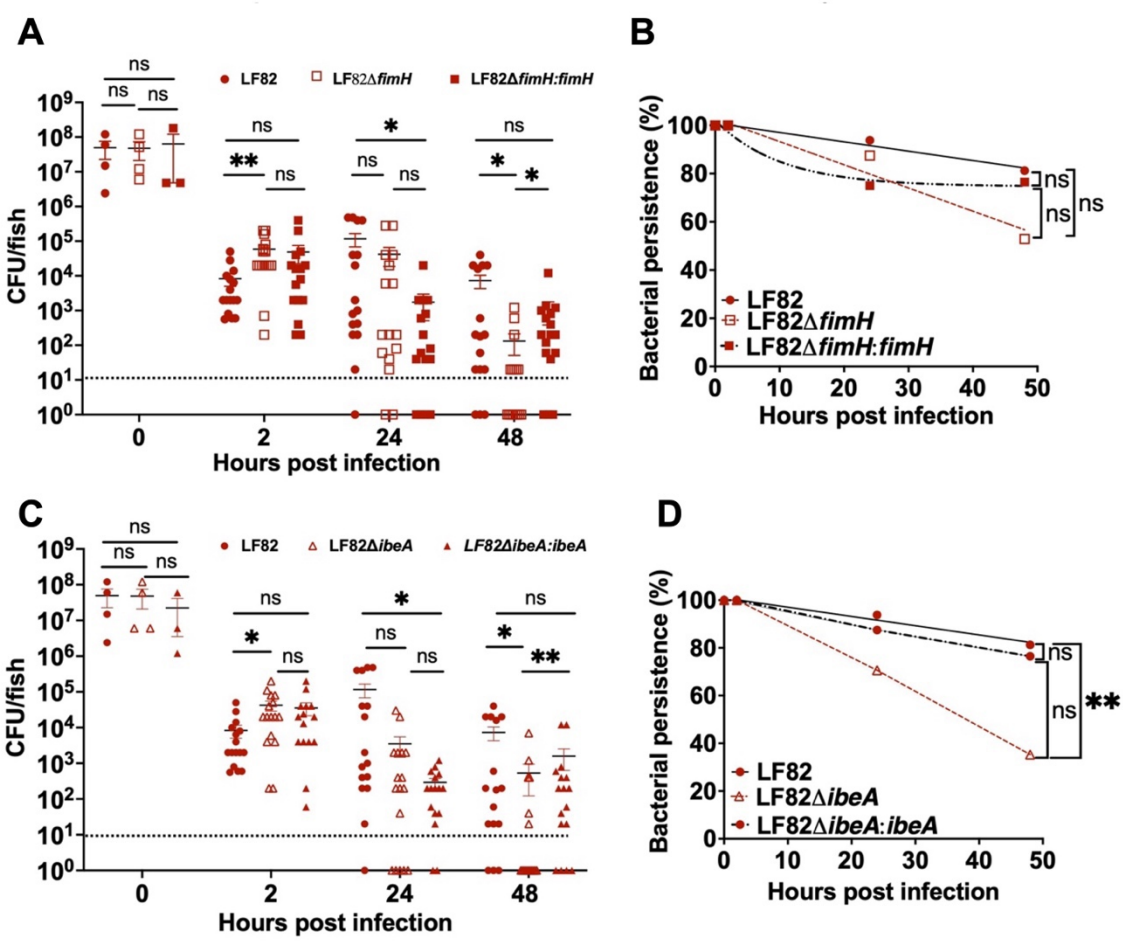

Figure 4- 14. Deletion and complementation of *fimH* and *ibeA* in AIEC LF82 changes the burden of LF82 inside of larval zebrafish

Quantification of the burden **(A and C)** and persistence **(B and D)** of LF82, **(A)** LF82Δ*fimH*, LF82Δ*fimH:fimH*, **(C)** LF82Δ*ibeA*, and LF82Δ*ibeA:ibeA* in DSS-treated larvae from 2-48 hpi, The burden was analyzed using a Kruskal-Wallis test, n ≥ 16. Bacterial persistence was defined as the percent of fish with a burden of AIEC above the detection limit and was analyzed using a log-rank test. The detection limit was 10^1 CFU/fish (dashed line). Non-linear regression, first order decay graph used to model bacterial persistence. *, P ≤ 0.05; **, P ≤ 0.01.

Previous reports show that the IbeA adhesin of AIEC NRG857c mediates the invasion, but not adhesion, of AIEC to the intestinal epithelium [222]. Therefore, the next question to address was whether the deletion of *ibeA* in AIEC LF82 affected the invasion of AIEC into the intestinal epithelium. We also investigated whether the deletion of *fimH* influenced to invasion of LF82. Infected larvae were euthanized, fixed, and stained with anti-laminin to visualize the localization of LF82Δ*ibeA* and LF82Δ*fimH* over the course of 48 hpi. Based on image analyses, LF82Δ*fimH* was observed inside of the epithelium from 2 to 48 hpi (Fig. 4-15, B), however there were less cells observed at 24 and 48 hpi, compared to the parent strain and LF82Δ*fimH:fimH* (Fig. 4-15, B compared to A and C.) Interestingly, LF82Δ*ibeA* was observed colonizing the surface of the epithelial cells (along the cytoplasm) at 2 and 48 hpi (Fig. 4-15 Di and Diii), while the parent and complemented strains were both found inside of the epithelium at these time points (Fig. 4-15 A and E). These observations suggested that the deletion of *ibeA* may affect the invasion of AIEC LF82 into the intestinal epithelium.

In these images, the localization of AIEC within the lamina propria was not observed. However, there was a striking difference in the AIEC colonies formed inside of the intestine of LF82Δ*fimH*, LF82Δ*fimH:fimH*, LF82Δ*ibeA*, and LF82Δ*ibeA:ibeA* compared to the parent strain (Fig. 4-15 B-E compared to A). As the infection time progressed, LF82 formed larger biofilm-like colonies, whereas LF82Δ*fimH*, LF82Δ*fimH:fimH*, LF82Δ*ibeA*, and LF82Δ*ibeA:ibeA* remained as individual cells. Additional experiments are required to confirm whether LF82 forms biofilms inside of larvae and whether there is a difference in biofilm-formation in the mutant strains.

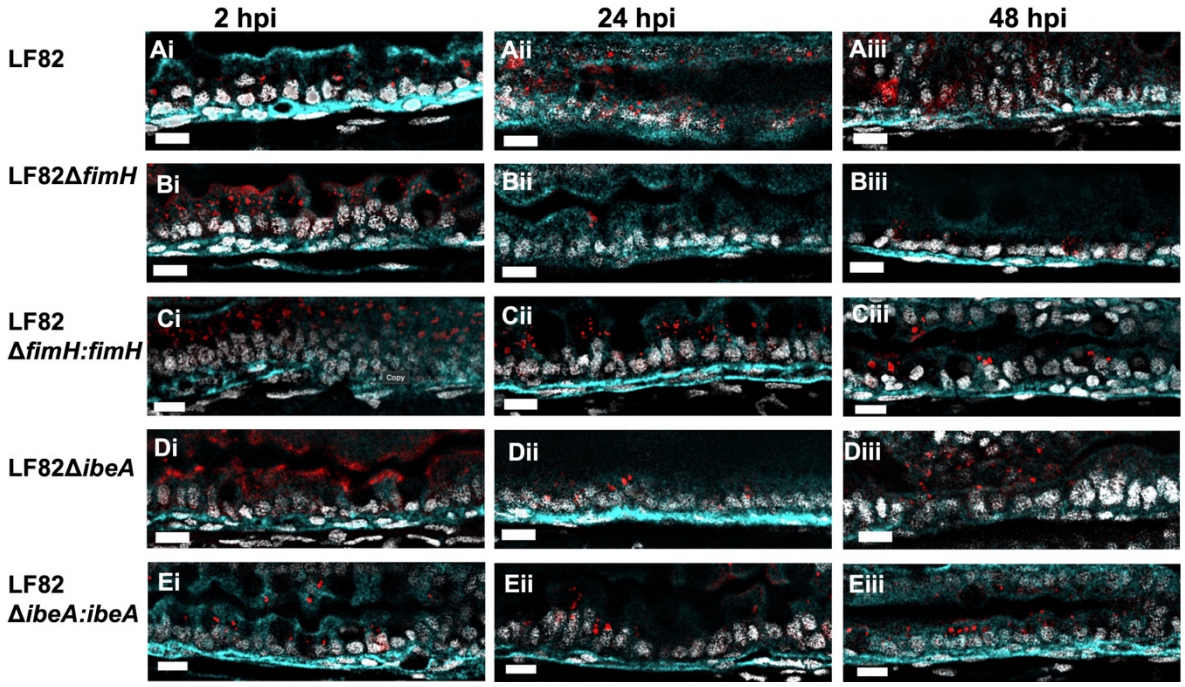

Figure 4- 15. Deletion of ibeA, but not fimH, results in the localization of AIEC LF82 along the surface of the epithelium.

Representative images of the mid-intestine of larvae infected with LF82 **(A)**, LF82Δ*fimH* **(B)**, *LF82ΔfimH*:*fimH* **(C)**, LF82Δ*ibeA* **(D)**, or LF82Δi*beA:ibeA* **(E)** at 2, 24, and 48 hpi. AIEC LF82 (red) is observed inside of the epithelium (outlined in cyan); nuclei (white). Single plane view of the midgut, n=3. Scale bars represent 10 μm.

Surprisingly, although the burden of the of LF82Δ*fimH* and LF82Δ*ibeA* strains was significantly higher than expected at 2 hpi, the mid-intestine of larvae harboring these deletion strains seemed to be less damaged than that of larvae infected with the parent or complemented strains (Fig.4-16 B and D compared to A, C, and E). At 2 hpi the mid-intestine epithelium of larvae infected with LF82, LF82Δ*fimH:fimH*, and LF82Δ*ibeA:ibeA* appeared flattened and thinner than the epithelium of fish harboring LF82Δ*fimH* and LF82Δ*ibeA* (Fig.4-16 Ai, Ci, and Di compared to Bi and Di). At 24 hpi, the epithelium of fish infected with LF82Δ*fimH* exhibited intestinal folds that were not observed in fish infected LF82, LF82Δ*ibeA*, and the complemented strains (Fig. 4-16 Bii compared to Aii, Cii, Dii, and Eii). By 8 dpf, the epithelium of larvae infected with all LF82 strains, except the parent strain, appeared thicker (Fig. 4-16, Biii, Ciii, Diii, and Eiii compared to Aiii).

A plausible reason that the intestinal epithelium of larvae infected with LF82Δ*ibeA* and LF82Δ*fimH* was not significantly damaged may be due to lower neutrophil recruitment to the intestine (Fig. 4-16 F). Larval zebrafish infected with LF82 were shown to have more neutrophils recruited to the intestine compared to fish harboring LF82Δ*fimH* and LF82Δ*ibeA* (Fig. 4-16, F). Complementation of *fimH* and *ibeA* also resulted in higher neutrophil recruitment in comparison to fish infected with LF82Δ*fimH* and LF82Δ*ibeA* (Fig. 4-16) and even more so when compared to those carrying LF82 (in the case LF82Δ*ibeA*). Altogether, these data suggested that FimH and IbeA have an immunogenic effect in the larval zebrafish intestine.

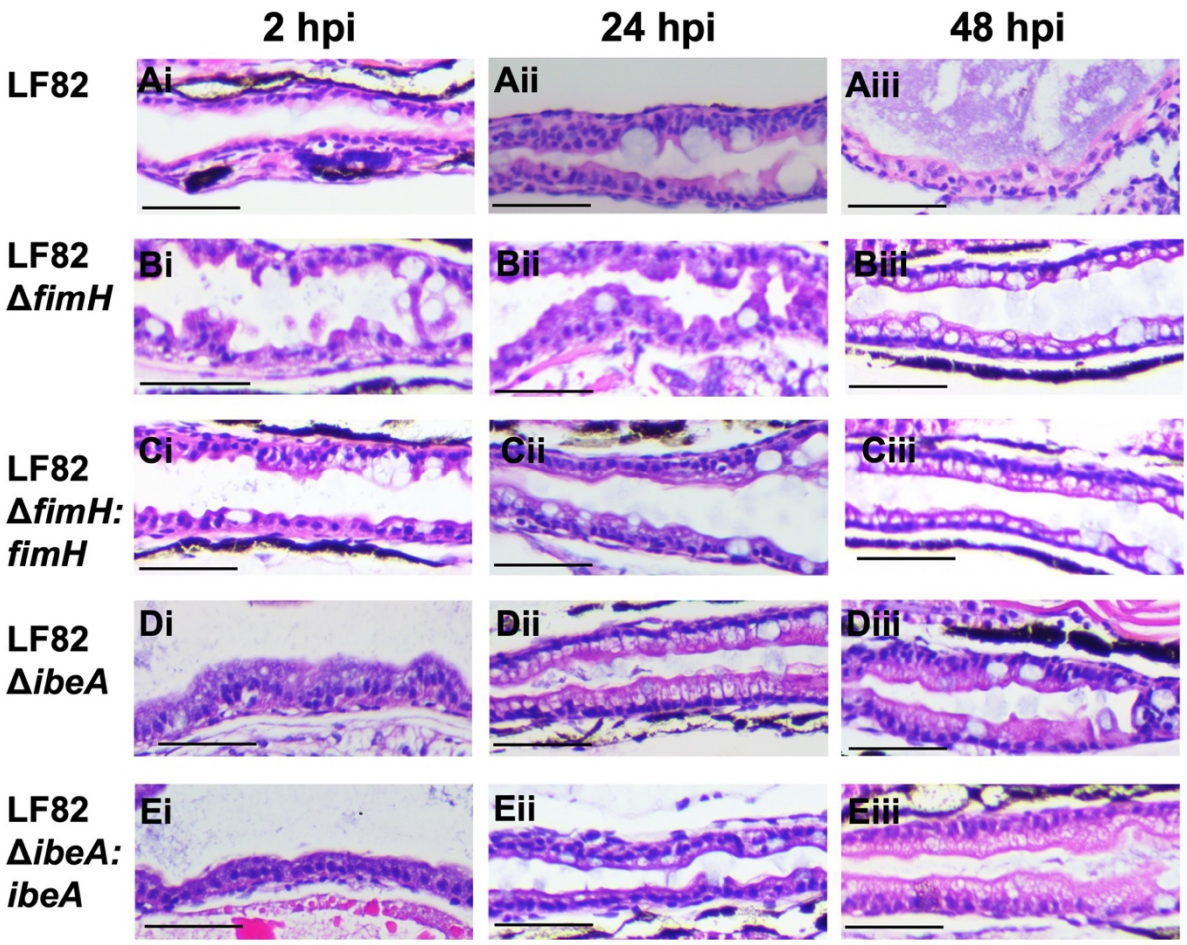
2 hpi
24 hpi
48 hpi
LF82
Ai
Aii
Aiii
LF82 ΔfimH
Bi
Bii
Biii
LF82 ΔfimH: fimH
Ci
Cii
Ciii
LF82 ΔibeA
Di
Dii
Diii
LF82 ΔibeA: ibeA
Ei
Eii
Eiii

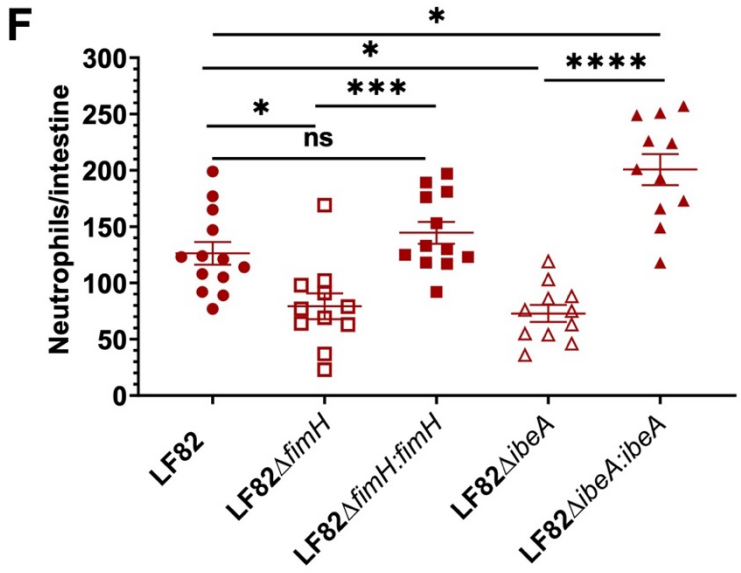
F
Neutrophils/intestine
300
250
200
150
100
50
0
*
*
****
***
*
ns
LF82
LF82ΔfimH
LF82ΔfimH:fimH
LF82ΔibeA
LF82ΔibeA:ibeA

Figure 4- 16. Deletion of fimH and ibeA in AIEC LF82 results in less tissue damage and decreased neutrophil recruitment to the intestine compared to LF82.

H&E longitudinal sections of the mid-intestine of larvae infected with LF82 **(A)** LF82Δ*fimH* **(B),** LF82Δ*fimH:fimH* **(C),** LF82Δ*ibeA* **(D),** and LF82Δ*ibeA:ibeA* **(E)** at 2, 24, and 48 hpi. Representative images for n=3. Scale bars represent 50 μm. **(F)** Quantification of neutrophils per intestine for DSS-treated fish infected with above mentioned LF82 strains or paramecia only control. Kruskal-Wallis test. n = ≥11. *, P ≤ 0.05; **, P ≤ 0.01; ***, P ≤ 0.001; ****P ≤ 0.0001.

Discussion

The overall goal of this project was to assess the consequences of AIEC LF82 colonization in larval zebrafish to determine whether larval zebrafish are a suitable model of AIEC colonization and infection. This goal was further expanded to address whether AIEC exacerbates preexisting inflammation in larvae, and if this was dependent on previously described AIEC virulence factors. To address these questions, paramecia were used as vehicles to deliver *E. coli* to the zebrafish intestine. Previous studies from the Krachler lab showed that MG1655 and EHEC survive acidification inside of paramecia vacuoles and are successfully delivered to the zebrafish intestine [314]. As a result, the paramecia model was expanded to include AIEC. Data presented in figure 4-3 suggests that AIEC have a similar stability in paramecia compared to other *E. coli*, and that the incubation of AIEC-loaded paramecia with larvae for 2 hours is sufficient for the delivery of 10^5 CFUs of AIEC to the gut.

Studies that have previously used larval zebrafish to study intestinal infections have typically administered 10^4-10^8 CFUs of different bacterial species, however 10^7-10^8 CFUs are generally considered to be on the high end and cause high mortality rates[397, 410, 411]. Further, previous studies from our lab on EHEC and others suggest that zebrafish infections with 10^4-10^5 CFUs of *E. coli* is a suitable range to study colonization and pathogenesis [314, 412]. Therefore, the original protocol was adapted to include 2 hours of AIEC feeding to paramecia and another 2 hours for the preying of zebrafish on AIEC-loaded paramecia. *E. coli* not internalized into paramecia are removed by several washing steps.

An advantage of using this foodborne model is that it facilitates the colonization of the GI tract by bacterial species that are not native zebrafish colonizers, and/or strains that do not colonize well through immersion infection. Members of the zebrafish microbiota belong to the phyla Proteobacteria and to a lesser extent Fusobacteria, Bacteroidetes, and Firmicutes [150, 413]. Prior metagenomics studies by our lab (unpublished) and others have shown that *E. coli* are not natural members of the larval zebrafish intestinal microbiome, but here we found that paramecia efficiently deliver *E. coli* to the intestine, where it persists for several days. Further, this protocol has also been successfully used to deliver of *Salmonella enterica* and *Vibrio cholerae* to larvae [319, 414, 415]. In addition to bacteria, paramecia are also able to engulf amoeba and yeasts, however this model has not yet been tested with these microbes [416].

Following ingestion of *E. coli*-loaded paramecia by larvae, paramecia are degraded in the foregut, and bacteria are released into the intestine [319]. During the initial hours post infection, AIEC is observed in the foregut and the midgut, however over the course of infection, AIEC shows a preference for colonizing the midgut of larvae, similar to EHEC [314]. This region of the intestine contains absorptive enterocytes, mucin secreting goblet cells, and M-like cells, all of which are also found in the mammalian small intestine [302]. As previously mentioned, AIEC are predominantly found colonizing the ileum of CD patients and adhere to the CEACAM6 glycoprotein expressed in transgenic CEABAC10 mice. One drawback of CEABAC10 mice is that the expression of CEACAM6 is directed to colonic epithelial cells [279]. However, this model has been the gold standard for studying AIEC infections since

the discovery that the CEACAM6 receptor is abnormally expressed in the ileum of CD patients [417]. In CEABAC10 and commonly used C57/BL6 mice administered DSS, AIEC causes histopathological damage in the colonic mucosa, which suggests that this may be the site of colonization *in vivo* [280, 418].

In the present study, the colonization of AIEC LF82 was determined under 2 host conditions: untreated (healthy) hosts, and hosts with preexisting inflammation (enterocolitis). AIEC colonization was also assessed in comparison to nonpathogenic *E. coli* MG1655 in both host conditions. We observed that AIEC LF82 colonized better than MG1655 in hosts with and without intestinal inflammation, an observation also reported in murine studies [403]. Figure 4-4 (C-D) suggests that although AIEC LF82 colonizes a bit longer than MG1655, it is only present up to 24 hpi in UT larvae. Furthermore, although preexisting inflammation caused by DSS enhanced the persistence and colonization of AIEC LF82 in fish, it only did so for an additional 24 hpi (Fig. 4-6 B-C).

Wild-type and CEBAC10 mice treated with DSS are colonized with AIEC LF82 up to 6 days post infection, however there is a significant difference in the amount of LF82 present in these groups by 6 dpi (10^4 compared to 10^6 CFU/g of feces, in wild-type and DSS-treated larvae, respectively) [280]. In contrast, LF82 is rarely observed past 24 hpi in UT larval zebrafish, but persists in DSS-treated fish until 48 hpi. One striking difference between mice studies and this zebrafish study is that transgenic and wild-type mice are usually challenged with 10^8-10^9 LF82 CFUs through oral gavage for daily 3 or 15 days, respectively, and treated with broad-spectrum antibiotics for multiple days to deplete most of their endogenous microbiome [280,

286, 419]. In contrast, here roughly 10^4-10^5 AIEC CFUs are consumed through foodborne infections once, making the model less labor intensive. It is also not necessary to pretreat with antibiotics, and AIEC colonization can be studied with the natural microbiota intact. Although it may seem that LF82 do not persist long enough in larvae, longer colonization times may be achieved through multiple bacterial challenges to study readouts over a longer time period.

Although the paramecia model may be less technically challenging than traditional oral gavage, it introduces a few limitations. For example, the reason for the lack of detection of AIEC in some larvae is unknown (Figure 4-4 C and 4-6 B). There are two plausible causes for this observation: (1) the larvae did not eat any/enough paramecia or (2) AIEC was more rapidly cleared from the intestine prior to sampling, for example through differences in peristalsis between individual larvae. These are issues that could potentially be addressed if a fixed number of bacteria was administered through oral gavage. Another limitation is that using the paramecia model prevents the introduction of AIEC to severely inflamed larvae, which may skew the final results. This is because larvae with higher inflammation are moribund and become unable to prey on paramecia. Therefore, this study may be lacking key readouts from AIEC infections in hosts with higher proinflammatory responses.

Here, it was also shown that the survival of DSS-treated larvae infected with LF82 is significantly decreased compared to DSS-treated fish that were uninfected or infected with MG1655 (Fig. 4-7). Similarly, DSS-treated CEABAC10 mice also experience decreased survival rates beginning at 2 dpi, and by 7 dpi the percent survival is only 20% [280]. In contrast, wild-type mice administered DSS and infected

with AIEC LF82 do experience lower survival rates compared to controls, but the survival is not as strikingly low. A plausible reason for a decreased survival rate in infected larvae may be due to the host being unable to regulate the proinflammatory response that LF82 exerts, in addition to the preexisting inflammation induced by DSS. Further, although AIEC decreases the survival rate in larvae, the percent survival is between 40%-50% and is not as low as observed in mice. A reason that AIEC may not induce a high mortality rate in infected larvae, as observed in mice, may be because *E. coli* is not a natural member of the zebrafish microbiome and does not persist in the larvae for long periods of time. For example, the colonization of larval zebrafish with *Aeromonas hydrophila*, a natural fish pathogen, results in higher persistence and higher mortality rates using lower bacterial dosages than used here [379].

Based on the data presented in figure 4-10 AIEC LF82 does exacerbate intestinal inflammation in infected hosts with preexisting inflammation. This is supported by an increase in neutrophil recruitment to the intestine, the inability of the mid-intestine to heal while colonized with AIEC, and the increased relative expression of the genes encoding the proinflammatory cytokines *cxcl8, il1b, mmp9*. Recently published work by Dr. Withey's lab at the Wayne State University School of Medicine, established adult zebrafish as model organisms of AIEC infections and showed that adult zebrafish produce S100A-10b, a protein homologous to calprotectin, in response to intestinal inflammation caused by LF82 [373]. As mentioned in Chapter 3, the production of S100A-10b was not investigated here, but may be examined in future work to quantify inflammation. Moreover, Dr. Withey's work further supports that AIEC

induce inflammation in zebrafish. Their work showed that AIEC LF82 persists at a high burden (10^4 CFU/fish) in adult zebrafish intestine up to 3 dpi and at a lower burden (10^2 CFU/fish) for up to 10 days, increase the relative expression of genes encoding TNFα, IL1β, and interferon-γ (IFNγ), and damage the intestinal villi [373]. However, in contrast to my study, the colonization of AIEC LF82 in adult larval zebrafish did not cause any mortality in infected fish. Furthermore, although AIEC caused inflammation in untreated adult zebrafish in Dr. Withey's study, here I see that AIEC only induce inflammation when the larvae are pretreated with DSS. The reason that AIEC trigger inflammation in UT adult zebrafish, and not in UT larvae is unknown, however it may be due to differences in AIEC colonization and persistence. The decision to use adult or larval zebrafish to study AIEC depends on the type of readouts for which one is searching. Furthermore although, LF82 may persist in the adult zebrafish longer, adult zebrafish are not transparent, so *in vivo* host responses to the infection cannot be visualized by live imaging. On the other hand, it may be possible to study the interaction of AIEC with B and T cells using adult zebrafish.

Although the burden of LF82 inside of larvae drops approximately 2-fold from 2 to 48 hpi, it is possible that the immune response is still activated even after AIEC have cleared, since AIEC-derived antigens may still be present. For example, neutrophils remain active along the notochord of larvae days after the clearance of *E. coli* K12, which prevents resolution of inflammation [382]. Further, two phenotypes commonly used to assess intestinal inflammation in mice are the presence of bloody diarrhea and changes in body weight [325]. A limitation of using larval zebrafish is that these phenotypes are not easily quantifiable, although changes in gut motility may

be observable in infected larvae and may signify important intestinal changes in hosts colonized by AIEC [420].

The reason why AIEC colonizes hosts with preexisting inflammation more efficiently than untreated fish is not well understood. However, there are three possible reasons for this observation. The first most obvious reason is that DSS damages the intestinal barrier and facilitates the adhesion and invasion of AIEC, which results in bacterial localization closer to the epithelial basement membrane (Fig. 4-9). As a result, the bacteria are farther away from the lumen and fail to be cleared out by peristaltic contractions [421]. Within the basement membrane, fibronectin, collagen types IV, VII and XVIII, and laminin are abundant, and these host proteins are all known to bind several bacterial adhesins [422]. Previously published studies from the Krachler lab have shown that the *E. coli* MAM adhesin, which is highly similar to that of AIEC, binds fibronectin and collagen, and to a lower extent laminin [76]. Additionally, FimH binds mammalian laminin, fibronectin, and type I and IV collagens [407]. Therefore, it may be possible that AIEC can also bind these proteins.

A second reason may be that DSS changes the composition of the intestinal microbiota that may otherwise limit AIEC colonization. Studies show that the administration of TNBS to larval zebrafish changes the proportion of species belonging to the Proteobacteria and Firmicutes phyla [423]. TNBS-treated fish experience an increase in Proteobacteria and a decrease in Firmicutes, an observation that has been found to be positively correlated with severity of intestinal inflammation [423]. Moreover, treatment of mice with DSS also results in dysbiosis of the colonic microflora and these changes are also correlated with severity of the

disease [424]. Further, it has also been shown that AIEC prevents the restoration of the normal intestinal microbiota in DSS-treated mice [425].

The third potential reason may be that intestinal inflammation causes the overexpression of a receptor important for binding of AIEC. *In vitro* studies suggest that AIEC can increase the expression of host adhesins. For example, the binding of LF82 through FimH to CEACAM6 induces blebbing of apoptotic cell-derived membranous vesicles, which exposes oligomannosidic glycans that serve as AIEC binding sites [283]. Moreover, others have shown that the expression of CECAM6 is increased by TNF-α and IFN-γ following AIEC infections [278]. To date, only one CEACAM ortholog (CEACAMz1) has been characterized in larval zebrafish. This protein has been shown to be predominantly expressed in gills and to a lesser extent in the intestine [426]. Interestingly, mammalian CEACAM6 is also expressed in the alveolar and airway epithelial cells of the lungs under homeostatic conditions and is highly expressed in the gut only during intestinal disease [427]. Further, larval zebrafish express a CEACAM6-like protein (encoded by the *zgc:198329* gene) in the intestine that is 29% identical to human CEACAM6 [428]. More studies are required to investigate whether the CECAM6-like protein is mannosylated, like human CEACAM6.

In an effort to investigate whether *fimH* and *ibeA* are important for AIEC colonization in the zebrafish intestine, these 2 genes were deleted from the parent strain. The reasoning was that FimH and IbeA are known virulence factors in other *in vitro* and *in vivo* models, so we wanted test if this was also the case in zebrafish larvae to address if our model is suitable for the discovery of virulence factors that mediate

in vivo infections. We reasoned that the phenotypes of known virulence factors would serve as a benchmark. It was surprising to see a slightly higher burden of LF82Δf*imH* and LF82Δ*ibeA* compared to the parent strain at the initial time point (Fig. 4-14 A and C). The reason for this is unknown, but it could be that the deletion of important virulence genes induces an overexpression of other adhesins. Although *fimH* and *ibeA* are important, AIEC possess numerous adhesins (as outlined in Chapter 1). As a result, the burden of AIEC LF82Δ*fimH* is not significantly decreased until 2 dpi in CEABAC10 mice and until 10 dpi in Vill-*hCC*6 mice with mammalian CEACAM6 expression in the ileum [221;[279]. Moreover, deletion of *ibeA* does not significantly impact the burden of AIEC in mice across 14 dpi [222, 280]. Based on the data presented here, FimH and IbeA may be more important for the retention of LF82 inside of larvae as the infection progresses. Interestingly though, the intestinal epithelium of larvae colonized with LF82Δ*fimH* and LF82Δ*ibeA* displayed less flattening through 48 hpi compared to the epithelium of fish infected with LF82, LF82Δ*fimH:fimH* and LF82Δ*ibeA:ibeA*. Furthermore, the infection of larvae with LF82Δf*imH* or LF82Δ*ibeA* also led to less neutrophil recruitment compared to fish infected with LF82, LF82Δ*fimH:fimH,* and LF82Δ*ibeA:ibeA*. Although, FimH and IbeA may be dispensable for early colonization to the zebrafish intestine, these 2 proteins do induce an immunogenic effect in the larval zebrafish intestine.

Inside of the larval intestine, LF82 appeared to form bacterial cell aggregates that were not observed when larvae were infected with the LF82Δ*fimH* and LF82Δ*ibeA* strains. Bacterial adhesion to the surface is an essential step in biofilm formation [429]. Since FimH plays a role in bacterial adhesion, it is plausible that its deletion interferes

with the biofilm formation process. Further, the FimH adhesins of uropathogenic *E. coli* and *Salmonella enterica* are highly similar to the FimH of AIEC LF82, and have been shown to be essential for biofilm formation in these strains [282, 430, 431]. Moreover, the deletion of *ibeA* in avian pathogenic *E. coli* also decreases biofilm formation, in comparison to the parent strain [432]. These observations suggest that the deletion of FimH and IbeA in AIEC LF82 may contribute to loss of biofilm formation and may explain why the deletion strains do not form bacterial cell aggregates inside of the larval zebrafish intestine.

For unknown reasons, the complementation of the *fimH* and *ibeA* in the AIEC LF82 deletion mutants did not restore the parent phenotypes (including bacterial cell aggregation and epithelial cell flattening at 48 hpi). However, whole genome sequencing showed that *fimH* and *ibeA* (as well as the Tn7 site from the mini-Tn7 vector used to insert the genes to the bacterial chromosome) were present at the Tn7 attachment site (attTn7) that is located downstream of the *glms1* gene in LF82. These data indicated that the complementation process was successful.

Based on immunofluorescence images, LF82Δ*ibeA* colonized the surface of cytoplasm at 2 and 48 hpi (Fig. 4-15, Di and Diii). However, at 24 hpi, LF82Δ*ibeA* was observed inside of the intestinal epithelium, like the parent and complemented strains. These data suggests that LF82 may employ other as of yet unidentified factors to invade. Interestingly, a phenotype that was seen several times during live imaging was what appeared to be the replication of AIEC LF82 inside of macrophages. Replication of AIEC inside of macrophages was usually observed outside the intestine. It is plausible that if AIEC breached the lamina propria, it moved into the

bloodstream, where it might have been engulfed by macrophages. Another reason might be that AIEC was internalized by epithelium-associated macrophages that sample the intestinal lumen [433]. Longer imaging experiments may be necessary to confirm this phenotype and to investigate how AIEC behave inside of macrophages *in vivo*. *In vitro* experiments suggest that the formation of a phagolysosome may be essential for the replication of AIEC inside of macrophages, however whether this occurs in a live animal is unknown [246].

Chapter 5: Overall Discussion and Perspectives

Overall discussion

The overall goal of my thesis was to determine whether larval zebrafish are a suitable model of AIEC colonization and pathogenesis. To address this question, the consequences of AIEC colonization in healthy and diseased hosts was investigated. Initial findings showed that the colonization and persistence of LF82 in untreated larvae was higher than that of MG1655. This model was then expanded to address how preexisting inflammation modulated AIEC colonization and persistence. The data presented in Chapter 3, showed that 0.5% DSS was a suitable concentration to induce intestinal inflammation in zebrafish larvae. This is in agreement with previous studies from Dr. Stefan Oehlers' lab, however some modifications were made to the E3 buffer to neutralize the acidification caused by 0.5% DSS. Treatment of larvae with 0.5% DSS resulted in increased colonization and persistence of AIEC LF82 compared to untreated larvae. Moreover, the colonization of LF82 in larvae with preexisting inflammation (caused by DSS) resulted in a significant increase in larval mortality compared to the survival of UT fish colonized with LF82, DSS-treated fish colonized with MG1655, and uninfected DSS-treated fish. These data suggest that DSS treatment of larvae enhanced the death of fish with existing inflammation infected with LF82, but LF82 alone did not induce larval death. Thus, the next question was why do AIEC cause mortality in larvae with preexisting inflammation. Intestinal neutrophil recruitment, histology, and qPCR analyses suggested that LF82 exacerbates inflammation in DSS-treated hosts. Further, image analysis showed that the burden of AIEC LF82 invading the intestinal epithelium was higher in DSS-treated fish compared to untreated controls, and that AIEC localized closer to lamina propria in fish with preexisting inflammation.

To investigate whether two virulence factors that mediate AIEC adhesion and invasion played a role in exacerbating inflammation, *fimH* and *ibeA*, were deleted from the parent LF82 strain, respectively. Based on the data presented in Chapter 4, it was concluded that the deletion of *ibeA* and *fimH* alone did not significantly affect burden and persistence during the first 24 hpi, but does significantly decrease AIEC burden at 48 hpi. As previously discussed in the Chapter 4 discussion, the deletion of *fimH* in LF82 does not significantly impact the AIEC burden in transgenic mice that express the type 1 pili receptor, CEACAM6, until later infection time points [221;279]. And the deletion of *ibeA* in AIEC NRG857c does not impact the burden of AIEC in mice across 14 dpi [222, 280]. Thus, although IbeA and FimH may not be essential for early LF82 colonization, they seem to be important for colonization at later time points in zebrafish larvae. Moreover, these data suggest that AIEC LF82 may express additional virulence factors that promote its survival inside of larvae. Interestingly, the colonization of LF82Δ*ibeA* and LF82Δ*fimH* resulted in decreased intestinal neutrophil recruitment and less epithelial damage compared to larvae that were infected with LF82, LF82 Δ*ibeA:ibeA,* and LF82Δ*fimH:fimH*. In mice, the colonization of AIEC NRG857 results in epithelial desquamation (flattening), severe ulceration, and complete loss of villi and crypts, however mice infected with AIEC NRG857cΔ*ibeA* do not exhibit severe damages, other than minor epithelial desquamation (flattening) [222]. Similarly, colonization of LF82Δ*fimH* causes less severe colonic epithelial damage compared to mice colonized with the parent LF82 strain [280]. Altogether these data suggest that larval zebrafish with preexisting inflammation exhibit similar

results as mice colonized with AIEC and may be used to model AIEC infections and to complement established mouse models.

The colonization of AIEC LF82 resulted in a significant increase in preexisting intestinal inflammation, suggesting that AIEC LF82 cause an immunogenic response that was not observed in larvae fed paramecia without bacteria. It is important to note that larvae fed paramecia, also potentially contained a small amount of the nonpathogenic *E. coli* strain MG1665, since all paramecia cultures are prepared and maintained using MG1655 as a food source. The presence of MG1655 (usually less than 10^2 CFU/fish) was sometimes observed on CHROMagar plates with homogenates of larvae fed paramecia only, indicating MG1655 might have been present in larvae during the initial infection times (2 hpi). However, inflammation was not exacerbated in larvae fed paramecia, as shown by the quantification of the relative expression of the proinflammatory cytokines and neutrophil recruitment to the intestine in these larvae compared to LF82-infected fish.

One major difference between larval zebrafish and mammals is the difference in body temperature. While mammals have an average body temperature of 37 ^{o}C, larval zebrafish are maintained at 30 ^{o}C [434]. However, this change in temperature has not hindered the modeling of bacterial infections in larvae, based on previously published studies [314, 415]. Controls to verify the expression of well-studied virulence genes may include a fluorescent gene reporter that monitors the expression of the gene inside the fish or by detecting the expression of the gene in AIEC grown at 30 ^{o}C.

Although this study included key readouts used to quantify intestinal inflammation in zebrafish larvae, there were two phenotypes that were not assessed after infection with AIEC. Clinical studies show that in humans, AIEC infections induce granulomas along the luminal mucosal surface of the intestine, but this was not assessed in larvae [187-189]. Although the aggregation of macrophages and neutrophils was observed during live imaging, the formation of granulomas was not further confirmed by transmission electron micrographs here. However, this method is commonly used in embryonic zebrafish infected with *Mycobacterium marinum,* and could be pursued in follow-up studies [435].

Another phenotype that was not studied in larval zebrafish infected with AIEC was intestinal permeability. Previous studies using monolayers of human colon-derived epithelial cells show that the parent LF82 strain, but not LF82Δ*fimH*, decreases intestinal barrier function [206]. Although it is unknown whether AIEC increase intestinal permeability in larvae, I attempted to investigate it here. Due to the lack of equipment for the oral gavage method, which is commonly used to deliver fluorescent dextran into the zebrafish intestine, infected larvae were incubated with 10 kD dextran conjugated to AlexaFluor 680, to visualize the translocation of dextran from the lumen into the bloodstream by microscopy. However, the dextran was difficult to wash away from the outside of the body of the larvae. To properly carry out this assay, oral gavage is required.

Future studies will investigate whether there are any significant changes in the transcription of proinflammatory cytokines in the zebrafish larvae infected with LF82 WT, LF82Δ*fimH* and LF82Δ*ibeA* at 6, 7, and 8 dpf (2, 24, and 48 hpi). Previous work

showed that mice colonized with LF82Δ*fimH* have lower levels of *il1b*, *il-6*, and *il-17* mRNAs [280]. Therefore, it would be interesting to know if larvae infected with the parent LF82 strain have increased markers of inflammation relative to those infected with LF82Δ*fimH*.

In addition, another challenge that was encountered was finding antibodies that target proinflammatory cytokines for Western blot analyses. In an effort to confirm our data from qRT-PCR experiments that quantified the transcription of proinflammatory genes, I performed Western Blot and immunofluorescence analyses with antibodies targeting proinflammatory markers, by testing zebrafish homogenates and fixed larval specimens. Ultimately, I did identify an IL-8 antibody that worked in the immunofluorescence assay, but the others did not work due to a lack of cross-specificity of the antibodies for zebrafish protein homologs. In general, this is an issue for many studies and a current limitation in the zebrafish field. However, as the field continues to grow, it is likely that new antibodies specifically targeting zebrafish inflammatory markers will become available.

Perspectives

As previously mentioned, the larval zebrafish model is not meant to replace mouse models of AIEC infections. Rather it is meant to complement mouse studies. In comparison to mammals, zebrafish larvae are cheaper to maintain, produce large numbers of offspring, and have a functional digestive system by 6 dpf. Additionally, many transgenic lines are available from repositories, and microscopy can be used to image tissues from the whole-organism level down to single cell detail. These characteristics make larval zebrafish advantageous for modeling intestinal diseases

and infections during early time points. Positive results regarding microbial virulence factors, host factors contributing to disease progression, and initial drug candidates in larval zebrafish, may then be further evaluated in mammals. Ultimately, this method will save researchers time and money.

There is an ongoing effort to identify a common AIEC molecular genetic signature in genotypically diverse strains to provide a means to develop diagnostics and alternative therapeutics for IBD patients, and to determine if there is a correlation between the presence of AIEC and disease severity. Some researchers argue that the reason that such biomarkers have not yet been discovered arises from the limitations of currently used infection models and *in vitro* models to classify *E. coli* strains as AIEC [196]. Previous attempts to identify molecular markers of AIEC have relied on *in vitro* systems to quantify adhesion, invasion, and replication inside of infected cells, since there are no widely conserved genetic features, such as the LEE pathogenicity islands in EHEC/EPEC, or certain toxins, such as in the case of STEC (Shiga-like toxins) and ETEC (LT/ST enterotoxins). However, it is plausible that there may be genes essential for AIEC *in vivo* colonization that are not expressed in a simplified *in vitro* model. In addition, other experts in the field believe that there are yet undiscovered AIEC genes, not commonly found in nonpathogenic *E. coli* strains that are yet to be identified. These are hypotheses that may be addressed using transposon mutagenesis and high-throughput assays in larval zebrafish.

A major drawback of using DSS to induce intestinal inflammation is that approximately 50% of the larvae are lost after treatment. A second drawback is that although DSS creates an inflammatory environment, it does not completely mimic the

mechanisms behind IBD. As outlined in chapter 1, IBD is a complex disease that arises from mutations in genes that are essential for the clearance of foreign microbes. However, with the rapid expansion of the zebrafish field it may be possible to investigate the consequences of AIEC colonization in zebrafish with genetic mutations similar to those carried in IBD patients. Recently, a novel IBD zebrafish model with a knockout in the tRNA methyltransferase 5 (*trmt5*) gene, a mutated gene in IBD patients, was generated and shown to develop spontaneous inflammation [436]. The development of the *trmt5−/−* larval zebrafish shows that larvae are generating more traction for the study of IBD and opens the possibilities for future studies to investigate the effect of AIEC colonization in a host with impaired bacterial sensing and autophagy.

One reason this project was developed was to use it in future studies to investigate the interactions of AIEC with the mucin, MUC2. Previous work from our lab has shown that the gut commensal strain *E. coli* HS*,* possesses a MAM adhesin, that is 99% identical to the MAM adhesion of AIEC, and that binds sulfate moieties of MUC2 [76]. This study also showed that sulfatase-secreting bacteria influence the retention of *E. coli* HS by the mucus layer. Further, clinical studies suggest that there is a correlation between sulfatase-secreting bacteria and IBD. For instance, mucosal tissue samples isolated from patients with IBD have an overabundance of sulfatase secreting *Bacteroidetes* and *Prevotella* species, compared to healthy controls [437]. Moreover, *B. thetaiotaomicron,* induces colitis in genetically susceptible mice through secretion of sulfatases via OMVs [438]. Additionally, increased sulfatase activity has been observed in fecal samples from IBD patients compared to healthy patients [439].

Further, as previously mentioned in Chapter 1 there is a positive correlation between a decreased expression of sulfotransferases (SULTs) and IBD [71, 72]. Altogether these data suggest that mucin sulfation plays a role in maintaining intestinal mucosal defenses, and that determining the role of mucin sulfation and sulfatases in AIEC colonization and IBD may be beneficial for the development of therapeutics that restore the integrity of the mucus barrier.

The larval zebrafish is a suitable model organism for this study because the zebrafish MUC2.1 mucin protein is homologous to mammalian MUC2 and its expression in the intestinal tract is conserved [440]. Zebrafish MUC2.1 also contains proline threonine serine-rich (PTS) domains that undergo O-glycosylation, fucosylation, sialylation, and sulfation [440]. Furthermore, zebrafish express homologs of two human intestinal enzymes responsible for mucin sulfation: carbohydrate sulfotransferase 5 (CHST5) and galactose-3-O-sulfotransferase-2 (GAL3ST2) [441, 442]. These features make zebrafish an appropriate model for potentially elucidating mucin-associated mechanisms of AIEC retention in the mucus layer *in vivo*. Currently, our lab is investigating whether the colonization of AIEC LF82 influences the expression of GAL3ST2 and CHST5. We hope that these studies will further the AIEC and IBD field and eventually translate into meaningful outcomes for patients.

References

1. Baumgart DC, Carding SR. Inflammatory bowel disease: cause and immunobiology. Lancet. 2007;369(9573):1627-40. doi: 10.1016/S0140-6736(07)60750-8. PubMed PMID: 17499605.

2. Kaplan GG. The global burden of IBD: from 2015 to 2025. Nat Rev Gastroenterol Hepatol. 2015;12(12):720-7. Epub 20150901. doi: 10.1038/nrgastro.2015.150. PubMed PMID: 26323879.

3. Loftus EV. Clinical epidemiology of inflammatory bowel disease: Incidence, prevalence, and environmental influences. Gastroenterology. 2004;126(6):1504-17. doi: 10.1053/j.gastro.2004.01.063. PubMed PMID: 15168363.

4. Shaw KA, Bertha M, Hofmekler T, Chopra P, Vatanen T, Srivatsa A, Prince J, Kumar A, Sauer C, Zwick ME, Satten GA, Kostic AD, Mulle JG, Xavier RJ, Kugathasan S. Dysbiosis, inflammation, and response to treatment: a longitudinal study of pediatric subjects with newly diagnosed inflammatory bowel disease. Genome Med. 2016;8(1):75. Epub 20160713. doi: 10.1186/s13073-016-0331-y. PubMed PMID: 27412252; PubMed Central PMCID: PMCPMC4944441.

5. Flynn S, Eisenstein S. Inflammatory Bowel Disease Presentation and Diagnosis. Surg Clin North Am. 2019;99(6):1051-62. Epub 20190911. doi: 10.1016/j.suc.2019.08.001. PubMed PMID: 31676047.

6. Wehkamp J, Götz M, Herrlinger K, Steurer W, Stange EF. Inflammatory Bowel Disease. Dtsch Arztebl Int. 2016;113(5):72-82. doi: 10.3238/arztebl.2016.0072. PubMed PMID: 26900160; PubMed Central PMCID: PMCPMC4782273.

7. Rhodes JM, Campbell BJ. Inflammation and colorectal cancer: IBD-associated and sporadic cancer compared. Trends Mol Med. 2002;8(1):10-6. doi: 10.1016/s1471-4914(01)02194-3. PubMed PMID: 11796261.

8. Seyedian SS, Nokhostin F, Malamir MD. A review of the diagnosis, prevention, and treatment methods of inflammatory bowel disease. J Med Life. 2019;12(2):113-22. doi: 10.25122/jml-2018-0075. PubMed PMID: 31406511; PubMed Central PMCID: PMCPMC6685307.

9. Axelrad JE, Lichtiger S, Yajnik V. Inflammatory bowel disease and cancer: The role of inflammation, immunosuppression, and cancer treatment. World J Gastroenterol. 2016;22(20):4794-801. doi: 10.3748/wjg.v22.i20.4794. PubMed PMID: 27239106; PubMed Central PMCID: PMCPMC4873872.

10. Sevim Y, Akyol C, Aytac E, Baca B, Bulut O, Remzi FH. Laparoscopic surgery for complex and recurrent Crohn's disease. World J Gastrointest Endosc. 2017;9(4):149-52. doi: 10.4253/wjge.v9.i4.149. PubMed PMID: 28465780; PubMed Central PMCID: PMCPMC5394720.

11. Liu S, Eisenstein S. State-of-the-art surgery for ulcerative colitis. Langenbecks Arch Surg. 2021;406(6):1751-61. Epub 20210828. doi: 10.1007/s00423-021-02295-6. PubMed PMID: 34453611; PubMed Central PMCID: PMCPMC8481179.

12. Bach SP, Mortensen NJ. Ileal pouch surgery for ulcerative colitis. World J Gastroenterol. 2007;13(24):3288-300. doi: 10.3748/wjg.v13.i24.3288. PubMed PMID: 17659667; PubMed Central PMCID: PMCPMC4172708.

13. Turpin W, Goethel A, Bedrani L, Croitoru Mdcm K. Determinants of IBD Heritability: Genes, Bugs, and More. Inflamm Bowel Dis. 2018;24(6):1133-48. doi:

10.1093/ibd/izy085. PubMed PMID: 29701818; PubMed Central PMCID: PMCPMC6093195.

14. Buttó LF, Schaubeck M, Haller D. Mechanisms of Microbe-Host Interaction in Crohn's Disease: Dysbiosis vs. Pathobiont Selection. Front Immunol. 2015;6:555. Epub 20151119. doi: 10.3389/fimmu.2015.00555. PubMed PMID: 26635787; PubMed Central PMCID: PMCPMC4652232.

15. Graham DB, Xavier RJ. Pathway paradigms revealed from the genetics of inflammatory bowel disease. Nature. 2020;578(7796):527-39. Epub 20200226. doi: 10.1038/s41586-020-2025-2. PubMed PMID: 32103191; PubMed Central PMCID: PMCPMC7871366.

16. Vancamelbeke M, Vermeire S. The intestinal barrier: a fundamental role in health and disease. Expert Rev Gastroenterol Hepatol. 2017;11(9):821-34. Epub 20170626. doi: 10.1080/17474124.2017.1343143. PubMed PMID: 28650209; PubMed Central PMCID: PMCPMC6104804.

17. Johansson ME, Ambort D, Pelaseyed T, Schütte A, Gustafsson JK, Ermund A, Subramani DB, Holmén-Larsson JM, Thomsson KA, Bergström JH, van der Post S, Rodriguez-Piñeiro AM, Sjövall H, Bäckström M, Hansson GC. Composition and functional role of the mucus layers in the intestine. Cell Mol Life Sci. 2011;68(22):3635-41. Epub 20110925. doi: 10.1007/s00018-011-0822-3. PubMed PMID: 21947475.

18. Johansson ME, Hansson GC. Immunological aspects of intestinal mucus and mucins. Nat Rev Immunol. 2016;16(10):639-49. Epub 20160808. doi:

10.1038/nri.2016.88. PubMed PMID: 27498766; PubMed Central PMCID: PMCPMC6435297.

19. Yeap YY, Lock J, Lerkvikarn S, Semin T, Nguyen N, Carrier RL. Intestinal mucus is capable of stabilizing supersaturation of poorly water-soluble drugs. J Control Release. 2019;296:107-13. Epub 20181206. doi: 10.1016/j.jconrel.2018.11.023. PubMed PMID: 30527813; PubMed Central PMCID: PMCPMC6467574.

20. Atuma C, Strugala V, Allen A, Holm L. The adherent gastrointestinal mucus gel layer: thickness and physical state in vivo. Am J Physiol Gastrointest Liver Physiol. 2001;280(5):G922-9. doi: 10.1152/ajpgi.2001.280.5.G922. PubMed PMID: 11292601.

21. Hansson GC. Role of mucus layers in gut infection and inflammation. Curr Opin Microbiol. 2012;15(1):57-62. Epub 20111214. doi: 10.1016/j.mib.2011.11.002. PubMed PMID: 22177113; PubMed Central PMCID: PMCPMC3716454.

22. Johansson ME, Larsson JM, Hansson GC. The two mucus layers of colon are organized by the MUC2 mucin, whereas the outer layer is a legislator of host-microbial interactions. Proc Natl Acad Sci U S A. 2011;108 Suppl 1(Suppl 1):4659-65. Epub 20100625. doi: 10.1073/pnas.1006451107. PubMed PMID: 20615996; PubMed Central PMCID: PMCPMC3063600.

23. Johansson ME, Phillipson M, Petersson J, Velcich A, Holm L, Hansson GC. The inner of the two Muc2 mucin-dependent mucus layers in colon is devoid of bacteria. Proc Natl Acad Sci U S A. 2008;105(39):15064-9. Epub 20080919. doi: 10.1073/pnas.0803124105. PubMed PMID: 18806221; PubMed Central PMCID: PMCPMC2567493.

24. Hsiao WW, Metz C, Singh DP, Roth J. The microbes of the intestine: an introduction to their metabolic and signaling capabilities. Endocrinol Metab Clin North Am. 2008;37(4):857-71. doi: 10.1016/j.ecl.2008.08.006. PubMed PMID: 19026936; PubMed Central PMCID: PMCPMC4411945.

25. Cullen PJ. Post-translational regulation of signaling mucins. Curr Opin Struct Biol. 2011;21(5):590-6. Epub 20110831. doi: 10.1016/j.sbi.2011.08.007. PubMed PMID: 21889329; PubMed Central PMCID: PMCPMC3189326.

26. Kong S, Zhang YH, Zhang W. Regulation of Intestinal Epithelial Cells Properties and Functions by Amino Acids. Biomed Res Int. 2018;2018:2819154. Epub 20180509. doi: 10.1155/2018/2819154. PubMed PMID: 29854738; PubMed Central PMCID: PMCPMC5966675.

27. Peterson LW, Artis D. Intestinal epithelial cells: regulators of barrier function and immune homeostasis. Nat Rev Immunol. 2014;14(3):141-53. doi: 10.1038/nri3608. PubMed PMID: 24566914.

28. Noah TK, Donahue B, Shroyer NF. Intestinal development and differentiation. Exp Cell Res. 2011;317(19):2702-10. Epub 20110924. doi: 10.1016/j.yexcr.2011.09.006. PubMed PMID: 21978911; PubMed Central PMCID: PMCPMC3210330.

29. Worthington JJ, Reimann F, Gribble FM. Enteroendocrine cells-sensory sentinels of the intestinal environment and orchestrators of mucosal immunity. Mucosal Immunol. 2018;11(1):3-20. Epub 20170830. doi: 10.1038/mi.2017.73. PubMed PMID: 28853441.

30. Porter EM, Bevins CL, Ghosh D, Ganz T. The multifaceted Paneth cell. Cell Mol Life Sci. 2002;59(1):156-70. doi: 10.1007/s00018-002-8412-z. PubMed PMID: 11846026.

31. Mei X, Gu M, Li M. Plasticity of Paneth cells and their ability to regulate intestinal stem cells. Stem Cell Res Ther. 2020;11(1):349. Epub 20200812. doi: 10.1186/s13287-020-01857-7. PubMed PMID: 32787930; PubMed Central PMCID: PMCPMC7425583.

32. Kanaya T, Sakakibara S, Jinnohara T, Hachisuka M, Tachibana N, Hidano S, Kobayashi T, Kimura S, Iwanaga T, Nakagawa T, Katsuno T, Kato N, Akiyama T, Sato T, Williams IR, Ohno H. Development of intestinal M cells and follicle-associated epithelium is regulated by TRAF6-mediated NF-κB signaling. J Exp Med. 2018;215(2):501-19. Epub 20180116. doi: 10.1084/jem.20160659. PubMed PMID: 29339448; PubMed Central PMCID: PMCPMC5789402.

33. Groschwitz KR, Hogan SP. Intestinal barrier function: molecular regulation and disease pathogenesis. J Allergy Clin Immunol. 2009;124(1):3-20; quiz 1-2. doi: 10.1016/j.jaci.2009.05.038. PubMed PMID: 19560575; PubMed Central PMCID: PMCPMC4266989.

34. Tsukita S, Furuse M. The structure and function of claudins, cell adhesion molecules at tight junctions. Ann N Y Acad Sci. 2000;915:129-35. doi: 10.1111/j.1749-6632.2000.tb05235.x. PubMed PMID: 11193568.

35. Morita K, Tsukita S, Miyachi Y. Tight junction-associated proteins (occludin, ZO-1, claudin-1, claudin-4) in squamous cell carcinoma and Bowen's disease. Br J

Dermatol. 2004;151(2):328-34. doi: 10.1111/j.1365-2133.2004.06029.x. PubMed PMID: 15327539.

36. Schneeberger EE, Lynch RD. Structure, function, and regulation of cellular tight junctions. Am J Physiol. 1992;262(6 Pt 1):L647-61. doi: 10.1152/ajplung.1992.262.6.L647. PubMed PMID: 1616050.

37. Kowalczyk AP, Green KJ. Structure, function, and regulation of desmosomes. Prog Mol Biol Transl Sci. 2013;116:95-118. doi: 10.1016/B978-0-12-394311-8.00005-4. PubMed PMID: 23481192; PubMed Central PMCID: PMCPMC4336551.

38. Saito M, Tucker DK, Kohlhorst D, Niessen CM, Kowalczyk AP. Classical and desmosomal cadherins at a glance. J Cell Sci. 2012;125(Pt 11):2547-52. doi: 10.1242/jcs.066654. PubMed PMID: 22833291; PubMed Central PMCID: PMCPMC3403229.

39. Krug SM, Schulzke JD, Fromm M. Tight junction, selective permeability, and related diseases. Semin Cell Dev Biol. 2014;36:166-76. Epub 20140916. doi: 10.1016/j.semcdb.2014.09.002. PubMed PMID: 25220018.

40. Bruewer M, Samarin S, Nusrat A. Inflammatory bowel disease and the apical junctional complex. Ann N Y Acad Sci. 2006;1072:242-52. doi: 10.1196/annals.1326.017. PubMed PMID: 17057204.

41. Picut CA, Coleman GD. Chapter 5 - Gastrointestinal Tract. In: Parker GA, Picut CA, editors. Atlas of Histology of the Juvenile Rat. Boston: Academic Press; 2016. p. 127-71.

42. Berek C, Beller A, Chu VT. Isolation of Eosinophils from the Lamina Propria of the Murine Small Intestine. Methods Mol Biol. 2016;1422:213-21. doi: 10.1007/978-1-4939-3603-8_20. PubMed PMID: 27246036.

43. Boudry G, Yang P-C, Perdue MH. Small Intestine, Anatomy. In: Johnson LR, editor. Encyclopedia of Gastroenterology. New York: Elsevier; 2004. p. 404-9.

44. Persson EK, Scott CL, Mowat AM, Agace WW. Dendritic cell subsets in the intestinal lamina propria: ontogeny and function. Eur J Immunol. 2013;43(12):3098-107. Epub 20130821. doi: 10.1002/eji.201343740. PubMed PMID: 23966272; PubMed Central PMCID: PMCPMC3933733.

45. Lee E, Schiller LR, Fordtran JS. Quantification of colonic lamina propria cells by means of a morphometric point-counting method. Gastroenterology. 1988;94(2):409-18. doi: 10.1016/0016-5085(88)90430-1. PubMed PMID: 3335315.

46. Marshall JS, Warrington R, Watson W, Kim HL. An introduction to immunology and immunopathology. Allergy, Asthma & Clinical Immunology. 2018;14(2):49. doi: 10.1186/s13223-018-0278-1.

47. Silva MT, Correia-Neves M. Neutrophils and macrophages: the main partners of phagocyte cell systems. Front Immunol. 2012;3:174. Epub 20120704. doi: 10.3389/fimmu.2012.00174. PubMed PMID: 22783254; PubMed Central PMCID: PMCPMC3389340.

48. Stock AJ, Kasus-Jacobi A, Pereira HA. The role of neutrophil granule proteins in neuroinflammation and Alzheimer's disease. J Neuroinflammation. 2018;15(1):240. Epub 20180827. doi: 10.1186/s12974-018-1284-4. PubMed PMID: 30149799; PubMed Central PMCID: PMCPMC6112130.

49. Fukata M, Arditi M. The role of pattern recognition receptors in intestinal inflammation. Mucosal Immunol. 2013;6(3):451-63. Epub 20130320. doi: 10.1038/mi.2013.13. PubMed PMID: 23515136; PubMed Central PMCID: PMCPMC3730813.

50. Jang JH, Shin HW, Lee JM, Lee HW, Kim EC, Park SH. An Overview of Pathogen Recognition Receptors for Innate Immunity in Dental Pulp. Mediators Inflamm. 2015;2015:794143. Epub 20151020. doi: 10.1155/2015/794143. PubMed PMID: 26576076; PubMed Central PMCID: PMCPMC4630409.

51. Michielan A, D'Incà R. Intestinal Permeability in Inflammatory Bowel Disease: Pathogenesis, Clinical Evaluation, and Therapy of Leaky Gut. Mediators Inflamm. 2015;2015:628157. Epub 20151025. doi: 10.1155/2015/628157. PubMed PMID: 26582965; PubMed Central PMCID: PMCPMC4637104.

52. Irvine EJ, Marshall JK. Increased intestinal permeability precedes the onset of Crohn's disease in a subject with familial risk. Gastroenterology. 2000;119(6):1740-4. doi: 10.1053/gast.2000.20231. PubMed PMID: 11113095.

53. Vogelsang H. Do changes in intestinal permeability predict disease relapse in Crohn's disease? Inflamm Bowel Dis. 2008;14 Suppl 2:S162-3. doi: 10.1002/ibd.20617. PubMed PMID: 18816766.

54. Wang F, Graham WV, Wang Y, Witkowski ED, Schwarz BT, Turner JR. Interferon-gamma and tumor necrosis factor-alpha synergize to induce intestinal epithelial barrier dysfunction by up-regulating myosin light chain kinase expression. Am J Pathol. 2005;166(2):409-19. doi: 10.1016/s0002-9440(10)62264-x. PubMed PMID: 15681825; PubMed Central PMCID: PMCPMC1237049.

55. Noth R, Stüber E, Häsler R, Nikolaus S, Kühbacher T, Hampe J, Bewig B, Schreiber S, Arlt A. Anti-TNF-α antibodies improve intestinal barrier function in Crohn's disease. J Crohns Colitis. 2012;6(4):464-9. Epub 20111111. doi: 10.1016/j.crohns.2011.10.004. PubMed PMID: 22398062.

56. Pullan RD, Thomas GA, Rhodes M, Newcombe RG, Williams GT, Allen A, Rhodes J. Thickness of adherent mucus gel on colonic mucosa in humans and its relevance to colitis. Gut. 1994;35(3):353-9. doi: 10.1136/gut.35.3.353. PubMed PMID: 8150346; PubMed Central PMCID: PMCPMC1374589.

57. Gersemann M, Becker S, Kübler I, Koslowski M, Wang G, Herrlinger KR, Griger J, Fritz P, Fellermann K, Schwab M, Wehkamp J, Stange EF. Differences in goblet cell differentiation between Crohn's disease and ulcerative colitis. Differentiation. 2009;77(1):84-94. Epub 20081022. doi: 10.1016/j.diff.2008.09.008. PubMed PMID: 19281767.

58. Hanski C, Born M, Foss HD, Marowski B, Mansmann U, Arastéh K, Bachler B, Papenfuss M, Niedobitek F. Defective post-transcriptional processing of MUC2 mucin in ulcerative colitis and in Crohn's disease increases detectability of the MUC2 protein core. J Pathol. 1999;188(3):304-11. doi: 10.1002/(SICI)1096-9896(199907)188:3<304::AID-PATH375>3.0.CO;2-A. PubMed PMID: 10419600.

59. Sun J, Shen X, Li Y, Guo Z, Zhu W, Zuo L, Zhao J, Gu L, Gong J, Li J. Therapeutic Potential to Modify the Mucus Barrier in Inflammatory Bowel Disease. Nutrients. 2016;8(1). Epub 20160114. doi: 10.3390/nu8010044. PubMed PMID: 26784223; PubMed Central PMCID: PMCPMC4728657.

60. McCormick DA, Horton LW, Mee AS. Mucin depletion in inflammatory bowel disease. J Clin Pathol. 1990;43(2):143-6. doi: 10.1136/jcp.43.2.143. PubMed PMID: 2318990; PubMed Central PMCID: PMCPMC502296.

61. Zheng X, Tsuchiya K, Okamoto R, Iwasaki M, Kano Y, Sakamoto N, Nakamura T, Watanabe M. Suppression of hath1 gene expression directly regulated by hes1 via notch signaling is associated with goblet cell depletion in ulcerative colitis. Inflamm Bowel Dis. 2011;17(11):2251-60. Epub 20110106. doi: 10.1002/ibd.21611. PubMed PMID: 21987298.

62. Raouf AH, Tsai HH, Parker N, Hoffman J, Walker RJ, Rhodes JM. Sulphation of colonic and rectal mucin in inflammatory bowel disease: reduced sulphation of rectal mucus in ulcerative colitis. Clin Sci (Lond). 1992;83(5):623-6. doi: 10.1042/cs0830623. PubMed PMID: 1335401.

63. Corfield AP, Myerscough N, Bradfield N, Corfield CoA, Gough M, Clamp JR, Durdey P, Warren BF, Bartolo DC, King KR, Williams JM. Colonic mucins in ulcerative colitis: evidence for loss of sulfation. Glycoconj J. 1996;13(5):809-22. doi: 10.1007/BF00702345. PubMed PMID: 8910008.

64. Rho JH, Wright DP, Christie DL, Clinch K, Furneaux RH, Roberton AM. A novel mechanism for desulfation of mucin: identification and cloning of a mucin-desulfating glycosidase (sulfoglycosidase) from Prevotella strain RS2. J Bacteriol. 2005;187(5):1543-51. doi: 10.1128/JB.187.5.1543-1551.2005. PubMed PMID: 15716424; PubMed Central PMCID: PMCPMC1064001.

65. Tobisawa Y, Imai Y, Fukuda M, Kawashima H. Sulfation of colonic mucins by N-acetylglucosamine 6-O-sulfotransferase-2 and its protective function in

experimental colitis in mice. J Biol Chem. 2010;285(9):6750-60. Epub 20091216. doi: 10.1074/jbc.M109.067082. PubMed PMID: 20018871; PubMed Central PMCID: PMCPMC2825469.

66. Felgentreff K, Beisswenger C, Griese M, Gulder T, Bringmann G, Bals R. The antimicrobial peptide cathelicidin interacts with airway mucus. Peptides. 2006;27(12):3100-6. Epub 20060911. doi: 10.1016/j.peptides.2006.07.018. PubMed PMID: 16963160.

67. Antoni L, Nuding S, Wehkamp J, Stange EF. Intestinal barrier in inflammatory bowel disease. World J Gastroenterol. 2014;20(5):1165-79. doi: 10.3748/wjg.v20.i5.1165. PubMed PMID: 24574793; PubMed Central PMCID: PMCPMC3921501.

68. Slomiany BL, Liau YH, Carter SR, Sarosiek J, Tsukada H, Slomiany A. Enzymatic sulfation of mucin in gastric mucosa: effect of sofalcone, sucralfate and aspirin. Digestion. 1987;38(3):178-86. doi: 10.1159/000199588. PubMed PMID: 3481699.

69. Osawa H, Ohnishi H, Kita H, Igari T, Hayashi Y, Iwamori M, Kawakami M, Sugano K. Reduced expression of sulfatides and galactosylceramide 3'-sulfotransferase in the gastric mucosa of chronic gastritis. J Clin Gastroenterol. 2008;42(1):23-8. doi: 10.1097/01.mcg.0000225663.61297.03. PubMed PMID: 18097285.

70. Denys A, Allain F. The Emerging Roles of Heparan Sulfate 3-. Front Oncol. 2019;9:507. Epub 20190612. doi: 10.3389/fonc.2019.00507. PubMed PMID: 31249810; PubMed Central PMCID: PMCPMC6582251.

71. Low S, Hirakawa J, Hoshino H, Uchimura K, Kawashima H, Kobayashi M. Role of MAdCAM-1-Expressing High Endothelial Venule-Like Vessels in Colitis Induced in Mice Lacking Sulfotransferases Catalyzing L-Selectin Ligand Biosynthesis. J Histochem Cytochem. 2018;66(6):415-25. Epub 20180119. doi: 10.1369/0022155417753363. PubMed PMID: 29350564; PubMed Central PMCID: PMCPMC5977439.

72. Suzuki K, Arumugam S, Yokoyama J, Kawauchi Y, Honda Y, Sato H, Aoyagi Y, Terai S, Okazaki K, Suzuki Y, Mizumoto S, Sugahara K, Atreya R, Neurath MF, Watanabe K, Hashiguchi T, Yoneyama H, Asakura H. Pivotal Role of Carbohydrate Sulfotransferase 15 in Fibrosis and Mucosal Healing in Mouse Colitis. PLoS One. 2016;11(7):e0158967. Epub 20160713. doi: 10.1371/journal.pone.0158967. PubMed PMID: 27410685; PubMed Central PMCID: PMCPMC4943596.

73. Jahnel J, Fickert P, Hauer AC, Högenauer C, Avian A, Trauner M. Inflammatory bowel disease alters intestinal bile acid transporter expression. Drug Metab Dispos. 2014;42(9):1423-31. Epub 20140625. doi: 10.1124/dmd.114.058065. PubMed PMID: 24965812.

74. Croix JA, Bhatia S, Gaskins HR. Inflammatory cues modulate the expression of secretory product genes, Golgi sulfotransferases and sulfomucin production in LS174T cells. Exp Biol Med (Maywood). 2011;236(12):1402-12. Epub 20111118. doi: 10.1258/ebm.2011.011186. PubMed PMID: 22101519.

75. Luis AS, Jin C, Pereira GV, Glowacki RWP, Gugel SR, Singh S, Byrne DP, Pudlo NA, London JA, Baslé A, Reihill M, Oscarson S, Eyers PA, Czjzek M, Michel G, Barbeyron T, Yates EA, Hansson GC, Karlsson NG, Cartmell A, Martens EC. A single

sulfatase is required to access colonic mucin by a gut bacterium. Nature. 2021;598(7880):332-7. Epub 20211006. doi: 10.1038/s41586-021-03967-5. PubMed PMID: 34616040; PubMed Central PMCID: PMCPMC9128668.

76. Al-Saedi F, Vaz DP, Stones DH, Krachler AM. 3-Sulfogalactosyl-dependent adhesion of. J Biol Chem. 2017;292(48):19792-803. Epub 20171005. doi: 10.1074/jbc.M117.817908. PubMed PMID: 28982977; PubMed Central PMCID: PMCPMC5712619.

77. Cunliffe RN, Rose FR, Keyte J, Abberley L, Chan WC, Mahida YR. Human defensin 5 is stored in precursor form in normal Paneth cells and is expressed by some villous epithelial cells and by metaplastic Paneth cells in the colon in inflammatory bowel disease. Gut. 2001;48(2):176-85. doi: 10.1136/gut.48.2.176. PubMed PMID: 11156637; PubMed Central PMCID: PMCPMC1728187.

78. Watanabe H. Experimentally induced intestinal metaplasia in Wistar rats by X-ray irradiation. Gastroenterology. 1978;75(5):796-9. PubMed PMID: 700322.

79. Wehkamp J, Harder J, Weichenthal M, Schwab M, Schäffeler E, Schlee M, Herrlinger KR, Stallmach A, Noack F, Fritz P, Schröder JM, Bevins CL, Fellermann K, Stange EF. NOD2 (CARD15) mutations in Crohn's disease are associated with diminished mucosal alpha-defensin expression. Gut. 2004;53(11):1658-64. doi: 10.1136/gut.2003.032805. PubMed PMID: 15479689; PubMed Central PMCID: PMCPMC1774270.

80. Cadwell K, Liu JY, Brown SL, Miyoshi H, Loh J, Lennerz JK, Kishi C, Kc W, Carrero JA, Hunt S, Stone CD, Brunt EM, Xavier RJ, Sleckman BP, Li E, Mizushima N, Stappenbeck TS, Virgin HW. A key role for autophagy and the autophagy gene

Atg16l1 in mouse and human intestinal Paneth cells. Nature. 2008;456(7219):259-63. Epub 20081005. doi: 10.1038/nature07416. PubMed PMID: 18849966; PubMed Central PMCID: PMCPMC2695978.

81. Wehkamp J, Salzman NH, Porter E, Nuding S, Weichenthal M, Petras RE, Shen B, Schaeffeler E, Schwab M, Linzmeier R, Feathers RW, Chu H, Lima H, Fellermann K, Ganz T, Stange EF, Bevins CL. Reduced Paneth cell alpha-defensins in ileal Crohn's disease. Proc Natl Acad Sci U S A. 2005;102(50):18129-34. Epub 20051205. doi: 10.1073/pnas.0505256102. PubMed PMID: 16330776; PubMed Central PMCID: PMCPMC1306791.

82. Wesener DA, Wangkanont K, McBride R, Song X, Kraft MB, Hodges HL, Zarling LC, Splain RA, Smith DF, Cummings RD, Paulson JC, Forest KT, Kiessling LL. Recognition of microbial glycans by human intelectin-1. Nat Struct Mol Biol. 2015;22(8):603-10. Epub 20150706. doi: 10.1038/nsmb.3053. PubMed PMID: 26148048; PubMed Central PMCID: PMCPMC4526365.

83. Nonnecke EB, Castillo PA, Akahoshi DT, Goley SM, Bevins CL, Lönnerdal B. Characterization of an intelectin-1 (Front Immunol. 2022;13:894649. Epub 20220822. doi: 10.3389/fimmu.2022.894649. PubMed PMID: 36072603; PubMed Central PMCID: PMCPMC9441953.

84. Nonnecke EB, Castillo PA, Dugan AE, Almalki F, Underwood MA, De La Motte CA, Yuan W, Lu W, Shen B, Johansson MEV, Kiessling LL, Hollox EJ, Lönnerdal B, Bevins CL. Human intelectin-1 (ITLN1) genetic variation and intestinal expression. Sci Rep. 2021;11(1):12889. Epub 20210618. doi: 10.1038/s41598-021-92198-9. PubMed PMID: 34145348; PubMed Central PMCID: PMCPMC8213764.

85. Wehkamp J, Stange EF. An Update Review on the Paneth Cell as Key to Ileal Crohn's Disease. Front Immunol. 2020;11:646. Epub 20200415. doi: 10.3389/fimmu.2020.00646. PubMed PMID: 32351509; PubMed Central PMCID: PMCPMC7174711.

86. Berkowitz L, Pardo-Roa C, Salazar GA, Salazar-Echegarai F, Miranda JP, Ramírez G, Chávez JL, Kalergis AM, Bueno SM, Álvarez-Lobos M. Mucosal Exposure to Cigarette Components Induces Intestinal Inflammation and Alters Antimicrobial Response in Mice. Front Immunol. 2019;10:2289. Epub 20190925. doi: 10.3389/fimmu.2019.02289. PubMed PMID: 31608070; PubMed Central PMCID: PMCPMC6773925.

87. Mak JWY, Yang S, Stanley A, Lin X, Morrison M, Ching JYL, Niu J, Wilson-O'Brien AL, Feng R, Tang W, Hamilton AL, Or L, Trakman GL, Lin WYY, Sung JJY, Chen MH, Mao Y, Kamm MA, Ng SC. Childhood antibiotics as a risk factor for Crohn's disease: The ENIGMA International Cohort Study. JGH Open. 2022;6(6):369-77. Epub 20220601. doi: 10.1002/jgh3.12755. PubMed PMID: 35774350; PubMed Central PMCID: PMCPMC9218523.

88. Kronman MP, Zaoutis TE, Haynes K, Feng R, Coffin SE. Antibiotic exposure and IBD development among children: a population-based cohort study. Pediatrics. 2012;130(4):e794-803. Epub 20120924. doi: 10.1542/peds.2011-3886. PubMed PMID: 23008454; PubMed Central PMCID: PMCPMC4074626.

89. Virta L, Auvinen A, Helenius H, Huovinen P, Kolho KL. Association of repeated exposure to antibiotics with the development of pediatric Crohn's disease--a nationwide, register-based finnish case-control study. Am J Epidemiol.

2012;175(8):775-84. Epub 20120224. doi: 10.1093/aje/kwr400. PubMed PMID: 22366379.

90. Ozkul C, Ruiz VE, Battaglia T, Xu J, Roubaud-Baudron C, Cadwell K, Perez-Perez GI, Blaser MJ. A single early-in-life antibiotic course increases susceptibility to DSS-induced colitis. Genome Med. 2020;12(1):65. Epub 20200725. doi: 10.1186/s13073-020-00764-z. PubMed PMID: 32711559; PubMed Central PMCID: PMCPMC7382806.

91. Su D, Nie Y, Zhu A, Chen Z, Wu P, Zhang L, Luo M, Sun Q, Cai L, Lai Y, Xiao Z, Duan Z, Zheng S, Wu G, Hu R, Tsukamoto H, Lugea A, Liu Z, Pandol SJ, Han YP. Vitamin D Signaling through Induction of Paneth Cell Defensins Maintains Gut Microbiota and Improves Metabolic Disorders and Hepatic Steatosis in Animal Models. Front Physiol. 2016;7:498. Epub 20161115. doi: 10.3389/fphys.2016.00498. PubMed PMID: 27895587; PubMed Central PMCID: PMCPMC5108805.

92. Mineta K, Yamamoto Y, Yamazaki Y, Tanaka H, Tada Y, Saito K, Tamura A, Igarashi M, Endo T, Takeuchi K, Tsukita S. Predicted expansion of the claudin multigene family. FEBS Letters. 2011;585(4):606-12. doi: https://doi.org/10.1016/j.febslet.2011.01.028.

93. Tang VW, Goodenough DA. Paracellular ion channel at the tight junction. Biophys J. 2003;84(3):1660-73. doi: 10.1016/S0006-3495(03)74975-3. PubMed PMID: 12609869; PubMed Central PMCID: PMCPMC1302736.

94. Buckley A, Turner JR. Cell Biology of Tight Junction Barrier Regulation and Mucosal Disease. Cold Spring Harb Perspect Biol. 2018;10(1). Epub 20180102. doi:

10.1101/cshperspect.a029314. PubMed PMID: 28507021; PubMed Central PMCID: PMCPMC5749156.

95. Landy J, Ronde E, English N, Clark SK, Hart AL, Knight SC, Ciclitira PJ, Al-Hassi HO. Tight junctions in inflammatory bowel diseases and inflammatory bowel disease associated colorectal cancer. World J Gastroenterol. 2016;22(11):3117-26. doi: 10.3748/wjg.v22.i11.3117. PubMed PMID: 27003989; PubMed Central PMCID: PMCPMC4789987.

96. Anderson JM, Van Itallie CM. Physiology and function of the tight junction. Cold Spring Harb Perspect Biol. 2009;1(2):a002584. doi: 10.1101/cshperspect.a002584. PubMed PMID: 20066090; PubMed Central PMCID: PMCPMC2742087.

97. Luettig J, Rosenthal R, Barmeyer C, Schulzke JD. Claudin-2 as a mediator of leaky gut barrier during intestinal inflammation. Tissue Barriers. 2015;3(1-2):e977176. Epub 20150403. doi: 10.4161/21688370.2014.977176. PubMed PMID: 25838982; PubMed Central PMCID: PMCPMC4372021.

98. Patel RM, Myers LS, Kurundkar AR, Maheshwari A, Nusrat A, Lin PW. Probiotic bacteria induce maturation of intestinal claudin 3 expression and barrier function. Am J Pathol. 2012;180(2):626-35. Epub 20111205. doi: 10.1016/j.ajpath.2011.10.025. PubMed PMID: 22155109; PubMed Central PMCID: PMCPMC3349863.

99. Tamura A, Hayashi H, Imasato M, Yamazaki Y, Hagiwara A, Wada M, Noda T, Watanabe M, Suzuki Y, Tsukita S. Loss of claudin-15, but not claudin-2, causes Na+ deficiency and glucose malabsorption in mouse small intestine. Gastroenterology. 2011;140(3):913-23. Epub 20100818. doi: 10.1053/j.gastro.2010.08.006. PubMed PMID: 20727355.

100. Holmes JL, Van Itallie CM, Rasmussen JE, Anderson JM. Claudin profiling in the mouse during postnatal intestinal development and along the gastrointestinal tract reveals complex expression patterns. Gene Expr Patterns. 2006;6(6):581-8. Epub 20060202. doi: 10.1016/j.modgep.2005.12.001. PubMed PMID: 16458081.

101. Garcia-Hernandez V, Quiros M, Nusrat A. Intestinal epithelial claudins: expression and regulation in homeostasis and inflammation. Ann N Y Acad Sci. 2017;1397(1):66-79. Epub 20170510. doi: 10.1111/nyas.13360. PubMed PMID: 28493289; PubMed Central PMCID: PMCPMC5545801.

102. Kuo WT, Zuo L, Odenwald MA, Madha S, Singh G, Gurniak CB, Abraham C, Turner JR. The Tight Junction Protein ZO-1 Is Dispensable for Barrier Function but Critical for Effective Mucosal Repair. Gastroenterology. 2021;161(6):1924-39. Epub 20210831. doi: 10.1053/j.gastro.2021.08.047. PubMed PMID: 34478742; PubMed Central PMCID: PMCPMC8605999.

103. Kuo W-T, Zuo L, Turner J. THE TIGHT JUNCTION PROTEIN ZO-1 REGULATES MITOTIC SPINDLE ORIENTATION TO ENABLE EFFICIENT MUCOSAL REPAIR. Inflammatory Bowel Diseases. 2021;27(Supplement_1):S28-S. doi: 10.1093/ibd/izaa347.064.

104. Heller F, Florian P, Bojarski C, Richter J, Christ M, Hillenbrand B, Mankertz J, Gitter AH, Bürgel N, Fromm M, Zeitz M, Fuss I, Strober W, Schulzke JD. Interleukin-13 is the key effector Th2 cytokine in ulcerative colitis that affects epithelial tight junctions, apoptosis, and cell restitution. Gastroenterology. 2005;129(2):550-64. doi: 10.1016/j.gastro.2005.05.002. PubMed PMID: 16083712.

105. Suzuki T, Yoshinaga N, Tanabe S. Interleukin-6 (IL-6) regulates claudin-2 expression and tight junction permeability in intestinal epithelium. J Biol Chem. 2011;286(36):31263-71. Epub 20110719. doi: 10.1074/jbc.M111.238147. PubMed PMID: 21771795; PubMed Central PMCID: PMCPMC3173073.

106. Huang X, Oshima T, Tomita T, Fukui H, Miwa H. Butyrate Alleviates Cytokine-Induced Barrier Dysfunction by Modifying Claudin-2 Levels. Biology (Basel). 2021;10(3). Epub 20210309. doi: 10.3390/biology10030205. PubMed PMID: 33803334; PubMed Central PMCID: PMCPMC8000923.

107. Davies JM, Abreu MT. The innate immune system and inflammatory bowel disease. Scandinavian Journal of Gastroenterology. 2015;50(1):24-33. doi: 10.3109/00365521.2014.966321.

108. Glick D, Barth S, Macleod KF. Autophagy: cellular and molecular mechanisms. J Pathol. 2010;221(1):3-12. doi: 10.1002/path.2697. PubMed PMID: 20225336; PubMed Central PMCID: PMCPMC2990190.

109. Salem M, Ammitzboell M, Nys K, Seidelin JB, Nielsen OH. ATG16L1: A multifunctional susceptibility factor in Crohn disease. Autophagy. 2015;11(4):585-94. doi: 10.1080/15548627.2015.1017187. PubMed PMID: 25906181; PubMed Central PMCID: PMCPMC4502774.

110. Runwal G, Stamatakou E, Siddiqi FH, Puri C, Zhu Y, Rubinsztein DC. LC3-positive structures are prominent in autophagy-deficient cells. Sci Rep. 2019;9(1):10147. Epub 20190712. doi: 10.1038/s41598-019-46657-z. PubMed PMID: 31300716; PubMed Central PMCID: PMCPMC6625982.

111. Kinchen JM, Ravichandran KS. Phagosome maturation: going through the acid test. Nat Rev Mol Cell Biol. 2008;9(10):781-95. doi: 10.1038/nrm2515. PubMed PMID: 18813294; PubMed Central PMCID: PMCPMC2908392.

112. Hampe J, Franke A, Rosenstiel P, Till A, Teuber M, Huse K, Albrecht M, Mayr G, De La Vega FM, Briggs J, Günther S, Prescott NJ, Onnie CM, Häsler R, Sipos B, Fölsch UR, Lengauer T, Platzer M, Mathew CG, Krawczak M, Schreiber S. A genome-wide association scan of nonsynonymous SNPs identifies a susceptibility variant for Crohn disease in ATG16L1. Nat Genet. 2007;39(2):207-11. Epub 20061231. doi: 10.1038/ng1954. PubMed PMID: 17200669.

113. Fujita N, Itoh T, Omori H, Fukuda M, Noda T, Yoshimori T. The Atg16L complex specifies the site of LC3 lipidation for membrane biogenesis in autophagy. Mol Biol Cell. 2008;19(5):2092-100. Epub 20080305. doi: 10.1091/mbc.e07-12-1257. PubMed PMID: 18321988; PubMed Central PMCID: PMCPMC2366860.

114. Van Limbergen J, Kabakchiev B, Stempak J, Schumm P, Xu W, Henderson P, Griffiths A, Girardin S, Philpott D, Silverberg M. OC-010 Detailed analysis of ATG16L1 demonstrates gene-wide extent of association with crohn's disease susceptibility. Gut. 2012;61(Suppl 2):A4. doi: 10.1136/gutjnl-2012-302514a.10.

115. Boada-Romero E, Serramito-Gómez I, Sacristán MP, Boone DL, Xavier RJ, Pimentel-Muiños FX. The T300A Crohn's disease risk polymorphism impairs function of the WD40 domain of ATG16L1. Nat Commun. 2016;7:11821. Epub 20160608. doi: 10.1038/ncomms11821. PubMed PMID: 27273576; PubMed Central PMCID: PMCPMC4899871.

116. Lassen KG, Kuballa P, Conway KL, Patel KK, Becker CE, Peloquin JM, Villablanca EJ, Norman JM, Liu TC, Heath RJ, Becker ML, Fagbami L, Horn H, Mercer J, Yilmaz OH, Jaffe JD, Shamji AF, Bhan AK, Carr SA, Daly MJ, Virgin HW, Schreiber SL, Stappenbeck TS, Xavier RJ. Atg16L1 T300A variant decreases selective autophagy resulting in altered cytokine signaling and decreased antibacterial defense. Proc Natl Acad Sci U S A. 2014;111(21):7741-6. Epub 20140512. doi: 10.1073/pnas.1407001111. PubMed PMID: 24821797; PubMed Central PMCID: PMCPMC4040621.

117. Murthy A, Li Y, Peng I, Reichelt M, Katakam AK, Noubade R, Roose-Girma M, DeVoss J, Diehl L, Graham RR, van Lookeren Campagne M. A Crohn's disease variant in Atg16l1 enhances its degradation by caspase 3. Nature. 2014;506(7489):456-62. Epub 20140219. doi: 10.1038/nature13044. PubMed PMID: 24553140.

118. Saitoh T, Fujita N, Jang MH, Uematsu S, Yang BG, Satoh T, Omori H, Noda T, Yamamoto N, Komatsu M, Tanaka K, Kawai T, Tsujimura T, Takeuchi O, Yoshimori T, Akira S. Loss of the autophagy protein Atg16L1 enhances endotoxin-induced IL-1beta production. Nature. 2008;456(7219):264-8. Epub 20081005. doi: 10.1038/nature07383. PubMed PMID: 18849965.

119. Martin PK, Marchiando A, Xu R, Rudensky E, Yeung F, Schuster SL, Kernbauer E, Cadwell K. Autophagy proteins suppress protective type I interferon signalling in response to the murine gut microbiota. Nat Microbiol. 2018;3(10):1131-41. Epub 20180910. doi: 10.1038/s41564-018-0229-0. PubMed PMID: 30202015; PubMed Central PMCID: PMCPMC6179362.

120. Hamaoui D, Subtil A. ATG16L1 functions in cell homeostasis beyond autophagy. FEBS J. 2022;289(7):1779-800. Epub 20210408. doi: 10.1111/febs.15833. PubMed PMID: 33752267.

121. Consortium WTCC. Genome-wide association study of 14,000 cases of seven common diseases and 3,000 shared controls. Nature. 2007;447(7145):661-78. doi: 10.1038/nature05911. PubMed PMID: 17554300; PubMed Central PMCID: PMCPMC2719288.

122. Baskaran K, Pugazhendhi S, Ramakrishna BS. Association of IRGM gene mutations with inflammatory bowel disease in the Indian population. PLoS One. 2014;9(9):e106863. Epub 20140905. doi: 10.1371/journal.pone.0106863. PubMed PMID: 25191865; PubMed Central PMCID: PMCPMC4156415.

123. Chauhan S, Mandell MA, Deretic V. IRGM governs the core autophagy machinery to conduct antimicrobial defense. Mol Cell. 2015;58(3):507-21. Epub 20150416. doi: 10.1016/j.molcel.2015.03.020. PubMed PMID: 25891078; PubMed Central PMCID: PMCPMC4427528.

124. Parkes M, Barrett JC, Prescott NJ, Tremelling M, Anderson CA, Fisher SA, Roberts RG, Nimmo ER, Cummings FR, Soars D, Drummond H, Lees CW, Khawaja SA, Bagnall R, Burke DA, Todhunter CE, Ahmad T, Onnie CM, McArdle W, Strachan D, Bethel G, Bryan C, Lewis CM, Deloukas P, Forbes A, Sanderson J, Jewell DP, Satsangi J, Mansfield JC, Cardon L, Mathew CG, Consortium WTCC. Sequence variants in the autophagy gene IRGM and multiple other replicating loci contribute to Crohn's disease susceptibility. Nat Genet. 2007;39(7):830-2. Epub 20070606. doi:

10.1038/ng2061. PubMed PMID: 17554261; PubMed Central PMCID: PMCPMC2628541.

125. Inohara N, Koseki T, del Peso L, Hu Y, Yee C, Chen S, Carrio R, Merino J, Liu D, Ni J, Núñez G. Nod1, an Apaf-1-like activator of caspase-9 and nuclear factor-kappaB. J Biol Chem. 1999;274(21):14560-7. doi: 10.1074/jbc.274.21.14560. PubMed PMID: 10329646.

126. Ogura Y, Inohara N, Benito A, Chen FF, Yamaoka S, Nunez G. Nod2, a Nod1/Apaf-1 family member that is restricted to monocytes and activates NF-kappaB. J Biol Chem. 2001;276(7):4812-8. Epub 20001121. doi: 10.1074/jbc.M008072200. PubMed PMID: 11087742.

127. Sellati TJ, Sahay B. Cells of Innate Immunity: Mechanisms of Activation. In: McManus LM, Mitchell RN, editors. Pathobiology of Human Disease. San Diego: Academic Press; 2014. p. 258-74.

128. Ogura Y, Lala S, Xin W, Smith E, Dowds TA, Chen FF, Zimmermann E, Tretiakova M, Cho JH, Hart J, Greenson JK, Keshav S, Nuñez G. Expression of NOD2 in Paneth cells: a possible link to Crohn's ileitis. Gut. 2003;52(11):1591-7. doi: 10.1136/gut.52.11.1591. PubMed PMID: 14570728; PubMed Central PMCID: PMCPMC1773866.

129. Yamamoto S, Ma X. Role of Nod2 in the development of Crohn's disease. Microbes Infect. 2009;11(12):912-8. Epub 20090630. doi: 10.1016/j.micinf.2009.06.005. PubMed PMID: 19573617; PubMed Central PMCID: PMCPMC2924159.

130. Horowitz JE, Warner N, Staples J, Crowley E, Gosalia N, Murchie R, Van Hout C, Fiedler K, Welch G, King AK, Reid JG, Overton JD, Baras A, Shuldiner AR, Griffiths A, Gottesman O, Muise AM, Gonzaga-Jauregui C. Mutation spectrum of NOD2 reveals recessive inheritance as a main driver of Early Onset Crohn's Disease. Sci Rep. 2021;11(1):5595. Epub 20210310. doi: 10.1038/s41598-021-84938-8. PubMed PMID: 33692434; PubMed Central PMCID: PMCPMC7946957.

131. Brain O, Allan P, Simmons A. NOD2-mediated autophagy and Crohn disease. Autophagy. 2010;6(3):412-4. Epub 20100403. doi: 10.4161/auto.6.3.11389. PubMed PMID: 20212355.

132. Ogura Y, Bonen DK, Inohara N, Nicolae DL, Chen FF, Ramos R, Britton H, Moran T, Karaliuskas R, Duerr RH, Achkar JP, Brant SR, Bayless TM, Kirschner BS, Hanauer SB, Nuñez G, Cho JH. A frameshift mutation in NOD2 associated with susceptibility to Crohn's disease. Nature. 2001;411(6837):603-6. doi: 10.1038/35079114. PubMed PMID: 11385577.

133. Chamaillard M, Philpott D, Girardin SE, Zouali H, Lesage S, Chareyre F, Bui TH, Giovannini M, Zaehringer U, Penard-Lacronique V, Sansonetti PJ, Hugot JP, Thomas G. Gene-environment interaction modulated by allelic heterogeneity in inflammatory diseases. Proc Natl Acad Sci U S A. 2003;100(6):3455-60. Epub 20030307. doi: 10.1073/pnas.0530276100. PubMed PMID: 12626759; PubMed Central PMCID: PMCPMC152314.

134. van Heel DA, Ghosh S, Butler M, Hunt KA, Lundberg AM, Ahmad T, McGovern DP, Onnie C, Negoro K, Goldthorpe S, Foxwell BM, Mathew CG, Forbes A, Jewell DP, Playford RJ. Muramyl dipeptide and toll-like receptor sensitivity in NOD2-

associated Crohn's disease. Lancet. 2005;365(9473):1794-6. doi: 10.1016/S0140-6736(05)66582-8. PubMed PMID: 15910952.

135. Caruso R, Warner N, Inohara N, Núñez G. NOD1 and NOD2: signaling, host defense, and inflammatory disease. Immunity. 2014;41(6):898-908. Epub 20141206. doi: 10.1016/j.immuni.2014.12.010. PubMed PMID: 25526305; PubMed Central PMCID: PMCPMC4272446.

136. Homer CR, Richmond AL, Rebert NA, Achkar JP, McDonald C. ATG16L1 and NOD2 interact in an autophagy-dependent antibacterial pathway implicated in Crohn's disease pathogenesis. Gastroenterology. 2010;139(5):1630-41, 41.e1-2. Epub 20100714. doi: 10.1053/j.gastro.2010.07.006. PubMed PMID: 20637199; PubMed Central PMCID: PMCPMC2967588.

137. Travassos LH, Carneiro LA, Ramjeet M, Hussey S, Kim YG, Magalhães JG, Yuan L, Soares F, Chea E, Le Bourhis L, Boneca IG, Allaoui A, Jones NL, Nuñez G, Girardin SE, Philpott DJ. Nod1 and Nod2 direct autophagy by recruiting ATG16L1 to the plasma membrane at the site of bacterial entry. Nat Immunol. 2010;11(1):55-62. Epub 20091108. doi: 10.1038/ni.1823. PubMed PMID: 19898471.

138. Kim H, Zhao Q, Zheng H, Li X, Zhang T, Ma X. A novel crosstalk between TLR4- and NOD2-mediated signaling in the regulation of intestinal inflammation. Sci Rep. 2015;5:12018. Epub 20150708. doi: 10.1038/srep12018. PubMed PMID: 26153766; PubMed Central PMCID: PMCPMC4495563.

139. Cario E. Bacterial interactions with cells of the intestinal mucosa: Toll-like receptors and NOD2. Gut. 2005;54(8):1182-93. Epub 20050419. doi:

10.1136/gut.2004.062794. PubMed PMID: 15840688; PubMed Central PMCID: PMCPMC1774880.

140. Hugot JP, Zaccaria I, Cavanaugh J, Yang H, Vermeire S, Lappalainen M, Schreiber S, Annese V, Jewell DP, Fowler EV, Brant SR, Silverberg MS, Cho J, Rioux JD, Satsangi J, Parkes M, Consortium IIG. Prevalence of CARD15/NOD2 mutations in Caucasian healthy people. Am J Gastroenterol. 2007;102(6):1259-67. Epub 20070223. doi: 10.1111/j.1572-0241.2007.01149.x. PubMed PMID: 17319929.

141. Lu Y, Li X, Liu S, Zhang Y, Zhang D. Toll-like Receptors and Inflammatory Bowel Disease. Front Immunol. 2018;9:72. Epub 20180130. doi: 10.3389/fimmu.2018.00072. PubMed PMID: 29441063; PubMed Central PMCID: PMCPMC5797585.

142. West AP, Koblansky AA, Ghosh S. Recognition and signaling by toll-like receptors. Annu Rev Cell Dev Biol. 2006;22:409-37. doi: 10.1146/annurev.cellbio.21.122303.115827. PubMed PMID: 16822173.

143. Park BS, Song DH, Kim HM, Choi BS, Lee H, Lee JO. The structural basis of lipopolysaccharide recognition by the TLR4-MD-2 complex. Nature. 2009;458(7242):1191-5. Epub 20090301. doi: 10.1038/nature07830. PubMed PMID: 19252480.

144. Moura-Assis A, Nogueira PAS, de-Lima-Junior JC, Simabuco FM, Gaspar JM, Donato J, Velloso LA. TLR4-interactor with leucine-rich repeats (TRIL) is involved in diet-induced hypothalamic inflammation. Sci Rep. 2021;11(1):18015. Epub 20210909. doi: 10.1038/s41598-021-97291-7. PubMed PMID: 34504172; PubMed Central PMCID: PMCPMC8429592.

145. Ciesielska A, Matyjek M, Kwiatkowska K. TLR4 and CD14 trafficking and its influence on LPS-induced pro-inflammatory signaling. Cell Mol Life Sci. 2021;78(4):1233-61. Epub 20201015. doi: 10.1007/s00018-020-03656-y. PubMed PMID: 33057840; PubMed Central PMCID: PMCPMC7904555.

146. Kang Y, Su G, Sun J, Zhang Y. Activation of the TLR4/MyD88 signaling pathway contributes to the development of human hepatocellular carcinoma via upregulation of IL-23 and IL-17A. Oncol Lett. 2018;15(6):9647-54. Epub 20180426. doi: 10.3892/ol.2018.8586. PubMed PMID: 29928340; PubMed Central PMCID: PMCPMC6004652.

147. Gazouli M, Mantzaris G, Kotsinas A, Zacharatos P, Papalambros E, Archimandritis A, Ikonomopoulos J, Gorgoulis VG. Association between polymorphisms in the Toll-like receptor 4, CD14, and CARD15/NOD2 and inflammatory bowel disease in the Greek population. World J Gastroenterol. 2005;11(5):681-5. doi: 10.3748/wjg.v11.i5.681. PubMed PMID: 15655821; PubMed Central PMCID: PMCPMC4250738.

148. Szumilas D, Krysiak R, Okopień B. [The role of TLR4 receptor in development of inflammation and carcinogenesis in ulcerative colitis and pharmacotherapy of this disorder]. Wiad Lek. 2013;66(1):3-9. PubMed PMID: 23905422.

149. Toiyama Y, Araki T, Yoshiyama S, Hiro J, Miki C, Kusunoki M. The expression patterns of Toll-like receptors in the ileal pouch mucosa of postoperative ulcerative colitis patients. Surg Today. 2006;36(3):287-90. doi: 10.1007/s00595-005-3144-y. PubMed PMID: 16493544.

150. Eckburg PB, Bik EM, Bernstein CN, Purdom E, Dethlefsen L, Sargent M, Gill SR, Nelson KE, Relman DA. Diversity of the human intestinal microbial flora. Science. 2005;308(5728):1635-8. Epub 20050414. doi: 10.1126/science.1110591. PubMed PMID: 15831718; PubMed Central PMCID: PMCPMC1395357.

151. Stojanov S, Berlec A, Štrukelj B. The Influence of Probiotics on the Firmicutes/Bacteroidetes Ratio in the Treatment of Obesity and Inflammatory Bowel disease. Microorganisms. 2020;8(11). Epub 20201101. doi: 10.3390/microorganisms8111715. PubMed PMID: 33139627; PubMed Central PMCID: PMCPMC7692443.

152. Rowland I, Gibson G, Heinken A, Scott K, Swann J, Thiele I, Tuohy K. Gut microbiota functions: metabolism of nutrients and other food components. Eur J Nutr. 2018;57(1):1-24. Epub 20170409. doi: 10.1007/s00394-017-1445-8. PubMed PMID: 28393285; PubMed Central PMCID: PMCPMC5847071.

153. Canani RB, Costanzo MD, Leone L, Pedata M, Meli R, Calignano A. Potential beneficial effects of butyrate in intestinal and extraintestinal diseases. World J Gastroenterol. 2011;17(12):1519-28. doi: 10.3748/wjg.v17.i12.1519. PubMed PMID: 21472114; PubMed Central PMCID: PMCPMC3070119.

154. Hamer HM, Jonkers D, Venema K, Vanhoutvin S, Troost FJ, Brummer RJ. Review article: the role of butyrate on colonic function. Aliment Pharmacol Ther. 2008;27(2):104-19. Epub 20071025. doi: 10.1111/j.1365-2036.2007.03562.x. PubMed PMID: 17973645.

155. Hatayama H, Iwashita J, Kuwajima A, Abe T. The short chain fatty acid, butyrate, stimulates MUC2 mucin production in the human colon cancer cell line,

LS174T. Biochem Biophys Res Commun. 2007;356(3):599-603. Epub 20070312. doi: 10.1016/j.bbrc.2007.03.025. PubMed PMID: 17374366.

156. Peng L, Li ZR, Green RS, Holzman IR, Lin J. Butyrate enhances the intestinal barrier by facilitating tight junction assembly via activation of AMP-activated protein kinase in Caco-2 cell monolayers. J Nutr. 2009;139(9):1619-25. Epub 20090722. doi: 10.3945/jn.109.104638. PubMed PMID: 19625695; PubMed Central PMCID: PMCPMC2728689.

157. Quince C, Ijaz UZ, Loman N, Eren AM, Saulnier D, Russell J, Haig SJ, Calus ST, Quick J, Barclay A, Bertz M, Blaut M, Hansen R, McGrogan P, Russell RK, Edwards CA, Gerasimidis K. Extensive Modulation of the Fecal Metagenome in Children With Crohn's Disease During Exclusive Enteral Nutrition. Am J Gastroenterol. 2015;110(12):1718-29; quiz 30. Epub 20151103. doi: 10.1038/ajg.2015.357. PubMed PMID: 26526081; PubMed Central PMCID: PMCPMC4697132.

158. Gong D, Gong X, Wang L, Yu X, Dong Q. Involvement of Reduced Microbial Diversity in Inflammatory Bowel Disease. Gastroenterol Res Pract. 2016;2016:6951091. Epub 20161215. doi: 10.1155/2016/6951091. PubMed PMID: 28074093; PubMed Central PMCID: PMCPMC5198157.

159. Ott SJ, Musfeldt M, Wenderoth DF, Hampe J, Brant O, Fölsch UR, Timmis KN, Schreiber S. Reduction in diversity of the colonic mucosa associated bacterial microflora in patients with active inflammatory bowel disease. Gut. 2004;53(5):685-93. doi: 10.1136/gut.2003.025403. PubMed PMID: 15082587; PubMed Central PMCID: PMCPMC1774050.

160. Loh G, Blaut M. Role of commensal gut bacteria in inflammatory bowel diseases. Gut Microbes. 2012;3(6):544-55. Epub 20121011. doi: 10.4161/gmic.22156. PubMed PMID: 23060017; PubMed Central PMCID: PMCPMC3495792.

161. Mirsepasi-Lauridsen HC, Vrankx K, Engberg J, Friis-Møller A, Brynskov J, Nordgaard-Lassen I, Petersen AM, Krogfelt KA. Disease-Specific Enteric Microbiome Dysbiosis in Inflammatory Bowel Disease. Front Med (Lausanne). 2018;5:304. Epub 20181120. doi: 10.3389/fmed.2018.00304. PubMed PMID: 30525037; PubMed Central PMCID: PMCPMC6256240.

162. Andoh A, Nishida A. Alteration of the Gut Microbiome in Inflammatory Bowel Disease. Digestion. 2022:1-8. Epub 20220728. doi: 10.1159/000525925. PubMed PMID: 35901721.

163. Sokol H, Pigneur B, Watterlot L, Lakhdari O, Bermúdez-Humarán LG, Gratadoux JJ, Blugeon S, Bridonneau C, Furet JP, Corthier G, Grangette C, Vasquez N, Pochart P, Trugnan G, Thomas G, Blottière HM, Doré J, Marteau P, Seksik P, Langella P. Faecalibacterium prausnitzii is an anti-inflammatory commensal bacterium identified by gut microbiota analysis of Crohn disease patients. Proc Natl Acad Sci U S A. 2008;105(43):16731-6. Epub 20081020. doi: 10.1073/pnas.0804812105. PubMed PMID: 18936492; PubMed Central PMCID: PMCPMC2575488.

164. Chen L, Wang W, Zhou R, Ng SC, Li J, Huang M, Zhou F, Wang X, Shen B, A Kamm M, Wu K, Xia B. Characteristics of fecal and mucosa-associated microbiota in Chinese patients with inflammatory bowel disease. Medicine (Baltimore).

2014;93(8):e51. doi: 10.1097/MD.0000000000000051. PubMed PMID: 25121355; PubMed Central PMCID: PMCPMC4602441.

165. Takahashi K, Nishida A, Fujimoto T, Fujii M, Shioya M, Imaeda H, Inatomi O, Bamba S, Sugimoto M, Andoh A. Reduced Abundance of Butyrate-Producing Bacteria Species in the Fecal Microbial Community in Crohn's Disease. Digestion. 2016;93(1):59-65. Epub 20160114. doi: 10.1159/000441768. PubMed PMID: 26789999.

166. Sinha SR, Haileselassie Y, Nguyen LP, Tropini C, Wang M, Becker LS, Sim D, Jarr K, Spear ET, Singh G, Namkoong H, Bittinger K, Fischbach MA, Sonnenburg JL, Habtezion A. Dysbiosis-Induced Secondary Bile Acid Deficiency Promotes Intestinal Inflammation. Cell Host Microbe. 2020;27(4):659-70.e5. Epub 20200225. doi: 10.1016/j.chom.2020.01.021. PubMed PMID: 32101703; PubMed Central PMCID: PMCPMC8172352.

167. Sellon RK, Tonkonogy S, Schultz M, Dieleman LA, Grenther W, Balish E, Rennick DM, Sartor RB. Resident enteric bacteria are necessary for development of spontaneous colitis and immune system activation in interleukin-10-deficient mice. Infect Immun. 1998;66(11):5224-31. doi: 10.1128/IAI.66.11.5224-5231.1998. PubMed PMID: 9784526; PubMed Central PMCID: PMCPMC108652.

168. Taurog JD, Richardson JA, Croft JT, Simmons WA, Zhou M, Fernández-Sueiro JL, Balish E, Hammer RE. The germfree state prevents development of gut and joint inflammatory disease in HLA-B27 transgenic rats. J Exp Med. 1994;180(6):2359-64. doi: 10.1084/jem.180.6.2359. PubMed PMID: 7964509; PubMed Central PMCID: PMCPMC2191772.

169. Martinez JE, Kahana DD, Ghuman S, Wilson HP, Wilson J, Kim SCJ, Lagishetty V, Jacobs JP, Sinha-Hikim AP, Friedman TC. Unhealthy Lifestyle and Gut Dysbiosis: A Better Understanding of the Effects of Poor Diet and Nicotine on the Intestinal Microbiome. Front Endocrinol (Lausanne). 2021;12:667066. Epub 20210608. doi: 10.3389/fendo.2021.667066. PubMed PMID: 34168615; PubMed Central PMCID: PMCPMC8218903.

170. Wei S, Bahl MI, Baunwall SMD, Hvas CL, Licht TR. Determining Gut Microbial Dysbiosis: a Review of Applied Indexes for Assessment of Intestinal Microbiota Imbalances. Appl Environ Microbiol. 2021;87(11). Epub 20210511. doi: 10.1128/AEM.00395-21. PubMed PMID: 33741632; PubMed Central PMCID: PMCPMC8208139.

171. Su W, Chen Y, Cao P, Guo Y, Wang S, Dong W. Promotes the Development of Ulcerative Colitis by Inducing the Autophagic Cell Death of Intestinal Epithelial. Front Cell Infect Microbiol. 2020;10:594806. Epub 20201127. doi: 10.3389/fcimb.2020.594806. PubMed PMID: 33330137; PubMed Central PMCID: PMCPMC7728699.

172. Wang L, Tang L, Feng Y, Zhao S, Han M, Zhang C, Yuan G, Zhu J, Cao S, Wu Q, Li L, Zhang Z. A purified membrane protein from Akkermansia muciniphila or the pasteurised bacterium blunts colitis associated tumourigenesis by modulation of CD8⁺ T cells in mice. Gut. 2020;69(11):1988. doi: 10.1136/gutjnl-2019-320105.

173. Ganesh BP, Klopfleisch R, Loh G, Blaut M. Commensal Akkermansia muciniphila exacerbates gut inflammation in Salmonella Typhimurium-infected

gnotobiotic mice. PLoS One. 2013;8(9):e74963. Epub 20130910. doi: 10.1371/journal.pone.0074963. PubMed PMID: 24040367; PubMed Central PMCID: PMCPMC3769299.

174. Bálint A, Farkas K, Méhi O, Kintses B, Vásárhelyi BM, Ari E, Pál C, Madácsy T, Maléth J, Szántó KJ, Nagy I, Rutka M, Bacsur P, Szűcs D, Szepes Z, Nagy F, Fábián A, Bor R, Milassin Á, Molnár T. Functional Anatomical Changes in Ulcerative Colitis Patients Determine Their Gut Microbiota Composition and Consequently the Possible Treatment Outcome. Pharmaceuticals (Basel). 2020;13(11). Epub 20201028. doi: 10.3390/ph13110346. PubMed PMID: 33126430; PubMed Central PMCID: PMCPMC7692875.

175. Haberman Y, Tickle TL, Dexheimer PJ, Kim MO, Tang D, Karns R, Baldassano RN, Noe JD, Rosh J, Markowitz J, Heyman MB, Griffiths AM, Crandall WV, Mack DR, Baker SS, Huttenhower C, Keljo DJ, Hyams JS, Kugathasan S, Walters TD, Aronow B, Xavier RJ, Gevers D, Denson LA. Pediatric Crohn disease patients exhibit specific ileal transcriptome and microbiome signature. J Clin Invest. 2014;124(8):3617-33. Epub 20140708. doi: 10.1172/JCI75436. PubMed PMID: 25003194; PubMed Central PMCID: PMCPMC4109533.

176. Vester-Andersen MK, Mirsepasi-Lauridsen HC, Prosberg MV, Mortensen CO, Träger C, Skovsen K, Thorkilgaard T, Nøjgaard C, Vind I, Krogfelt KA, Sørensen N, Bendtsen F, Petersen AM. Increased abundance of proteobacteria in aggressive Crohn's disease seven years after diagnosis. Sci Rep. 2019;9(1):13473. Epub 20190917. doi: 10.1038/s41598-019-49833-3. PubMed PMID: 31530835; PubMed Central PMCID: PMCPMC6748953.

177. Mirsepasi-Lauridsen HC, Vallance BA, Krogfelt KA, Petersen AM. Pathobionts Associated with Inflammatory Bowel Disease. Clin Microbiol Rev. 2019;32(2). Epub 20190130. doi: 10.1128/CMR.00060-18. PubMed PMID: 30700431; PubMed Central PMCID: PMCPMC6431131.

178. Zhang Y, Rowehl L, Krumsiek JM, Orner EP, Shaikh N, Tarr PI, Sodergren E, Weinstock GM, Boedeker EC, Xiong X, Parkinson J, Frank DN, Li E, Gathungu G. Identification of Candidate Adherent-Invasive E. coli Signature Transcripts by Genomic/Transcriptomic Analysis. PLoS One. 2015;10(6):e0130902. Epub 20150630. doi: 10.1371/journal.pone.0130902. PubMed PMID: 26125937; PubMed Central PMCID: PMCPMC4509574.

179. Conte MP, Longhi C, Marazzato M, Conte AL, Aleandri M, Lepanto MS, Zagaglia C, Nicoletti M, Aloi M, Totino V, Palamara AT, Schippa S. Adherent-invasive Escherichia coli (AIEC) in pediatric Crohn's disease patients: phenotypic and genetic pathogenic features. BMC Res Notes. 2014;7:748. Epub 20141022. doi: 10.1186/1756-0500-7-748. PubMed PMID: 25338542; PubMed Central PMCID: PMCPMC4210564.

180. Darfeuille-Michaud A, Boudeau J, Bulois P, Neut C, Glasser AL, Barnich N, Bringer MA, Swidsinski A, Beaugerie L, Colombel JF. High prevalence of adherent-invasive Escherichia coli associated with ileal mucosa in Crohn's disease. Gastroenterology. 2004;127(2):412-21. doi: 10.1053/j.gastro.2004.04.061. PubMed PMID: 15300573.

181. López-Siles M, Camprubí-Font C, Gómez Del Pulgar EM, Sabat Mir M, Busquets D, Sanz Y, Martinez-Medina M. Prevalence, Abundance, and Virulence of

Adherent-Invasive. Front Immunol. 2022;13:748839. Epub 20220310. doi: 10.3389/fimmu.2022.748839. PubMed PMID: 35359974; PubMed Central PMCID: PMCPMC8960851.

182. Darfeuille-Michaud A, Neut C, Barnich N, Lederman E, Di Martino P, Desreumaux P, Gambiez L, Joly B, Cortot A, Colombel JF. Presence of adherent Escherichia coli strains in ileal mucosa of patients with Crohn's disease. Gastroenterology. 1998;115(6):1405-13. doi: 10.1016/s0016-5085(98)70019-8. PubMed PMID: 9834268.

183. Palmela C, Chevarin C, Xu Z, Torres J, Sevrin G, Hirten R, Barnich N, Ng SC, Colombel JF. Adherent-invasive. Gut. 2018;67(3):574-87. Epub 20171115. doi: 10.1136/gutjnl-2017-314903. PubMed PMID: 29141957.

184. Buisson A, Sokol H, Hammoudi N, Nancey S, Treton X, Nachury M, Fumery M, Hébuterne X, Rodrigues M, Hugot JP, Boschetti G, Stefanescu C, Wils P, Seksik P, Le Bourhis L, Bezault M, Sauvanet P, Pereira B, Allez M, Barnich N, group Rs. Role of adherent and invasive. Gut. 2023;72(1):39-48. Epub 20220331. doi: 10.1136/gutjnl-2021-325971. PubMed PMID: 35361684.

185. Freeman HJ. Granuloma-positive Crohn's disease. Can J Gastroenterol. 2007;21(9):583-7. doi: 10.1155/2007/917649. PubMed PMID: 17853953; PubMed Central PMCID: PMCPMC2657987.

186. Meconi S, Vercellone A, Levillain F, Payré B, Al Saati T, Capilla F, Desreumaux P, Darfeuille-Michaud A, Altare F. Adherent-invasive Escherichia coli isolated from Crohn's disease patients induce granulomas in vitro. Cell Microbiol. 2007;9(5):1252-

61. Epub 20070111. doi: 10.1111/j.1462-5822.2006.00868.x. PubMed PMID: 17223928.

187. Simpson KW, Dogan B, Rishniw M, Goldstein RE, Klaessig S, McDonough PL, German AJ, Yates RM, Russell DG, Johnson SE, Berg DE, Harel J, Bruant G, McDonough SP, Schukken YH. Adherent and invasive Escherichia coli is associated with granulomatous colitis in boxer dogs. Infect Immun. 2006;74(8):4778-92. doi: 10.1128/IAI.00067-06. PubMed PMID: 16861666; PubMed Central PMCID: PMCPMC1539603.

188. Ishii PE, Suchodolski JS, Duarte R, Pereira ARC, Lidbury JA, Steiner JM, Giaretta PR. Detection of invasive. J Vet Diagn Invest. 2022;34(6):990-4. Epub 20220822. doi: 10.1177/10406387221119712. PubMed PMID: 35993285; PubMed Central PMCID: PMCPMC9597337.

189. Ryan P, Kelly RG, Lee G, Collins JK, O'Sullivan GC, O'Connell J, Shanahan F. Bacterial DNA within granulomas of patients with Crohn's disease--detection by laser capture microdissection and PCR. Am J Gastroenterol. 2004;99(8):1539-43. doi: 10.1111/j.1572-0241.2004.40103.x. PubMed PMID: 15307874.

190. Ryan P, Bennett MW, Aarons S, Lee G, Collins JK, O'Sullivan GC, O'Connell J, Shanahan F. PCR detection of Mycobacterium paratuberculosis in Crohn's disease granulomas isolated by laser capture microdissection. Gut. 2002;51(5):665-70. doi: 10.1136/gut.51.5.665. PubMed PMID: 12377804; PubMed Central PMCID: PMCPMC1773423.

191. Glasser AL, Boudeau J, Barnich N, Perruchot MH, Colombel JF, Darfeuille-Michaud A. Adherent invasive Escherichia coli strains from patients with Crohn's

disease survive and replicate within macrophages without inducing host cell death. Infect Immun. 2001;69(9):5529-37. doi: 10.1128/IAI.69.9.5529-5537.2001. PubMed PMID: 11500426; PubMed Central PMCID: PMCPMC98666.

192. Miquel S, Peyretaillade E, Claret L, de Vallée A, Dossat C, Vacherie B, Zineb eH, Segurens B, Barbe V, Sauvanet P, Neut C, Colombel JF, Medigue C, Mojica FJ, Peyret P, Bonnet R, Darfeuille-Michaud A. Complete genome sequence of Crohn's disease-associated adherent-invasive E. coli strain LF82. PLoS One. 2010;5(9). Epub 20100917. doi: 10.1371/journal.pone.0012714. PubMed PMID: 20862302; PubMed Central PMCID: PMCPMC2941450.

193. Nash JH, Villegas A, Kropinski AM, Aguilar-Valenzuela R, Konczy P, Mascarenhas M, Ziebell K, Torres AG, Karmali MA, Coombes BK. Genome sequence of adherent-invasive Escherichia coli and comparative genomic analysis with other E. coli pathotypes. BMC Genomics. 2010;11:667. Epub 20101125. doi: 10.1186/1471-2164-11-667. PubMed PMID: 21108814; PubMed Central PMCID: PMCPMC3091784.

194. Nowrouzian FL, Wold AE, Adlerberth I. Escherichia coli strains belonging to phylogenetic group B2 have superior capacity to persist in the intestinal microflora of infants. J Infect Dis. 2005;191(7):1078-83. Epub 20050302. doi: 10.1086/427996. PubMed PMID: 15747243.

195. Fang X, Monk JM, Mih N, Du B, Sastry AV, Kavvas E, Seif Y, Smarr L, Palsson BO. Escherichia coli B2 strains prevalent in inflammatory bowel disease patients have distinct metabolic capabilities that enable colonization of intestinal mucosa. BMC Syst

Biol. 2018;12(1):66. Epub 20180611. doi: 10.1186/s12918-018-0587-5. PubMed PMID: 29890970; PubMed Central PMCID: PMCPMC5996543.

196. Camprubí-Font C, Martinez-Medina M. Why the discovery of adherent-invasive. World J Biol Chem. 2020;11(1):1-13. doi: 10.4331/wjbc.v11.i1.1. PubMed PMID: 32405343; PubMed Central PMCID: PMCPMC7205867.

197. Picard B, Garcia JS, Gouriou S, Duriez P, Brahimi N, Bingen E, Elion J, Denamur E. The link between phylogeny and virulence in Escherichia coli extraintestinal infection. Infect Immun. 1999;67(2):546-53. doi: 10.1128/IAI.67.2.546-553.1999. PubMed PMID: 9916057; PubMed Central PMCID: PMCPMC96353.

198. Martinez-Medina M, Mora A, Blanco M, López C, Alonso MP, Bonacorsi S, Nicolas-Chanoine MH, Darfeuille-Michaud A, Garcia-Gil J, Blanco J. Similarity and divergence among adherent-invasive Escherichia coli and extraintestinal pathogenic E. coli strains. J Clin Microbiol. 2009;47(12):3968-79. Epub 20091014. doi: 10.1128/JCM.01484-09. PubMed PMID: 19828750; PubMed Central PMCID: PMCPMC2786640.

199. Camprubí-Font C, Bustamante P, Vidal RM, O'Brien CL, Barnich N, Martinez-Medina M. Study of a classification algorithm for AIEC identification in geographically distinct E. coli strains. Sci Rep. 2020;10(1):8094. Epub 20200515. doi: 10.1038/s41598-020-64894-5. PubMed PMID: 32415168; PubMed Central PMCID: PMCPMC7229014.

200. Schaale K, Peters KM, Murthy AM, Fritzsche AK, Phan MD, Totsika M, Robertson AA, Nichols KB, Cooper MA, Stacey KJ, Ulett GC, Schroder K, Schembri MA, Sweet MJ. Strain- and host species-specific inflammasome activation, IL-1β

release, and cell death in macrophages infected with uropathogenic Escherichia coli. Mucosal Immunol. 2016;9(1):124-36. Epub 20150520. doi: 10.1038/mi.2015.44. PubMed PMID: 25993444.

201. Sarowska J, Futoma-Koloch B, Jama-Kmiecik A, Frej-Madrzak M, Ksiazczyk M, Bugla-Ploskonska G, Choroszy-Krol I. Virulence factors, prevalence and potential transmission of extraintestinal pathogenic. Gut Pathog. 2019;11:10. Epub 20190221. doi: 10.1186/s13099-019-0290-0. PubMed PMID: 30828388; PubMed Central PMCID: PMCPMC6383261.

202. Agus A, Massier S, Darfeuille-Michaud A, Billard E, Barnich N. Understanding host-adherent-invasive Escherichia coli interaction in Crohn's disease: opening up new therapeutic strategies. Biomed Res Int. 2014;2014:567929. Epub 20141215. doi: 10.1155/2014/567929. PubMed PMID: 25580435; PubMed Central PMCID: PMCPMC4279263.

203. Boudeau J, Barnich N, Darfeuille-Michaud A. Type 1 pili-mediated adherence of Escherichia coli strain LF82 isolated from Crohn's disease is involved in bacterial invasion of intestinal epithelial cells. Mol Microbiol. 2001;39(5):1272-84. doi: 10.1111/j.1365-2958.2001.02315.x. PubMed PMID: 11251843.

204. Capitani G, Eidam O, Glockshuber R, Grütter MG. Structural and functional insights into the assembly of type 1 pili from Escherichia coli. Microbes Infect. 2006;8(8):2284-90. Epub 20060602. doi: 10.1016/j.micinf.2006.03.013. PubMed PMID: 16793308.

205. Jones CH, Pinkner JS, Roth R, Heuser J, Nicholes AV, Abraham SN, Hultgren SJ. FimH adhesin of type 1 pili is assembled into a fibrillar tip structure in the

Enterobacteriaceae. Proc Natl Acad Sci U S A. 1995;92(6):2081-5. doi: 10.1073/pnas.92.6.2081. PubMed PMID: 7892228; PubMed Central PMCID: PMCPMC42427.

206. Elatrech I, Marzaioli V, Boukemara H, Bournier O, Neut C, Darfeuille-Michaud A, Luis J, Dubuquoy L, El-Benna J, My-Chan Dang P, Marie JC. Escherichia coli LF82 differentially regulates ROS production and mucin expression in intestinal epithelial T84 cells: implication of NOX1. Inflamm Bowel Dis. 2015;21(5):1018-26. doi: 10.1097/MIB.0000000000000365. PubMed PMID: 25822013.

207. Mancini NL, Rajeev S, Jayme TS, Wang A, Keita Å, Workentine ML, Hamed S, Söderholm JD, Lopes F, Shutt TE, Shearer J, McKay DM. Crohn's Disease Pathobiont Adherent-Invasive E coli Disrupts Epithelial Mitochondrial Networks With Implications for Gut Permeability. Cell Mol Gastroenterol Hepatol. 2021;11(2):551-71. Epub 20200928. doi: 10.1016/j.jcmgh.2020.09.013. PubMed PMID: 32992049; PubMed Central PMCID: PMCPMC7797367.

208. Wine E, Ossa JC, Gray-Owen SD, Sherman PM. Adherent-invasive Escherichia coli, strain LF82 disrupts apical junctional complexes in polarized epithelia. BMC Microbiol. 2009;9:180. Epub 20090826. doi: 10.1186/1471-2180-9-180. PubMed PMID: 19709415; PubMed Central PMCID: PMCPMC2741472.

209. Hao LJ, Lin Y, Zhang W, Tian J, Wang Y, Chen PD, Hu CK, Zeng LC, Yang J, Wang BX, Jiang X. [Effect of eicosapentaenoic acid on mRNA expression of tight junction protein ZO-1 in intestinal epithelial cells after Escherichia coli LF82 infection]. Zhongguo Dang Dai Er Ke Za Zhi. 2017;19(6):693-8. doi: 10.7499/j.issn.1008-

8830.2017.06.016. PubMed PMID: 28606239; PubMed Central PMCID: PMCPMC7390293.

210. Claret L, Miquel S, Vieille N, Ryjenkov DA, Gomelsky M, Darfeuille-Michaud A. The flagellar sigma factor FliA regulates adhesion and invasion of Crohn disease-associated Escherichia coli via a cyclic dimeric GMP-dependent pathway. J Biol Chem. 2007;282(46):33275-83. Epub 20070907. doi: 10.1074/jbc.M702800200. PubMed PMID: 17827157.

211. Simonsen KT, Nielsen G, Bjerrum JV, Kruse T, Kallipolitis BH, Møller-Jensen J. A role for the RNA chaperone Hfq in controlling adherent-invasive Escherichia coli colonization and virulence. PLoS One. 2011;6(1):e16387. Epub 20110126. doi: 10.1371/journal.pone.0016387. PubMed PMID: 21298102; PubMed Central PMCID: PMCPMC3027648.

212. Rooks MG, Veiga P, Reeves AZ, Lavoie S, Yasuda K, Asano Y, Yoshihara K, Michaud M, Wardwell-Scott L, Gallini CA, Glickman JN, Sudo N, Huttenhower C, Lesser CF, Garrett WS. QseC inhibition as an antivirulence approach for colitis-associated bacteria. Proc Natl Acad Sci U S A. 2017;114(1):142-7. Epub 20161215. doi: 10.1073/pnas.1612836114. PubMed PMID: 27980034; PubMed Central PMCID: PMCPMC5224399.

213. Sevrin G, Massier S, Chassaing B, Agus A, Delmas J, Denizot J, Billard E, Barnich N. Adaptation of adherent-invasive. Gut Microbes. 2020;11(3):364-80. Epub 20180301. doi: 10.1080/19490976.2017.1421886. PubMed PMID: 29494278; PubMed Central PMCID: PMCPMC7524368.

214. Fitzgerald DM, Bonocora RP, Wade JT. Comprehensive mapping of the Escherichia coli flagellar regulatory network. PLoS Genet. 2014;10(10):e1004649. Epub 20141002. doi: 10.1371/journal.pgen.1004649. PubMed PMID: 25275371; PubMed Central PMCID: PMCPMC4183435.

215. Kim JM, Garcia-Alcala M, Balleza E, Cluzel P. Stochastic transcriptional pulses orchestrate flagellar biosynthesis in. Sci Adv. 2020;6(6):eaax0947. Epub 20200205. doi: 10.1126/sciadv.aax0947. PubMed PMID: 32076637; PubMed Central PMCID: PMCPMC7002133.

216. Ko M, Park C. Two novel flagellar components and H-NS are involved in the motor function of Escherichia coli. J Mol Biol. 2000;303(3):371-82. doi: 10.1006/jmbi.2000.4147. PubMed PMID: 11031114.

217. Zorraquino V, García B, Latasa C, Echeverz M, Toledo-Arana A, Valle J, Lasa I, Solano C. Coordinated cyclic-di-GMP repression of Salmonella motility through YcgR and cellulose. J Bacteriol. 2013;195(3):417-28. Epub 20121116. doi: 10.1128/JB.01789-12. PubMed PMID: 23161026; PubMed Central PMCID: PMCPMC3554008.

218. Morson BC. The early histological lesion of Crohn's disease. Proc R Soc Med. 1972;65(1):71-2. PubMed PMID: 5015484; PubMed Central PMCID: PMCPMC1644285.

219. Fujimura Y, Kamoi R, Iida M. Pathogenesis of aphthoid ulcers in Crohn's disease: correlative findings by magnifying colonoscopy, electron microscopy, and immunohistochemistry. Gut. 1996;38(5):724-32. doi: 10.1136/gut.38.5.724. PubMed PMID: 8707119; PubMed Central PMCID: PMCPMC1383155.

220. Chassaing B, Rolhion N, de Vallée A, Salim SY, Prorok-Hamon M, Neut C, Campbell BJ, Söderholm JD, Hugot JP, Colombel JF, Darfeuille-Michaud A. Crohn disease--associated adherent-invasive E. coli bacteria target mouse and human Peyer's patches via long polar fimbriae. J Clin Invest. 2011;121(3):966-75. Epub 20110221. doi: 10.1172/JCI44632. PubMed PMID: 21339647; PubMed Central PMCID: PMCPMC3049390.

221. Keita Å, Alkaissi LY, Holm EB, Heil SDS, Chassaing B, Darfeuille-Michaud A, McKay DM, Söderholm JD. Enhanced E. coli LF82 Translocation through the Follicle-associated Epithelium in Crohn's Disease is Dependent on Long Polar Fimbriae and CEACAM6 expression, and Increases Paracellular Permeability. J Crohns Colitis. 2020;14(2):216-29. doi: 10.1093/ecco-jcc/jjz144. PubMed PMID: 31393983; PubMed Central PMCID: PMCPMC7008151.

222. Cieza RJ, Hu J, Ross BN, Sbrana E, Torres AG. The IbeA invasin of adherent-invasive Escherichia coli mediates interaction with intestinal epithelia and macrophages. Infect Immun. 2015;83(5):1904-18. Epub 20150223. doi: 10.1128/IAI.03003-14. PubMed PMID: 25712929; PubMed Central PMCID: PMCPMC4399045.

223. Chassaing B, Etienne-Mesmin L, Bonnet R, Darfeuille-Michaud A. Bile salts induce long polar fimbriae expression favouring Crohn's disease-associated adherent-invasive Escherichia coli interaction with Peyer's patches. Environ Microbiol. 2013;15(2):355-71. Epub 20120713. doi: 10.1111/j.1462-2920.2012.02824.x. PubMed PMID: 22789019.

224. Delmas J, Gibold L, Faïs T, Batista S, Leremboure M, Sinel C, Vazeille E, Cattoir V, Buisson A, Barnich N, Dalmasso G, Bonnet R. Metabolic adaptation of adherent-invasive Escherichia coli to exposure to bile salts. Sci Rep. 2019;9(1):2175. Epub 20190218. doi: 10.1038/s41598-019-38628-1. PubMed PMID: 30778122; PubMed Central PMCID: PMCPMC6379400.

225. Ormsby MJ, Logan M, Johnson SA, McIntosh A, Fallata G, Papadopoulou R, Papachristou E, Hold GL, Hansen R, Ijaz UZ, Russell RK, Gerasimidis K, Wall DM. Inflammation associated ethanolamine facilitates infection by Crohn's disease-linked adherent-invasive Escherichia coli. EBioMedicine. 2019;43:325-32. Epub 20190426. doi: 10.1016/j.ebiom.2019.03.071. PubMed PMID: 31036531; PubMed Central PMCID: PMCPMC6557746.

226. Gonyar LA, Kendall MM. Ethanolamine and choline promote expression of putative and characterized fimbriae in enterohemorrhagic Escherichia coli O157:H7. Infect Immun. 2014;82(1):193-201. Epub 20131014. doi: 10.1128/IAI.00980-13. PubMed PMID: 24126525; PubMed Central PMCID: PMCPMC3911853.

227. Coppens F, Iyyathurai J, Ruer S, Fioravanti A, Taganna J, Vereecke L, De Greve H, Remaut H. Structural and adhesive properties of the long polar fimbriae protein LpfD from adherent-invasive Escherichia coli. Acta Crystallogr D Biol Crystallogr. 2015;71(Pt 8):1615-26. Epub 20150728. doi: 10.1107/S1399004715009803. PubMed PMID: 26249343.

228. Derkacz A, Olczyk P, Olczyk K, Komosinska-Vassev K. The Role of Extracellular Matrix Components in Inflammatory Bowel Diseases. J Clin Med.

2021;10(5). Epub 20210308. doi: 10.3390/jcm10051122. PubMed PMID: 33800267; PubMed Central PMCID: PMCPMC7962650.

229. Rolhion N, Barnich N, Claret L, Darfeuille-Michaud A. Strong decrease in invasive ability and outer membrane vesicle release in Crohn's disease-associated adherent-invasive Escherichia coli strain LF82 with the yfgL gene deleted. J Bacteriol. 2005;187(7):2286-96. doi: 10.1128/JB.187.7.2286-2296.2005. PubMed PMID: 15774871; PubMed Central PMCID: PMCPMC1065249.

230. Rolhion N, Barnich N, Bringer MA, Glasser AL, Ranc J, Hébuterne X, Hofman P, Darfeuille-Michaud A. Abnormally expressed ER stress response chaperone Gp96 in CD favours adherent-invasive Escherichia coli invasion. Gut. 2010;59(10):1355-62. Epub 20100629. doi: 10.1136/gut.2010.207456. PubMed PMID: 20587550; PubMed Central PMCID: PMCPMC2976078.

231. Arnott ID, Landers CJ, Nimmo EJ, Drummond HE, Smith BK, Targan SR, Satsangi J. Sero-reactivity to microbial components in Crohn's disease is associated with disease severity and progression, but not NOD2/CARD15 genotype. Am J Gastroenterol. 2004;99(12):2376-84. doi: 10.1111/j.1572-0241.2004.40417.x. PubMed PMID: 15571586.

232. Mow WS, Vasiliauskas EA, Lin YC, Fleshner PR, Papadakis KA, Taylor KD, Landers CJ, Abreu-Martin MT, Rotter JI, Yang H, Targan SR. Association of antibody responses to microbial antigens and complications of small bowel Crohn's disease. Gastroenterology. 2004;126(2):414-24. doi: 10.1053/j.gastro.2003.11.015. PubMed PMID: 14762777.

233. Kenney LJ, Anand GS. EnvZ/OmpR Two-Component Signaling: An Archetype System That Can Function Noncanonically. EcoSal Plus. 2020;9(1). doi: 10.1128/ecosalplus.ESP-0001-2019. PubMed PMID: 32003321; PubMed Central PMCID: PMCPMC7192543.

234. Rolhion N, Carvalho FA, Darfeuille-Michaud A. OmpC and the sigma(E) regulatory pathway are involved in adhesion and invasion of the Crohn's disease-associated Escherichia coli strain LF82. Mol Microbiol. 2007;63(6):1684-700. doi: 10.1111/j.1365-2958.2007.05638.x. PubMed PMID: 17367388.

235. Lucchini V, Sivignon A, Pieren M, Gitzinger M, Lociuro S, Barnich N, Kemmer C, Trebosc V. The Role of OmpR in Bile Tolerance and Pathogenesis of Adherent-Invasive. Front Microbiol. 2021;12:684473. Epub 20210628. doi: 10.3389/fmicb.2021.684473. PubMed PMID: 34262546; PubMed Central PMCID: PMCPMC8273539.

236. Barnich N, Bringer MA, Claret L, Darfeuille-Michaud A. Involvement of lipoprotein NlpI in the virulence of adherent invasive Escherichia coli strain LF82 isolated from a patient with Crohn's disease. Infect Immun. 2004;72(5):2484-93. doi: 10.1128/IAI.72.5.2484-2493.2004. PubMed PMID: 15102755; PubMed Central PMCID: PMCPMC387872.

237. Boudeau J, Glasser AL, Masseret E, Joly B, Darfeuille-Michaud A. Invasive ability of an Escherichia coli strain isolated from the ileal mucosa of a patient with Crohn's disease. Infect Immun. 1999;67(9):4499-509. doi: 10.1128/IAI.67.9.4499-4509.1999. PubMed PMID: 10456892; PubMed Central PMCID: PMCPMC96770.

238. Jarry A, Crémet L, Caroff N, Bou-Hanna C, Mussini JM, Reynaud A, Servin AL, Mosnier JF, Liévin-Le Moal V, Laboisse CL. Subversion of human intestinal mucosa innate immunity by a Crohn's disease-associated E. coli. Mucosal Immunol. 2015;8(3):572-81. Epub 20141001. doi: 10.1038/mi.2014.89. PubMed PMID: 25269707.

239. Cleynen I, Vazeille E, Artieda M, Verspaget HW, Szczypiorska M, Bringer MA, Lakatos PL, Seibold F, Parnell K, Weersma RK, Mahachie John JM, Morgan-Walsh R, Staelens D, Arijs I, De Hertogh G, Müller S, Tordai A, Hommes DW, Ahmad T, Wijmenga C, Pender S, Rutgeerts P, Van Steen K, Lottaz D, Vermeire S, Darfeuille-Michaud A. Genetic and microbial factors modulating the ubiquitin proteasome system in inflammatory bowel disease. Gut. 2014;63(8):1265-74. Epub 20131003. doi: 10.1136/gutjnl-2012-303205. PubMed PMID: 24092863.

240. Negroni A, Costanzo M, Vitali R, Superti F, Bertuccini L, Tinari A, Minelli F, Di Nardo G, Nuti F, Pierdomenico M, Cucchiara S, Stronati L. Characterization of adherent-invasive Escherichia coli isolated from pediatric patients with inflammatory bowel disease. Inflamm Bowel Dis. 2012;18(5):913-24. Epub 20111012. doi: 10.1002/ibd.21899. PubMed PMID: 21994005.

241. Mazzarella G, Perna A, Marano A, Lucariello A, Rotondi Aufiero V, Sorrentino A, Melina R, Guerra G, Taccone FS, Iaquinto G, De Luca A. Pathogenic Role of Associated Adherent-Invasive Escherichia coli in Crohn's Disease. J Cell Physiol. 2017;232(10):2860-8. Epub 20170515. doi: 10.1002/jcp.25717. PubMed PMID: 27925192.

242. Bringer MA, Billard E, Glasser AL, Colombel JF, Darfeuille-Michaud A. Replication of Crohn's disease-associated AIEC within macrophages is dependent on TNF-α secretion. Lab Invest. 2012;92(3):411-9. Epub 20111031. doi: 10.1038/labinvest.2011.156. PubMed PMID: 22042084.

243. Häcker H, Fürmann C, Wagner H, Häcker G. Caspase-9/-3 activation and apoptosis are induced in mouse macrophages upon ingestion and digestion of Escherichia coli bacteria. J Immunol. 2002;169(6):3172-9. doi: 10.4049/jimmunol.169.6.3172. PubMed PMID: 12218135.

244. Legarda D, Justus SJ, Ang RL, Rikhi N, Li W, Moran TM, Zhang J, Mizoguchi E, Zelic M, Kelliher MA, Blander JM, Ting AT. CYLD Proteolysis Protects Macrophages from TNF-Mediated Auto-necroptosis Induced by LPS and Licensed by Type I IFN. Cell Rep. 2016;15(11):2449-61. Epub 20160602. doi: 10.1016/j.celrep.2016.05.032. PubMed PMID: 27264187; PubMed Central PMCID: PMCPMC4909532.

245. Dhuriya YK, Sharma D. Necroptosis: a regulated inflammatory mode of cell death. J Neuroinflammation. 2018;15(1):199. Epub 20180706. doi: 10.1186/s12974-018-1235-0. PubMed PMID: 29980212; PubMed Central PMCID: PMCPMC6035417.

246. Bringer MA, Glasser AL, Tung CH, Méresse S, Darfeuille-Michaud A. The Crohn's disease-associated adherent-invasive Escherichia coli strain LF82 replicates in mature phagolysosomes within J774 macrophages. Cell Microbiol. 2006;8(3):471-84. doi: 10.1111/j.1462-5822.2005.00639.x. PubMed PMID: 16469058.

247. Thompson AP, O'Neill I, Smith EJ, Catchpole J, Fagan A, Burgess KEV, Carmody RJ, Clarke DJ. Glycolysis and pyrimidine biosynthesis are required for

replication of adherent-invasive Escherichia coli in macrophages. Microbiology (Reading). 2016;162(6):954-65. Epub 20160406. doi: 10.1099/mic.0.000289. PubMed PMID: 27058922.

248. Bringer MA, Barnich N, Glasser AL, Bardot O, Darfeuille-Michaud A. HtrA stress protein is involved in intramacrophagic replication of adherent and invasive Escherichia coli strain LF82 isolated from a patient with Crohn's disease. Infect Immun. 2005;73(2):712-21. doi: 10.1128/IAI.73.2.712-721.2005. PubMed PMID: 15664909; PubMed Central PMCID: PMCPMC546957.

249. Bringer MA, Rolhion N, Glasser AL, Darfeuille-Michaud A. The oxidoreductase DsbA plays a key role in the ability of the Crohn's disease-associated adherent-invasive Escherichia coli strain LF82 to resist macrophage killing. J Bacteriol. 2007;189(13):4860-71. Epub 20070420. doi: 10.1128/JB.00233-07. PubMed PMID: 17449627; PubMed Central PMCID: PMCPMC1913465.

250. Hansen G, Hilgenfeld R. Architecture and regulation of HtrA-family proteins involved in protein quality control and stress response. Cell Mol Life Sci. 2013;70(5):761-75. Epub 20120718. doi: 10.1007/s00018-012-1076-4. PubMed PMID: 22806565.

251. Bardwell JC, McGovern K, Beckwith J. Identification of a protein required for disulfide bond formation in vivo. Cell. 1991;67(3):581-9. doi: 10.1016/0092-8674(91)90532-4. PubMed PMID: 1934062.

252. Rossi E, Leccese G, Baldelli V, Bibi A, Scalone E, Camilloni C, Paroni M, Landini P. Inactivation of the Pyrimidine Biosynthesis. Microorganisms. 2022;10(3).

Epub 20220228. doi: 10.3390/microorganisms10030537. PubMed PMID: 35336113; PubMed Central PMCID: PMCPMC8956108.

253. Saunthararajah Y. Mysteries of partial dihydroorotate dehydrogenase inhibition and leukemia terminal differentiation. Haematologica. 2020;105(9):2191-3. Epub 20200901. doi: 10.3324/haematol.2020.254482. PubMed PMID: 33054042; PubMed Central PMCID: PMCPMC7556521.

254. Hou CW, Mohanan V, Zachara NE, Grimes CL. Identification and biological consequences of the O-GlcNAc modification of the human innate immune receptor, Nod2. Glycobiology. 2016;26(1):13-8. Epub 20150914. doi: 10.1093/glycob/cwv076. PubMed PMID: 26369908; PubMed Central PMCID: PMCPMC4672147.

255. Sun QH, Wang YS, Liu G, Zhou HL, Jian YP, Liu MD, Zhang D, Ding Q, Zhao RX, Chen JF, Li YN, Liang J, Li YL, Quan CS, Xu ZX. Enhanced O-linked Glcnacylation in Crohn's disease promotes intestinal inflammation. EBioMedicine. 2020;53:102693. Epub 20200227. doi: 10.1016/j.ebiom.2020.102693. PubMed PMID: 32114385; PubMed Central PMCID: PMCPMC7047186.

256. Demarre G, Prudent V, Schenk H, Rousseau E, Bringer MA, Barnich N, Tran Van Nhieu G, Rimsky S, De Monte S, Espéli O. The Crohn's disease-associated Escherichia coli strain LF82 relies on SOS and stringent responses to survive, multiply and tolerate antibiotics within macrophages. PLoS Pathog. 2019;15(11):e1008123. Epub 20191114. doi: 10.1371/journal.ppat.1008123. PubMed PMID: 31725806; PubMed Central PMCID: PMCPMC6855411.

257. Podlesek Z, Žgur Bertok D. The DNA Damage Inducible SOS Response Is a Key Player in the Generation of Bacterial Persister Cells and Population Wide

Tolerance. Front Microbiol. 2020;11:1785. Epub 20200804. doi: 10.3389/fmicb.2020.01785. PubMed PMID: 32849403; PubMed Central PMCID: PMCPMC7417476.

258. Fanelli G, Pasqua M, Colonna B, Prosseda G, Grossi M. Expression Profile of Multidrug Resistance Efflux Pumps During Intracellular Life of Adherent-Invasive. Front Microbiol. 2020;11:1935. Epub 20200817. doi: 10.3389/fmicb.2020.01935. PubMed PMID: 33013734; PubMed Central PMCID: PMCPMC7462009.

259. Carrière J, Bretin A, Darfeuille-Michaud A, Barnich N, Nguyen HT. Exosomes Released from Cells Infected with Crohn's Disease-associated Adherent-Invasive Escherichia coli Activate Host Innate Immune Responses and Enhance Bacterial Intracellular Replication. Inflamm Bowel Dis. 2016;22(3):516-28. doi: 10.1097/MIB.0000000000000635. PubMed PMID: 26595556.

260. Nguyen HT, Dalmasso G, Müller S, Carrière J, Seibold F, Darfeuille-Michaud A. Crohn's disease-associated adherent invasive Escherichia coli modulate levels of microRNAs in intestinal epithelial cells to reduce autophagy. Gastroenterology. 2014;146(2):508-19. Epub 20131019. doi: 10.1053/j.gastro.2013.10.021. PubMed PMID: 24148619.

261. Larabi A, Dalmasso G, Delmas J, Barnich N, Nguyen HTT. Exosomes transfer miRNAs from cell-to-cell to inhibit autophagy during infection with Crohn's disease-associated adherent-invasive. Gut Microbes. 2020;11(6):1677-94. Epub 20200625. doi: 10.1080/19490976.2020.1771985. PubMed PMID: 32583714; PubMed Central PMCID: PMCPMC7524154.

262. Lu C, Chen J, Xu HG, Zhou X, He Q, Li YL, Jiang G, Shan Y, Xue B, Zhao RX, Wang Y, Werle KD, Cui R, Liang J, Xu ZX. MIR106B and MIR93 prevent removal of bacteria from epithelial cells by disrupting ATG16L1-mediated autophagy. Gastroenterology. 2014;146(1):188-99. Epub 20130911. doi: 10.1053/j.gastro.2013.09.006. PubMed PMID: 24036151; PubMed Central PMCID: PMCPMC3870037.

263. Dalmasso G, Nguyen HTT, Faïs T, Massier S, Barnich N, Delmas J, Bonnet R. Crohn's Disease-Associated Adherent-Invasive Escherichia coli Manipulate Host Autophagy by Impairing SUMOylation. Cells. 2019;8(1). Epub 20190109. doi: 10.3390/cells8010035. PubMed PMID: 30634511; PubMed Central PMCID: PMCPMC6357120.

264. Lapaquette P, Bringer MA, Darfeuille-Michaud A. Defects in autophagy favour adherent-invasive Escherichia coli persistence within macrophages leading to increased pro-inflammatory response. Cell Microbiol. 2012;14(6):791-807. Epub 20120301. doi: 10.1111/j.1462-5822.2012.01768.x. PubMed PMID: 22309232.

265. Bretin A, Carrière J, Dalmasso G, Bergougnoux A, B'chir W, Maurin AC, Müller S, Seibold F, Barnich N, Bruhat A, Darfeuille-Michaud A, Nguyen HT. Activation of the EIF2AK4-EIF2A/eIF2α-ATF4 pathway triggers autophagy response to Crohn disease-associated adherent-invasive Escherichia coli infection. Autophagy. 2016;12(5):770-83. Epub 20160317. doi: 10.1080/15548627.2016.1156823. PubMed PMID: 26986695; PubMed Central PMCID: PMCPMC4854551.

266. Lapaquette P, Glasser AL, Huett A, Xavier RJ, Darfeuille-Michaud A. Crohn's disease-associated adherent-invasive E. coli are selectively favoured by impaired

autophagy to replicate intracellularly. Cell Microbiol. 2010;12(1):99-113. Epub 20090911. doi: 10.1111/j.1462-5822.2009.01381.x. PubMed PMID: 19747213; PubMed Central PMCID: PMCPMC3743084.

267. Dalmasso G, Nguyen HTT, Faïs T, Massier S, Chevarin C, Vazeille E, Barnich N, Delmas J, Bonnet R. Yersiniabactin Siderophore of Crohn's Disease-Associated Adherent-Invasive. Int J Mol Sci. 2021;22(7). Epub 20210329. doi: 10.3390/ijms22073512. PubMed PMID: 33805299; PubMed Central PMCID: PMCPMC8037853.

268. Cooney R, Baker J, Brain O, Danis B, Pichulik T, Allan P, Ferguson DJ, Campbell BJ, Jewell D, Simmons A. NOD2 stimulation induces autophagy in dendritic cells influencing bacterial handling and antigen presentation. Nat Med. 2010;16(1):90-7. Epub 20091206. doi: 10.1038/nm.2069. PubMed PMID: 19966812.

269. Negroni A, Colantoni E, Vitali R, Palone F, Pierdomenico M, Costanzo M, Cesi V, Cucchiara S, Stronati L. NOD2 induces autophagy to control AIEC bacteria infectiveness in intestinal epithelial cells. Inflamm Res. 2016;65(10):803-13. Epub 20160622. doi: 10.1007/s00011-016-0964-8. PubMed PMID: 27335178.

270. Prudent V, Demarre G, Vazeille E, Wery M, Quenech'Du N, Ravet A, Dauverd-Girault J, van Dijk E, Bringer MA, Descrimes M, Barnich N, Rimsky S, Morillon A, Espéli O. The Crohn's disease-related bacterial strain LF82 assembles biofilm-like communities to protect itself from phagolysosomal attack. Commun Biol. 2021;4(1):627. Epub 20210525. doi: 10.1038/s42003-021-02161-7. PubMed PMID: 34035436; PubMed Central PMCID: PMCPMC8149705.

271. Ellermann M, Gharaibeh RZ, Fulbright L, Dogan B, Moore LN, Broberg CA, Lopez LR, Rothemich AM, Herzog JW, Rogala A, Gordon IO, Rieder F, Brouwer CR, Simpson KW, Jobin C, Sartor RB, Arthur JC. Yersiniabactin-Producing Adherent/Invasive Escherichia coli Promotes Inflammation-Associated Fibrosis in Gnotobiotic. Infect Immun. 2019;87(11). Epub 20191018. doi: 10.1128/IAI.00587-19. PubMed PMID: 31481410; PubMed Central PMCID: PMCPMC6803345.

272. Chassaing B, Garénaux E, Carriere J, Rolhion N, Guérardel Y, Barnich N, Bonnet R, Darfeuille-Michaud A. Analysis of the σE regulon in Crohn's disease-associated Escherichia coli revealed involvement of the waaWVL operon in biofilm formation. J Bacteriol. 2015;197(8):1451-65. Epub 20150209. doi: 10.1128/JB.02499-14. PubMed PMID: 25666140; PubMed Central PMCID: PMCPMC4372749.

273. Sicard JF, Vogeleer P, Le Bihan G, Rodriguez Olivera Y, Beaudry F, Jacques M, Harel J. -Acetyl-glucosamine influences the biofilm formation of. Gut Pathog. 2018;10:26. Epub 20180622. doi: 10.1186/s13099-018-0252-y. PubMed PMID: 29977346; PubMed Central PMCID: PMCPMC6013987.

274. Nickerson KP, McDonald C. Crohn's disease-associated adherent-invasive Escherichia coli adhesion is enhanced by exposure to the ubiquitous dietary polysaccharide maltodextrin. PLoS One. 2012;7(12):e52132. Epub 20121212. doi: 10.1371/journal.pone.0052132. PubMed PMID: 23251695; PubMed Central PMCID: PMCPMC3520894.

275. Ormsby MJ, Johnson SA, Carpena N, Meikle LM, Goldstone RJ, McIntosh A, Wessel HM, Hulme HE, McConnachie CC, Connolly JPR, Roe AJ, Hasson C, Boyd J, Fitzgerald E, Gerasimidis K, Morrison D, Hold GL, Hansen R, Walker D, Smith DGE,

Wall DM. Propionic Acid Promotes the Virulent Phenotype of Crohn's Disease-Associated Adherent-Invasive Escherichia coli. Cell Rep. 2020;30(7):2297-305.e5. doi: 10.1016/j.celrep.2020.01.078. PubMed PMID: 32075765; PubMed Central PMCID: PMCPMC7034058.

276. Rizeq B, Zakaria Z, Ouhtit A. Towards understanding the mechanisms of actions of carcinoembryonic antigen-related cell adhesion molecule 6 in cancer progression. Cancer Sci. 2018;109(1):33-42. Epub 20180102. doi: 10.1111/cas.13437. PubMed PMID: 29110374; PubMed Central PMCID: PMCPMC5765285.

277. Saiz-Gonzalo G, Hanrahan N, Rossini V, Singh R, Ahern M, Kelleher M, Hill S, O'Sullivan R, Fanning A, Walsh PT, Hussey S, Shanahan F, Nally K, O'Driscoll CM, Melgar S. Regulation of CEACAM Family Members by IBD-Associated Triggers in Intestinal Epithelial Cells, Their Correlation to Inflammation and Relevance to IBD Pathogenesis. Front Immunol. 2021;12:655960. Epub 20210729. doi: 10.3389/fimmu.2021.655960. PubMed PMID: 34394073; PubMed Central PMCID: PMCPMC8358819.

278. Barnich N, Carvalho FA, Glasser AL, Darcha C, Jantscheff P, Allez M, Peeters H, Bommelaer G, Desreumaux P, Colombel JF, Darfeuille-Michaud A. CEACAM6 acts as a receptor for adherent-invasive E. coli, supporting ileal mucosa colonization in Crohn disease. J Clin Invest. 2007;117(6):1566-74. Epub 20070524. doi: 10.1172/JCI30504. PubMed PMID: 17525800; PubMed Central PMCID: PMCPMC1868786.

279. Sivignon A, Chervy M, Chevarin C, Ragot E, Billard E, Denizot J, Barnich N. An adherent-invasive Escherichia coli-colonized mouse model to evaluate microbiota-targeting strategies in Crohn's disease. Dis Model Mech. 2022;15(10). Epub 20221024. doi: 10.1242/dmm.049707. PubMed PMID: 36172858; PubMed Central PMCID: PMCPMC9637268.

280. Carvalho FA, Barnich N, Sivignon A, Darcha C, Chan CH, Stanners CP, Darfeuille-Michaud A. Crohn's disease adherent-invasive Escherichia coli colonize and induce strong gut inflammation in transgenic mice expressing human CEACAM. J Exp Med. 2009;206(10):2179-89. Epub 20090908. doi: 10.1084/jem.20090741. PubMed PMID: 19737864; PubMed Central PMCID: PMCPMC2757893.

281. Aprikian P, Tchesnokova V, Kidd B, Yakovenko O, Yarov-Yarovoy V, Trinchina E, Vogel V, Thomas W, Sokurenko E. Interdomain interaction in the FimH adhesin of Escherichia coli regulates the affinity to mannose. J Biol Chem. 2007;282(32):23437-46. Epub 20070613. doi: 10.1074/jbc.M702037200. PubMed PMID: 17567583.

282. Dreux N, Denizot J, Martinez-Medina M, Mellmann A, Billig M, Kisiela D, Chattopadhyay S, Sokurenko E, Neut C, Gower-Rousseau C, Colombel JF, Bonnet R, Darfeuille-Michaud A, Barnich N. Point mutations in FimH adhesin of Crohn's disease-associated adherent-invasive Escherichia coli enhance intestinal inflammatory response. PLoS Pathog. 2013;9(1):e1003141. Epub 20130124. doi: 10.1371/journal.ppat.1003141. PubMed PMID: 23358328; PubMed Central PMCID: PMCPMC3554634.

283. Dumych T, Yamakawa N, Sivignon A, Garenaux E, Robakiewicz S, Coddeville B, Bongiovanni A, Bray F, Barnich N, Szunerits S, Slomianny C, Herrmann M, Gouin

SG, Lutsyk AD, Munoz LE, Lafont F, Rolando C, Bilyy R, Bouckaert JMJ. Oligomannose-Rich Membranes of Dying Intestinal Epithelial Cells Promote Host Colonization by Adherent-Invasive. Front Microbiol. 2018;9:742. Epub 20180418. doi: 10.3389/fmicb.2018.00742. PubMed PMID: 29720971; PubMed Central PMCID: PMCPMC5915571.

284. Aomatsu T, Imaeda H, Matsumoto K, Kimura E, Yoden A, Tamai H, Fujiyama Y, Mizoguchi E, Andoh A. Faecal chitinase 3-like-1: a novel biomarker of disease activity in paediatric inflammatory bowel disease. Aliment Pharmacol Ther. 2011;34(8):941-8. Epub 20110816. doi: 10.1111/j.1365-2036.2011.04805.x. PubMed PMID: 21848856.

285. Chen CC, Pekow J, Llado V, Kanneganti M, Lau CW, Mizoguchi A, Mino-Kenudson M, Bissonnette M, Mizoguchi E. Chitinase 3-like-1 expression in colonic epithelial cells as a potentially novel marker for colitis-associated neoplasia. Am J Pathol. 2011;179(3):1494-503. Epub 20110716. doi: 10.1016/j.ajpath.2011.05.038. PubMed PMID: 21763261; PubMed Central PMCID: PMCPMC3157229.

286. Low D, Tran HT, Lee IA, Dreux N, Kamba A, Reinecker HC, Darfeuille-Michaud A, Barnich N, Mizoguchi E. Chitin-binding domains of Escherichia coli ChiA mediate interactions with intestinal epithelial cells in mice with colitis. Gastroenterology. 2013;145(3):602-12.e9. Epub 20130516. doi: 10.1053/j.gastro.2013.05.017. PubMed PMID: 23684751; PubMed Central PMCID: PMCPMC3755095.

287. Mizoguchi E. Chitinase 3-like-1 exacerbates intestinal inflammation by enhancing bacterial adhesion and invasion in colonic epithelial cells.

Gastroenterology. 2006;130(2):398-411. doi: 10.1053/j.gastro.2005.12.007. PubMed PMID: 16472595.

288. Tran HT, Lee IA, Low D, Kamba A, Mizoguchi A, Shi HN, Lee CG, Elias JA, Mizoguchi E. Chitinase 3-like 1 synergistically activates IL6-mediated STAT3 phosphorylation in intestinal epithelial cells in murine models of infectious colitis. Inflamm Bowel Dis. 2014;20(5):835-46. doi: 10.1097/MIB.0000000000000033. PubMed PMID: 24694795; PubMed Central PMCID: PMCPMC4012618.

289. Alkaissi LY, Winberg ME, Heil SDS, Haapaniemi S, Myrelid P, Stange EF, Söderholm JD, Keita Å. Antagonism of Adherent Invasive E. coli LF82 With Human α-defensin 5 in the Follicle-associated Epithelium of Patients With Ileal Crohn's Disease. Inflamm Bowel Dis. 2021;27(7):1116-27. doi: 10.1093/ibd/izaa315. PubMed PMID: 33336693; PubMed Central PMCID: PMCPMC8205628.

290. McPhee JB, Small CL, Reid-Yu SA, Brannon JR, Le Moual H, Coombes BK. Host defense peptide resistance contributes to colonization and maximal intestinal pathology by Crohn's disease-associated adherent-invasive Escherichia coli. Infect Immun. 2014;82(8):3383-93. Epub 20140527. doi: 10.1128/IAI.01888-14. PubMed PMID: 24866805; PubMed Central PMCID: PMCPMC4136195.

291. Gibold L, Garenaux E, Dalmasso G, Gallucci C, Cia D, Mottet-Auselo B, Faïs T, Darfeuille-Michaud A, Nguyen HT, Barnich N, Bonnet R, Delmas J. The Vat-AIEC protease promotes crossing of the intestinal mucus layer by Crohn's disease-associated Escherichia coli. Cell Microbiol. 2016;18(5):617-31. Epub 20151123. doi: 10.1111/cmi.12539. PubMed PMID: 26499863.

292. Barnich N, Buisson A, Auzolle C, Rodrigues M, Stefanescu C, Nancey S, Desreumaux P, Marteau P, Fumery M, Sokol H, Treton X, Seksik P, Allez M. P772 The presence of adherent-invasive Escherichia coli strains on the surgical specimen is a predictor of severe endoscopic postoperative recurrence in Crohn's disease. Journal of Crohn's and Colitis. 2017;11(suppl_1):S475-S6. doi: 10.1093/ecco-jcc/jjx002.893.

293. Zheng L, Duan SL, Dai YC, Wu SC. Role of adherent invasive. World J Clin Cases. 2022;10(32):11671-89. doi: 10.12998/wjcc.v10.i32.11671. PubMed PMID: 36405271; PubMed Central PMCID: PMCPMC9669839.

294. Oberc AM, Fiebig-Comyn AA, Tsai CN, Elhenawy W, Coombes BK. Antibiotics Potentiate Adherent-Invasive E. coli Infection and Expansion. Inflamm Bowel Dis. 2019;25(4):711-21. doi: 10.1093/ibd/izy361. PubMed PMID: 30496418.

295. Dogan B, Fu J, Zhang S, Scherl EJ, Simpson KW. Rifaximin decreases virulence of Crohn's disease-associated Escherichia coli and epithelial inflammatory responses. J Antibiot (Tokyo). 2018;71(5):485-94. Epub 20180206. doi: 10.1038/s41429-017-0022-y. PubMed PMID: 29410518.

296. Li J, Dejanovic D, Zangara MT, Chandra J, McDonald C, Rieder F. Mouse Models of Intestinal Fibrosis. Methods Mol Biol. 2021;2299:385-403. doi: 10.1007/978-1-0716-1382-5_26. PubMed PMID: 34028756; PubMed Central PMCID: PMCPMC8844945.

297. Flores EM, Nguyen AT, Odem MA, Eisenhoffer GT, Krachler AM. The zebrafish as a model for gastrointestinal tract-microbe interactions. Cell Microbiol.

2020;22(3):e13152. Epub 20200107. doi: 10.1111/cmi.13152. PubMed PMID: 31872937; PubMed Central PMCID: PMCPMC7015812.

298. Howe K, Clark MD, Torroja CF, Torrance J, Berthelot C, Muffato M, Collins JE, Humphray S, McLaren K, Matthews L, McLaren S, Sealy I, Caccamo M, Churcher C, Scott C, Barrett JC, Koch R, Rauch GJ, White S, Chow W, Kilian B, Quintais LT, Guerra-Assunção JA, Zhou Y, Gu Y, Yen J, Vogel JH, Eyre T, Redmond S, Banerjee R, Chi J, Fu B, Langley E, Maguire SF, Laird GK, Lloyd D, Kenyon E, Donaldson S, Sehra H, Almeida-King J, Loveland J, Trevanion S, Jones M, Quail M, Willey D, Hunt A, Burton J, Sims S, McLay K, Plumb B, Davis J, Clee C, Oliver K, Clark R, Riddle C, Elliot D, Threadgold G, Harden G, Ware D, Begum S, Mortimore B, Kerry G, Heath P, Phillimore B, Tracey A, Corby N, Dunn M, Johnson C, Wood J, Clark S, Pelan S, Griffiths G, Smith M, Glithero R, Howden P, Barker N, Lloyd C, Stevens C, Harley J, Holt K, Panagiotidis G, Lovell J, Beasley H, Henderson C, Gordon D, Auger K, Wright D, Collins J, Raisen C, Dyer L, Leung K, Robertson L, Ambridge K, Leongamornlert D, McGuire S, Gilderthorp R, Griffiths C, Manthravadi D, Nichol S, Barker G, Whitehead S, Kay M, Brown J, Murnane C, Gray E, Humphries M, Sycamore N, Barker D, Saunders D, Wallis J, Babbage A, Hammond S, Mashreghi-Mohammadi M, Barr L, Martin S, Wray P, Ellington A, Matthews N, Ellwood M, Woodmansey R, Clark G, Cooper J, Tromans A, Grafham D, Skuce C, Pandian R, Andrews R, Harrison E, Kimberley A, Garnett J, Fosker N, Hall R, Garner P, Kelly D, Bird C, Palmer S, Gehring I, Berger A, Dooley CM, Ersan-Ürün Z, Eser C, Geiger H, Geisler M, Karotki L, Kirn A, Konantz J, Konantz M, Oberländer M, Rudolph-Geiger S, Teucke M, Lanz C, Raddatz G, Osoegawa K, Zhu B, Rapp A, Widaa S, Langford C, Yang F, Schuster SC, Carter

NP, Harrow J, Ning Z, Herrero J, Searle SM, Enright A, Geisler R, Plasterk RH, Lee C, Westerfield M, de Jong PJ, Zon LI, Postlethwait JH, Nüsslein-Volhard C, Hubbard TJ, Roest Crollius H, Rogers J, Stemple DL. The zebrafish reference genome sequence and its relationship to the human genome. Nature. 2013;496(7446):498-503. Epub 20130417. doi: 10.1038/nature12111. PubMed PMID: 23594743; PubMed Central PMCID: PMCPMC3703927.

299. Oehlers SH, Flores MV, Hall CJ, Swift S, Crosier KE, Crosier PS. The inflammatory bowel disease (IBD) susceptibility genes NOD1 and NOD2 have conserved anti-bacterial roles in zebrafish. Dis Model Mech. 2011;4(6):832-41. Epub 20110704. doi: 10.1242/dmm.006122. PubMed PMID: 21729873; PubMed Central PMCID: PMCPMC3209652.

300. Ng AN, de Jong-Curtain TA, Mawdsley DJ, White SJ, Shin J, Appel B, Dong PD, Stainier DY, Heath JK. Formation of the digestive system in zebrafish: III. Intestinal epithelium morphogenesis. Dev Biol. 2005;286(1):114-35. doi: 10.1016/j.ydbio.2005.07.013. PubMed PMID: 16125164.

301. Pack M, Solnica-Krezel L, Malicki J, Neuhauss SC, Schier AF, Stemple DL, Driever W, Fishman MC. Mutations affecting development of zebrafish digestive organs. Development. 1996;123:321-8. doi: 10.1242/dev.123.1.321. PubMed PMID: 9007252.

302. Wallace KN, Akhter S, Smith EM, Lorent K, Pack M. Intestinal growth and differentiation in zebrafish. Mech Dev. 2005;122(2):157-73. doi: 10.1016/j.mod.2004.10.009. PubMed PMID: 15652704.

303. Chen YH, Lu YF, Ko TY, Tsai MY, Lin CY, Lin CC, Hwang SP. Zebrafish cdx1b regulates differentiation of various intestinal cell lineages. Dev Dyn. 2009;238(5):1021-32. doi: 10.1002/dvdy.21908. PubMed PMID: 19253392.

304. Wang Z, Du J, Lam SH, Mathavan S, Matsudaira P, Gong Z. Morphological and molecular evidence for functional organization along the rostrocaudal axis of the adult zebrafish intestine. BMC Genomics. 2010;11:392. Epub 20100622. doi: 10.1186/1471-2164-11-392. PubMed PMID: 20565988; PubMed Central PMCID: PMCPMC2996925.

305. Park J, Levic DS, Sumigray KD, Bagwell J, Eroglu O, Block CL, Eroglu C, Barry R, Lickwar CR, Rawls JF, Watts SA, Lechler T, Bagnat M. Lysosome-Rich Enterocytes Mediate Protein Absorption in the Vertebrate Gut. Dev Cell. 2019;51(1):7-20.e6. Epub 20190829. doi: 10.1016/j.devcel.2019.08.001. PubMed PMID: 31474562; PubMed Central PMCID: PMCPMC6783362.

306. Li J, Prochaska M, Maney L, Wallace KN. Development and organization of the zebrafish intestinal epithelial stem cell niche. Dev Dyn. 2020;249(1):76-87. Epub 20190218. doi: 10.1002/dvdy.16. PubMed PMID: 30698914; PubMed Central PMCID: PMCPMC8432741.

307. Chen X, Yi Y, Bian C, You X, Shi Q. Putative Antimicrobial Peptides in Fish: Using Zebrafish as a Representative. Protein Pept Lett. 2020;27(11):1059-67. doi: 10.2174/0929866527666200517104610. PubMed PMID: 32416669.

308. Willms RJ, Jones LO, Hocking JC, Foley E. A cell atlas of microbe-responsive processes in the zebrafish intestine. Cell Rep. 2022;38(5):110311. doi: 10.1016/j.celrep.2022.110311. PubMed PMID: 35108531.

309. Lam SH, Chua HL, Gong Z, Lam TJ, Sin YM. Development and maturation of the immune system in zebrafish, Danio rerio: a gene expression profiling, in situ hybridization and immunological study. Dev Comp Immunol. 2004;28(1):9-28. doi: 10.1016/s0145-305x(03)00103-4. PubMed PMID: 12962979.

310. Meijer AH, Gabby Krens SF, Medina Rodriguez IA, He S, Bitter W, Ewa Snaar-Jagalska B, Spaink HP. Expression analysis of the Toll-like receptor and TIR domain adaptor families of zebrafish. Mol Immunol. 2004;40(11):773-83. doi: 10.1016/j.molimm.2003.10.003. PubMed PMID: 14687934.

311. Herbomel P, Thisse B, Thisse C. Ontogeny and behaviour of early macrophages in the zebrafish embryo. Development. 1999;126(17):3735-45. doi: 10.1242/dev.126.17.3735. PubMed PMID: 10433904.

312. Lieschke GJ, Oates AC, Crowhurst MO, Ward AC, Layton JE. Morphologic and functional characterization of granulocytes and macrophages in embryonic and adult zebrafish. Blood. 2001;98(10):3087-96. doi: 10.1182/blood.v98.10.3087. PubMed PMID: 11698295.

313. Torraca V, Mostowy S. Zebrafish Infection: From Pathogenesis to Cell Biology. Trends Cell Biol. 2018;28(2):143-56. Epub 20171121. doi: 10.1016/j.tcb.2017.10.002. PubMed PMID: 29173800; PubMed Central PMCID: PMCPMC5777827.

314. Stones DH, Fehr AGJ, Thompson L, Rocha J, Perez-Soto N, Madhavan VTP, Voelz K, Krachler AM. Zebrafish (mSphere. 2017;2(5). Epub 20170920. doi: 10.1128/mSphereDirect.00365-17. PubMed PMID: 28959735; PubMed Central PMCID: PMCPMC5607324.

315. Renshaw SA, Loynes CA, Trushell DM, Elworthy S, Ingham PW, Whyte MK. A transgenic zebrafish model of neutrophilic inflammation. Blood. 2006;108(13):3976-8. Epub 20060822. doi: 10.1182/blood-2006-05-024075. PubMed PMID: 16926288.

316. Ellett F, Pase L, Hayman JW, Andrianopoulos A, Lieschke GJ. mpeg1 promoter transgenes direct macrophage-lineage expression in zebrafish. Blood. 2011;117(4):e49-56. Epub 20101117. doi: 10.1182/blood-2010-10-314120. PubMed PMID: 21084707; PubMed Central PMCID: PMCPMC3056479.

317. Lee DJ, Bingle LE, Heurlier K, Pallen MJ, Penn CW, Busby SJ, Hobman JL. Gene doctoring: a method for recombineering in laboratory and pathogenic Escherichia coli strains. BMC Microbiol. 2009;9:252. Epub 20091209. doi: 10.1186/1471-2180-9-252. PubMed PMID: 20003185; PubMed Central PMCID: PMCPMC2796669.

318. Crépin S, Harel J, Dozois CM. Chromosomal complementation using Tn7 transposon vectors in Enterobacteriaceae. Appl Environ Microbiol. 2012;78(17):6001-8. Epub 20120615. doi: 10.1128/AEM.00986-12. PubMed PMID: 22706059; PubMed Central PMCID: PMCPMC3416591.

319. Flores E, Thompson L, Sirisaengtaksin N, Nguyen AT, Ballard A, Krachler AM. Using the Protozoan Paramecium caudatum as a Vehicle for Food-borne Infections in Zebrafish Larvae. J Vis Exp. 2019;(143). Epub 20190107. doi: 10.3791/58949. PubMed PMID: 30663701; PubMed Central PMCID: PMCPMC8376190.

320. Oehlers SH, Flores MV, Hall CJ, Okuda KS, Sison JO, Crosier KE, Crosier PS. Chemically induced intestinal damage models in zebrafish larvae. Zebrafish.

2013;10(2):184-93. Epub 20130228. doi: 10.1089/zeb.2012.0824. PubMed PMID: 23448252.

321. Peterson SM, Freeman JL. RNA isolation from embryonic zebrafish and cDNA synthesis for gene expression analysis. J Vis Exp. 2009;(30). Epub 20090807. doi: 10.3791/1470. PubMed PMID: 19684565; PubMed Central PMCID: PMCPMC3152201.

322. Schmittgen TD, Livak KJ. Analyzing real-time PCR data by the comparative CT method.

323. Grisham MB. Do different animal models of IBD serve different purposes? Inflamm Bowel Dis. 2008;14 Suppl 2:S132-3. doi: 10.1002/ibd.20682. PubMed PMID: 18816751.

324. Mizoguchi A. Animal models of inflammatory bowel disease. Prog Mol Biol Transl Sci. 2012;105:263-320. doi: 10.1016/B978-0-12-394596-9.00009-3. PubMed PMID: 22137435.

325. Baydi Z, Limami Y, Khalki L, Zaid N, Naya A, Mtairag EM, Oudghiri M, Zaid Y. An Update of Research Animal Models of Inflammatory Bowel Disease. ScientificWorldJournal. 2021;2021:7479540. Epub 20211213. doi: 10.1155/2021/7479540. PubMed PMID: 34938152; PubMed Central PMCID: PMCPMC8687830.

326. Randhawa PK, Singh K, Singh N, Jaggi AS. A review on chemical-induced inflammatory bowel disease models in rodents. Korean J Physiol Pharmacol. 2014;18(4):279-88. Epub 20140813. doi: 10.4196/kjpp.2014.18.4.279. PubMed PMID: 25177159; PubMed Central PMCID: PMCPMC4146629.

327. Dubińska-Magiera M, Daczewska M, Lewicka A, Migocka-Patrzałek M, Niedbalska-Tarnowska J, Jagla K. Zebrafish: A Model for the Study of Toxicants Affecting Muscle Development and Function. Int J Mol Sci. 2016;17(11). Epub 20161119. doi: 10.3390/ijms17111941. PubMed PMID: 27869769; PubMed Central PMCID: PMCPMC5133936.

328. Wirtz S, Popp V, Kindermann M, Gerlach K, Weigmann B, Fichtner-Feigl S, Neurath MF. Chemically induced mouse models of acute and chronic intestinal inflammation. Nat Protoc. 2017;12(7):1295-309. Epub 20170601. doi: 10.1038/nprot.2017.044. PubMed PMID: 28569761.

329. Chassaing B, Aitken JD, Malleshappa M, Vijay-Kumar M. Dextran sulfate sodium (DSS)-induced colitis in mice. Curr Protoc Immunol. 2014;104:15.25.1-15.25.14. Epub 20140204. doi: 10.1002/0471142735.im1525s104. PubMed PMID: 24510619; PubMed Central PMCID: PMCPMC3980572.

330. Eichele DD, Kharbanda KK. Dextran sodium sulfate colitis murine model: An indispensable tool for advancing our understanding of inflammatory bowel diseases pathogenesis. World J Gastroenterol. 2017;23(33):6016-29. doi: 10.3748/wjg.v23.i33.6016. PubMed PMID: 28970718; PubMed Central PMCID: PMCPMC5597494.

331. Oehlers SH, Flores MV, Hall CJ, Crosier KE, Crosier PS. Retinoic acid suppresses intestinal mucus production and exacerbates experimental enterocolitis. Dis Model Mech. 2012;5(4):457-67. Epub 20120419. doi: 10.1242/dmm.009365. PubMed PMID: 22563081; PubMed Central PMCID: PMCPMC3380709.

332. Oehlers SH, Flores MV, Okuda KS, Hall CJ, Crosier KE, Crosier PS. A chemical enterocolitis model in zebrafish larvae that is dependent on microbiota and responsive to pharmacological agents. Dev Dyn. 2011;240(1):288-98. doi: 10.1002/dvdy.22519. PubMed PMID: 21181946.

333. Antoniou E, Margonis GA, Angelou A, Pikouli A, Argiri P, Karavokyros I, Papalois A, Pikoulis E. The TNBS-induced colitis animal model: An overview. Ann Med Surg (Lond). 2016;11:9-15. Epub 20160819. doi: 10.1016/j.amsu.2016.07.019. PubMed PMID: 27656280; PubMed Central PMCID: PMCPMC5021709.

334. Fleming A, Jankowski J, Goldsmith P. In vivo analysis of gut function and disease changes in a zebrafish larvae model of inflammatory bowel disease: a feasibility study. Inflamm Bowel Dis. 2010;16(7):1162-72. doi: 10.1002/ibd.21200. PubMed PMID: 20128011.

335. Neurath MF, Fuss I, Kelsall BL, Stüber E, Strober W. Antibodies to interleukin 12 abrogate established experimental colitis in mice. J Exp Med. 1995;182(5):1281-90. doi: 10.1084/jem.182.5.1281. PubMed PMID: 7595199; PubMed Central PMCID: PMCPMC2192205.

336. Mannon PJ, Fuss IJ, Mayer L, Elson CO, Sandborn WJ, Present D, Dolin B, Goodman N, Groden C, Hornung RL, Quezado M, Yang Z, Neurath MF, Salfeld J, Veldman GM, Schwertschlag U, Strober W, Group A-I-CsDS. Anti-interleukin-12 antibody for active Crohn's disease. N Engl J Med. 2004;351(20):2069-79. doi: 10.1056/NEJMoa033402. PubMed PMID: 15537905.

337. Boirivant M, Fuss IJ, Chu A, Strober W. Oxazolone colitis: A murine model of T helper cell type 2 colitis treatable with antibodies to interleukin 4. J Exp Med.

1998;188(10):1929-39. doi: 10.1084/jem.188.10.1929. PubMed PMID: 9815270; PubMed Central PMCID: PMCPMC2212414.

338. Brugman S, Liu KY, Lindenbergh-Kortleve D, Samsom JN, Furuta GT, Renshaw SA, Willemsen R, Nieuwenhuis EE. Oxazolone-induced enterocolitis in zebrafish depends on the composition of the intestinal microbiota. Gastroenterology. 2009;137(5):1757-67.e1. Epub 20090819. doi: 10.1053/j.gastro.2009.07.069. PubMed PMID: 19698716.

339. Hedrera MI, Galdames JA, Jimenez-Reyes MF, Reyes AE, Avendaño-Herrera R, Romero J, Feijóo CG. Soybean meal induces intestinal inflammation in zebrafish larvae. PLoS One. 2013;8(7):e69983. Epub 20130723. doi: 10.1371/journal.pone.0069983. PubMed PMID: 23894568; PubMed Central PMCID: PMCPMC3720926.

340. Fuentes-Appelgren P, Opazo R, Barros L, Feijoó CG, Urzúa V, Romero J. Effect of the dietary inclusion of soybean components on the innate immune system in zebrafish. Zebrafish. 2014;11(1):41-9. Epub 20140107. doi: 10.1089/zeb.2013.0934. PubMed PMID: 24392798.

341. Solis CJ, Hamilton MK, Caruffo M, Garcia-Lopez JP, Navarrete P, Guillemin K, Feijoo CG. Intestinal Inflammation Induced by Soybean Meal Ingestion Increases Intestinal Permeability and Neutrophil Turnover Independently of Microbiota in Zebrafish. Front Immunol. 2020;11:1330. Epub 20200724. doi: 10.3389/fimmu.2020.01330. PubMed PMID: 32793187; PubMed Central PMCID: PMCPMC7393261.

342. Fitzpatrick FA. Cyclooxygenase enzymes: regulation and function. Curr Pharm Des. 2004;10(6):577-88. doi: 10.2174/1381612043453144. PubMed PMID: 14965321.

343. Goldsmith JR, Cocchiaro JL, Rawls JF, Jobin C. Glafenine-induced intestinal injury in zebrafish is ameliorated by μ-opioid signaling via enhancement of Atf6-dependent cellular stress responses. Dis Model Mech. 2013;6(1):146-59. Epub 20120823. doi: 10.1242/dmm.009852. PubMed PMID: 22917923; PubMed Central PMCID: PMCPMC3529347.

344. Mizoguchi A, Takeuchi T, Himuro H, Okada T, Mizoguchi E. Genetically engineered mouse models for studying inflammatory bowel disease. J Pathol. 2016;238(2):205-19. Epub 20151114. doi: 10.1002/path.4640. PubMed PMID: 26387641; PubMed Central PMCID: PMCPMC4689626.

345. Iyer SS, Cheng G. Role of interleukin 10 transcriptional regulation in inflammation and autoimmune disease. Crit Rev Immunol. 2012;32(1):23-63. doi: 10.1615/critrevimmunol.v32.i1.30. PubMed PMID: 22428854; PubMed Central PMCID: PMCPMC3410706.

346. Glocker EO, Kotlarz D, Boztug K, Gertz EM, Schäffer AA, Noyan F, Perro M, Diestelhorst J, Allroth A, Murugan D, Hätscher N, Pfeifer D, Sykora KW, Sauer M, Kreipe H, Lacher M, Nustede R, Woellner C, Baumann U, Salzer U, Koletzko S, Shah N, Segal AW, Sauerbrey A, Buderus S, Snapper SB, Grimbacher B, Klein C. Inflammatory bowel disease and mutations affecting the interleukin-10 receptor. N Engl J Med. 2009;361(21):2033-45. Epub 20091104. doi: 10.1056/NEJMoa0907206. PubMed PMID: 19890111; PubMed Central PMCID: PMCPMC2787406.

347. Kühn R, Löhler J, Rennick D, Rajewsky K, Müller W. Interleukin-10-deficient mice develop chronic enterocolitis. Cell. 1993;75(2):263-74. doi: 10.1016/0092-8674(93)80068-p. PubMed PMID: 8402911.

348. Morales RA, Rabahi S, Diaz OE, Salloum Y, Kern BC, Westling M, Luo X, Parigi SM, Monasterio G, Das S, Hernández PP, Villablanca EJ. Interleukin-10 regulates goblet cell numbers through Notch signaling in the developing zebrafish intestine. Mucosal Immunol. 2022;15(5):940-51. Epub 20220715. doi: 10.1038/s41385-022-00546-3. PubMed PMID: 35840681; PubMed Central PMCID: PMCPMC9385495.

349. Marjoram L, Alvers A, Deerhake ME, Bagwell J, Mankiewicz J, Cocchiaro JL, Beerman RW, Willer J, Sumigray KD, Katsanis N, Tobin DM, Rawls JF, Goll MG, Bagnat M. Epigenetic control of intestinal barrier function and inflammation in zebrafish. Proc Natl Acad Sci U S A. 2015;112(9):2770-5. Epub 20150217. doi: 10.1073/pnas.1424089112. PubMed PMID: 25730872; PubMed Central PMCID: PMCPMC4352795.

350. Qi S, Li Y, Dai Z, Xiang M, Wang G, Wang L, Wang Z. Uhrf1-Mediated Tnf-α Gene Methylation Controls Proinflammatory Macrophages in Experimental Colitis Resembling Inflammatory Bowel Disease. J Immunol. 2019;203(11):3045-53. Epub 20191014. doi: 10.4049/jimmunol.1900467. PubMed PMID: 31611260.

351. Ostanin DV, Bao J, Koboziev I, Gray L, Robinson-Jackson SA, Kosloski-Davidson M, Price VH, Grisham MB. T cell transfer model of chronic colitis: concepts, considerations, and tricks of the trade. Am J Physiol Gastrointest Liver Physiol. 2009;296(2):G135-46. Epub 20081125. doi: 10.1152/ajpgi.90462.2008. PubMed PMID: 19033538; PubMed Central PMCID: PMCPMC2643911.

352. Wan F, Hu CB, Ma JX, Gao K, Xiang LX, Shao JZ. Characterization of γδ T Cells from Zebrafish Provides Insights into Their Important Role in Adaptive Humoral Immunity. Front Immunol. 2016;7:675. Epub 20170109. doi: 10.3389/fimmu.2016.00675. PubMed PMID: 28119690; PubMed Central PMCID: PMCPMC5220103.

353. Pizarro TT, Pastorelli L, Bamias G, Garg RR, Reuter BK, Mercado JR, Chieppa M, Arseneau KO, Ley K, Cominelli F. SAMP1/YitFc mouse strain: a spontaneous model of Crohn's disease-like ileitis. Inflamm Bowel Dis. 2011;17(12):2566-84. Epub 20110506. doi: 10.1002/ibd.21638. PubMed PMID: 21557393; PubMed Central PMCID: PMCPMC3154989.

354. Matsumoto S, Okabe Y, Setoyama H, Takayama K, Ohtsuka J, Funahashi H, Imaoka A, Okada Y, Umesaki Y. Inflammatory bowel disease-like enteritis and caecitis in a senescence accelerated mouse P1/Yit strain. Gut. 1998;43(1):71-8. doi: 10.1136/gut.43.1.71. PubMed PMID: 9771408; PubMed Central PMCID: PMCPMC1727165.

355. Rohner N, Perathoner S, Frohnhöfer HG, Harris MP. Enhancing the efficiency of N-ethyl-N-nitrosourea-induced mutagenesis in the zebrafish. Zebrafish. 2011;8(3):119-23. Epub 20110823. doi: 10.1089/zeb.2011.0703. PubMed PMID: 21861612.

356. Basson AR, Gomez-Nguyen A, Menghini P, Buttó LF, Di Martino L, Aladyshkina N, Osme A, LaSalla A, Fischer D, Ezeji JC, Erkkila HL, Brennan CJ, Lam M, Rodriguez-Palacios A, Cominelli F. Human Gut Microbiome Transplantation in Ileitis Prone Mice: A Tool for the Functional Characterization of the Microbiota in

Inflammatory Bowel Disease Patients. Inflammatory Bowel Diseases. 2019;26(3):347-59. doi: 10.1093/ibd/izz242.

357. Kullberg MC, Ward JM, Gorelick PL, Caspar P, Hieny S, Cheever A, Jankovic D, Sher A. Helicobacter hepaticus triggers colitis in specific-pathogen-free interleukin-10 (IL-10)-deficient mice through an IL-12- and gamma interferon-dependent mechanism. Infect Immun. 1998;66(11):5157-66. doi: 10.1128/IAI.66.11.5157-5166.1998. PubMed PMID: 9784517; PubMed Central PMCID: PMCPMC108643.

358. Crawford KC, Vega Flores M, Oehlers SH, Hall CJ, Crosier KE, Crosier PS. Zebrafish heat shock protein a4 genes in the intestinal epithelium are up-regulated during inflammation. Genesis. 2011;49(12):905-11. Epub 20111013. doi: 10.1002/dvg.20767. PubMed PMID: 21557452.

359. Chuang LS, Morrison J, Hsu NY, Labrias PR, Nayar S, Chen E, Villaverde N, Facey JA, Boschetti G, Giri M, Castillo-Martin M, Thin TH, Sharma Y, Chu J, Cho JH. Zebrafish modeling of intestinal injury, bacterial exposures and medications defines epithelial. Dis Model Mech. 2019;12(8). Epub 20190813. doi: 10.1242/dmm.037432. PubMed PMID: 31337664; PubMed Central PMCID: PMCPMC6737949.

360. Di Paola D, Natale S, Iaria C, Cordaro M, Crupi R, Siracusa R, D'Amico R, Fusco R, Impellizzeri D, Cuzzocrea S, Spanò N, Gugliandolo E, Peritore AF. Intestinal Disorder in Zebrafish Larvae (Life (Basel). 2022;12(1). Epub 20220116. doi: 10.3390/life12010125. PubMed PMID: 35054518; PubMed Central PMCID: PMCPMC8778351.

361. Clark KJ, Boczek NJ, Ekker SC. Stressing zebrafish for behavioral genetics. Rev Neurosci. 2011;22(1):49-62. doi: 10.1515/RNS.2011.007. PubMed PMID: 21615261; PubMed Central PMCID: PMCPMC3470424.

362. Scheid P, Pelster B, Kobayashi H. Gas exchange in the fish swimbladder. Adv Exp Med Biol. 1990;277:735-42. doi: 10.1007/978-1-4684-8181-5_84. PubMed PMID: 1965765.

363. Yue MS, Peterson RE, Heideman W. Dioxin inhibition of swim bladder development in zebrafish: is it secondary to heart failure? Aquat Toxicol. 2015;162:10-7. Epub 20150302. doi: 10.1016/j.aquatox.2015.02.016. PubMed PMID: 25766903; PubMed Central PMCID: PMCPMC4397172.

364. Biton IE, Stettner N, Brener O, Erez A, Harmelin A, Garbow JR. Assessing Mucosal Inflammation in a DSS-Induced Colitis Mouse Model by MR Colonography. Tomography. 2018;4(1):4-13. doi: 10.18383/j.tom.2017.00021. PubMed PMID: 30042983; PubMed Central PMCID: PMCPMC6024430.

365. Erben U, Loddenkemper C, Doerfel K, Spieckermann S, Haller D, Heimesaat MM, Zeitz M, Siegmund B, Kühl AA. A guide to histomorphological evaluation of intestinal inflammation in mouse models. Int J Clin Exp Pathol. 2014;7(8):4557-76. Epub 20140715. PubMed PMID: 25197329; PubMed Central PMCID: PMCPMC4152019.

366. d'Alençon CA, Peña OA, Wittmann C, Gallardo VE, Jones RA, Loosli F, Liebel U, Grabher C, Allende ML. A high-throughput chemically induced inflammation assay in zebrafish. BMC Biol. 2010;8:151. Epub 20101222. doi: 10.1186/1741-7007-8-151. PubMed PMID: 21176202; PubMed Central PMCID: PMCPMC3022775.

367. Hall C, Flores MV, Crosier K, Crosier P. Live cell imaging of zebrafish leukocytes. Methods Mol Biol. 2009;546:255-71. doi: 10.1007/978-1-60327-977-2_16. PubMed PMID: 19378109.

368. Kim ND, Luster AD. The role of tissue resident cells in neutrophil recruitment. Trends Immunol. 2015;36(9):547-55. Epub 20150818. doi: 10.1016/j.it.2015.07.007. PubMed PMID: 26297103; PubMed Central PMCID: PMCPMC4567503.

369. Fujiwara N, Kobayashi K. Macrophages in inflammation. Curr Drug Targets Inflamm Allergy. 2005;4(3):281-6. doi: 10.2174/1568010054022024. PubMed PMID: 16101534.

370. Laroui H, Ingersoll SA, Liu HC, Baker MT, Ayyadurai S, Charania MA, Laroui F, Yan Y, Sitaraman SV, Merlin D. Dextran sodium sulfate (DSS) induces colitis in mice by forming nano-lipocomplexes with medium-chain-length fatty acids in the colon. PLoS One. 2012;7(3):e32084. Epub 20120309. doi: 10.1371/journal.pone.0032084. PubMed PMID: 22427817; PubMed Central PMCID: PMCPMC3302894.

371. Miskolci V, Squirrell J, Rindy J, Vincent W, Sauer JD, Gibson A, Eliceiri KW, Huttenlocher A. Distinct inflammatory and wound healing responses to complex caudal fin injuries of larval zebrafish. Elife. 2019;8. Epub 20190701. doi: 10.7554/eLife.45976. PubMed PMID: 31259685; PubMed Central PMCID: PMCPMC6602581.

372. Foundation CsC. How is IBD Diagnosed? 2022. Available from: https://www.crohnscolitisfoundation.org/what-is-ibd/diagnosing-ibd.

373. Nag D, Farr D, Raychaudhuri S, Withey JH. An adult zebrafish model for adherent-invasive. iScience. 2022;25(7):104572. Epub 20220609. doi: 10.1016/j.isci.2022.104572. PubMed PMID: 35769878; PubMed Central PMCID: PMCPMC9234234.

374. Geier MS, Smith CL, Butler RN, Howarth GS. Small-intestinal manifestations of dextran sulfate sodium consumption in rats and assessment of the effects of Lactobacillus fermentum BR11. Dig Dis Sci. 2009;54(6):1222-8. Epub 20081113. doi: 10.1007/s10620-008-0495-4. PubMed PMID: 19005763.

375. Colucci-Guyon E, Tinevez JY, Renshaw SA, Herbomel P. Strategies of professional phagocytes in vivo: unlike macrophages, neutrophils engulf only surface-associated microbes. J Cell Sci. 2011;124(Pt 18):3053-9. Epub 20110824. doi: 10.1242/jcs.082792. PubMed PMID: 21868367.

376. Butterfield TA, Best TM, Merrick MA. The dual roles of neutrophils and macrophages in inflammation: a critical balance between tissue damage and repair. J Athl Train. 2006;41(4):457-65. PubMed PMID: 17273473; PubMed Central PMCID: PMCPMC1748424.

377. Osawa Y, Nagaki M, Banno Y, Brenner DA, Asano T, Nozawa Y, Moriwaki H, Nakashima S. Tumor necrosis factor alpha-induced interleukin-8 production via NF-kappaB and phosphatidylinositol 3-kinase/Akt pathways inhibits cell apoptosis in human hepatocytes. Infect Immun. 2002;70(11):6294-301. doi: 10.1128/IAI.70.11.6294-6301.2002. PubMed PMID: 12379708; PubMed Central PMCID: PMCPMC130316.

378. Yabluchanskiy A, Ma Y, Iyer RP, Hall ME, Lindsey ML. Matrix metalloproteinase-9: Many shades of function in cardiovascular disease. Physiology (Bethesda). 2013;28(6):391-403. doi: 10.1152/physiol.00029.2013. PubMed PMID: 24186934; PubMed Central PMCID: PMCPMC3858212.

379. Saraceni PR, Romero A, Figueras A, Novoa B. Establishment of Infection Models in Zebrafish Larvae (Danio rerio) to Study the Pathogenesis of Aeromonas hydrophila. Front Microbiol. 2016;7:1219. Epub 20160804. doi: 10.3389/fmicb.2016.01219. PubMed PMID: 27540375; PubMed Central PMCID: PMCPMC4972827.

380. van Soest JJ, Stockhammer OW, Ordas A, Bloemberg GV, Spaink HP, Meijer AH. Comparison of static immersion and intravenous injection systems for exposure of zebrafish embryos to the natural pathogen Edwardsiella tarda. BMC Immunol. 2011;12:58. Epub 20111017. doi: 10.1186/1471-2172-12-58. PubMed PMID: 22003892; PubMed Central PMCID: PMCPMC3206475.

381. Schmidt JG, Korbut R, Ohtani M, Jørgensen LVG. Zebrafish (Danio rerio) as a model to visualize infection dynamics of Vibrio anguillarum following intraperitoneal injection and bath exposure. Fish Shellfish Immunol. 2017;67:692-7. Epub 20170627. doi: 10.1016/j.fsi.2017.06.052. PubMed PMID: 28663130.

382. Nguyen-Chi M, Phan QT, Gonzalez C, Dubremetz JF, Levraud JP, Lutfalla G. Transient infection of the zebrafish notochord with E. coli induces chronic inflammation. Dis Model Mech. 2014;7(7):871-82. doi: 10.1242/dmm.014498. PubMed PMID: 24973754; PubMed Central PMCID: PMCPMC4073276.

383. Stemple DL. Structure and function of the notochord: an essential organ for chordate development. Development. 2005;132(11):2503-12. doi: 10.1242/dev.01812.

384. Willis AR, Moore C, Mazon-Moya M, Krokowski S, Lambert C, Till R, Mostowy S, Sockett RE. Injections of Predatory Bacteria Work Alongside Host Immune Cells to Treat Shigella Infection in Zebrafish Larvae. Curr Biol. 2016;26(24):3343-51. Epub 20161123. doi: 10.1016/j.cub.2016.09.067. PubMed PMID: 27889262; PubMed Central PMCID: PMCPMC5196024.

385. Cocchiaro JL, Rawls JF. Microgavage of zebrafish larvae. J Vis Exp. 2013;(72):e4434. Epub 20130220. doi: 10.3791/4434. PubMed PMID: 23463135; PubMed Central PMCID: PMCPMC3605733.

386. Collymore C, Rasmussen S, Tolwani RJ. Gavaging adult zebrafish. J Vis Exp. 2013;(78). Epub 20130811. doi: 10.3791/50691. PubMed PMID: 23962977; PubMed Central PMCID: PMCPMC3855001.

387. Lee SW, Wendy W. Antibiotic and heavy metal resistance of. Vet World. 2017;10(7):803-7. Epub 20170721. doi: 10.14202/vetworld.2017.803-807. PubMed PMID: 28831226; PubMed Central PMCID: PMCPMC5553151.

388. Hawke JP, Kent M, Rogge M, Baumgartner W, Wiles J, Shelley J, Savolainen LC, Wagner R, Murray K, Peterson TS. Edwardsiellosis caused by Edwardsiella ictaluri in laboratory populations of Zebrafish Danio rerio. J Aquat Anim Health. 2013;25(3):171-83. doi: 10.1080/08997659.2013.782226. PubMed PMID: 23865817; PubMed Central PMCID: PMCPMC4077847.

389. Xu T, Su Y, Xu Y, He Y, Wang B, Dong X, Li Y, Zhang XH. Mutations of flagellar genes fliC12, fliA and flhDC of Edwardsiella tarda attenuated bacterial motility, biofilm formation and virulence to fish. J Appl Microbiol. 2014;116(2):236-44. Epub 20131025. doi: 10.1111/jam.12357. PubMed PMID: 24118854.

390. Okuda J, Takeuchi Y, Nakai T. Type III secretion system genes of Edwardsiella tarda associated with intracellular replication and virulence in zebrafish. Dis Aquat Organ. 2014;111(1):31-9. doi: 10.3354/dao02763. PubMed PMID: 25144115.

391. Dong X, Fan X, Wang B, Shi X, Zhang XH. Invasin of Edwardsiella tarda is essential for its haemolytic activity, biofilm formation and virulence towards fish. J Appl Microbiol. 2013;115(1):12-9. Epub 20130418. doi: 10.1111/jam.12198. PubMed PMID: 23600645.

392. Yang HT, Zou SS, Zhai LJ, Wang Y, Zhang FM, An LG, Yang GW. Pathogen invasion changes the intestinal microbiota composition and induces innate immune responses in the zebrafish intestine. Fish Shellfish Immunol. 2017;71:35-42. Epub 20170928. doi: 10.1016/j.fsi.2017.09.075. PubMed PMID: 28964859.

393. Hossain S, De Silva BCJ, Dahanayake PS, Heo GJ. Characterization of virulence properties and multi-drug resistance profiles in motile Aeromonas spp. isolated from zebrafish (Danio rerio). Lett Appl Microbiol. 2018;67(6):598-605. Epub 20181112. doi: 10.1111/lam.13075. PubMed PMID: 30229985.

394. Johnston JM, Becker SF, McFarland LM. Gastroenteritis in patients with stool isolates of Vibrio vulnificus. Am J Med. 1986;80(2):336-8. doi: 10.1016/0002-9343(86)90038-0. PubMed PMID: 3946453.

395. Tsai YH, Huang TJ, Hsu RW, Weng YJ, Hsu WH, Huang KC, Peng KT. Necrotizing soft-tissue infections and primary sepsis caused by Vibrio vulnificus and Vibrio cholerae non-O1. J Trauma. 2009;66(3):899-905. doi: 10.1097/TA.0b013e31816a9ed3. PubMed PMID: 19276771.

396. Runft DL, Mitchell KC, Abuaita BH, Allen JP, Bajer S, Ginsburg K, Neely MN, Withey JH. Zebrafish as a natural host model for Vibrio cholerae colonization and transmission. Appl Environ Microbiol. 2014;80(5):1710-7. Epub 20131227. doi: 10.1128/AEM.03580-13. PubMed PMID: 24375135; PubMed Central PMCID: PMCPMC3957598.

397. Manneh-Roussel J, Haycocks JRJ, Magán A, Perez-Soto N, Voelz K, Camilli A, Krachler AM, Grainger DC. cAMP Receptor Protein Controls Vibrio cholerae Gene Expression in Response to Host Colonization. mBio. 2018;9(4). Epub 20180710. doi: 10.1128/mBio.00966-18. PubMed PMID: 29991587; PubMed Central PMCID: PMCPMC6050953.

398. Tyrkalska SD, Candel S, Angosto D, Gómez-Abellán V, Martín-Sánchez F, García-Moreno D, Zapata-Pérez R, Sánchez-Ferrer Á, Sepulcre MP, Pelegrín P, Mulero V. Neutrophils mediate Salmonella Typhimurium clearance through the GBP4 inflammasome-dependent production of prostaglandins. Nat Commun. 2016;7:12077. Epub 20160701. doi: 10.1038/ncomms12077. PubMed PMID: 27363812; PubMed Central PMCID: PMCPMC4932187.

399. Nag D, Breen P, Raychaudhuri S, Withey JH. Glucose Metabolism by Escherichia coli Inhibits Vibrio cholerae Intestinal Colonization of Zebrafish. Infect

Immun. 2018;86(12). Epub 20181120. doi: 10.1128/IAI.00486-18. PubMed PMID: 30249745; PubMed Central PMCID: PMCPMC6246912.

400. Hudzicki J. Kirby-Bauer disk diffusion susceptibility test protocol. American society for microbiology. 2009;15:55-63.

401. Bragg AN, Hulpieu H. A METHOD OF DEMONSTRATING ACIDITY OF FOOD VACUOLES IN PARAMECIUM. Science. 1925;61(1580):392. doi: 10.1126/science.61.1580.392. PubMed PMID: 17732158.

402. Patterson BW, Abraham AO, MacIver MA, McLean DL. Visually guided gradation of prey capture movements in larval zebrafish. J Exp Biol. 2013;216(Pt 16):3071-83. Epub 20130425. doi: 10.1242/jeb.087742. PubMed PMID: 23619412; PubMed Central PMCID: PMCPMC4074221.

403. Bretin A, Lucas C, Larabi A, Dalmasso G, Billard E, Barnich N, Bonnet R, Nguyen HTT. AIEC infection triggers modification of gut microbiota composition in genetically predisposed mice, contributing to intestinal inflammation. Sci Rep. 2018;8(1):12301. Epub 20180817. doi: 10.1038/s41598-018-30055-y. PubMed PMID: 30120269; PubMed Central PMCID: PMCPMC6098085.

404. Imai J, Kitamoto S, Sugihara K, Nagao-Kitamoto H, Hayashi A, Morhardt TL, Kuffa P, Higgins PDR, Barnich N, Kamada N. Flagellin-mediated activation of IL-33-ST2 signaling by a pathobiont promotes intestinal fibrosis. Mucosal Immunol. 2019;12(3):632-43. Epub 20190211. doi: 10.1038/s41385-019-0138-4. PubMed PMID: 30742042; PubMed Central PMCID: PMCPMC6462251.

405. Hayashi Y, Nakase H. The Molecular Mechanisms of Intestinal Inflammation and Fibrosis in Crohn's Disease. Front Physiol. 2022;13:845078. Epub 20220211. doi:

10.3389/fphys.2022.845078. PubMed PMID: 35222098; PubMed Central PMCID: PMCPMC8874128.

406. Viladomiu M, Metz ML, Lima SF, Jin WB, Chou L, Guo CJ, Diehl GE, Simpson KW, Scherl EJ, Longman RS, Bank JLC. Adherent-invasive E. coli metabolism of propanediol in Crohn's disease regulates phagocytes to drive intestinal inflammation. Cell Host Microbe. 2021;29(4):607-19.e8. Epub 20210203. doi: 10.1016/j.chom.2021.01.002. PubMed PMID: 33539767; PubMed Central PMCID: PMCPMC8049981.

407. Sokurenko EV, Courtney HS, Maslow J, Siitonen A, Hasty DL. Quantitative differences in adhesiveness of type 1 fimbriated Escherichia coli due to structural differences in fimH genes. J Bacteriol. 1995;177(13):3680-6. doi: 10.1128/jb.177.13.3680-3686.1995. PubMed PMID: 7601831; PubMed Central PMCID: PMCPMC177083.

408. Martinez-Medina M, Denizot J, Dreux N, Robin F, Billard E, Bonnet R, Darfeuille-Michaud A, Barnich N. Western diet induces dysbiosis with increased E coli in CEABAC10 mice, alters host barrier function favouring AIEC colonisation. Gut. 2014;63(1):116-24. Epub 20130418. doi: 10.1136/gutjnl-2012-304119. PubMed PMID: 23598352.

409. Fléchard M, Cortes MA, Répérant M, Germon P. New role for the ibeA gene in H2O2 stress resistance of Escherichia coli. J Bacteriol. 2012;194(17):4550-60. Epub 20120622. doi: 10.1128/JB.00089-12. PubMed PMID: 22730120; PubMed Central PMCID: PMCPMC3415484.

410. Ran C, Qin C, Xie M, Zhang J, Li J, Xie Y, Wang Y, Li S, Liu L, Fu X, Lin Q, Li N, Liles MR, Zhou Z. Aeromonas veronii and aerolysin are important for the pathogenesis of motile aeromonad septicemia in cyprinid fish. Environ Microbiol. 2018;20(9):3442-56. Epub 20180920. doi: 10.1111/1462-2920.14390. PubMed PMID: 30136361.

411. Logan SL, Thomas J, Yan J, Baker RP, Shields DS, Xavier JB, Hammer BK, Parthasarathy R. The. Proc Natl Acad Sci U S A. 2018;115(16):E3779-E87. Epub 20180402. doi: 10.1073/pnas.1720133115. PubMed PMID: 29610339; PubMed Central PMCID: PMCPMC5910850.

412. Wiles TJ, Bower JM, Redd MJ, Mulvey MA. Use of zebrafish to probe the divergent virulence potentials and toxin requirements of extraintestinal pathogenic Escherichia coli. PLoS Pathog. 2009;5(12):e1000697. Epub 20091218. doi: 10.1371/journal.ppat.1000697. PubMed PMID: 20019794; PubMed Central PMCID: PMCPMC2785880.

413. Rawls JF, Mahowald MA, Ley RE, Gordon JI. Reciprocal gut microbiota transplants from zebrafish and mice to germ-free recipients reveal host habitat selection. Cell. 2006;127(2):423-33. doi: 10.1016/j.cell.2006.08.043. PubMed PMID: 17055441; PubMed Central PMCID: PMCPMC4839475.

414. Perez-Soto N, Moule L, Crisan DN, Insua I, Taylor-Smith LM, Voelz K, Fernandez-Trillo F, Krachler AM. Engineering microbial physiology with synthetic polymers: cationic polymers induce biofilm formation in. Chem Sci. 2017;8(8):5291-8. Epub 20170516. doi: 10.1039/c7sc00615b. PubMed PMID: 28970909; PubMed Central PMCID: PMCPMC5607900.

415. Fan Y, Thompson L, Lyu Z, Cameron TA, De Lay NR, Krachler AM, Ling J. Optimal translational fidelity is critical for Salmonella virulence and host interactions. Nucleic Acids Res. 2019;47(10):5356-67. doi: 10.1093/nar/gkz229. PubMed PMID: 30941426; PubMed Central PMCID: PMCPMC6547416.

416. Frager SZ, Chrisman CJ, Shakked R, Casadevall A. Paramecium species ingest and kill the cells of the human pathogenic fungus Cryptococcus neoformans. Med Mycol. 2010;48(5):775-9. doi: 10.3109/13693780903451810. PubMed PMID: 20233022; PubMed Central PMCID: PMCPMC4294704.

417. Glas J, Seiderer J, Fries C, Tillack C, Pfennig S, Weidinger M, Beigel F, Olszak T, Lass U, Göke B, Ochsenkühn T, Wolf C, Lohse P, Müller-Myhsok B, Diegelmann J, Czamara D, Brand S. CEACAM6 gene variants in inflammatory bowel disease. PLoS One. 2011;6(4):e19319. Epub 20110429. doi: 10.1371/journal.pone.0019319. PubMed PMID: 21559399; PubMed Central PMCID: PMCPMC3084820.

418. Chokr D, Cornu M, Neut C, Bortolus C, Charlet R, Desreumaux P, Speca S, Sendid B. Adherent invasive Escherichia coli (AIEC) strain LF82, but not Candida albicans, plays a profibrogenic role in the intestine. Gut Pathog. 2021;13(1):5. Epub 20210128. doi: 10.1186/s13099-021-00401-z. PubMed PMID: 33509285; PubMed Central PMCID: PMCPMC7842025.

419. Carvalho FA, Barnich N, Sauvanet P, Darcha C, Gelot A, Darfeuille-Michaud A. Crohn's disease-associated Escherichia coli LF82 aggravates colitis in injured mouse colon via signaling by flagellin. Inflamm Bowel Dis. 2008;14(8):1051-60. doi: 10.1002/ibd.20423. PubMed PMID: 18338780.

420. Bassotti G, Antonelli E, Villanacci V, Salemme M, Coppola M, Annese V. Gastrointestinal motility disorders in inflammatory bowel diseases. World J Gastroenterol. 2014;20(1):37-44. doi: 10.3748/wjg.v20.i1.37. PubMed PMID: 24415856; PubMed Central PMCID: PMCPMC3886030.

421. Cremer J, Segota I, Yang CY, Arnoldini M, Sauls JT, Zhang Z, Gutierrez E, Groisman A, Hwa T. Effect of flow and peristaltic mixing on bacterial growth in a gut-like channel. Proc Natl Acad Sci U S A. 2016;113(41):11414-9. Epub 20160928. doi: 10.1073/pnas.1601306113. PubMed PMID: 27681630; PubMed Central PMCID: PMCPMC5068270.

422. Steukers L, Glorieux S, Vandekerckhove AP, Favoreel HW, Nauwynck HJ. Diverse microbial interactions with the basement membrane barrier. Trends Microbiol. 2012;20(3):147-55. Epub 20120131. doi: 10.1016/j.tim.2012.01.001. PubMed PMID: 22300759; PubMed Central PMCID: PMCPMC7127156.

423. He Q, Wang L, Wang F, Wang C, Tang C, Li Q, Li J, Zhao Q. Microbial fingerprinting detects intestinal microbiota dysbiosis in Zebrafish models with chemically-induced enterocolitis. BMC Microbiology. 2013;13(1):289. doi: 10.1186/1471-2180-13-289.

424. Håkansson Å, Tormo-Badia N, Baridi A, Xu J, Molin G, Hagslätt ML, Karlsson C, Jeppsson B, Cilio CM, Ahrné S. Immunological alteration and changes of gut microbiota after dextran sulfate sodium (DSS) administration in mice. Clin Exp Med. 2015;15(1):107-20. Epub 20140111. doi: 10.1007/s10238-013-0270-5. PubMed PMID: 24414342; PubMed Central PMCID: PMCPMC4308640.

425. Xu Z, Dong X, Yang K, Chevarin C, Zhang J, Lin Y, Zuo T, Chu LC, Sun Y, Zhang F. Association of adherent-invasive Escherichia coli with severe gut mucosal dysbiosis in Hong Kong chinese population with Crohn's disease. Gut microbes. 2021;13(1):1994833.

426. Kowalewski J, Paris T, Gonzalez C, Lelièvre E, Castaño Valencia L, Boutrois M, Augier C, Lutfalla G, Yatime L. Characterization of a member of the CEACAM protein family as a novel marker of proton pump-rich ionocytes on the zebrafish epidermis. PLoS One. 2021;16(7):e0254533. Epub 20210712. doi: 10.1371/journal.pone.0254533. PubMed PMID: 34252160; PubMed Central PMCID: PMCPMC8274849.

427. Chapin C, Bailey NA, Gonzales LW, Lee JW, Gonzalez RF, Ballard PL. Distribution and surfactant association of carcinoembryonic cell adhesion molecule 6 in human lung. Am J Physiol Lung Cell Mol Physiol. 2012;302(2):L216-25. Epub 20111028. doi: 10.1152/ajplung.00055.2011. PubMed PMID: 22037359; PubMed Central PMCID: PMCPMC3349363.

428. zfin. gc:198329 2023. Available from: https://zfin.org/ZDB-GENE-080226-6#summary.

429. Hall-Stoodley L, Costerton JW, Stoodley P. Bacterial biofilms: from the natural environment to infectious diseases. Nature reviews microbiology. 2004;2(2):95-108.

430. Schembri MA, Klemm P. Biofilm formation in a hydrodynamic environment by novel fimh variants and ramifications for virulence. Infect Immun. 2001;69(3):1322-8. doi: 10.1128/IAI.69.3.1322-1328.2001. PubMed PMID: 11179294; PubMed Central PMCID: PMCPMC98023.

431. Dwyer BE, Newton KL, Kisiela D, Sokurenko EV, Clegg S. Single nucleotide polypmorphisms of fimH associated with adherence and biofilm formation by serovars of Salmonella enterica. Microbiology (Reading). 2011;157(Pt 11):3162-71. Epub 20110818. doi: 10.1099/mic.0.051425-0. PubMed PMID: 21852351; PubMed Central PMCID: PMCPMC3352275.

432. Wang S, Niu C, Shi Z, Xia Y, Yaqoob M, Dai J, Lu C. Effects of ibeA deletion on virulence and biofilm formation of avian pathogenic Escherichia coli. Infect Immun. 2011;79(1):279-87. Epub 20101025. doi: 10.1128/IAI.00821-10. PubMed PMID: 20974831; PubMed Central PMCID: PMCPMC3019902.

433. Graves CL, Chen A, Kwon V, Shiau CE. Zebrafish harbor diverse intestinal macrophage populations including a subset intimately associated with enteric neural processes. iScience. 2021;24(6):102496. Epub 20210503. doi: 10.1016/j.isci.2021.102496. PubMed PMID: 34142024; PubMed Central PMCID: PMCPMC8185245.

434. Avdesh A, Chen M, Martin-Iverson MT, Mondal A, Ong D, Rainey-Smith S, Taddei K, Lardelli M, Groth DM, Verdile G, Martins RN. Regular care and maintenance of a zebrafish (Danio rerio) laboratory: an introduction. J Vis Exp. 2012;(69):e4196. Epub 20121118. doi: 10.3791/4196. PubMed PMID: 23183629; PubMed Central PMCID: PMCPMC3916945.

435. Davis JM, Clay H, Lewis JL, Ghori N, Herbomel P, Ramakrishnan L. Real-time visualization of mycobacterium-macrophage interactions leading to initiation of granuloma formation in zebrafish embryos. Immunity. 2002;17(6):693-702. doi: 10.1016/s1074-7613(02)00475-2. PubMed PMID: 12479816.

436. Zhao Q, Chang H, Zheng J, Li P, Ye L, Pan R, Li D, Shao J-Z, Zhao RC, Chen Y. A novel Trmt5-deficient zebrafish model with spontaneous inflammatory bowel disease-like phenotype.

437. Kabeerdoss J, Jayakanthan P, Pugazhendhi S, Ramakrishna BS. Alterations of mucosal microbiota in the colon of patients with inflammatory bowel disease revealed by real time polymerase chain reaction amplification of 16S ribosomal ribonucleic acid. Indian J Med Res. 2015;142(1):23-32. doi: 10.4103/0971-5916.162091. PubMed PMID: 26261163; PubMed Central PMCID: PMCPMC4557246.

438. Hickey CA, Kuhn KA, Donermeyer DL, Porter NT, Jin C, Cameron EA, Jung H, Kaiko GE, Wegorzewska M, Malvin NP, Glowacki RW, Hansson GC, Allen PM, Martens EC, Stappenbeck TS. Colitogenic Bacteroides thetaiotaomicron Antigens Access Host Immune Cells in a Sulfatase-Dependent Manner via Outer Membrane Vesicles. Cell Host Microbe. 2015;17(5):672-80. doi: 10.1016/j.chom.2015.04.002. PubMed PMID: 25974305; PubMed Central PMCID: PMCPMC4432250.

439. Tsai HH, Dwarakanath AD, Hart CA, Milton JD, Rhodes JM. Increased faecal mucin sulphatase activity in ulcerative colitis: a potential target for treatment. Gut. 1995;36(4):570-6. doi: 10.1136/gut.36.4.570. PubMed PMID: 7737566; PubMed Central PMCID: PMCPMC1382499.

440. Jevtov I, Samuelsson T, Yao G, Amsterdam A, Ribbeck K. Zebrafish as a model to study live mucus physiology. Sci Rep. 2014;4:6653. Epub 20141017. doi: 10.1038/srep06653. PubMed PMID: 25323747; PubMed Central PMCID: PMCPMC4200417.

441. Medicine NLo, Information NCfB. galactose-3-O-sulfotransferase 2 [*Danio rerio* (zebrafish)] [cited 2023]. ZFIN Gene: gal3st2.]. Available from: https://www.ncbi.nlm.nih.gov/gene/556126.

442. Medicine NLo, Information NCfB. carbohydrate sulfotransferase 6 [*Danio rerio* (zebrafish)] [2023]. Available from: https://www.ncbi.nlm.nih.gov/gene/100170782.

Erika Flores entered The University of Texas MD Anderson Cancer Center UTHealth Graduate School of Biomedical Sciences in August of 2017 .